Forschungszentrum Karlsruhe
in der Helmholtz-Gemeinschaft

Wissenschaftliche Berichte
FZKA 7483

Definition of Procedures for Coil Electrical Testing and Preparation for PF Transient Analysis

(EFDA/06-1522)
FU06-CT-2006-00470
CPM 801514

Final Report
Version 26.05.2009

S. Fink, A. Winkler, W. Fietz, M. Noe
Institut für Technische Physik

Juli 2009

Forschungszentrum Karlsruhe

in der Helmholtz-Gemeinschaft

Wissenschaftliche Berichte

FZKA 7483

Definition of Procedures for Coil Electrical Testing and Preparation for PF Transient Analysis

(EFDA/06-1522)

FU06-CT-2006-00470

CPM 801514

Final Report

Version 26.05.2009

S. Fink, A. Winkler, W. Fietz, M. Noe

Institute for Technical Physics

Forschungszentrum Karlsruhe GmbH, Karlsruhe

2009

Forschungszentrum Karlsruhe GmbH
Postfach 3640, 76021 Karlsruhe

Mitglied der Hermann von Helmholtz-Gemeinschaft
Deutscher Forschungszentren (HGF)

ISSN 0947-8620

urn:nbn:de:0005-074831

Abstract

Three superconducting coil systems will be used at the ITER project. The 18 Toroidal Field coils (TF), will be used to confine the plasma in the plasma vessel. The main task of the 6 Poloidal Field coils (PF) is to control the position and the shape of the plasma during different operating scenarios. The Central Solenoid (CS) consisting of 6 CS coil modules will induce current in the plasma. During the lifetime of ITER all coils must withstand the high voltage stress because repairing or replacing a coil would cause considerable delay of the test program. Hence a verification of the high voltage design and a suitable definition of test voltages and test procedures are indispensable. This report presents the building-up of a model for the CS PF coil system with special consideration of the ability for a detailed voltage examination of the PF 3 and PF 6 coils. In addition test voltages and procedures for the ITER TF coils are proposed.

For all superconducting coils the high voltage excitation, e. g. during a fast discharge after a quench can lead to overvoltages on terminals and on the different kinds of insulation within the coil, e. g. turn, layer or ground insulation. The calculations of transient electrical behaviour of the coils provide a basis for high voltage insulation co-ordination and selection of test voltages. Such calculations are already available for ITER TF system [Fin04]. In contrast no models had been available for the investigation of PF coils. In the frame of this report such models are established for the coupled CS PF system. In addition the PF 3 and PF 6 coils were analysed in detail. PF 3 coil is the PF coil with the largest main radius and PF 6 coil is the PF coil with the largest number of turns.

The calculation strategy consists of calculations with Finite Element Method (FEM) program Maxwell2D and the network program PSpice. The Finite Element Method models of the coils were established with the specified geometry and materials. The values for frequency dependent inductances were calculated with FEM models. The values for frequency independent capacitances were calculated analytically by formulas for cylindrical and parallel-plate capacitor. The calculated values were taken into network models as lumped elements and the first resonance frequency of the coil was calculated. Due to the frequency dependence of inductance a calculation loop was started to calculate the final resonance frequency, which gives the first benchmark in the investigation of the transient electrical behaviour of the PF 3 and PF 6 coils. The voltage excitation of the PF 3 and PF 6 coils will be calculated depending on the operating state, e. g. normal operation mode, fast discharge and two fault cases.

Test voltages and waveforms for the ITER TF coils are described based on the results of prior investigations on an existing model of the TF system and detailed models of a single TF coil [Fin04]. 10 hour DC and AC tests on conductor and radial plate insulation of the ITER TF Model Coil show that no relevant degradation occurs with the proposed test voltages taking into account the proposed test time. A proposal of the test sequence and test procedures for ITER TF is presented under special consideration of a Paschen test.

TABLE OF CONTENTS

LIST OF TABLES

LIST OF FIGURES

1 Introduction

Three superconducting coil systems will be used at the ITER project. The 18 Toroidal Field coils (TF) will confine the plasma in the plasma vessel. The 6 Poloidal Field coils (PF) will control the position and the shape of the plasma. The Central Solenoid (CS) consisting of 6 CS coil modules will induce current in the plasma. The scheme of the ITER coil system is shown in Fig. 1-1.

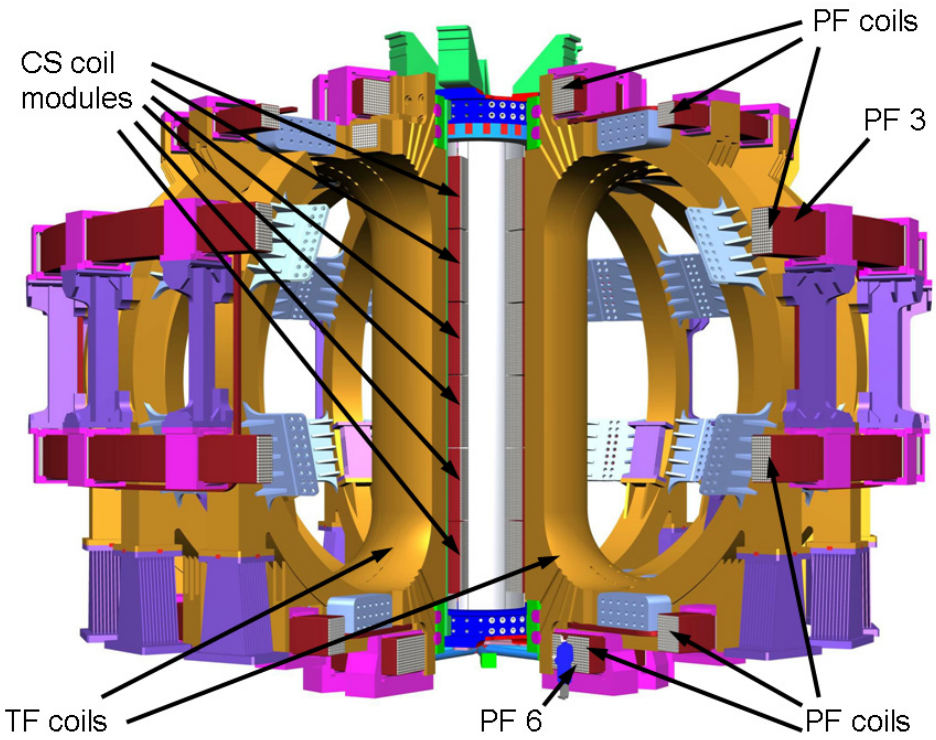

Fig. 1-1 Scheme of ITER coil system with Toroidal Field, Poloidal Field and Central Solenoid coils

The transient voltage excitations in large superconducting coils can lead to high voltage stress on different kinds of insulation within the coils, e. g. turn, layer or ground insulation, which may even exceed the terminal to terminal voltage of the coil. Because of the large dimensions, coil main diameter up to 24 m, and large number of turns in the coils, up to 549 turns, non linear voltage distribution may appear. Large internal voltages may especially appear, if an excitation contains relevant parts of the resonance frequency of the coil. The calculations of the transient electrical behaviour of the coils provide a basis for high voltage insulation co-ordination and selection of test voltages.

This report presents the building-up of a model for the CS PF coil system with special consideration of the ability for a detailed internal voltage investigation of the PF 3 and PF 6 coils. In addition test voltages and procedures for the ITER TF coils are proposed.

Most detailed calculations are made for the ITER PF 3 coil because it is the coil with the largest coil diameter and for the PF 6 coil because it is the PF coil with largest number of

turns. For both coils low resonance frequencies have been expected. With the established models it will be possible to investigate in a future task the transient electrical behaviour of the PF 3 and PF 6 coils for the case of a fast discharge, for the normal operation scenario and also for possible failure cases in electrical components of the circuit.

The strategy of the calculation of the voltage stress within the coil was also used in earlier projects in the Forschungszentrum Karlsruhe, e. g. [Fin04], in which the calculations were made for the ITER TF coils. The calculation strategy is shown in the flow chart in Fig. 1-2. At the beginning of the calculation the FEM model of the coil is established with specified geometry and materials from [DDD06]. The values for inductances are calculated with the FEM model. The values for capacitances are calculated with formulas for parallel plate and cylinder capacitor. The calculated values are taken as lumped elements into the network model of the coils. Further calculations are separated in two parts. Part one is the calculations in frequency domain. In frequency domain the resonance frequency of PF 3 and PF 6 coil is calculated, which gives the first benchmark for the calculation of voltage stress within the coils. Part two is the calculations in time domain which will be in the scope of a future report. In time domain the voltage stress on different kinds of insulation within the coil will be calculated. First the excitation voltage on the PF 3 and PF 6 coils will be calculated in a simplified CS PF coil system, in which the electrical and magnetic couplings between the coils are considered. Then the voltage stresses within the coils will be calculated with the network models of the PF 3 and PF 6 coils.

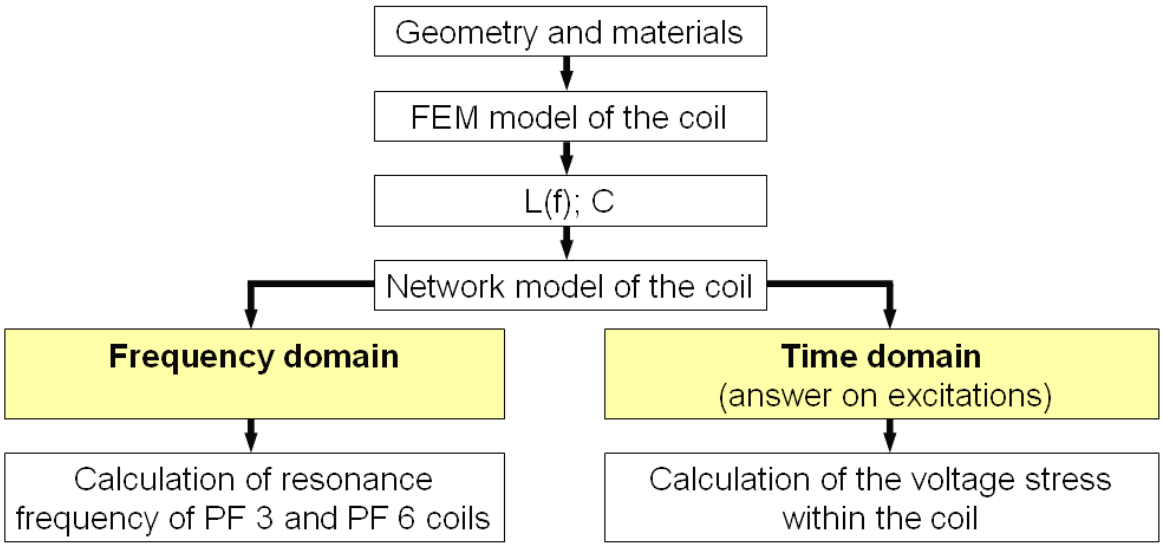

Fig. 1-2 Strategy for calculation of the resonance frequency of a coil and voltage stress within a coil

In the following chapters the calculation according this strategy will be described in detail. The overview about the ITER CS PF coil system is given in chapter 2. The detailed and simplified Finite Element Method (FEM) models of the coils are described in chapter 3. In chapter 4 the network model of the coil power supplies and network models of the PF 3 and PF 6 coils are shown in detail. The results of the calculation in frequency domain are discussed in chapter 5. The detailed data and results of the FEM calculation and network calculations for ITER PF are given in Annex A respectively in Annex B.

Test voltages and waveforms for the ITER TF coils are described in chapter 6 based on the calculated results of [Fin04] which was performed in the framework of a previous EFDA task [Con03]. In addition tests were performed which are not contained within this previous task. 10 hour DC and AC tests on conductor and radial plate insulation of the ITER TF Model Coil show that no relevant degradation occurs with the proposed test voltages taking into account the proposed test time. Chapter 7 presents a proposal of the test sequence and test procedures for ITER TF derived from the calculations and confirmed by the tests.

2 Overview about ITER CS PF Coil System

A detailed knowledge of the projected system is necessary for detailed investigation of the internal voltage of the coils. This chapter describes the dimensions of the CS PF coil system, the internal design of the PF coils and the materials which will be used for the coil construction.

2.1 Location and Size of PF and CS Coils

The rotational symmetry of the CS and PF coils can be used to build two dimensional models of the CS PF coil system. Fig. 2-1 shows the cross section of the ITER CS PF coil system with the axis of rotational symmetry and the magnet centre line. The magnet centre line is defined between the upper and the lower CS coil modules. The dimensions of the coils in Z-direction are specified with relation on the magnet centre line in [DDD06]. Further information about ITER can be taken from [ITER01].

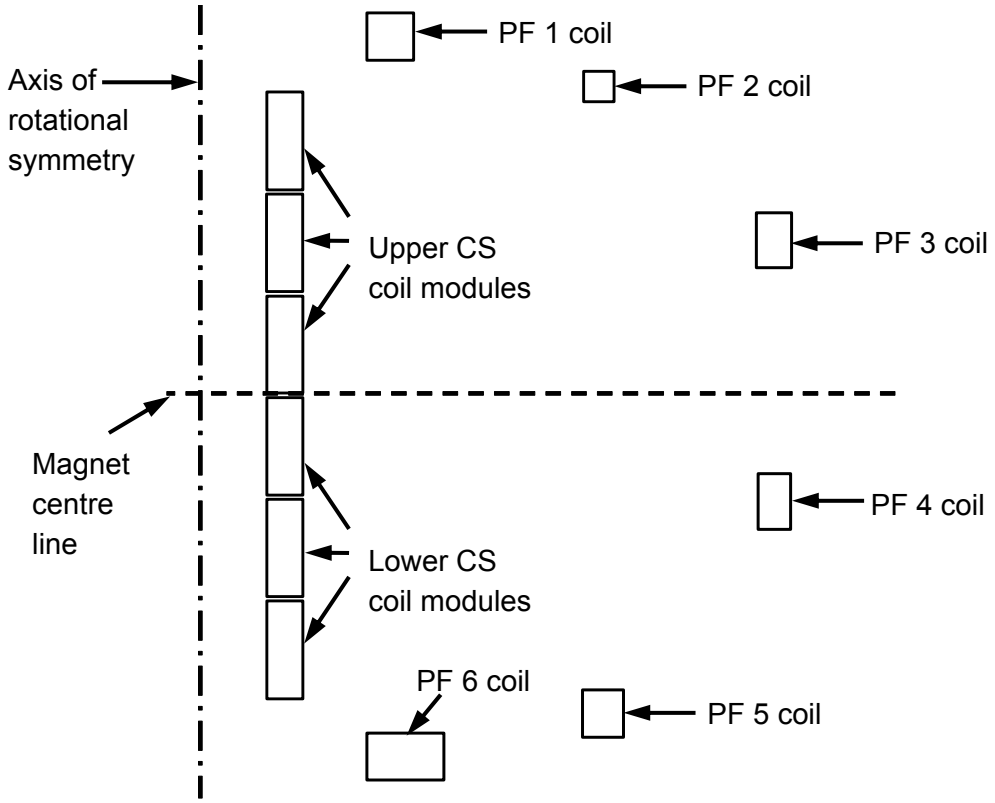

Fig. 2-1 Cross section of the ITER CS PF coil system

At the calculations of transient behaviour of the PF coils, the TF coils can be neglected, because the magnetic field caused by TF coils is orthogonal to the magnetic field of CS and PF coils. The CS coil has a conducting, hard grounded surface at the outside of each CS coil module [DDD06j]. The PF coils have protection covers, which are made from stainless steel [PPA3]. The magnetic coupling between the coils at higher frequencies will be weakened because of the metallic coil cases and other metallic parts between the coils. The eddy current which will be induced in these metallic parts reduces the coupling to negligible values at

higher frequencies. Thus at frequencies higher than 5 kHz every coil was considered as a coil without magnetic coupling to other coils which is explained in detail in 3.2.1.

The dimensions of the coils at 4.7 K are summarised in Tab. 2-1. The positions of the coil centres in Z-direction are specified from the magnet centre line of the coil system, which is shown in Fig. 2-1. Further information about ITER coils can be taken from [DDD06].

PF coil	Position of coil centre		Coil size without ground insulation and protector	
	Rc (m)	Zc (m)	ΔR (m)	ΔZ (m)
PF 1	3.943	7.557	0.968	0.976
PF 2	8.319	6.530	0.649	0.595
PF 3	11.997	3.265	0.708	0.966*
PF 4	11.967	-2.243	0.649	0.966*
PF 5	8.395	-6.730	0.820	0.945
PF 6	4.263	-7.557	1.633	0.976
CS3U	1.722	5.355	0.719	2.092
CS2U	1.722	3.213	0.719	2.092
CS1U	1.722	1.071	0.719	2.092
CS1L	1.722	-1.071	0.719	2.092
CS2L	1.722	-3.213	0.719	2.092
CS3L	1.722	-5.355	0.719	2.092

* For PF 3 and PF 4 coils the dimensions in Z-direction in [DDD06a] are specified for the design with separator plates which will not be used in the current design. The Z-dimensions of PF 3 and PF 4 coils were calculated with dimensions specified in [DDDD2] for room temperature and scaled down with factor -0.29 % [DDD06g] to 4.5 K.

Tab. 2-1 Location and size of PF and CS coils at 4.7 K [DDD06a]

2.2 PF Conductor Configuration

The design of all PF coils is described in this section although at the calculations of transient behaviour of ITER PF coils only the PF 3 and PF 6 coils will be analysed in detail.

All PF coils will be built with NbTi superconductor, which is cooled by liquid helium. The PF coils are designed for normal operation current of 45 kA at 5 K operation temperature. In the backup mode, when one of the damaged double pancakes of a coil will be disconnected and by-passed, the coil current will be increased to 52 kA. Although the PF 2 conductor is designed for 45 kA, the operating current at normal conditions is 41 kA. The PF 2 coil has only 5 double pancakes and in backup mode, with one double pancake less, the coil current is limited to 52 kA. Therefore the normal operating current has to be limited to 41 kA. Due to different magnetic fields on the conductors in normal and backup mode, there are three different designs of the PF coil conductors. All relevant data for the PF coils are summarised in the Tab. 2-2.

	PF 1 & PF 6	PF 2, PF 3 & PF 4	PF 5
Coolant normal/backup	Inlet 4.7 K/4.4 K	Inlet 4.7 K	Inlet 4.7 K
Type of strand	NbTi	NbTi	NbTi
Operating current (kA) normal/backup	45 / 52	45* / 52	45 / 52
Nominal peak field (T) normal/backup	6.0 / 6.4	4.0	5.0
Operating temperature (K) normal/backup	5.0 / 4.7	5.0	5.0
I_{OP}/I_C (Ratio of operating current to critical current) normal/backup mode	0.127 / 0.144	0.365 / 0.422	0.264 / 0.305
Cable diameter (mm)	38.2	34.5	35.4
Central spiral outer x inner diameter (mm)	12 x 10	12 x 10	12 x 10
Conductor outer dimensions (mm)	53.8 x 53.8	52.3 x 52.3	51.9 x 51.9
Jacket material	316L	316L	316L
SC strand diameter (mm)	0.73	0.73	0.72
SC strand cu:non-cu ratio	1.6	6.9	4.4
Cabling pattern (+ is Cu core)	3x4x4x5x6	((3x3x4+1)x 4+1)x6	((3x3x4+1)x 5+1)x6
SC strand number	1440	864	1080
Cu core 2/3/4 stage (mm)	0/0/0	0/1.8/3.5	0/1.2/2.7
Local void fraction (%) on strand bundle	34.5	34.2	34.3
SC strand weight/m of conductor (kg/m)	4.885	2.931	3.564

* For PF 2 coil the operation current at normal conditions is 41 kA.

Tab. 2-2 Data of the PF conductors [DDD06b]

The conductor in PF coils will be cooled by helium, which flows inside the cooling tube in the middle of the conductor. The cooling tube has a inner diameter of 10 mm and an outer diameter of 12 mm and is made as a spiral to get the helium easier into the superconducting

cable. The superconducting cable is placed directly on the outside of the cooling tube. The cross section and relevant dimensions of the PF conductors are shown in Fig. 2-2. The superconducting cable consists of up to 1440 superconducting strands [DDD06b], which are separated in five stages of sub bundles, the cabling pattern for superconducting cable of each PF coil is given in Tab. 2-2. The sub bundles in each stage are twisted against each other to make the current density in the superconducting strands and sub bundles more homogenous and avoid individual overload of one strand or bundle.

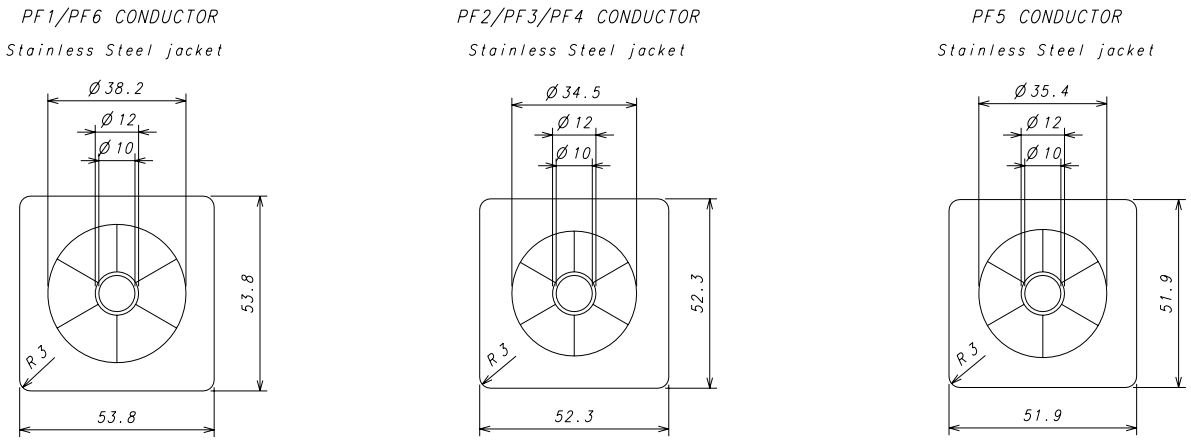

Fig. 2-2 Dimensions of the PF conductors (mm) [DDDD1]

The copper in superconducting cables is necessary to have a current path in case of the quench of superconductor. The superconducting strands have different copper non copper ratio, depending on the PF coil in which they will be used. Different sub bundles of the superconducting cable have an additional copper strand, to enlarge the copper ratio of the cable Tab. 2-2. For mechanical stabilisation the superconducting cables are put into a square stainless steel jacket. For protection during the pull through into the jacket, the superconducting cable is covered with 0.08 mm stainless steel wrap [DDD06c]. The outer dimensions of the jacket are between 51.9 mm and 53.8 mm, depending on the PF coil Fig. 2-2.

The insulation of the PF coils consists of several insulation types, the conductor, layer and ground insulation. Fig. 2-3 shows the dimensions of the insulation of the PF 6 coil, the dimensions of all PF coils are summarised in Tab. 2-3. The conductor insulation consists of two insulation layers 1.5 mm each with a 0.2 mm metal screen in between [DDD06d]. It is build up of half overlapped interleaved polyimide film and dry glass. After the winding of the double pancakes the conductor insulation is vacuum impregnated by epoxy resin. After the impregnation the double pancake insulation is placed on the double pancake and 8 double pancakes, 5 for PF 2 coil, are stacked to one winding pack. The ground insulation with a compacted thickness of 8 mm is wrapped on the whole winding pack [DDD06d]. The ground insulation consists of 0.25 mm thick glass, 0.05 mm thick polyimide film and 0.25 mm thick glass wrapped in nine 50 % overlapped layers [DDD06d]. The total not compacted thickness of ground insulation is 9.9 mm. In the second impregnation step the ground insulation is also vacuum impregnated with epoxy resin. In addition to the ground insulation, a protective cover of 2 mm thickness made of pre-cured G10 glass epoxy composite is applied to the PF coils [DDD06d].

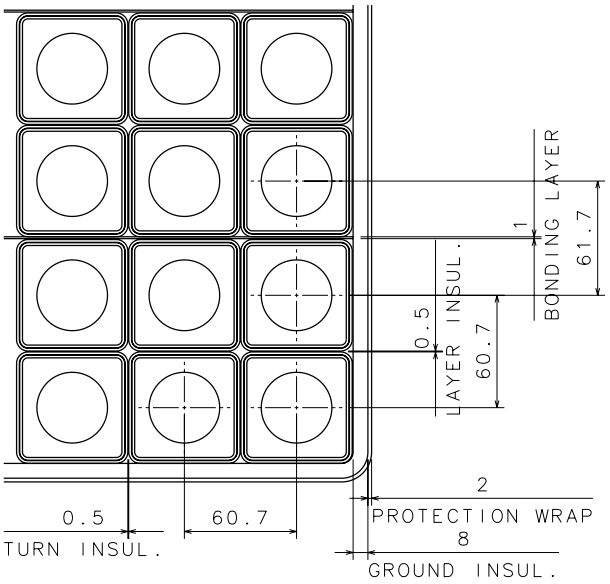

Fig. 2-3 Conductor and insulation dimensions of PF 6 coil (mm) [DDDD2]

	PF 1 / PF6	PF 2	PF 3 / PF 4	PF 5
Conductor insulation (mm)	3.2			
Turn insulation (mm)	0.5			
Distance between the windings centres (mm)	60.7	59.2	58.8	59.2
Layer insulation (mm)	0.5	0.5	1	0.5
Bonding layer (mm)	1	1	2	1
Ground insulation (mm)	8			
Protection wrap (mm)	2			

Tab. 2-3 Insulation dimensions of PF coils [DDDD2]

The PF coils are built as double pancake winding with the two-in-hand winding configuration. The two-in-hand winding scheme and stacking of double pancakes allows for all joints to be located at the pancake outer diameter, shown in Fig. 2-4.

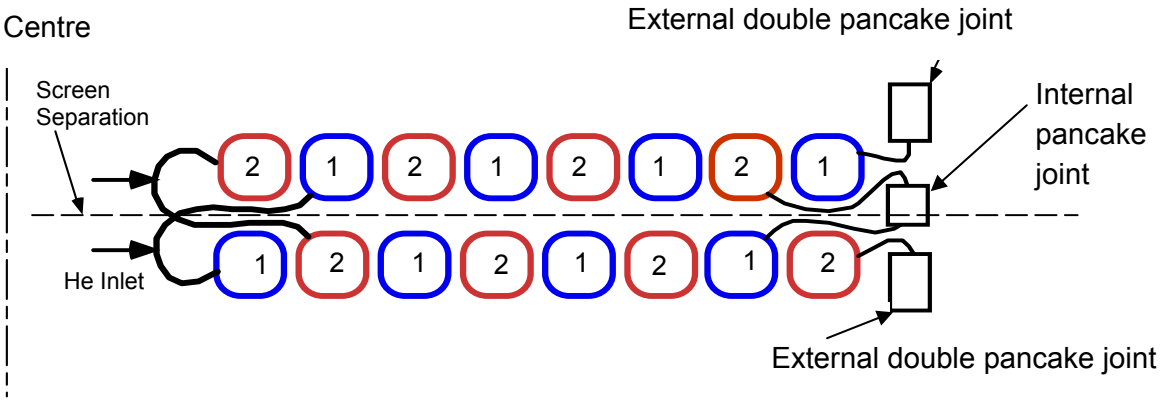

Fig. 2-4 Concept of two-in-hand double pancake winding [CDA4a]

There is a joint between the two conductors within a double pancake (internal pancake joint), as well as joints between neighbouring double pancakes (external double pancake joints). Having all joints on the outer diameter gives the ability to bypass a double pancake in the event of a short by opening three joints and reconnecting two of the joints. Bypass is accomplished by opening the joint between the two-in-hand sections in the faulted double pancake (internal pancake joint), thus the internal short circuit of the double pancake is open. The inlets of liquid helium are on the inner side of the double pancakes, thus the inner conductor of the coils get always colder coolant as the outer conductor. Further advantage of these windings configuration is that the possibility of a short circuit between the turns of the same conductor within the same pancake is strongly reduced because they are separated by the second conductor [CDA4].

The total number of turns, the winding configuration in the PF coils and the length of the conductor are given in Tab. 2-4.

PF coil	Conductor length (m)	Conductor unit length (m)	Conductor in hand	Number of pancakes	Number of turns	
					N_R x N_Z	Total
PF 1	6188	382	2	16	15.56 x 16	249
PF 2	5557	556	2	10	10.60 x 10	106
PF 3	13988	874	2	16	11.56 x 16	185
PF 4	12746	797	2	16	10.56 x 16	168
PF 5	11480	718	2	16	13.56 x 16	217
PF 6	11418	714	2	16	26.56 x 16	425

Tab. 2-4 PF coil winding configuration [DDD06e]

2.3 Power Supply Circuits of the PF and CS Coils

The power supplies of the PF and CS coils will be connected to the high voltage grid, which is capable to deliver large pulsed power. The design of the coil circuits is different depending on the coil of the circuit, shown in Fig. 2-5, Fig. 2-6 and Fig. 2-7. Further information about the power supplies of the coils can be taken from [PPS1].

The coils CS3U, CS3L, CS2U, CS2L, PF 1 and PF 6 are placed as a single coil in the coil power supply circuit, shown in Fig. 2-5. The 12-pulsed thyristor AC/DC main converter converts the alternating current from the high voltage grid to the direct current needed for the coil operation. Variations of the coil voltage during the normal operation required for breakdown and plasma initiation, which can not be generated only by the converter, will be produced by the switching network unit (SNU). In case of a quench in one of the coils in the CS PF coil system the fast discharge of all CS and PF coils will be started simultaneously by the respective fast discharge units (FDUs) in the coil circuits. Each coil terminal is symmetrically grounded by the grounding resistor network, consisting of two R_{TN} and one R_{NG} resistor. This will limit the terminal to ground voltage of the coils to the half, separated in equal positive and negative terminal voltage.

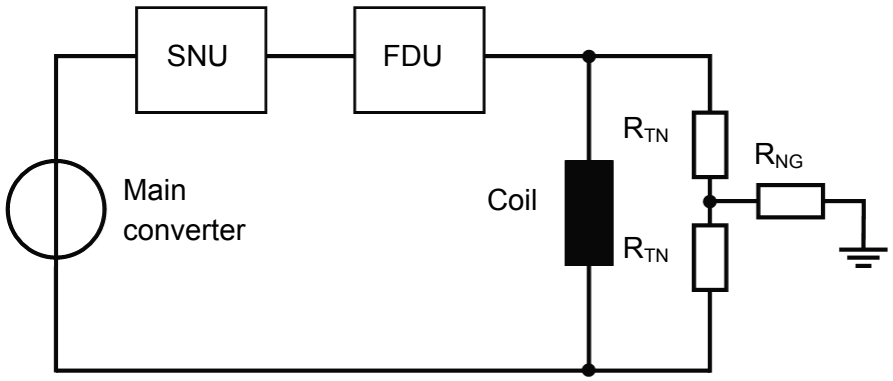

Fig. 2-5 Scheme of coil circuit for CS3U, CS3L, CS2U, CS2L, PF 1 and PF 6 derived from [PAF6Ba]

The CS1U and CS1L coil circuits are switched in series, shown in Fig. 2-6. They consist of the same elements like it was described for single coil circuits but with different values for the fast discharge resistor of the fast discharge unit (FDU) of CS1U and CS1L coil.

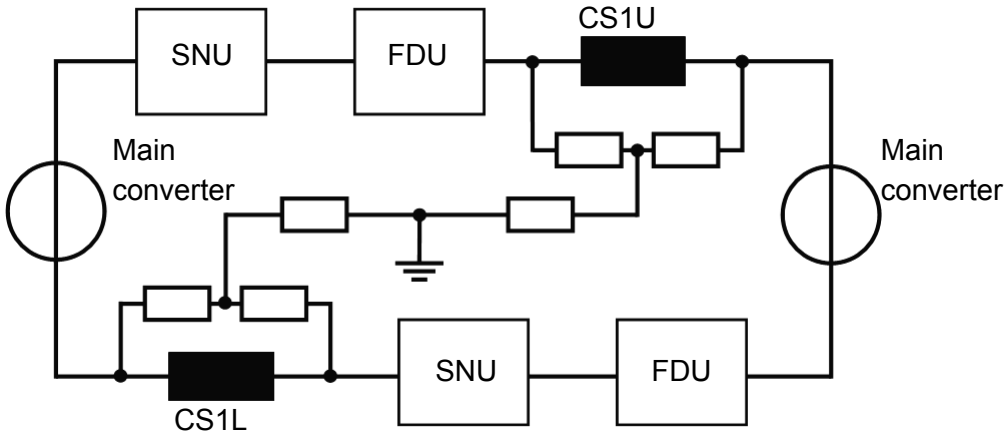

Fig. 2-6 Scheme of coil circuit for CS1U and CS1L derived from [PAF6Ba]

The PF 2, PF 3, PF 4 and PF 5 coils are connected in parallel in one electrical circuit, shown in Fig. 2-7. Due to requirement of fast control of the currents in these coils to stabilise the plasma vertical position, the vertical stabilisation converter is switched in parallel to the coil circuits of PF 2 - PF 5. The FDU and symmetrical resistor network for grounding have the same design like in other coil circuits but with different values for the fast discharge resistor of the FDU of each PF coil. The booster converters are used in the circuits of PF 2 – PF 5 coils instead of SNU in other coil circuits. The voltage on the PF 2 - PF 5 coils is higher than on the other coils due to cumulative voltage of main converter and the booster converter connected in series to each coil. A main converter and a booster converter are summarised to a branch converter (BRC), shown in Fig. 2-7. Detailed drawings of the power supplies of each coil can be taken from [PPSD1].

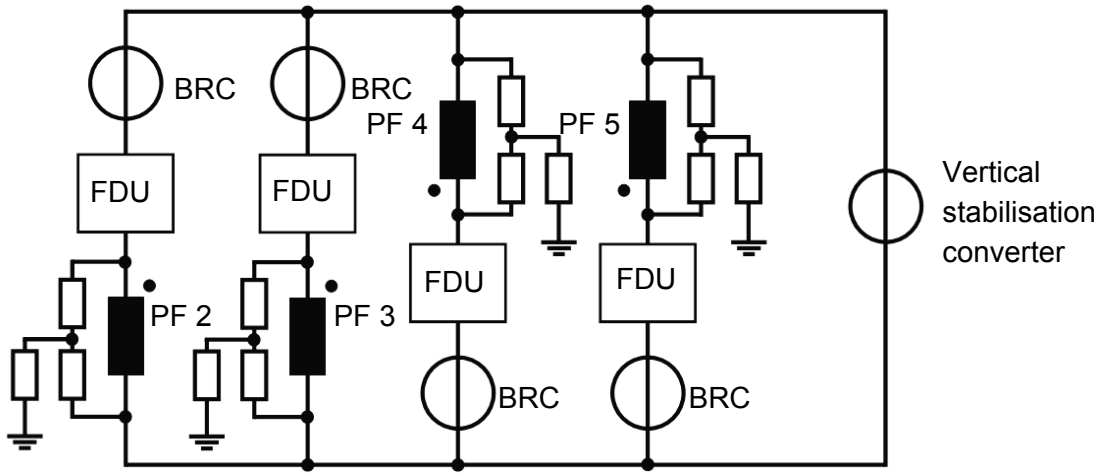

Fig. 2-7 Scheme of coil circuit for PF 2, PF 3, PF 4 and PF 5 derived from [PAF6Ba]

All CS and PF coils, despite PF 2 coil, have the same current during the normal operation of 45 kA. The current of the PF 2 coil during the normal operation is 41 kA. The no load, on load voltage and converter current are shown in Tab. 2-5.

	Maximal no load voltage	Maximal on load voltage	Converter operation current
Main converter	2 kV	1.5 kV	45 kA
Booster converter	2 x 2.8 kV	2 x 2.1 kV	10 kA
Vertical stabilisation converter	2 x 4 kV	2 x 3 kV	45 kA

Tab. 2-5 Power supply converter data [PAF6Ba], [PPS1a]

2.3.1 Fast Discharge Unit (FDU)

The FDU will be used for fast discharge of the coils, e. g. if a quench will be detected in the coils. The equivalent time constant for fast discharge for CS coils is 11.5 s. It consists of time for quench detection, 2 s action time of switching procedure and 7.5 s for current discharge time constant [DDD06f]. For PF coils the equivalent time constant for fast discharge is 18 s, separated in time for quench detection, 2 s action time and 14 s for current discharge time constant [DDD06c]. Fig. 2-8 shows the schematic drawing of the fast discharge unit.

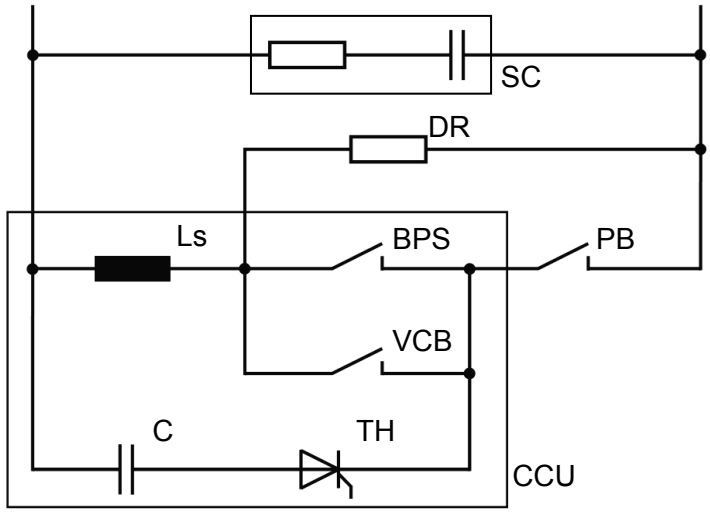

Fig. 2-8 Scheme of the fast discharge unit (FDU) derived from [PPSD1]

The FDU consists of the snubber circuit (SC), the discharge resistor (DR), the current commutation unit (CCU) and pyrobreaker (PB). The snubber circuit, which will limit the high frequency voltage oscillations caused by the FDU, consists of a resistor R = 0.15 Ω and a capacitor C = 0.35 mF [PPSA1a]. The current commutation unit commutates the current from the free wheeling path to a discharge resistor during the fast discharge of the coils. The CCU consists of bypass switch (BPS), the vacuum circuit breaker (VCB), the saturable inductor (Ls), the counterpulse capacitor (C) and the discharge thyristor switch (TH). The pyrobreaker (PB) will be used to switch the current to the DR if the CCU will not work correctly.

At the beginning of the fast discharge the power supply of the coils will be disconnected from the coil circuit and a free wheeling path for coil current will be created by a switch. Then the BPS will be opened and the coil current commutates to the parallel placed VCB. After the commutation is completed the VCB will be opened and an arc will appear inside the VCB for some ms. To erase the arc in the VCB the counterpulse capacitor will be discharged by the discharge thyristor. The counterpulse capacitor with capacity of 1.8 mF will be charged to a voltage of 7 kV [PPSA1a]. During the discharge of the capacitor the coil current through the VCB will be extinguished and then the coil current will commutate to the discharge resistor of the coil. The current commutation procedure to the discharge resistor is completed when the discharge resistor current reaches the same value as the coil current.

The saturable inductor (Ls) of the FDU is a non linear inductor depending on the current, which flows through the element. The saturable inductor is used to limit the current variation at low current values. The current dependence of the saturable inductor is shown in Tab. 2-6.

Current (A)	0	800	1200	1800	5000	20000
Inductance (μH)	156	110	77	39	10	2

Tab. 2-6 Current dependence of the saturable inductor for all FDUs [PPSA1b]

During the normal operation the BPS and VCB switched in parallel but the main current flows through BPS due to the 60 times higher resistance of the VCB. All relevant parameters of BPS, VCB and PB are taken from [PPS1], shown in Tab. 2-7.

	BPS	VCB	PB
Resistance at main contacts	1 μΩ	60 μΩ	10 μΩ
Opening time	230 ms	30 ms	0.2 ms
Continuous current	68 kA	3.5 kA	68 kA
Pulsed current (duration)	250 kA (0.1 s)	68 kA (0.4 s)	100 kA (1 s)

Tab. 2-7 Main parameters of the switching components of FDU [PPSA1b]

Due to the different values for energy stored in each coil the fast discharge resistors have different values to reach the time constant suggested for the coils. Data of fast discharge resistors are summarised in Tab. 2-8. Further data of the FDU components can be taken from [PPS1] and [PPSA1].

Coils	Max. FDU design energy (GJ)	Initial value of fast discharge resistor at 20 °C (Ω)	Maximum value for fast discharge resistor at 235 °C (Ω)
CS3U	1.01	0.090	0.212
CS2U	1.15	0.103	0.242
CS1U	1.14	0.102	0.240
CS1L	1.13	0.101	0.237
CS2L	1.15	0.103	0.242
CS3L	1.15	0.091	0.214
PF 1	1.03	0.046	0.108
PF 2	0.42	0.019	0.045
PF 3	1.80	0.080	0.188
PF 4	1.51	0.067	0.157
PF 5	1.59	0.071	0.167
PF 6	2.07	0.092	0.216

Tab. 2-8 Data of fast discharge resistors [PAF6Bb]

2.3.2 Switching Network Unit (SNU)

The resistors of the switching network unit provide the voltage, which is necessary for the breakdown and plasma initiation. They remain in the coil circuits during the ramp-up phase while the extraction of the stored energy continues. The relatively high breakdown voltage has to be provided at different currents between 40 % and 100 % of the nominal value. Therefore several resistor branches are switched in parallel to reach the required voltage, shown in Fig. 2-9.

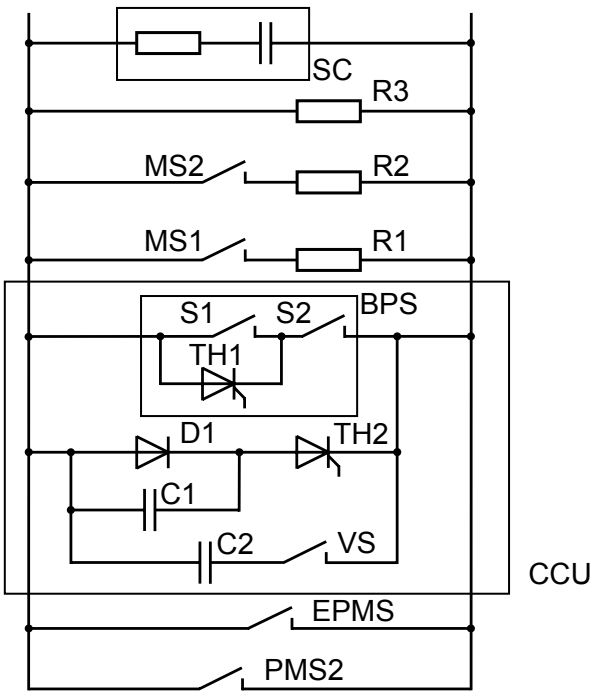

Fig. 2-9 Scheme of the switching network unit (SNU) derived from [PPSD1]

The current commutation unit (CCU) is needed to bypass the SNU during the charging of the coils. The CCU is designed for arc less commutation from BPS to the SNU resistors. The detailed function of the CCU is described in section 2.3.1. Additionally the CCU of SNU has two counterpulse capacitors (C1) and (C2) and a vacuum switch (VS). The C1 with 20 mF will be charged to 1 kV and C2 with 0.8 mF will be charged to 8 kV [PPSA1a]. The diode (D1) and thyristor (TH2) are summarised to thyristor circuit breaker (TCB). The explosively activated protective make switch (EPMS) is connected in parallel with the CCU. The snubber circuit (SC) is also placed in parallel to CCU and limits the high frequency voltage oscillations, caused by SNU. The components of SC are C with 0.1 mF and R with 0.2 Ω [PPSA1a]. The protective make switches (PMS1 and PMS2) are built with parallel BPS and VCB. PMS1 will be used to make the free wheeling circuit for coil current during the fast discharge (not shown in Fig. 2-9). The PMS2 will be used to bypass the SNU during the fast discharge. The fast make switches (MS) will be used to switch additional resistances parallel to achieve the required voltages during the plasma breakdown and ignition. All relevant data of the switches used in SNU are summarised in Tab. 2-9.

	BPS	TCB	MS	EPMS
Rated current (kA)	60	45 (for 10 ms)	60	68
Closing time (ms)	4.5	n/a	0.1	0.012
Resistance at main contacts (μΩ)	5	n/a	1	3

Tab. 2-9 Data of the switches used in switch network unit (SNU) [PPS1b]

The resistance network of the SNU consists of 9 modules switched in parallel to 3 module groups (R1, R2 and R3). The module group R3 is directly connected to the terminals. R1 and R2 can be switched with MS1 and MS2 in parallel to reduce the total resistance of SNU. The rated values for the resistor module for all CS coils and PF 1 is 10 Ω and for PF 6 13.6 Ω [PPS1b].

3 Finite Element Method CS and PF Models

The Finite Element Method (FEM) models will be described in this chapter. The simplified FEM model of the CS PF coil system is presented in section 3.1. The detailed FEM models of PF 3 and PF 6 coil are described in section 3.2 respectively 3.3.

3.1 Simplified Finite Element Method Model of the CS PF Coil System

For the models in Finite Element Method (FEM) program Maxwell2D [Max99], the rotational symmetry of the coil system was used to establish two dimensional models of the coils. First a simplified model of the CS PF coil system was established, which is shown in Fig. 3-1. The coils are shown as rectangles which have in cross section the outer dimensions of the coils. The positions of the coil centres and dimensions in Z- and R-directions were taken from [DDD06a] and are summarised in Tab. 2-1.

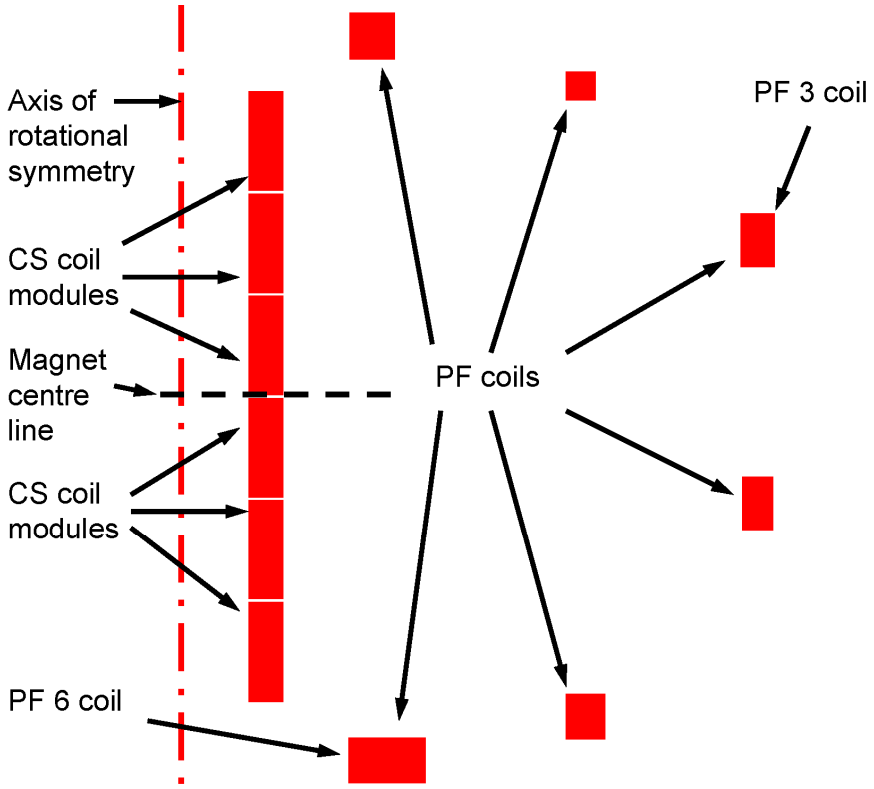

Fig. 3-1 Simplified FEM model of the CS PF coil system in Maxwell 2D

The self and mutual inductances of the simplified models of the coils were calculated with FEM program Maxwell 2D for DC. Copper was chosen as material for the rectangles which were equivalent to the cross section of the calculated coils. Vacuum was chosen as material for the space between the coils. Further the coil cross sections were defined as stranded conductor, which means that skin and proximity effects did not appear in the cross sections. The boundary of the model was set in Z-direction to ±30 m and in R-direction to 40 m. The boundaries were defined as magnetic neutral with magnetic zero potential which is infinitely far away from the model. The currents in the CS and PF coils were set to 45 kA. Triangular elements were used for the meshing of the model. Further information about the FEM model

of the CS PF coil system in Maxwell 2D are summarised in Annex A.1. As a calculation result the inductance for each cross section of the modelled coils was calculated. To obtain the results for the self inductance of the coils, the calculated value for inductance of the coil cross section have to be multiplied with the squared number of turns of the coil, calculated with formula (3.1).

$$L_C = w^2 \cdot L_{CS} \tag{3.1}$$

L_C : Inductance of the coil
w : Number of turns of the coil
L_{CS} : Inductance of the coil cross section calculated with FEM program

The calculated results for self inductances of CS and PF coils are summarised in Tab. 3-1. Due to the small coil diameter of CS coils compared with coil diameters of PF coils, the cross section of CS coil have relatively low inductance. But the CS coils have larger number of turns than the PF coils, thus the self inductance of the CS coils is higher than of the PF 1 and PF 2 coils, despite lower inductance of the cross section of the CS coil.

Coil Name	CS	PF 1	PF 2	PF 3	PF 4	PF 5	PF 6
FEM inductance of coil cross section (μH)	2.58	11.38	36.35	53.42	53.79	33.1	11.16
Number of turns	549	249	106	185	168	217	425
Calculated DC self inductance of the coil (H)	0.778	0.705	0.408	1.828	1.536	1.559	2.016

Tab. 3-1 FEM calculated DC values for self inductances with simplified CS and PF coil models

The mutual inductances between the coils were calculated first between the cross sections of the coils. The calculated values were multiplied one time with the number of turns of the first coil and one time with the number of turns of the second coil, calculated with formula (3.2). For example to calculate the mutual inductance between CS1U and PF 3 coil, the value for mutual inductance calculated by Maxwell 2D was multiplied with the number of turns of the CS1U and with the number of turns of the PF 3 coils.

$$M_{C1-C2} = w_{C1} \cdot w_{C2} \cdot M_{CS1-CS2} \tag{3.2}$$

M_{C1-C2} : Mutual inductance between coil 1 and coil 2
w_{C1} : Number of turns of coil1
w_{C2} : Number of turns of coil2
$M_{CS1-CS2}$: Mutual inductance between the cross section 1 and cross section 2

The calculated values for mutual DC inductances between CS and PF coils are given in Tab. 3-2 and Tab. 3-3.

	CS3U	CS2U	CS1U	CS1L	CS2L	CS3L
CS3U						
CS2U	0.241					
CS1U	0.052	0.241				
CS1L	0.018	0.052	0.241			
CS2L	0.008	0.018	0.052	0.241		
CS3L	0.004	0.008	0.018	0.052	0.241	
PF 1	0.136	0.061	0.028	0.014	0.008	0.005
PF 2	0.041	0.033	0.024	0.017	0.011	0.008
PF 3	0.048	0.050	0.048	0.042	0.034	0.027
PF 4	0.028	0.035	0.041	0.045	0.046	0.042
PF 5	0.015	0.022	0.033	0.048	0.066	0.081
PF 6	0.010	0.016	0.028	0.052	0.108	0.227

Tab. 3-2 Mutual DC inductance between the CS and PF coils (H)

	PF 1	PF 2	PF 3	PF 4	PF 5
PF 1					
PF 2	0.104				
PF 3	0.100	0.220			
PF 4	0.049	0.094	0.448		
PF 5	0.024	0.043	0.182	0.358	
PF 6	0.014	0.024	0.093	0.166	0.437

Tab. 3-3 Mutual DC inductance between the PF coils (H)

3.2 Detailed Finite Element Method Model of the PF 3 Coil

The establishing of the detailed Finite Element Method (FEM) model of the PF 3 coil at 4.5 K is described in this chapter. The dimensions and materials of the detailed FEM model of the PF 3 coil are shown in the first section. The results of the FEM calculation for the PF 3 coil are discussed in the second section.

3.2.1 Dimensions and Materials of the Detailed FEM Model of the PF 3 Coil at 4.5 K

For the calculation of the voltage stress within the coils the values for the elements of the network models have been calculated by the detailed FEM models of these coils. For each turn of the PF 3 coil the values for frequency dependent inductances were calculated with the detailed FEM model. The FEM models of the PF 3 coils consist of the cooling tube, the superconducting cable, the stainless steel jacket and the insulation shown in Fig. 3-2.

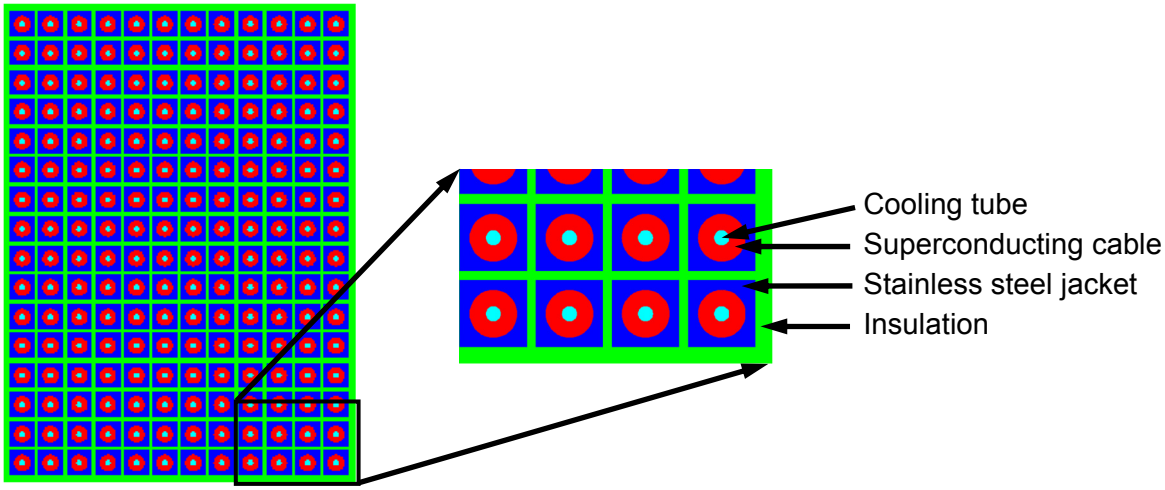

Fig. 3-2 Detailed FEM model of a cross section of the PF 3 coil in Maxwell 2D. The rotation axis (not shown in the figure) of the complete space is on the left side of the cross section. The zoomed area shows the outer lower corner of the PF 3 coil model

The outer diameter of the cooling tube is 12 mm. Liquid helium has a permittivity of $\varepsilon_r = 1.05$ [Fas70a] and a permeability of $\mu_r = 1$. Hence vacuum was selected as material instead of the definition of a new material in the FEM program. The thickness of the cooling tube wall and its metallic properties can be neglected for the calculations of inductances and capacitances because the cooling tube is placed inside the current leading superconducting cable and thus has no influence on the outer magnetic and electric fields of the conductor.

The superconducting cable of PF 3 coil consists of 864 superconducting strands, Tab. 2-2, thus the superconducting cable in FEM was defined as stranded conductor which means that the skin and proximity effects in the cable will not appear and thus the uniform current density at the whole cable cross section is defined. The copper with the conductivity of 6.4E9 S/m at 4.5 K [DRGAa] was chosen as the material for the superconducting cable in the FEM models. The superconducting cable has an outer diameter of 34.4 mm which means a contraction of -0.29 % [DDD06g] compared to room temperature dimensions of the cable [DDDD1] due to the cooling down at 4.5 K. The value of -0.29 % contraction is given for the

stainless steel jacket, because of the stranded structure of the superconducting cable the stainless steel jacket have strong influence on the cable dimensions at 4.5 K. The stainless steel protection wrap of 0.08 mm with 50 % overlapping [DDD06c], is used to protect the cable during the pull through processes through the stainless steel jacket. The thickness of the protection wrap was added to the stainless steel jacket in the FEM model of the PF 3 coil.

The stainless steel jacket will be used to give the superconducting cable mechanical stability during the manufacturing and operation of the coils. The outer dimensions of the jacket are 52.1 mm which means a contraction of -0.29 % compared to dimensions at room temperature which are given in Fig. 2-2. The conductivity of stainless steel was set to 1.88E6 S/m at 4.5 K which is given in [DRGAa].

The different kinds of insulation e. g. turn, layer and ground insulation were summarised to one insulation type because of the similar permittivity of about $\varepsilon_r = 4$ [DRG1a].

Each conductor has 3.2 mm conductor insulation. Further there is a turn insulation of 0.5 mm between two turns of the same pancake. Hence the total insulation between two turns in the same pancake is 6.9 mm. The insulation in Z-direction depends on the location of the conductors in the coil. The layer insulation in one double pancake is 1 mm, thus the total insulation between two layers in one double pancake is 7.4 mm. An additional insulation layer called bounding layer is placed between the double pancakes and has a thickness of 2 mm. The total insulation between the conductors of two different double pancakes is 9.4 mm [DDDD2].

The ground insulation of 8 mm and outer protection layer of 2 mm, which cover all conductors of the PF 3 coil, were summarised to an outer insulation with a thickness of 10 mm. The total dimensions of the PF 3 coil with ground insulation are 728 mm in R-direction and 986 mm in Z-direction. Compared with the values for coil dimensions which are given for 4.7 K with 708 mm and 966 mm without ground insulation in Tab. 2-1, there is additionally 10 mm of ground insulation on both sides of the coil which were considered in the detailed FEM model of the PF 3 coil.

The detailed FEM model of the PF 3 coil shown in Fig. 3-2 was used for FEM calculations at DC. With increasing frequencies of the FEM models two additional FEM models of the PF 3 coil were used because the models at higher frequencies need more memory but Maxwell2D can not manage more than 2 GB of the memory. At frequencies higher than DC and lower than 5 kHz a FEM model of the PF 3 coil with even line symmetry was used, which is shown in Fig. 3-3. Using of the even line symmetry in Maxwell 2D allows to draw only the upper half of the whole model. With the definition of the even line symmetry the lower part of the model will be considered at the calculations of the magnetic fields and also in the impedance matrix. The only difference between the FEM model shown in Fig. 3-2 and Fig. 3-3 is that the model in Fig. 3-3 is the half of the real PF 3 coil. All other dimensions of the coil remain the same.

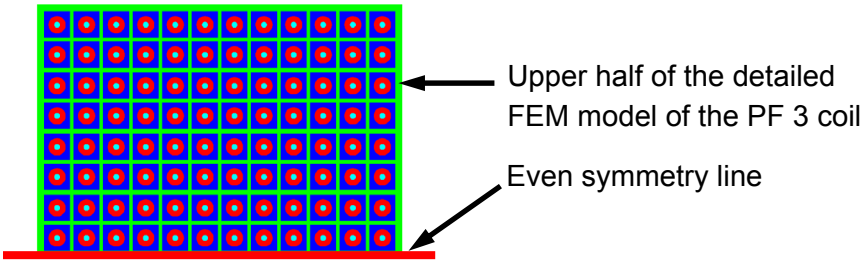

Fig. 3-3 FEM model of a cross section of the half of PF 3 coil with even line symmetry axis. The rotation axis is on the left side (not shown in the figure)

With the increasing frequency of the calculations the value for the inductance of the conductor is decreasing due to the higher currents which are induced in the stainless steel jacket of each conductor. The induction of the eddy currents in the stainless steel jacket means that both the self inductance of one conductor and the mutual inductance between two conductors are decreasing. For frequencies higher than 5 kHz the magnetic coupling between the conductors is lower than 1 % of the value for the self inductance of the conductor. Thus the mutual inductance between the conductors was neglected. For frequencies higher than 5 kHz the FEM model of only one pancake of the PF 3 coil was used, which is shown in Fig. 3-4.

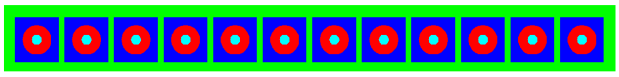

Fig. 3-4 FEM model of a cross section of one pancake of PF 3 coil

The dimensions of the conductors and insulation between them were the same like in the models in Fig. 3-2 and Fig. 3-3. The values for the inductance of each conductor in one pancake were calculated and were used for other pancakes.

3.2.2 Results of the FEM Calculations for Detailed Model of the PF 3 Coil

The detailed results of the FEM calculations of the PF 3 coil are summarised in Annex A.2. In this section only a part of the results will be shown to explain the different mechanisms of the frequency dependence of the inductances in PF 3 coil.

The inductance of a conductor is the factor which shows the connection between the current of the conductor and the magnetic energy which is stored in the space around and in the conductor, which is caused by this current. The self inductance of each conductor is the sum of the inner and the outer inductance of it. The inner inductance defines the connection between the current and the magnetic energy which is stored in the space which is in the conductor. The outer inductance is the connection between the current and the magnetic energy which is stored in the space around the conductor. The inner inductance of a conductor stays the same over the whole frequency range if the skin and proximity effects do not appear in this conductor. The superconducting cables used in PF coils consist of many thin filaments which have low dependence on skin and proximity effects. Thus the inner inductance of the superconducting cable stays the same over the relevant frequency range.

The outer inductance of the conductor depends on the design of the conductor and has strong frequency dependence for the PF coils. The eddy currents which are induced in the stainless steel jacket of the conductor decrease the magnetic field around the conductors and thus the magnetic energy which is used for calculation of the outer inductance. With increasing frequency the eddy currents in the stainless steel jacket are also increasing and thus the outer inductance of the conductor is decreasing. The frequency dependence of the self inductance of the upper left conductor (i. e. turn) is shown in Tab. 3-4. The upper left conductor has the number 1_1. The first number stands for the conductor number from the inner side of the coil, the second for the pancake number. So the next conductor in the same pancake has the number 2_1, the next one 3_1 and so on. The first left conductor of the next pancake has the number 1_2. The calculated values for the self inductance of the conductor were taken from the calculations which were made for the frequencies relevant for the calculation of resonance frequency of the PF 3 coil shown in chapter 5.

In Tab. 3-4 the strongest drop of self inductance is between DC and 0.42 kHz with the factor of 11.3. At 0.42 kHz the induced eddy currents in the stainless steel jacket which are weakening the outer magnetic field of the conductor are very strong compared to no eddy currents at DC. The value of the outer inductance is decreasing with increasing frequency and at 295 kHz only the inner inductance of the conductor is relevant for calculation of the self inductance.

Frequency (kHz)	0	0.42	9.5	20.7	200	295
Self inductance of the conductor 1_1 (H)	9.88e-05	8.68e-06	4.55e-06	4.03e-06	3.32e-06	3.26e-06
Relative factor to the self inductance of the conductor 1_1 at DC	1	0.088	0.046	0.041	0.034	0.033

Tab. 3-4 Frequency dependence of the self inductance of the upper left conductor of PF 3 coil shown for single frequencies which are relevant for calculation of the resonance frequency of the coil

The cable in conduit design of the PF coil conductor has also strong influence on the frequency dependence of the mutual inductance between the conductors shown in Tab. 3-5. The eddy currents which are induced in the stainless steel jacket of the conductors of the PF coils weaken the mutual inductance between the conductors. With increasing frequency the mutual inductance between two conductors is decreasing. The mutual inductance continues its strong decreasing also at very high frequencies compared to the self inductance of the conductor, which reaches a convergence value of inner inductance at a frequency of about 295 kHz.

Frequency (kHz)	0	0.42	9.5	20.7	200	295
Mutual inductance between the conductors 1_1 and 2_1 (H)	7.80e-05	1.35e-06	1.25e-09	4.75e-11	1.20e-18	2.22e-19
Coupling factor between the conductors 1_1 and 2_1	0.786	0.148	2.7e-04	1e-5	4e-18	7e-19

Tab. 3-5 Mutual inductance between the upper left conductors 1_1 and 2_1 of the PF 3 coil shown for single frequencies which are relevant for calculation of the resonance frequency of the coil

With increasing distance between the conductors their mutual inductance is decreasing. At DC this effect is lower, for example the mutual inductance between conductor 1_1 and 2_1 is 7.80e-05 H and between 1_1 and 12_1 is 4.43E-05 H, there is only a factor of 1.76 between these values. Selected mutual inductances between conductors of the upper pancake at DC are shown in Tab. 3-6. For frequency of 295 kHz the mutual inductance between conductor 1_1 and 2_1 is 2.22e-19 H and between 1_1 and 12_1 is only 7.55E-22 H, the factor between these values is 294. Selected mutual inductances between conductors of the upper pancake at 295 kHz are shown in Tab. 3-7.

	2_1	4_1	6_1	8_1	10_1	12_1
Mutual inductance to conductor 1_1 (H)	7.80E-05	6.23E-05	5.51E-05	5.04E-05	4.70E-05	4.43E-05
Coupling factor to conductor 1_1	0.786	0.625	0.55	0.5	0.46	0.43

Tab. 3-6 Selected mutual inductances and coupling factors between the conductors in the upper pancake of PF 3 coil at DC

	2_1	4_1	6_1	8_1	10_1	12_1
Mutual inductance to conductor 1_1 (H)	2.22E-19	4.16E-21	9.81E-22	1.42E-21	9.00E-22	7.55E-22
Coupling factor to conductor 1_1	7e-14	1e-15	3e-16	4e-16	2e-16	2e-16

Tab. 3-7 Selected mutual inductances and coupling factors between the conductors in the upper pancake of the PF 3 coil at 295 kHz

The cumulative inductance of each conductor was calculated by the summarising of all mutual inductances of a conductor to all other conductors of the PF 3 coil and addition of the self inductance of this conductor. The value for cumulative inductance for DC of the conductor 1_1 is 8.9e-3 H. This value is very high compared to the self inductance of the same conductor of 9.88e-05 H. This high cumulative inductance is the result of the high values of the mutual inductances between the conductors at DC shown in Tab. 3-6. With increasing frequency the value for mutual inductance decreases faster than for the self inductance shown in Tab. 3-4 and Tab. 3-5. Thus for frequencies higher than 5 kHz the mutual inductances between the conductors were neglected because their values were lower than 1 % of the self inductance and only self inductance of the conductors was take in to account. The frequency dependence of the cumulative inductance of the conductor 1_1 is shown in Tab. 3-8. The values for relevant frequencies of the cumulative inductance of each conductor of PF 3 coil are summarised in Annex A.2(d).

Frequency (kHz)	0	0.42	9.5	20.7	200	295
Cumulative inductance of conductor 1_1 (H)	8.90E-03	1.20E-05	4.55E-06	4.03E-06	3.32E-06	3.26E-06

Tab. 3-8 Frequency dependence of the cumulative inductance of the PF 3 conductor 1_1

The total inductance for the PF 3 coil, which was calculated with the detailed FEM model, was compared with the inductance of the PF 3 coil, which was calculated with the simplified model of CS PF coil system. The comparison was made for the total inductances at DC because the inductance calculation with the simplified model of the coil system was only made for DC. To calculate the total inductance of the detailed FEM model of PF 3 coil, all cumulative inductances of each conductor were summarised. The total inductance of the PF 3 coil calculated with detailed FEM model is 1.94 H. The total inductance of PF 3 coil calculated with simplified model of the CS PF coil system is 1.83 H. The difference between the results

is 5.6 %. Further the self inductance of the PF 3 coil was calculated with formula given in [Gro62] for DC. The value for self inductance calculated with this formula is 1.8 H. The relative difference to the value calculated by detailed FEM model of the PF 3 coil is 7.2 %. The relative difference to the inductance of the PF 3 coil calculated with simplified model of the CS PF coil system is 1.6 %.

3.3 Detailed Finite Element Method Model of the PF 6 Coil

The establishing of the detailed Finite Element Method (FEM) model of the PF 6 coil at 4.5 K is described in this chapter. The dimensions and materials of the detailed FEM model of the PF 6 coil are shown in the first section. The results of the FEM calculation for the PF 6 coil are discussed in the second section.

3.3.1 Dimensions and Materials of the Detailed FEM Model of the PF 6 Coil at 4.5 K

The calculations of the frequency dependent inductances for the PF 6 coil was made with the same strategy as for the PF 3 coil, despite of it, all relevant information for the establishing of the detailed model of the PF 6 coil are described in detail in this section.

For each conductor of the PF 6 coil the values for frequency dependent inductances were calculated with the detailed FEM model. The FEM models of the PF 6 coils consist of the cooling tube, the superconducting cable, the stainless steel jacket and the insulation shown in Fig. 3-5.

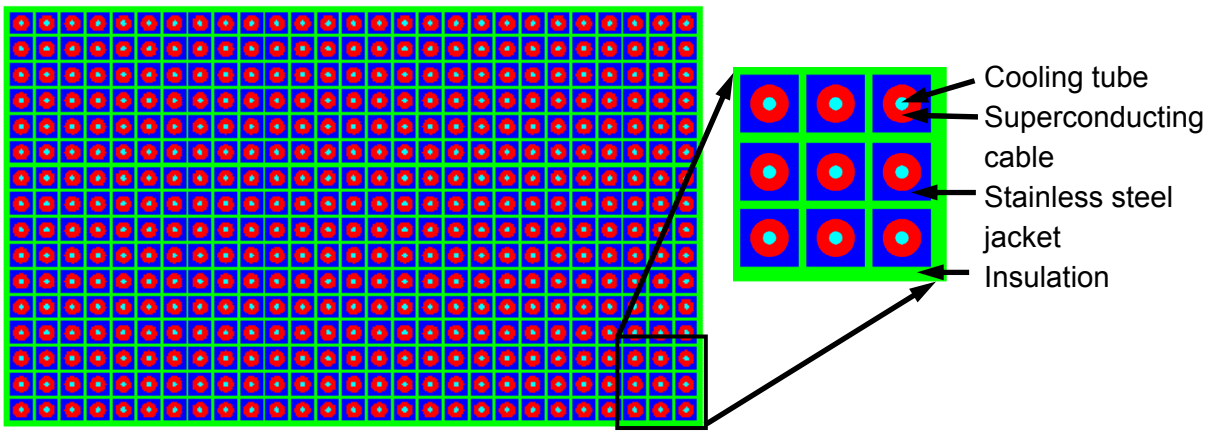

Fig. 3-5 Detailed FEM model of the cross section of the PF 6 coil in Maxwell 2D. The rotation axis (not shown in the figure) is on the left side of the cross section. The zoomed area shows the outer lower corner

The outer diameter of the cooling tube is 12 mm. Liquid helium has a permittivity of $\varepsilon_r = 1.05$ [Fas70a] and a permeability of $\mu_r = 1$. Hence vacuum was selected as material instead of the definition of a new material in the FEM program. The thickness of the cooling tube wall and its metallic properties can be neglected for the calculations of inductances and capacitances because the cooling tube is placed inside the current leading superconducting cable and thus has no influence on the outer magnetic and electric fields of the conductor.

The superconducting cable of PF 6 coil consists of 1440 superconducting strands, Tab. 2-2, thus the superconducting cable in FEM was defined as stranded conductor which means that the skin and proximity effects in the cable will not appear and thus the uniform current density is defined at the whole cable cross section. The copper with the conductivity of 6.4E9 S/m at 4.5 K [DRGAa] was chosen as the material for the superconducting cable in the FEM models. The superconducting cable has an outer diameter of 38.1 mm which means a

contraction of -0.29 % [DDD06g] compared to room temperature dimensions of the cable [DDDD1] due to the cooling down at 4.5 K. The value of -0.29 % contraction is specified for the stainless steel jacket, because of the stranded structure of the superconducting cable the stainless steel jacket have strong influence on the dimensions at 4.5 K. The stainless steel protection wrap of 0.08 mm with 50 % overlapping [DDD06c] is used to protect the cable during the pull through processes through the stainless steel jacket. The thickness of the protection wrap was added to the stainless steel jacket in the FEM model of the PF 6 coil.

The stainless steel jacket will be used to give the superconducting cable mechanical stability during the manufacturing and operation of the coils. The outer dimensions of the jacket are 53.6 mm which means a contraction of -0.29 % compared to dimensions at room temperature which are given in Fig. 2-2. The conductivity of stainless steel was set to 1.88E6 S/m at 4.5 K which is given in [DRGAa].

The different kinds of insulation e. g. turn, layer and ground insulation were summarised to one insulation type because of the similar permittivity of about $\varepsilon_r = 4$ [DRG1a].

Each conductor has 3.2 mm conductor insulation. Further there is a turn insulation of 0.5 mm between two turns in the same pancake of the coil. In the sum the total insulation between two turns in one pancake is 6.9 mm. The insulation in Z-direction depends on the location of the conductors in the coil. The layer insulation in one double pancake is 0.5 mm, thus the total insulation between two layers in one double pancake is 6.9 mm. An additional insulation layer called bounding layer is placed between the double pancakes and has a thickness of 1 mm. The total insulation between the conductors of two different double pancakes is 7.9 mm.

The ground insulation of 8 mm and outer protection layer of 2 mm which cover all conductors of the PF 6 coil were summarised to an outer insulation with a thickness of 10 mm. The total dimensions of the PF 6 coil with ground insulation are 996 mm in Z-direction and 1653 mm in R-direction. Compared with the values for coil dimensions which are specified for 4.7 K with 976 mm and 1633 mm without ground insulation in Tab. 2-1, there is additionally 10 mm of ground insulation on both sides of the coil which were considered in the detailed FEM model of the PF 6 coil.

The detailed FEM model of the PF 6 coil shown in Fig. 3-5 was used for FEM calculations at DC. With increasing frequencies of the FEM models two additional FEM models of the PF 6 coil were used because the models at higher frequencies need more memory but Maxwell2D can not mange more than 2 GB of the memory. At frequencies higher than DC and lower than 5 kHz a FEM model of the PF 6 coil with even line symmetry was used, which is shown in Fig. 3-6. Using of the even line symmetry in Maxwell 2D allows to draw only the upper half of the whole model. With the definition of the even line symmetry the lower part of the model will be considered at the calculations of the magnetic fields and also in the impedance matrix. The only difference between the FEM model shown in Fig. 3-5 and Fig. 3-6 is that the model in Fig. 3-6 is the half of the cross section of the PF 6 coil. All other dimensions of the coil remain the same.

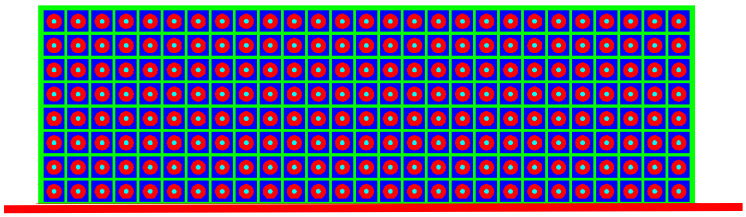

Fig. 3-6 Detailed FEM model of the half cross section of the PF 6 coil with line symmetry axis. The rotation axis is on the left side (not shown in the figure)

With the increasing frequency of the calculations the value for the inductance of the conductor is decreasing due to the higher currents which are induced in the stainless steel jacket of each conductor. The inducing of the eddy current in the stainless steel jacket means that both the self inductance of one conductor and the mutual inductance between two conductors is decreasing. For frequencies higher than 5 kHz the magnetic coupling between the conductors is lower than 1 % of the value for the self inductance of the conductor. Thus the mutual inductance between the conductors was neglected. For frequencies higher than 5 kHz the FEM model of only one pancake of the PF 6 coil were used, which is shown in Fig. 3-7.

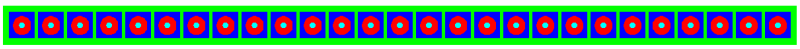

Fig. 3-7 FEM model of one pancake of PF 6 coil

The dimensions of the conductors and insulation were the same like in the models in Fig. 3-5 and Fig. 3-6. The values for the inductance of each conductor in one pancake were calculated and were used for other pancakes.

3.3.2 Results of the FEM calculations for detailed model of the PF 6 coil

The detailed results of the FEM calculations of the PF 6 coil are summarised in Annex A.3(d). In this section only a part of the results will be shown to explain the different mechanisms of the frequency dependence of the inductances in PF 6 coil.

The inner inductance of the conductor stays the same over the whole frequency range if the skin and proximity effects do not appear in the conductor. The superconducting cable has due to the multi filament design low influence of skin and proximity effects and thus no reduction of the inner inductance appears in the relevant frequency range. The eddy currents which are induced in the stainless steel jacket of the conductor decrease the magnetic field around the conductors and also decrease the magnetic energy which is used for calculation of the outer inductance. With increasing frequency the eddy currents in the stainless steel jacket are also increasing and thus the outer inductance of the conductor is decreasing. The frequency dependence of the self inductance of the upper left conductor (i. e. turn) with conductor number 1_1 is shown in Tab. 3-9. The values for the self inductance of the conductor were taken from the calculations which were made for the frequencies relevant for the calculation of resonance frequency of the PF 6 coil shown in chapter 5.

The strongest drop of self inductance is between DC and 0.5 kHz with the factor of 10.3. At 0.5 kHz the induced eddy currents in the stainless steel jacket which are weaken the outer magnetic field of the conductor are very strong compared to no eddy currents at DC. The value of the outer inductance is decreasing with increasing frequency and at 295 kHz only the inner inductance of the conductor is relevant for calculation of the self inductance.

Frequency (kHz)	0	0.5	12.9	28.6	200	295
Self inductance of the conductor 1_1 (H)	2.40e-05	2.34e-06	1.28e-06	1.16e-06	1.00e-06	9.88e-07
Relative factor to the self inductance of the conductor 1_1 at DC	1	0.098	0.05	0.048	0.042	0.041

Tab. 3-9 Frequency dependence of the self inductance of the upper inner conductor of PF 6 coil shown for single frequencies which are relevant for calculation of the resonance frequency of the PF 6 coil

The cable in conduit design of the PF coil conductor has also strong influence on the frequency dependence of the mutual inductance between the conductors shown in Tab. 3-10. The eddy currents which are induced in the stainless steel jacket of the conductors of the PF coils weakening the mutual inductance between the conductors. With increasing frequency the mutual inductance between two conductors is decreasing. The mutual inductance continues its strong decreasing also at very high frequencies compared to the self inductance of the conductor, which reaches a convergence value of inner inductance at frequency of about 295 kHz.

Frequency (kHz)	0	0.5	12.9	28.6	200	295
Mutual inductance between the conductors 1_1 and 2_1 (H)	1.82e-05	3.35e-07	2.07e-10	7.60e-12	3.73e-18	1.81e-20
Coupling factor between the conductors 1_1 and 2_1	0.76	0.14	1.6e-4	6e-6	4e-12	2e-14

Tab. 3-10 Mutual inductance between the upper inner conductors 1_1 and 2_1 of the PF 6 coil shown for single frequencies which are relevant for calculation of the resonance frequency

With increasing distance between the conductors the mutual inductance between them is decreasing. At DC this effect is lower, for example the mutual inductance between conductor 1_1 and 2_1 is 1.82E-05 H and between 1_1 and 27_1 is 5.84E-06 H with a factor of 3.1 between the values. Selected mutual inductances between conductors of the upper pancake at DC are shown in Tab. 3-11. For frequency of 295 kHz the mutual inductance between conductor 1_1 and 2_1 is 1.81E-20 H and between 1_1 and 27_1 is only 4.83E-22 H with a factor of 37 between the values. Selected mutual inductances between conductors of the upper pancake at 295 kHz are shown in Tab. 3-12.

	2_1	7_1	12_1	17_1	22_1	27_1
Mutual inductance to conductor 1_1 (H)	1.82E-05	1.09E-05	8.69E-06	7.39E-06	6.50E-06	5.84E-06
Coupling factor to conductor 1_1	0.76	0.45	0.36	0.31	0.27	0.24

Tab. 3-11 Selected mutual inductances and coupling factors between the conductors in upper pancake at DC

	2_1	7_1	12_1	17_1	22_1	27_1
Mutual inductance to conductor 1_1 (H)	1.81E-20	1.91E-23	7.47E-24	4.64E-24	3.14E-24	4.83E-22
Coupling factor to conductor 1_1	2e-14	2e-17	7e-18	5e-18	3e-18	5e-16

Tab. 3-12 Selected mutual inductances and coupling factors between the conductors in upper pancake at 295 kHz

The cumulative inductance of each conductor was calculated by the summarising of all mutual inductances of a conductor to all other conductors of the PF 6 coil and addition of the self inductance of this conductor. The value for cumulative inductance for DC of the conductor 1_1 is 3.29E-03 H, which is very high compared to the self inductance of the same conductor of 2.40e-05 H. This high value is the result of the high values of the mutual inductances between the conductors at DC shown before. With increasing frequency the value for mutual inductance decreases faster than for the self inductance shown in Tab. 3-9 and Tab. 3-10. Thus for frequencies higher than 5 kHz the mutual inductances between the conductors were neglected because their values were lower than 1 % of the self inductance and only self inductances of the conductors were taken in to account. The frequency dependence of the cumulative inductance of the conductor 1_1 is shown in Tab. 3-13. The values for relevant frequencies of the cumulative inductance for each conductor of PF 6 coil are summarised in Annex A.3(d).

Frequency (kHz)	0	0.5	12.9	28.6	200	295
Cumulative inductance of conductor 1_1 (H)	3.29E-03	2.81E-06	1.28E-06	1.16E-06	1.00E-06	9.88E-07

Tab. 3-13 Frequency dependence of the cumulative inductance of conductor 1_1 of PF 6 coil

The result of the calculation of the total inductance for the PF 6 coil, which was calculated with detailed FEM model, was compared with the inductance of the PF 6 coil, which was calculated with the simplified model of CS PF coil system. The comparison was made for total inductances at DC because the inductance calculation with the simplified model of the coil system was only made for DC. To calculate the total inductance of the detailed FEM model

of PF 6 coil, all cumulative inductances of each conductor were summarised. The total inductance of the PF 6 coil calculated with detailed FEM model is 2.06 H. The total inductance of PF 6 coil calculated with simplified model of the CS PF coil system is 2.016 H. The difference between the results was 2.1 %. Further the self inductance of the PF 6 coil was calculated with formula given in [Gro62] for DC. The value for self inductance calculated with this formula is 2 H. The relative difference to the inductance value calculated by detailed FEM model of the PF 6 coil is 2.9 %. The relative difference to the inductance of the PF 6 coil calculated with simplified model of the CS PF coil system is 0.8 %.

3.4 Finite Element Models of the Bus Bars for Power Supply

For the network model of the CS PF coil system the values for the resistances, inductances and capacitances to ground of the bus bars for the power supplies of the coils had to be calculated. These values were not given for superconducting bus bars in [DDD06] and [DDD01]. The values for the resistance of the water cooled bus bars in [PPSA1] are given with 2.97 mΩ/m, the inductance with 1 µH/m. This values were controlled by the FEM calculation of water cooled bus bars.

3.4.1 Superconducting Bus Bars

The superconducting bus bars will be used to connect the coil terminals with the Coil Terminal Box (CTB), which will be located outside of the vacuum vessel and the coil cryostat [DDD06i]. The FEM model of the cross section of a superconducting bus bar is shown in Fig. 3-8.

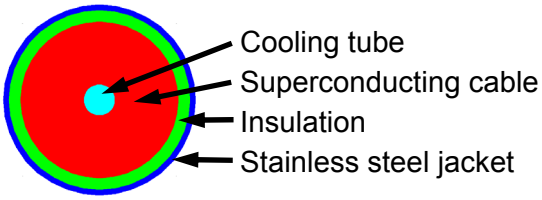

Fig. 3-8 FEM Model of the superconducting bus bar

Vacuum was used as the material for the cooling tube because of the similar magnetic properties as helium. The inner diameter of the cooling tube and its metallic structure was neglected for the FEM model of the superconducting bus bar, because the cooling tube is inside of the current leading superconducting cable and has no influence on its inductance and capacitance to the ground.

The cable of the superconducting bus bar which consists of 1800 superconducting filaments [DDD06h] was defined in the FEM model of the bus bar as stranded conductor. This means that in the cable the current density is uniform and the skin and proximity effects do not appear. Copper with conductivity of 6.4E9 S/m at 4.5 K [DRGAa] was defined as the material for the FEM model of the superconducting cable.

The insulation of the superconducting bus bars is made from polyimide film-glass impregnated with epoxy resin and has the same dielectric constant as the insulation of PF coils with $\varepsilon_r = 4$ [DRG1a]. The stainless steel jacket surrounding the cable was specified with the conductivity of 1.88E6 S/m at 4.5 K which is given in [DRGAa]. All relevant dimensions of superconducting bus bars are summarised in Tab. 3-14.

The results of the FEM calculation for the superconducting bus bars are summarised in Tab. 3-15. The resistance of the superconducting bus bars which was calculated by FEM model was ignored and was set to 1 pΩ/m, because the superconducting filaments of the bus bars have no electrical resistivity during the normal operation. The value of 1 pΩ/m was needed for the network model, because it does not work without any resistance in the circuit. To cal-

culate the inductance, resistance and capacitance to the ground these values will be multiplied with the length of bus bars for each coil of the system.

Bus bar dimension	Size
Cooling tube outer diameter	8 mm
Cable space diameter	41 mm
Conductor outer diameter	47 mm
Jacket thickness	3 mm

Tab. 3-14 Dimensions of the PF and CS superconducting bus bars taken from [DDD06h]

Inductance	1.4 µH/m
Capacitance to ground	1.79 nF/m

Tab. 3-15 Results of FEM calculation for superconducting bus bars

3.4.2 Water Cooled Bus Bars

Water cooled bus bars are needed as the connection of the FDU and SNU with the power supply of the coils. The FEM model of the cross section of the water cooled bus bar is shown in Fig. 3-9. The bus bar has a height of 106 mm and width of 200 mm. The diameter of the water cooling tubes is 20 mm. The location of their centre is 50 mm from the left and right side and 27 mm from the upper and lower side of the bus bar. These dimensions were taken from [PPSD2]. The material for the bus bar is aluminium with a conductivity of 3.3e7 S/m at continuous operation temperature of 60°C, which was derived from [DRGAb]. Because of the location inside the current leading bus bar the cooling tubes have no influence on the inductance and capacitance of the bus bar. For the cooling tubes vacuum was chosen as the material because the properties of the cooling liquid have no influence.

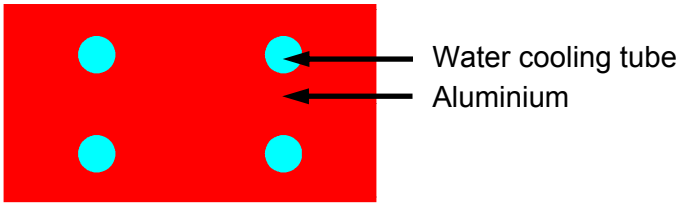

Fig. 3-9 FEM Model of the water cooled bus bar for power supply of the coils

The results of the FEM calculations are shown in Tab. 3-16. To calculate the inductance, resistance and capacitance to the ground these values will be multiplied with the length of bus bars for each coil of the system.

Inductance at DC	1.39 µH/m
Resistance at DC	1.39 µΩ/m
Capacitance to ground	13 pF/m
Capacitance to the parallel bus bar	35 pF/m

Tab. 3-16 Results of FEM calculation for water cooled bus bars

Compared to the values which are specified for the water cooled bus bars in [PPSA1] for the resistance 2.97 mΩ/m, the calculated value of the resistance with FEM is lower more than 2000 times. For the further calculations the calculated value for the resistance 1.39 µΩ/m was used. Compared to the value of the inductance of the water cooled bus bars which was given in [PPSA1] with 1 µH/m, the calculated value of 1.39 µH/m has a relative difference of 40 %. For the further calculations the calculated value for the inductance 1.39 µH/m was used.

3.5 Simplifications Used in the Finite Element Method Models

- The crossover of the conductors between the pancakes and double pancakes are ignored, the conductors have only rotational symmetry.

- The cooling tube with 10 mm inner and 12 mm outer diameter with its metallic properties was replaced with a tube with an outer diameter of 12 mm. Liquid helium has a permittivity of εr = 1.05 [Fas70a] and a permeability of μ_r = 1. Hence vacuum was selected as material instead of the definition of a new material in the FEM program.

- The superconducting cable of PF coils is made of up to 1440 superconducting strands, which means that the influence of skin and proximity effects in the cables is very low. Further the stranded and twisted design allows uniform current density in the whole cross section of the cable. To consider the cable design in the FEM model of the superconducting cable the cross section of the cable, excluding the cross section of the cooling tube, was defined as stranded copper conductor with a conductivity of 6.4E9 S/m at 4.5 K. Because of the stranded superconducting cable model no skin and proximity effects do appear in the cable. The jacket has still the skin and proximity effect.

- In the FEM model outer corners of the jacket are rectangular, which is in contradiction to the specified rounding of 3 mm radius.

- Several layers of insulation were summarised to one insulation layer with homogeneous permittivity of ε_r = 4 [DRG1a].

- At FEM calculations with frequencies higher than 5 kHz one layer FEM model of the coil was used to manage the memory problems of the Maxwell2D. The magnetic coupling between the conductors for these frequencies are lower than 1 % and can be neglected

- The sub cable have a 0.1 mm thin stainless steel wrap with 50 % coverage to allow the helium penetration [PAC1]. Further there is a stainless steel final cable wrap with total 0.2 mm thickness with 50 % overlapping for protection of the cable during the pull through the jacket. The superconducting cable and the stainless steel jacket were taken into model as separated and insulated parts. The stainless steel wrap were added to the stainless steel jacket in the detailed FEM models of the PF 3 and PF 6 coil.

- The value for the water cooled bus bars specified in [PPSA1] for the resistance 2.97 mΩ/m and the inductance 1 µH/m were not used in network models. Instead of them the FEM calculated values for resistance 1.39 µΩ/m and inductance 1.39 µH/m were used in further calculations.

4 Network Models of the CS and PF Coils

In this chapter the network models of the coils are described. The network model of the complete CS PF coil system with FDU, SNU and power supply is shown in section 4.1. The detailed network models of the PF 3 and PF 6 coils with and without instrumentation cables are described in section 4.2 and 4.3. The network calculations were made with the program PSpice [Orc07].

4.1 Network Model of the CS PF Coil System

The network model of the CS PF coil system will be used to calculate the voltage behaviour on the coil terminals for PF 3 and PF 6 coils. These calculated voltages will be used in detailed network models of the coils as excitation voltages and thus the voltage stress between each conductor of the PF 3 and PF 6 coils will be calculated. The settings of the network model of CS PF coil system are given in Annex B.1.

The network model of the CS PF coil system consists of the parts of the electrical circuits of the CS and PF coils which were shown in section 2.3 with simplifications which will be described in detail in this section and summarised in section 4.4.

The overview about the network models of all CS and PF coil circuits is shown in Fig. 4-1. Due to the high amount of parts in the network models of the CS PF coils system the overview figure can not be shown closer. The details of the circuits are shown in the following figures.

The circuits of the CS3U, CS2U, CS2L, CS3L, PF 1 and PF 6 coils are single coil electrical circuits which consist of power supply, SNU, FDU and the simplified network model of the coil. The coils CS1U and CS1L are switched in series in one electrical circuit, which consists of one power supply, two FDUs, two SNUs and the simplified network models of the CS1U and CS1L coils. The PF 2, PF 3, PF 4 and PF 5 coils are switched in parallel in one electrical circuit which consists of four power supplies, four FDUs and the simplified network models of the PF 2 – PF 5 coils. The magnetic coupling between all the coils which were calculated with the simplified FEM model of the CS PF coil system described in section 3.1 is also considered in the network model.

The coils in the CS PF coil system have partly different winding direction of the turns. The winding direction of the PF 2 – PF 5 coils is specified in [PAF6Ba]. The PF 2 and PF 3 coils have the same winding direction. The PF 4 and PF 5 coils have also the same winding direction, but different to PF 2 and PF 3 coils. The winding direction for other coils, PF 1, PF 6 and all CS coils, is not explicitly specified in the documentation. In [DDDD3] the winding direction of the CS coils, PF 3 and PF 6 coil is drawn for upper and lower pancake of the double pancake one and also in a side view of these coils. The winding direction of CS, PF 3 and PF 6 coils are the same in these drawings, thus the winding direction of PF 1 was assumed to be the same like PF 3 coil. Only PF 4 and PF 5 coils are winded in opposite direction to other PF and all CS coils.

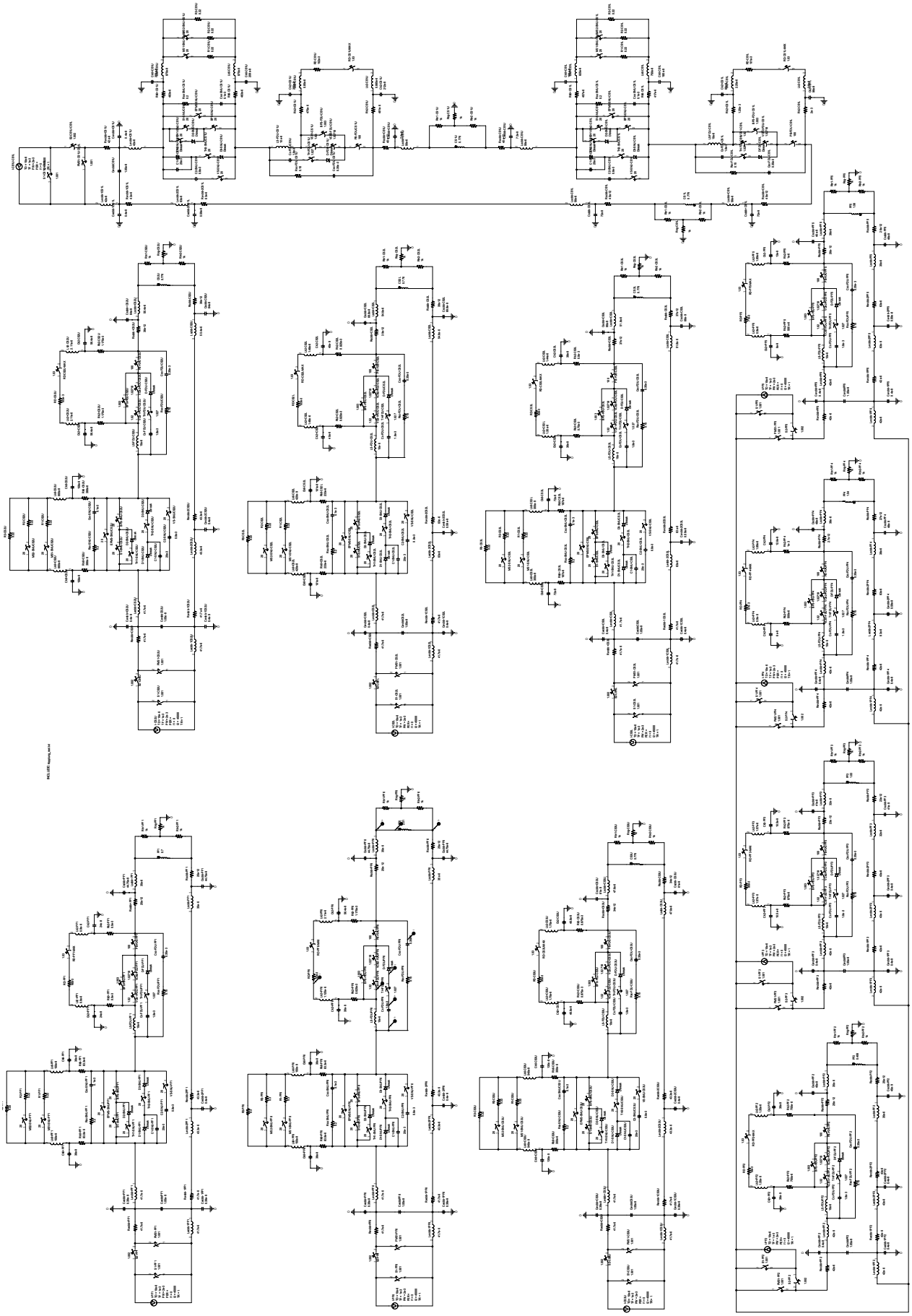

Fig. 4-1 Network models of the electrical circuits of the CS and PF coils

The detailed discussion of a network model of a coil circuit will be made exemplary with the PF 6 coil, which is shown in Fig. 4-2. To show the details of the network model, it was separated in four parts: the power supply, the switching network unit, the fast discharge unit and the simplified model of the PF 6 coil which are shown in detail in Fig. 4-3, Fig. 4-4, Fig. 4-5 and Fig. 4-6.

The power supply of the PF 6 coil which is shown in Fig. 4-3 consists of the current source I-PF6 which supplies the coil circuit with current up to 45 kA. The free wheeling switch of the power supply S1-PF6 will be closed before the fast discharge of the coil will be started. First the free wheeling path of the coil current will be made by the switch PMS1-PF6. The switch S2-PF6 will separate, 1 ms after the closing of the PMS1-PF6 and S1-PF6, the power supply from the coil circuit during the fast discharge. In the network model the switching times of these three switches were set to 1 µs. In reality the switching times are much slower but this has no relevance for the calculation of the coil voltages.

The connection of the power supply with the PF 6 coil and its SNU will be made with the water cooled bus bars, the FEM model of which is shown in section 3.4.2. With the calculated values for resistance with 1.39 µΩ/m, inductance with 1.39 µH/m, the capacitance to the ground with 13 pF/m and capacitance between the water cooled bus bars with 35 pF/m and with the distances between the CTB of the coil, the power supply and the SNU, the values for the water cooled bus bars were calculated for positive and negative polarity of the connections to the power supply. These distances were derived from [SLBD1] and [SLBa].

The bus bar with positive polarity was defined as the connection between the coil power supply and the SNU. Its length was estimated from site layouts ([SLBD1], [SLBa]) to 30 m for the PF 6 coil. The elements of the water cooled bus bar with positive polarity have the indexes “wcbb+PF6”. The bus bar with negative polarity was defined as the connection between the CTB of the coil and the coil power supply. Its total length was estimated to 75 m. The first part of the water cooled bus bars with negative polarity is placed parallel to the positive polarity for about 30 m. This distance is equal to the distance between SNU and power supply of the coils. The other part of the bus bar is placed between CTB and SNU and has only a bus bar in one direction for 31 m respectively 45 m, depending on the distance of the coil connection to the power supply. The elements of the water cooled bus bar with negative polarity which are placed in parallel to the bus bars with positive polarity have the indexes “wcbb-1PF6” and the part of the bus bars with negative polarity which have no parallel bus bar with positive polarity have the indexes “wcbb-2PF6”.

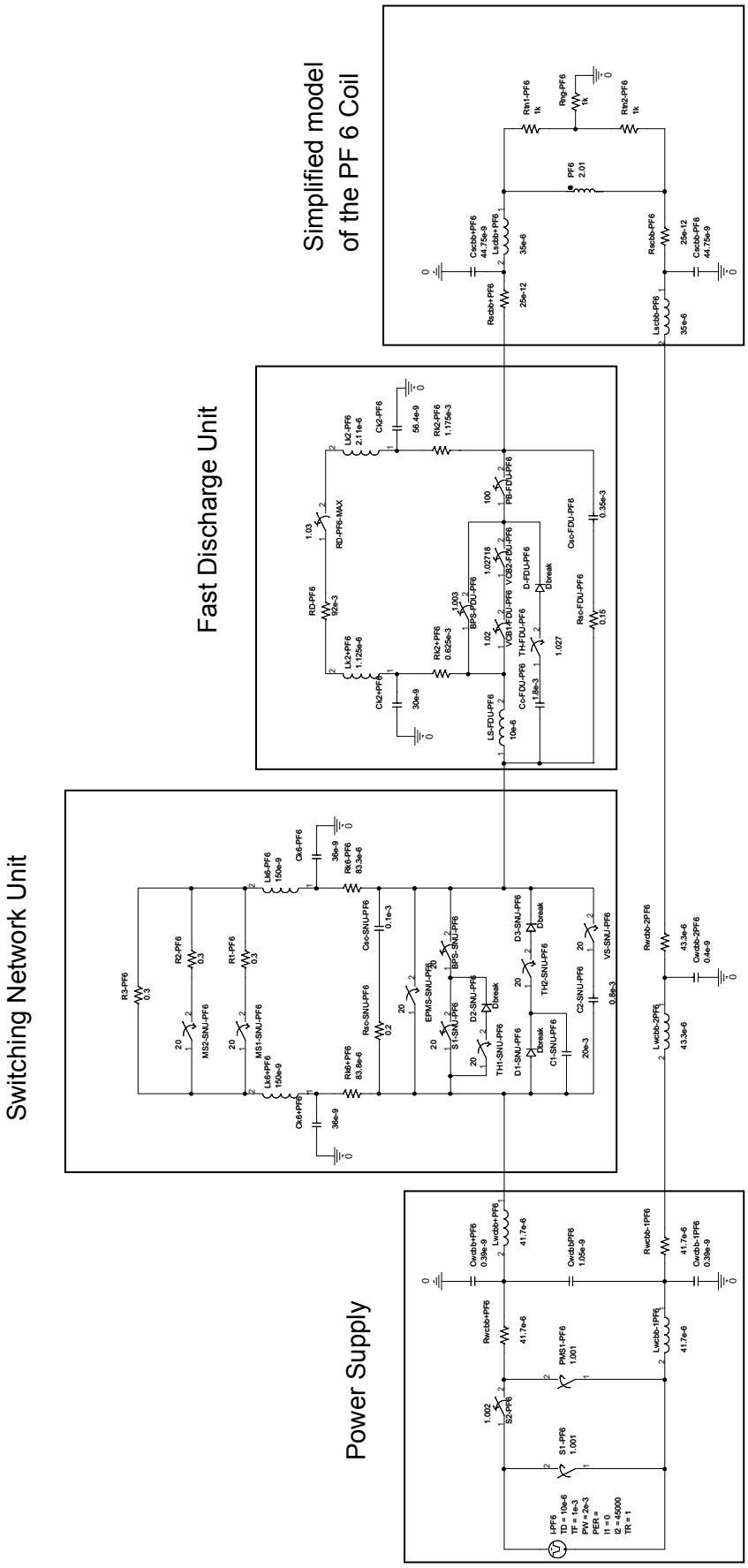

Fig. 4-2 Network model of the electrical circuit of the PF 6 coil with the parts which are shown in detail in Fig. 4-3, Fig. 4-4, Fig. 4-5 and Fig. 4-6

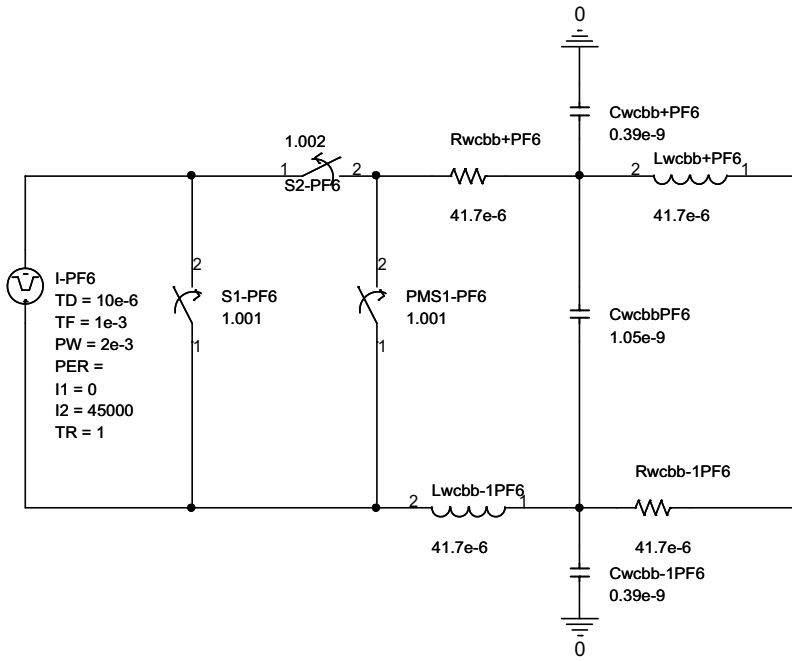

Fig. 4-3 Network model of the power supply of the PF 6 coil with water cooled bus bars

The length of the water cooled bus bars for all coils are summarised in Tab. 4-1 and Tab. 4-2. Because the parallel coils PF 2, PF 3, PF 4 and PF 5 have no SNU in their electrical circuits the power supplies of these coils are directly connected to FDUs. The values of the resistances, inductances and capacitances used for water cooled bus bars in the network model of the CS PF coil system are given in Tab. B.1-1 in Annex B.1.

Coil Name	Length of the connection from CTB to power supply	Length of the connection from power supply to SNU
CS3U	61 m	30 m
CS2U	61 m	30 m
CS1U	75 m	30 m
CS1L	75 m	30 m
CS2L	75 m	30 m
CS3L	75 m	30 m
PF 1	61 m	30 m
PF 6	61 m	30 m

Tab. 4-1 Length of the water cooled bus bars to SNU for CS, PF 1 and PF 6 coils derived from [SLBD1] and [SLBa]

Coil Name	Length of the connection from CTB to power supply	Length of the connection from power supply to FDU
PF 2	61 m	30 m
PF 3	61 m	30 m
PF 4	75 m	30 m
PF 5	75 m	30 m

Tab. 4-2 Length of the water cooled bus bars to FDU for PF 2, PF 3, PF 4 and PF 5 coils derived from [SLBD1] and [SLBa]

The network model of the SNU of the PF 6 coil is shown in Fig. 4-4. The values for the elements of the SNU were taken from section 2.3.2 and established in the network model. The switching network resistors R1-PF6, R2-PF6 and R3-PF6 have all the same resistance value. The task of the switching network resistors is to deliver 10 kV voltages for ignition of the plasma at different currents through the coils [PAF6Bc]. To achieve this task the resistances R1-PF6 and R2-PF6 can be switched in and off from the SNU circuit by the main switches MS1-SNU-PF6 and MS2-SNU-PF6.

The power cables are used for the connection between the switching unit and the switching network resistors (SNR). These cables are made from copper with a cross section of 800 mm². The element values for one cable are taken from [Bar05]. The capacitance to ground is 0.6 nF/m, the inductance of one cable is 90 nH/m and the resistance is 50 µΩ/m. For connection of switching unit to SNR six parallel cables will be used because of the high currents which will flow to the SNR during the normal operation scenarios. The lengths of the connection with power cables between the SNU and SNR are given in Tab. 4-3. The values for the cables for the connection between SNU and SNR are given in Tab. B.1-2 in Annex B.1.

The snubber circuit which consists of a resistance Rsc-SNU-PF6 = 0.2 Ω and a capacitance Csc-SNU-PF6 = 0.1 mF will limit the high frequency voltage oscillations which will be caused by switching of the SNU. The explosively activated protective make switch EPMS-SNU-PF6 will be used to make the free wheeling path for the current and to bridge the SNU if other current switches are disabled.

The current will flow at the normal operation through the switch S1-SNU-PF6 and the bypass switch BPS-SNU-PF6. The switch TH1-SNU-PF6 will be used to make the free wheeling current path and to bridge the SNU during the normal operation. The diode D2-SNU-PF6 together with the switch TH1-SNU-PF6 is used to simulate the function of a thyristor, which will be used. The diode D1-SNU-PF6 will be used to limit the current flow to one direction. The capacitor C1-SNU-PF6 = 20mF is charged to a voltage of 1 kV. The switch TH2-SNU-PF6 and the diode D3-SNU-PF6 simulate the thyristor which will be used to discharge the C1-SNU-PF6 and thus make the current free opening of the BPS-SNU-PF6. The capacitor C2-SNU-PF6 = 0.8 mF is charged to a voltage of 8 kV. The vacuum switch VS-SNU-PF6 will be

used to discharge the C2-SNU-PF6 and to support the current less opening of the BPS-SNU-PF6.

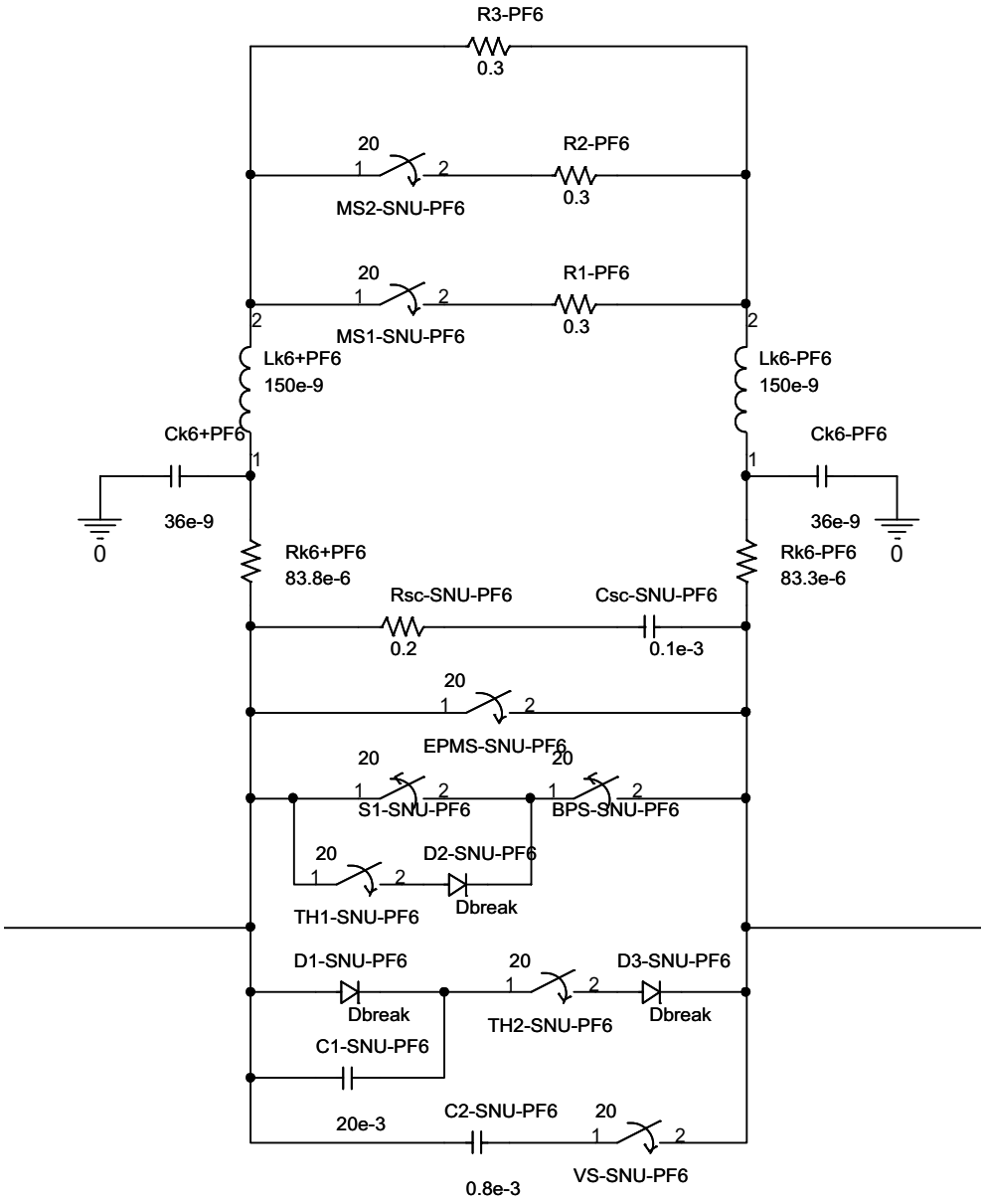

Fig. 4-4 Network model of the SNU of the PF 6 coil

The FDU will be used to commutate the current to the fast discharge resistor (FDR) during the fast discharge of the coils. The network model of the FDU of the PF 6 coil is shown in Fig. 4-5. The fast discharge resistor of the PF 6 coil RD-FDU-PF6 has an initial value of 92 mΩ. During the fast discharge the value of the resistance is increasing due to the heating up of the resistor to 216 mΩ. This process is simulated with an additional switch RD-PF6-MAX. Its initial resistance is set to 1e-12 Ω. During the closing time the value of the resistance of the PD-PF6-MAX is increasing and reaches its maximum of 124 mΩ. The closing time of PD-PF6-MAX is selected to 13 s which corresponds to the equivalent discharge time constant of the PF 6 coil.

The power cables which were used for connection from FDU to Fast Discharge Resistor (FDR) are made of copper with a cross section of 800 mm^2. The values for one cable were taken from [Bar05]. The capacitance to ground is 0.6 nF/m, the inductance of one cable is 90 nH/m and the resistance is 50 µΩ/m. For the connection of FDU with FDR only two parallel cables were used because the currents to FDR will flow only during the fast discharge process. The lengths of the connection of power cables between FDU and FDR are summarised in Tab. 4-3. The values for the resistances, inductances and capacitances of the cables for the connection between FDU and FDR are given in Tab. B.1-3 in Annex B.1.

The switch BPS-FDU-PF6 will simulate the BPS of the FDU with the same switching times and resistances like the real BPS. The switches VCB1-FDU-PF6 and VCB2-FDU-PF6 will simulate the vacuum circuit breaker. The VCB1-FDU-PF6 will simulate the arcing in a real VCB of the FDU before the extinguishing of the arc starts. The VCB2-FDU-PF6 will simulate the extinguishing of the arc in a real VCB. The pyrobreaker PB-FDU-PF6 will commutate the current in case of the failure when the VCB does not work properly. The circuit with the capacitance Cc-FDU-PF6 = 1.8 mF which is charged to a voltage of 7 kV, the switch TH-FDU-PF6 and the diode D-FDU-PF6 will be used to extinguish the arc in the VCB by discharging of the capacitor. TH-FDU-PF6 and D-FDU-PF6 will simulate the real thyristor of the circuit. The switching time of TH-FDU-PF6 was set to 2 µs [Dat1]. The snubber circuit which consists of a resistance Rsc-FDU-PF6 = 0.15 Ω and a capacitance Csc-FDU-PF6 = 0.35 mF will limit the high frequency voltage oscillations which will be caused by switching of the FDU.

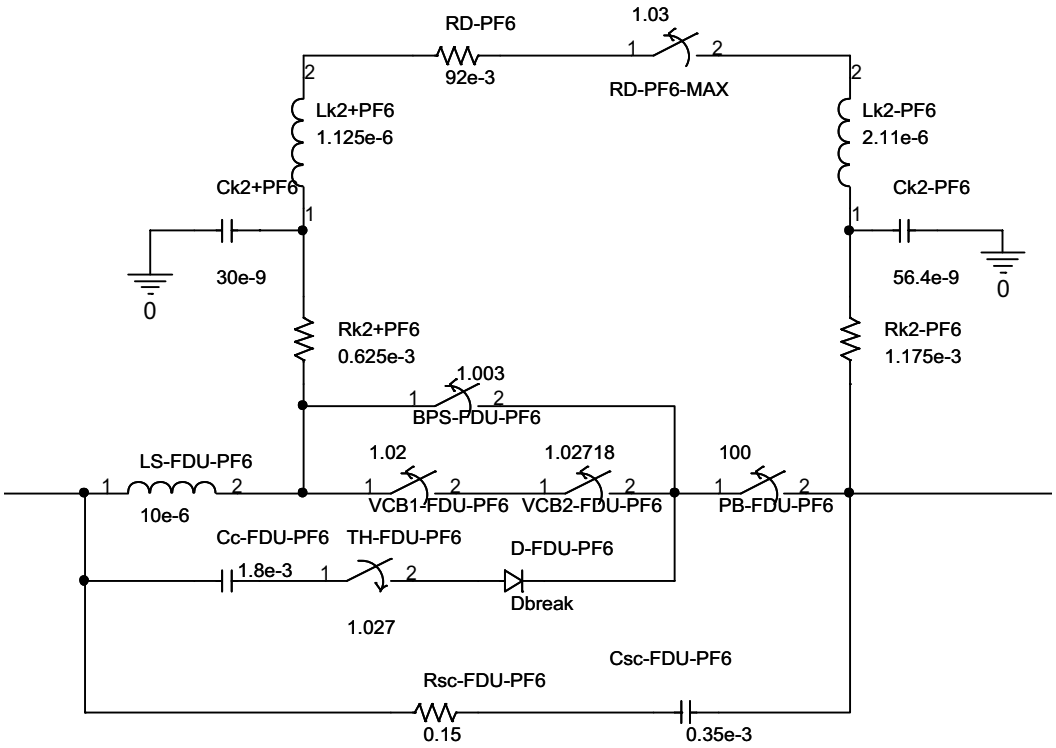

Fig. 4-5 Network model of the FDU of the PF 6 coil

The network model with simplified PF 6 coil, the superconducting bus bars and symmetrical grounding of the coil is shown in Fig. 4-6. The connection of the CTB with the PF 6 coil will be made with the superconducting bus bars, the FEM model of which is shown in section

3.4.1. To simulate the superconductivity of the filaments the resistance of the superconducting bus bars was set to 1 pΩ/m. With the calculated values for inductance 1.4 µH/m and the capacitance 1.79 nF/m and with the distances between the CTB and the coil which were derived from [SLBD1] and [SLBa], the values for the superconducting bus bars were calculated for positive and negative polarity of the connections of PF 6 coil, which have the same distance of 25 m. The elements of the positive polarity of the superconducting bus bar have the indexes “scbb+PF6”. The elements of the negative polarity of the water cooled bus bar have the indexes “scbb-PF6”. The lengths of the connections with superconducting bus bars between the CTB and the coil terminals are given in Tab. 4-3. The values for inductances and capacitances of the superconducting bus bars for the connection between CTB and the coil terminals are given in Tab. B.1-4 in Annex B.1. The symmetrical grounding of the coil [PAF6Bd] will be made with two identical terminal to neutral resistances Rtn1-PF6 and Rtn2-PF6 and the neutral to ground resistance Rng-PF6 with values of 1 kΩ each.

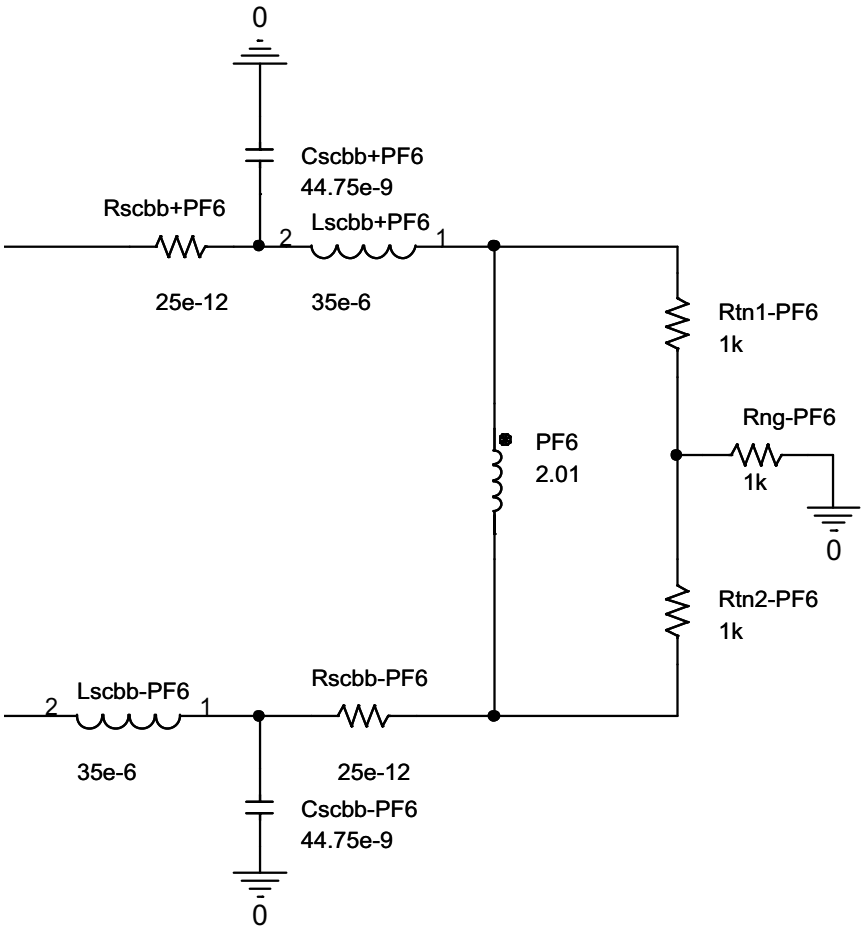

Fig. 4-6 Network model of the simplified PF 6 coil with superconducting bus bars and symmetrical grounding

Coil Name	Distance from SNU to SNR with 6 parallel power cables	Distance from SNR to FDU with 6 parallel power cables	Distance from FDU to FDR with 2 parallel power cables	Distance from FDR to CTB with 2 parallel power cables	Distance from CTB to coil with superconducting bus bars
CS3U	36 m	36 m	39 m	39 m	34 m
CS2U	44 m	44 m	47 m	47 m	36 m
CS1U	58 m	58 m	19 m	20 m	40 m
CS1L	55 m	50 m	50 m	80 m	40 m
CS2L	28 m	28 m	33 m	33 m	39 m
CS3L	20 m	20 m	30 m	32 m	37 m
PF 1	10 m	10 m	20 m	20 m	25 m
PF 2	-	-	30 m	30 m	25 m
PF 3	-	-	35 m	35 m	23 m
PF 4	-	-	20 m	40 m	27 m
PF 5	-	-	20 m	40 m	26 m
PF 6	10 m	10 m	25 m	47 m	25 m

Tab. 4-3 Distances for superconducting bus bars and power cables for SNU and FDU derived from [SLBD1] and [SLBa]

4.2 Detailed Network Model of the PF 3 Coil

The detailed network models of the PF 3 coil will be described in this chapter. The detailed network model of the PF 3 coil without instrumentation cables will be discussed in the first section. The influence of the instrumentation cables will be described in the second section.

4.2.1 Detailed Network Model of the PF 3 Coil without Instrumentation Cable

The detailed network models of the PF 3 coil were used to calculate the resonance frequency of the coil and also will be used for calculation of voltage stress between the conductors of the PF 3 coil during the normal operation, fast discharge and failure cases. The network program settings of the detailed network model of the PF 3 coil are given in Annex B.2. The values for inductances, which were calculated with detailed FEM models of the PF 3 coil shown in section 3.2, were taken into the network model as lumped elements. The calculation of the values for the capacitances of the PF 3 coil between the conductors and the outer conductors to ground was made with formulas (4.1) and (4.2).

Cylinder capacitor:

$$C_{cyl} = 2\pi\varepsilon_0\varepsilon_r \frac{l_c}{\ln(r_a / r_i)} \tag{4.1}$$

Parallel plate capacitor:

$$C_{pp} = \pi\varepsilon_0\varepsilon_r \frac{r_a - r_i}{d} \tag{4.2}$$

l_c = Height of the cylinder capacitor; r_a = Outer radius of the capacitor;
d = Distance between the plates of the capacitor; r_i = Inner radius of the capacitor.

The values for capacitances between the conductors of one pancake vary between 19.7 nF and 20.7 nF, depending on the location of the conductors. The capacitances between the conductors of two pancakes in one double pancake vary from 18 nF to 19.3 nF. The capacitances between the conductors of two different double pancakes vary between 14 nF and 15 nF. The capacitances of the outer conductors to the ground vary between 9.6 nF and 20.5 nF. The detailed results of the calculations of the capacitances are given in Annex A.2(d).

The resistances of the conductors were set to 1e-12 Ω because of the superconducting cable which will be used in the coils. The overview about the detailed network model of the PF 3 coil is shown in Fig. 4-7. The zoomed right upper part of the network model is shown in Fig. 4-8.

The designations for the elements were given at following scheme: First letter is the element type, e. g. R for resistance. Next is the number of the pancake separated with an underline, e. g. P01. If the designation is given for an element which is placed between two pancakes, than the number of the second pancake is also given separated by an underline, e. g.

P01_02. Next is the number of the conductor (i. e. turn) separated by underline, e. g. C01. If the designation is given for an element which is placed between two conductors the number of the second conductor is also given separated by an underline, e. g. C10_12. For example the capacitance between conductor 10 and 11 of the pancake 01 has the designation C_P01_C10_11. The capacitance of the conductor 12 between the pancake 01 and 02 has the designation C_P01_02_C12. For the outer conductors the capacitors to ground have an E which is placed between the pancake and conductor number, e. g. C_P01_E_C12 in Fig. 4-8.

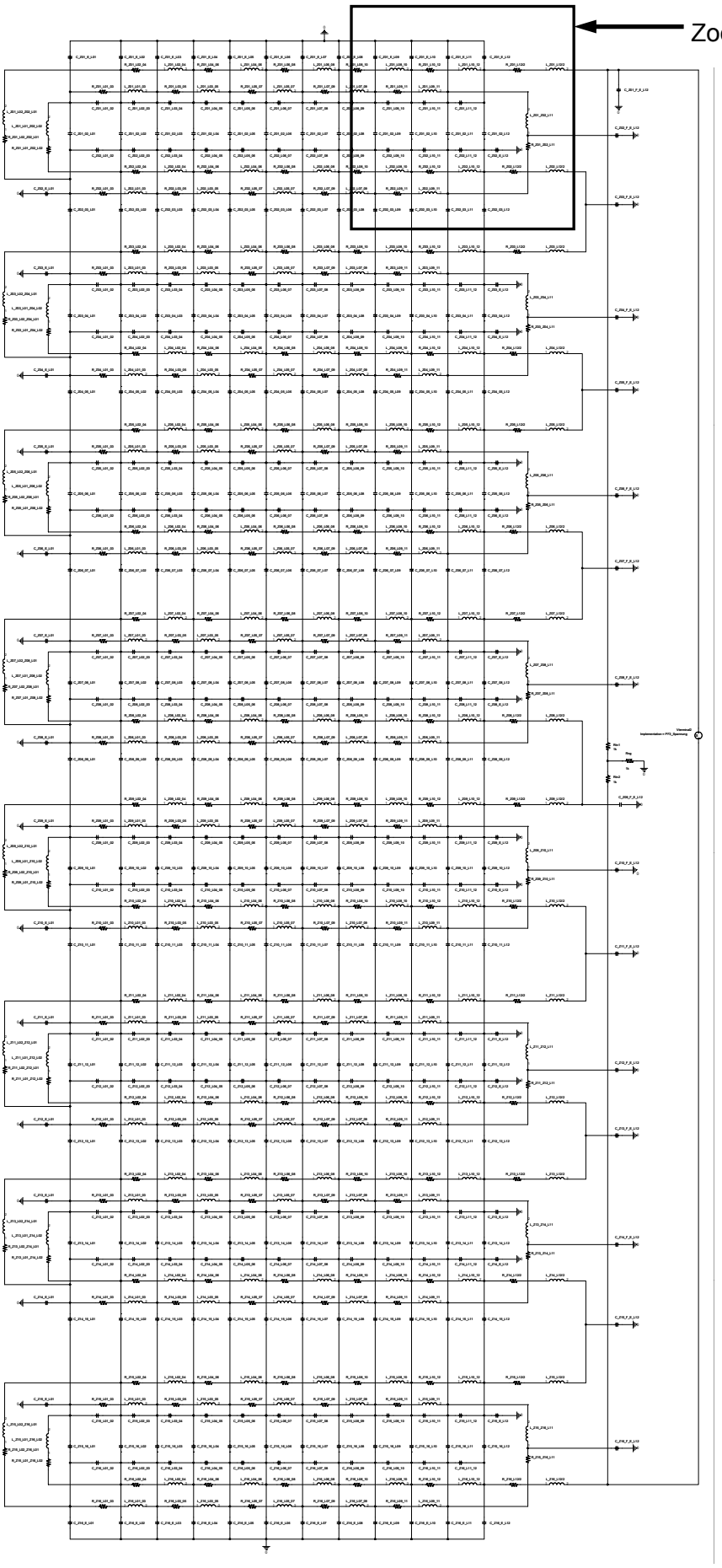

Fig. 4-7 Detailed network model of the PF 3 coil

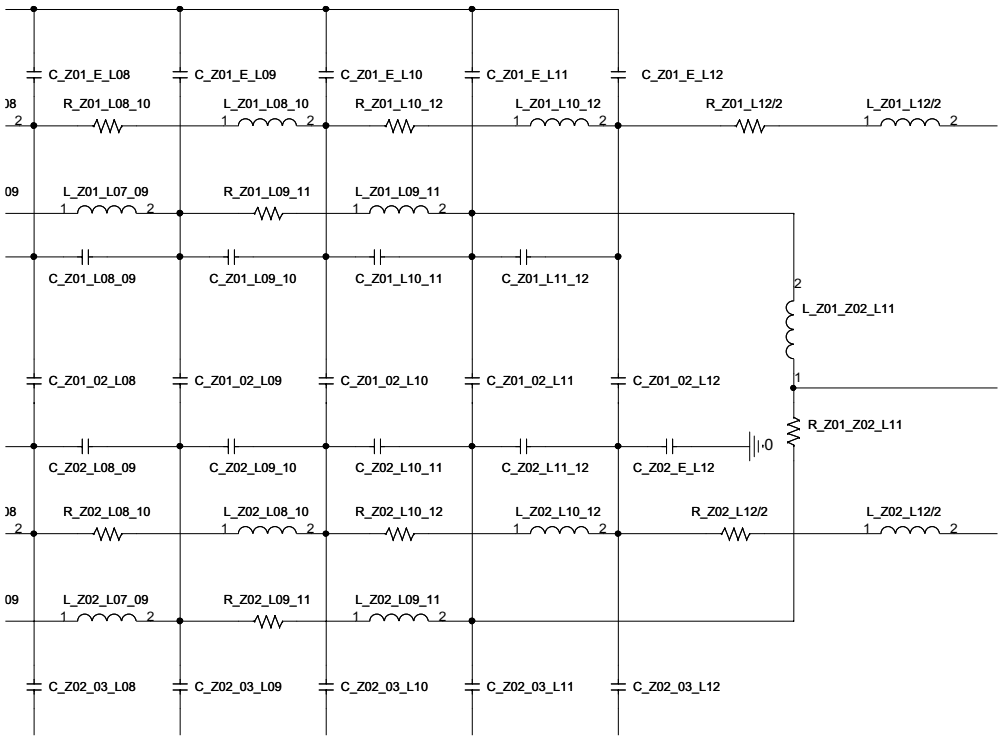

Fig. 4-8 Zoomed right upper part of the detailed network model of the PF 3 coil

The coil terminals are on the right side of the PF 3 network model. The numbers for the conductors were given from left to the right, thus the connection of the voltage source is placed on the winding with the greatest number for conductor P01_C12. Due to the large dimensions of the windings all inductances and resistances of each conductor were separated in two parts. The number of the conductor was placed between these two parts, e.g. P01_C12 in Fig. 4-8. This point was also the connection for the capacitor to the neighbouring conductors and for the capacitors to the ground.

The values for the conductors at the beginning and the end of a double pancake stay with the values divided by two, e. g. R_P01_C12/2 and L_P01_C12/2 in Fig. 4-8. The resistance and inductance values for other conductors were summarised because of the switching in series of two resistances and two inductances, e. g. R_P01_C12/2 and R_P01_C10/2 were summarised to R_P01_C10_12; L_P01_C12/2 and L_P01_C10/2 were summarised to L_P01_C10_12. Thus the number of the elements of resistances and inductances could be reduced by a factor of nearly two.

The detailed network model of the PF 3 coil was used for calculation in frequency domain and in time domain. In the frequency domain the resonance frequency of the coil was calculated. In time domain the voltage stress between the conductors will be calculated.

4.2.2 Detailed Network Model of the PF 3 Coil with Instrumentation Cables

The influence of the instrumentation cables on the resonance frequency and the voltage distribution within the PF 3 coil was analysed by consideration of the instrumentation cables in the detailed network model. The instrumentation cables will be placed on the joints between the double pancakes but the type of cables is not exactly defined in [CDA3]. Thus it was calculated with the same instrumentation cable type [Bau98] which was used for the ITER TF Model Coil (TFMC) [Ulb05]. The capacitance of these cables was calculated to 437 pF/m. The cables were taken into the network model as additionally capacitances on the double pancake joints. The designation “IC” was used for the capacitances of the instrumentation cables. The length of the instrumentation cables were derived from [CDA3] and [DDDD4]. The values for the length of the cables and their capacitances are summarised in Tab. 4-4.

	Length (m)	Capacitance (nF)
C_IC_E_P01	53	23
C_IC_E_P02_P03	45	19.6
C_IC_E_P04_P05	62	27
C_IC_E_P06_P07	45	19.6
C_IC_E_P08_P09	32	14
C_IC_E_P10_P11	46	20
C_IC_E_P12_P13	62	27
C_IC_E_P14_P15	46	20
C_IC_E_P16	60	26

Tab. 4-4 Length and capacitance values for the instrumentation cables of the PF 3 coil

4.3 Detailed Network Model of the PF 6 Coil

In this chapter the detailed network models of the PF 6 coil will be described. The detailed network model of the PF 6 coil without instrumentation cables will be discussed in the first section. The influence of the instrumentation cables will be specified in the second section.

4.3.1 Detailed Network Model of the PF 6 Coil without Instrumentation Cable

The detailed network models of the PF 6 coil were used to calculate the resonance frequency of the coil and also will be used for calculation of voltage stress between the conductors of the PF 6 coil during the normal operation, fast discharge and failure cases. The network program settings of the detailed network model of the PF 6 coil are given in Annex B.3. The values for inductances, which were calculated with detailed FEM models of the PF 3 coil shown in section 3.3, were taken into the network model as lumped elements. The calculation of the values for the capacitances of the PF 6 coil between the conductors and the outer conductors to ground was made with formulas (4.1) and (4.2) with the procedure which was described in section 4.2.

The values for capacitances between the conductors of one pancake vary between 6.1 nF and 8.7 nF, depending on the location of the conductors. The capacitances between the conductors of two pancakes in one double pancake vary from 5.8 nF to 8.5 nF. The capacitances between the conductors of two different double pancakes vary between 5.1 nF and 7.4 nF. The capacitances of the outer conductors to the ground vary between 3.1 nF and 8.9 nF. The detailed results of the calculations of the capacitances are given in Annex A.3(d).

The resistances of the conductors were set to 1e-12 Ω because of the superconducting cable which will be used in the coils. The overview about the detailed network model of the PF 6 coil is shown in Fig. 4-9. The zoomed right upper part of the network model is shown in Fig. 4-10.

The designations for the elements were given at following scheme: First letter is the element type, e. g. R for resistance. Next is the number of the pancake separated with an underline, e. g. P01. If the designation is given for an element which is placed between two pancakes, than the number of the second pancake is also given separated by an underline, e. g. P01_02 or P10_11. Next is the number of the conductor separated by underline, e. g. C01. If the designation is given for an element which is placed between two conductors the number of the second conductor is also given separated by an underline, e. g. C25_26. For example the capacitance between conductor 25 and 26 of the pancake 01 has the designation C_P01_C25_26. The capacitance of the conductors 27 between the pancake 01 and 02 has the designation C_P01_02_C27. The capacitors to ground of the outer conductors have an E which is placed between the pancake and conductor number, e. g. C_P01_E_C27 in Fig. 4-10.

The detailed network model of the PF 6 coil was used for calculation in frequency domain and in time domain. In the frequency domain the resonance frequency of the coil was calculated. In time domain the voltage stress between the conductors will be calculated.

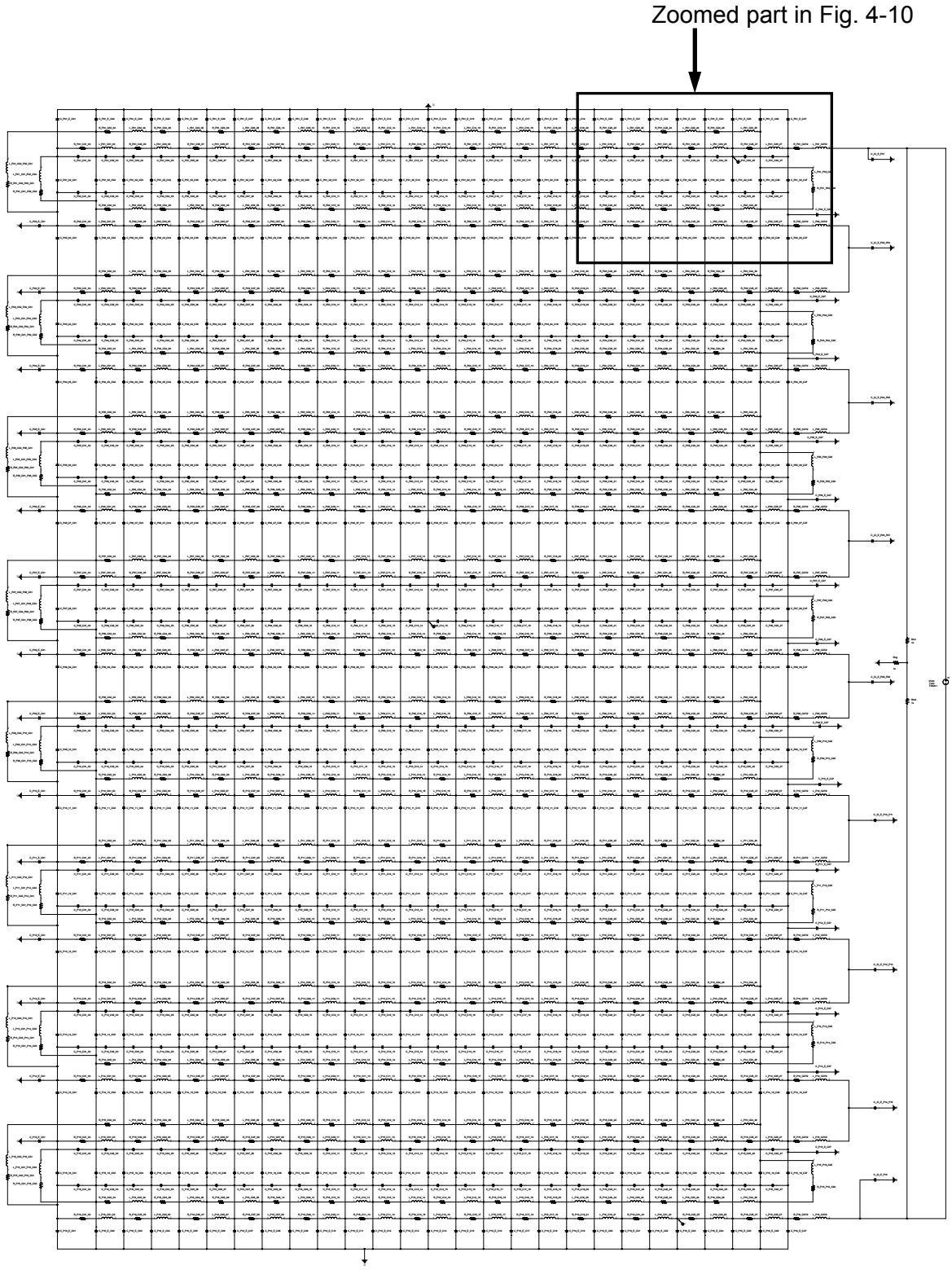

Fig. 4-9 Detailed network model of the PF 6 coil

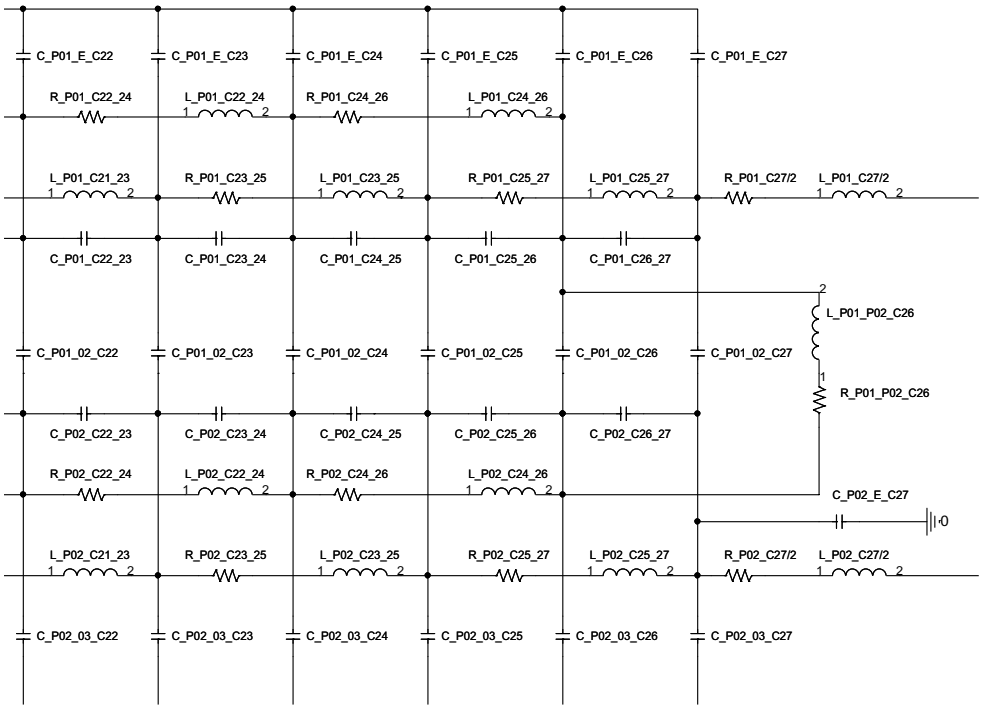

Fig. 4-10 Zoomed right upper part of the detailed network model of the PF 6 coil

4.3.2 Detailed Network Model of the PF 6 Coil with Instrumentation Cables

The influence of the instrumentation cables on the resonance frequency and the voltage distribution within the PF 6 coil was analysed by consideration of the instrumentation cables in the detailed network model. The instrumentation cables will be placed on the joints between the double pancakes but the type of cables is not exactly defined in [CDA3]. Thus it was calculated with the same instrumentation cable type [Bau98] which was used for the ITER TF Model Coil (TFMC) [Ulb05]. The capacitance of these cables was calculated to 437 pF/m. The cables were taken into the network model as additionally capacitances on the double pancake joints. The designation “IC” was used for the capacitances of the instrumentation cables. The length of the instrumentation cables were derived from [CDA3] and [DDDD4]. The values for the length of the cables and their capacitances are summarised in Tab. 4-5.

	Length (m)	Capacitance (nF)
C_IC_E_P01	44	20
C_IC_E_P02_P03	34	15
C_IC_E_P04_P05	38	16.5
C_IC_E_P06_P07	41	18
C_IC_E_P08_P09	46	20
C_IC_E_P10_P11	46	20
C_IC_E_P12_P13	41	18
C_IC_E_P14_P15	38	16.5
C_IC_E_P16	46	20

Tab. 4-5 Length and capacitance values for the instrumentation cables of the PF 6 coil

4.4 Simplifications Used in the Network Models

- In the detailed network models of PF 3 and PF 6 coils only one RLC circuit was used for each turn of the coils

- All mutual inductances and self inductance were summarised to one cumulative inductance of one turn

- The connection of the instrumentation cables on the joints between the pancakes and double pancakes was considered as an additional capacitance on the joints

- AC/DC converter (Ves) was neglected during the fast discharge network simulation, because it will be bypassed during the fast discharge

- In the PF 2-PF 5 coil network the main and booster converters were summarised to one converter

- In the CS1L-CS1U coil network the two converters of each coil were summarised to one converter in the network, because the converters are in series

- The winding direction of the PF 1 coil was not given in the [DDDD3] it was assumed to be the same like PF 3, PF 6 and CS coils

5 Results of Calculations in Frequency Domain for PF 3 and PF 6

In the frequency domain the resonance frequency of the PF 3 and PF 6 coils was calculated, which gives a first benchmark of the transient behaviour of these coils.

The calculation strategy, which was used for calculation of resonance frequency of PF 3 and PF 6 coils, is shown in Fig. 5-1. Due to the frequency dependence of the inductances of the coils, the calculations include an iterative loop.

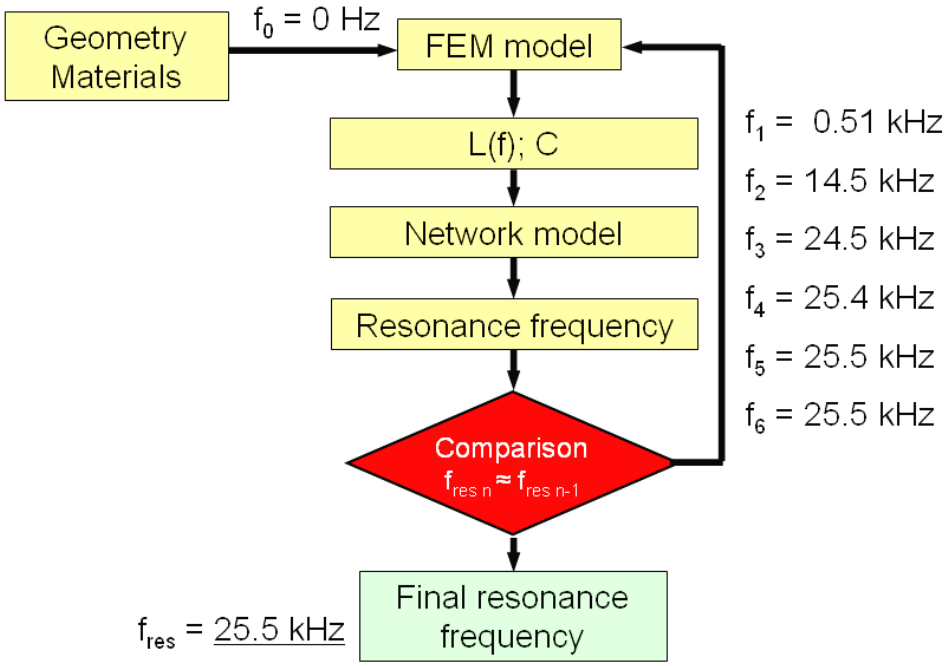

Fig. 5-1 Strategy for calculation of resonance frequency on example of PF 3 coil

In the following the calculation strategy will be explained on the example of the PF 3 coil. At the beginning of the calculations the detailed FEM model of the coil without instrumentation cables was established with the given geometries and materials, which is described in section 3.2. Because the range, in which the resonance frequency of the coil lies, was unknown the calculations were started with the frequency of 0 Hz. The values for frequency dependent inductances were calculated with the FEM model of the coil for the frequency of 0 Hz. The values for frequency independent capacitances were calculated by formulas for cylindrical and parallel plate capacitor, shown in section 4.2. The resistances of the superconducting cables were defined to 1 pΩ. The calculated values were taken into the network model as lumped elements. The calculations in frequency domain were made by the excitation of the network model with a voltage of 1 V. The answer on the excitation was calculated for all frequencies in a defined frequency range, shown in Fig. 5-2. The first calculated resonance frequency was taken into account, because it is the natural frequency of the coil. The natural frequency is the frequency of free vibrations. It seems that the first peak in Fig. 5-2 is at 0.98 kHz with a value of 8.4 V. The closer view at the frequency behaviour at the frequency

range lower than 0.9 kHz, shows a peak at 0.51 kHz with a value of 1.07 V, Fig. 5-3. Thus the first resonance frequency of the first loop was calculated to 0.51 kHz.

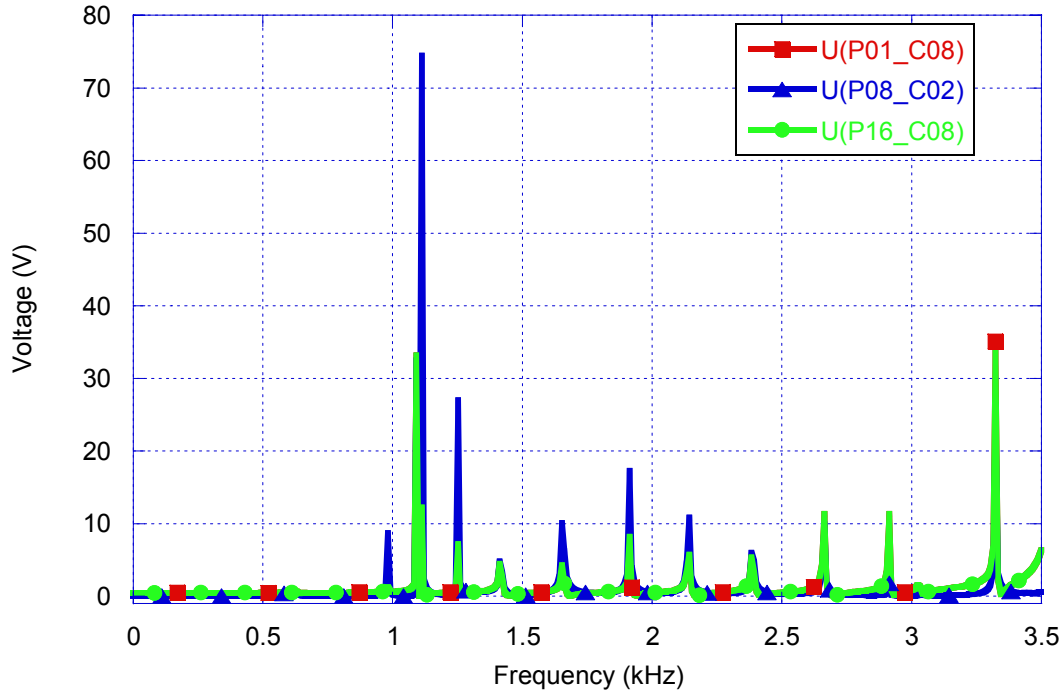

Fig. 5-2 Voltage answer on the excitation for the conductors P01_C08, P08_C02 and P16_C08 in a frequency range lower than 3.5 kHz for a terminal excitation with 1 V and DC values of the PF 3 coil elements.

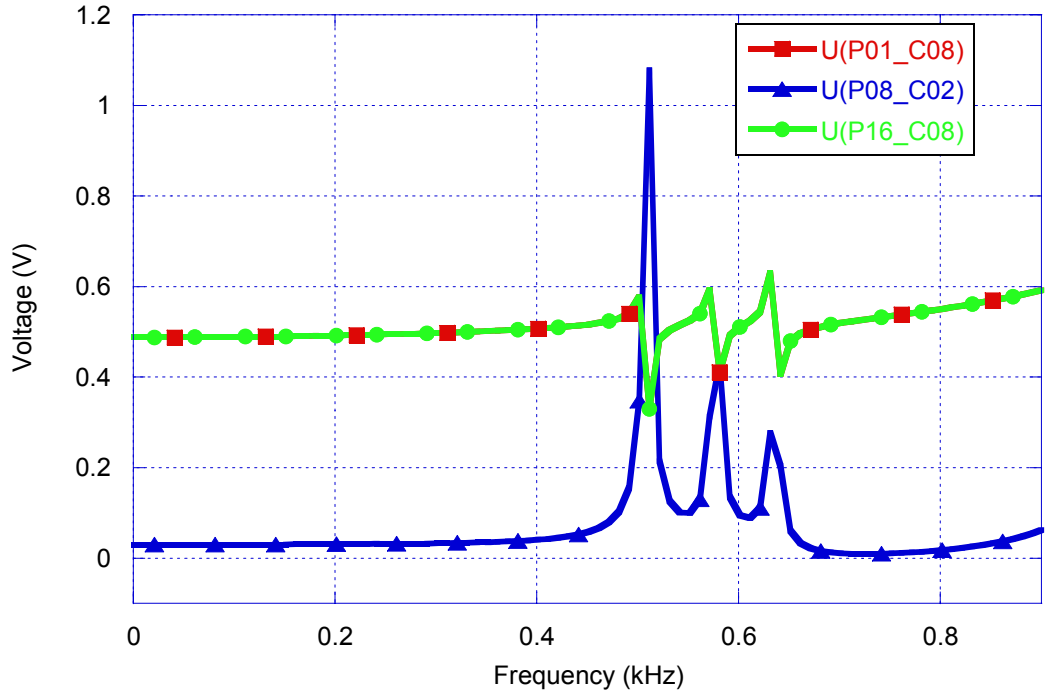

Fig. 5-3 Voltage answer on the excitation for the conductors P01_C08, P08_C02 and P16_C08 in a frequency range lower than 0.9 kHz for a terminal excitation with 1 V and DC values of the PF 3 coil elements.

The comparison between the calculated frequency of the first loop and the frequency of 0 Hz, at which the FEM model of the coil was established, shows relatively big difference. Thus a second calculation loop was started. The new values for the frequency dependent inductances were calculated at 0.51 kHz. The values were taken into the network model as lumped elements and the resonance frequency of the second loop was calculated to 14.5 kHz. The relative difference between the resonance frequency of the first loop 0.51 kHz and the second loop 14.5 kHz was still big, thus the third loop of calculation was started. The values for the inductances were calculated for the frequency of 14.5 kHz and taken into network model of the coil. The resonance frequency of the third loop was calculated to 24.5 kHz.

The difference of 0.1 % between the resonance frequencies of following loops was defined as the break out criterion of the calculation loop. This criterion was reached after the sixth calculation loop and so the final resonance frequency of 25.5 kHz for PF 3 coil was calculated.

To verify that the resonance frequency converges only to one value of 25.5 kHz, the calculation were realised with the start frequency of 200 kHz. The calculations were made with the same strategy, like with the start frequency of 0 Hz. The break out criterion was the achievement of the converged resonance frequency of 25.5 kHz. This criterion was fulfilled after the third calculation loop. The results of the resonance frequency calculations of the PF 3 coil with symmetrical grounding are shown in Tab. 5-1.

	Without instrumentation cables with start frequency 0 Hz (kHz)	Without instrumentation cables with start frequency 200 kHz (kHz)	With instrumentation cables with start frequency 0 Hz (kHz)
1st Loop	0.51	27.8	0.49
2nd Loop	14.5	25.6	14
3rd Loop	24.5	25.5	23.5
4th Loop	25.4		24.3
5th Loop	25.5		24.4
6th Loop	25.5		

Tab. 5-1 Calculated resonance frequencies of PF 3 coil with symmetrical grounding

Additionally the influence of the instrumentation cables on the resonance frequency of the PF 3 coil was analysed. The network model of the PF 3 coil with instrumentation cables and symmetrical grounding, which was described in 4.2.2, was used for these calculations. After the fifth calculation loop the resonance frequency with instrumentation cables was calculated to 24.4 kHz.

The comparison of the results between the calculations with and without instrumentation cables shows that the instrumentation cables have an influence on the resonance frequency of the coils and displace it to lower frequencies.

The calculations of resonance frequency for the PF 6 coil were made with the same strategy like for the PF 3 coil. The results of the calculations with start frequency of 0 Hz without instrumentation cables, with start frequency of 200 kHz without instrumentation cables and the calculations with instrumentation cables with start frequency of 0 Hz are shown in Tab. 5-2.

	Without instrumentation cables with start frequency 0 Hz (kHz)	Without instrumentation cables with start frequency 200 kHz (kHz)	With instrumentation cables with start frequency 0 Hz (kHz)
1st Loop	0.55	34.2	0.58
2nd Loop	18.7	32.1	18.1
3rd Loop	30.8	32.0	29.6
4th Loop	31.9		30.6
5th Loop	32.0		30.7
6th Loop	32.0		30.7

Tab. 5-2 Calculated resonance frequencies of PF 6 coil with symmetrical grounding

Additionally the influence of the unsymmetrical grounding, e. g. in case of a ground fault on one terminal, on the resonance frequency was analysed. The results of the calculation of the resonance frequency with unsymmetrical grounding for PF 3 coil are shown in Tab. 5-3. The resonance frequency of PF 3 coil without instrumentation cables with symmetrical grounding was calculated to 25.5 kHz, with unsymmetrical grounding the resonance frequency is displaced to lower value of 20.7 kHz. The instrumentation cables at unsymmetrical grounding displace the resonance frequency of the PF 3 coil to much lower value of 17.0 kHz.

The values of the resonance frequency of PF 6 coil with unsymmetrical grounding are summarised in Tab. 5-4. The unsymmetrical grounding displace also the resonance frequency of the PF 6 coil to lower value of 28.6 kHz, compared with 32.0 kHz with symmetrical grounding of the PF 6 coil. The instrumentation cables have strong influence on the resonance frequency of the PF 6 coil with unsymmetrical grounding and displace it to 22.9 kHz.

	Without instrumentation cables with start frequency 0 Hz (kHz)	Without instrumentation cables with start frequency 200 kHz (kHz)	With instrumentation cables with start frequency 0 Hz (kHz)
1st Loop	0.422	22.80	0.354
2nd Loop	11.94	20.78	9.50
3rd Loop	19.85	20.66	16.3
4th Loop	20.60		17.0
5th Loop	20.66		17.0
6th Loop	20.66		

Tab. 5-3 Calculated resonance frequencies of PF 3 coil with unsymmetrical grounding

	Without instrumentation cables with start frequency 0 Hz (kHz)	Without instrumentation cables with start frequency 200 kHz (kHz)	With instrumentation cables with start frequency 0 Hz (kHz)
1st Loop	0.5	30.8	0.4
2nd Loop	16.8	28.74	12.9
3rd Loop	27.75	28.63	22.1
4th Loop	28.63		22.9
5th Loop	28.63		22.9

Tab. 5-4 Calculated resonance frequencies of PF 6 coil with unsymmetrical grounding

6 Test voltages and waveforms for TF coils

Insulation co-ordination is the selection of the dielectric strength of equipment in relation to the operating voltages and overvoltages which can appear on the system for which the equipment is intended and taking into account the service environment and the characteristics of the available preventing and protective devices [IEC60071]. Insulation co-ordination in conventional high voltage engineering delivers the selection of the standard rated withstand voltages from a list. This standard rated withstand voltages are standardised test voltages. Although such sets of standard test voltages cannot be simply taken for fusion magnets the procedure for the determination of the test voltages can be applied. As the first step the system analysis is performed which delivers the voltages and overvoltages for defined cases, e. g. fast discharge with perfect synchronisation of all fast discharge units and no fault.

The following proposal for test voltages and waveforms is based on previous investigations on TF coils [Fin04]. A short summary of these investigations is presented and the test voltages and waveforms are described in this chapter. Some of the proposed test voltage waveforms are applied in “long-term tests” (10 h for each voltage step) on ITER TFMC in order to demonstrate that the proposed test voltages do not require a modification of the ITER TF design.

6.1 TF coil, TF system and models description

The examined ITER TF coil system is based on the ITER document status 2002 at the beginning of the activities for [Fin04]. A list of simplifications is available in [Fin04] in order to perform the calculations on a single PC.

The insulated conductor of an ITER TF coil is embedded in 7 stainless steel plates (so called radial plates) to handle the occurring Lorentz forces. The radial plates are insulated by vacuum impregnation and stacked to a winding pack. This winding pack is enclosed in a D-shaped stainless steel case (Fig. 6-1).

All 5 inner radial plates have two pancakes with 11 turns each. Both outer radial plates have a pancake with 9 turns and a pancake with 3 turns. This leads to total number of 134 turns per TF coil.

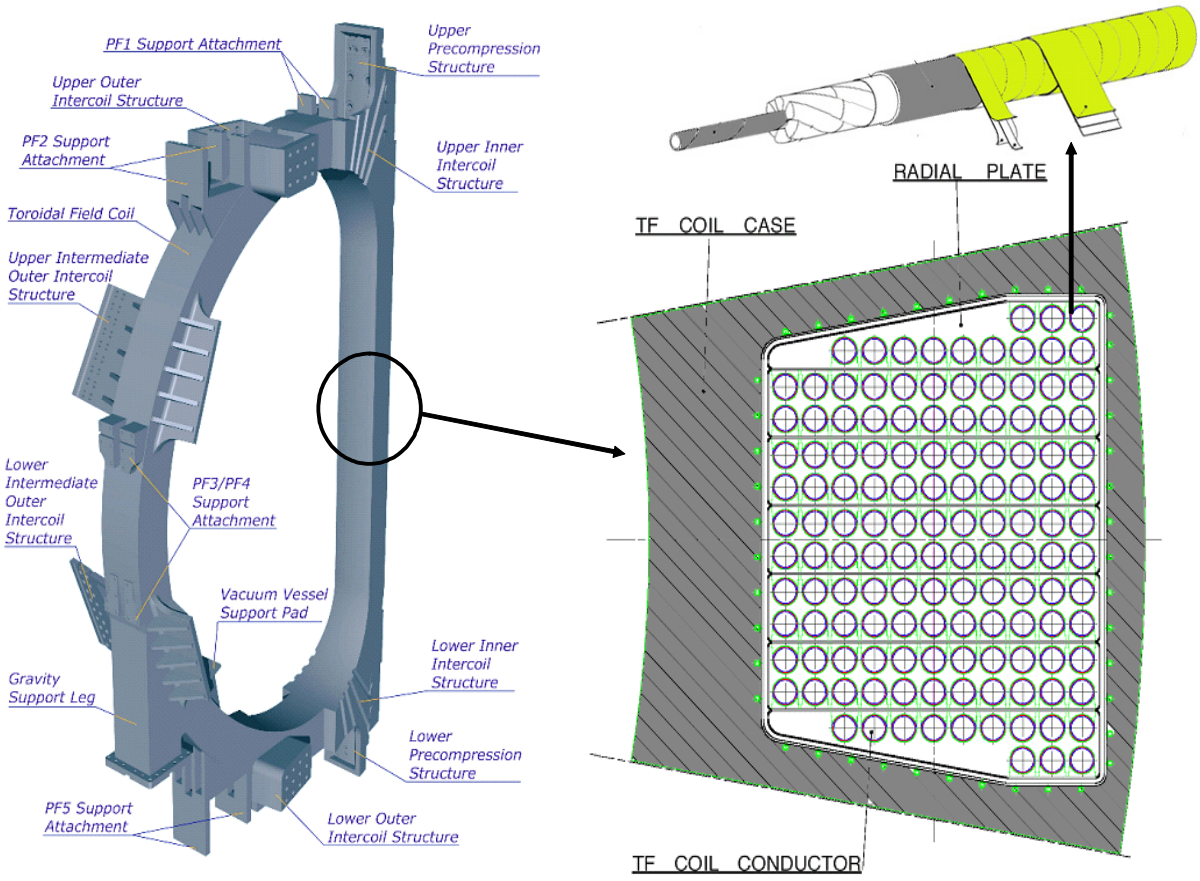

Fig. 6-1 D-shaped steel case, cross section of this steel case in the mid plane of the straight section (inboard leg) and the design of the conductor insulation of the ITER TF coils.

The ITER TF system consists of 18 TF coils with 9 fast discharge units (FDUs) (Fig. 6-2). In the FDUs the energy is dissipated in discharge resistors during fast discharge. The symmetrical “soft” grounding (i. e. grounding on both sides of a fast discharge unit with 500 Ω resistors) allows to halve the coil terminal to ground voltage and limits the fault current in case of a single earth fault.

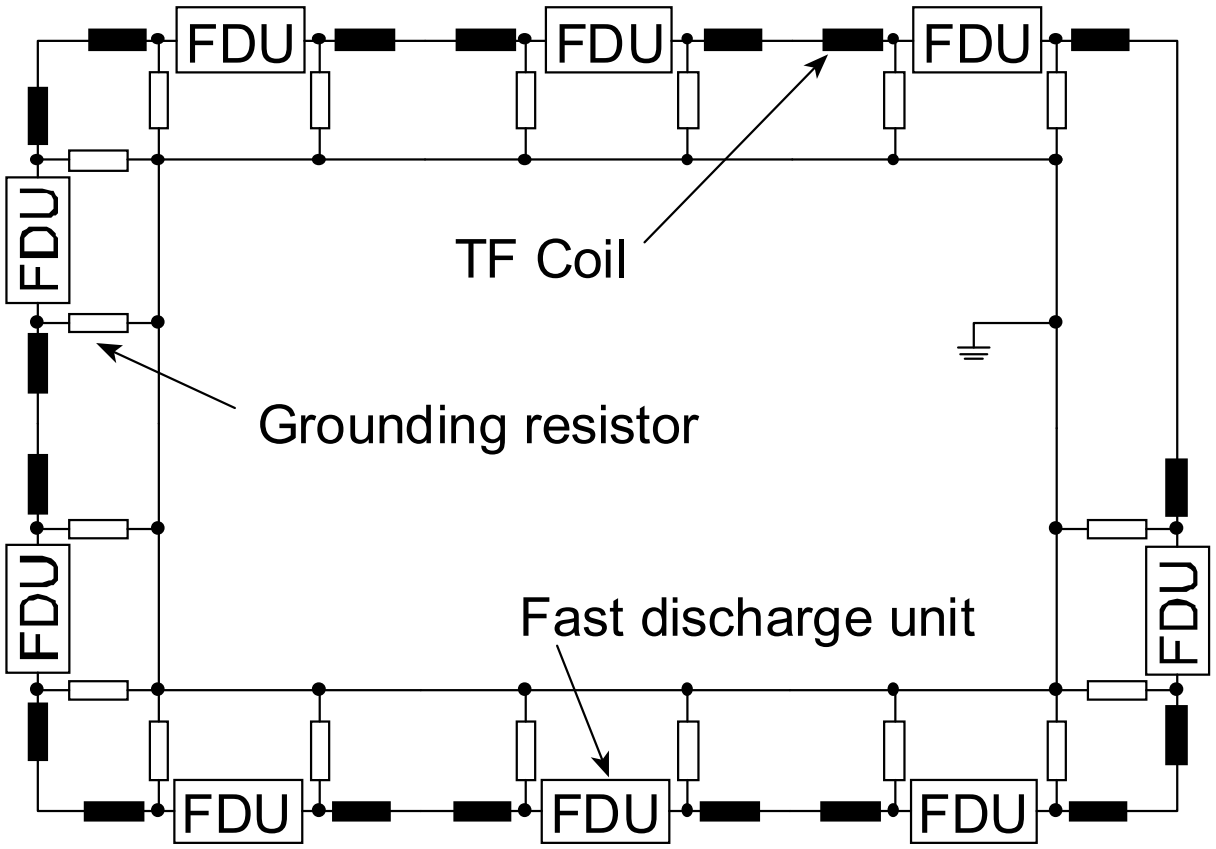

Fig. 6-2 Simplified analogue circuit of the TF coil system during fast discharge (power supply already disconnected).

According to the design of the TF coil its insulation system consists of three different types: the conductor insulation between the conductor and the surrounding radial plates, the radial plate insulation between two neighbouring radial plates and the ground insulation between the radial plates and the grounded coil case.

The calculation of the maximum voltages for all 3 types of insulation during a fast discharge was performed step by step. In fact, it was not possible to integrate all conditions and solve all problems in a frequency dependent network model directly because in every coil the transient current is superposed to the transport current with the much longer equivalent discharge time constant of 11 s.

For the first step the detailed network model of a single TF coil was established by determination of one capacitance, one resistance and one inductance per turn. The turn capacitances were calculated as cylinder capacitors. Radial plate and case capacitances were calculated as plate capacitors; additional capacitances were assumed for the instrumentation cables. The resistances, inductances and mutual inductances were calculated for several frequencies with the FEM program Maxwell.

The established network model was treated by the code PSpice, which does not allow the use of frequency dependent lumped elements. So several network models were established for different frequencies. The natural frequency (i.e. first resonance frequency) for a single ITER TF coil was calculated to be at 50 kHz, which is considerable lower as the value of 300 kHz which was calculated and measured for the TF Model Coil [Ulb05].

For the second step a network model of the TF FDU system was built up with 18 simplified coils and 9 models of a FDU. This network model allows the determination of the coil terminal voltages. The coils act in this step as coupled superconducting DC coils and were excited with the rated current of 68 kA.

The coils of the system are subjected to different voltage excitations in case of a malfunction of a FDU or an earth fault. Hence for the fault cases, the maximum terminal to terminal voltages and the maximum terminal to earth voltages (which do not occur at the same coils) were identified.

In the last step, these terminal voltages from the system network are used for the excitation of the detailed single coil model. For this purpose the models with the natural frequency (50 kHz) and with a rise time in the ms range (chosen: 1 kHz, which corresponds roughly to a rise time of 0.25 ms) are used. For the fast discharge, one terminal was earthed and the other one was excited with the calculated terminal voltages. In the fault cases it was necessary to excite both terminals.

6.2 Calculated fault cases

Firstly a fast discharge with no fault and perfect synchronised FDUs were examined.

Then a fault case (fault case 1) with the simultaneous failure or delay of 2 neighbouring FDUs during a fast discharge was assumed, i.e. that for these units the current remains “for a long time” in the short circuit path and the energy of all coils dissipates in only 7 discharge resistors instead of 9. The term “for a long time” means in this sense long compared to the rise time of the fast discharge process causing to reach the same maximum overvoltages as if the commutation in this FDU does not operate at all. This fault case 1 causes an imbalance of the TF system. Hence the coils have different terminal to ground voltages.

For the second fault case it was assumed that the voltage imbalance in the system, caused by fault 1, with the increase of terminal to earth voltages, leads to an earth fault at the time and location of the maximum voltage to earth.

6.3 Calculated voltages for fast discharge and two fault cases

The simulation of the fast discharge starts with the current commutation from the short circuit path (that bridges the resistor path during DC current operation) to the discharge resistor path in the FDUs. This commutation produces a maximum voltage of about $U = R \cdot I_0$ at the resistor R of the FDUs. Assuming an initial rated current of 68 kA and a discharge resistance of 0.1 Ω the voltage across one FDU is about 7 kV. For a perfect symmetrical ITER system, this causes a voltage to ground of +U / 2 or –U / 2 at every FDU terminal because the FDUs are symmetrically grounded over resistors with 500 Ω [PAF6A]. For such a "soft grounded" symmetrical ITER system, every coil has one terminal with a maximum voltage of +U / 2 or –U / 2 (the one which is connected to the FDU) and one terminal with ground potential (the one which is connected to the neighbouring coil). Hence all coils have the same terminal to terminal voltage and the same voltage to ground (neglecting polarity) or 3.5 kV during the

fast discharge. It is therefore sufficient to collect the data of one coil terminal that is connected with the FDU.

The voltage values for the fast discharge without a fault and for fault case 1 are preferably chosen from the 1 kHz model because the rise times are 1.5 ms or longer.

For the second fault case, the rise times are in the range of few µs for the maximum radial plate and conductor insulation voltage and in the range of some ms for the ground insulation voltage. The reason for such a difference between the rise times is that the maximum values were not found at the same coil.

Tab. 6-1 shows the collection of all calculated maximum voltages, the time and rise time of these voltages and the location.

		No fault				Failure of FDU 2 and FDU 3								Failure of FDU 2, 3 and earth fault at L3:1							
		Coil voltage and voltage to ground for all coils 3.467 kV				Coil with maximum coil voltage 3.644 kV: L14 (L15)				Coil with maximum voltage to ground 8.061 kV: L8:2 (L3:1)				Coil with maximum coil voltage 13.49 kV: L2				Coil with maximum voltage to ground 16.35 kV: L8:2			
	fmodel / kHz	location	U / kV	t / s	TA / s	location	U / kV	t / s	TA / s	location	U / kV	t / s	TA / s	location	U / kV	t / s	TA / s (from x V))	location	U / kV	t / s	TA / s (from x kV)
Terminal	1	terminal 2	3.47	8.5 m	1.6 m	L14:2	3.46	8.1 m	1.6 m	L8:2	8.06	80.4 m	17 m	L2:2	9.66	81.9 m	2.4 µ (-1145)	L8:2	16.35	87.7 m	3.5 m (8.06)
	50	terminal 2	3.47	8.5 m	1.6 m	L14:2	3.46	8.1 m	1.6 m	L8:2	8.06	80.4 m	17 m	L2:2	9.66	81.9 m	2.4 µ (-1145)	L8:2	16.35	87.7 m	3.5 m (8.06)
Ground insulation	1	terminal 2	3.47	8.5 m	1.6 m	L14:2	3.46	8.1 m	1.6 m	L8:2	8.06	80.4 m	17 m	DPJ45	10.56	82.7 m	some µs	L8:2	16.35	87.7 m	3.5 m (8.06)
	50	terminal 2	3.47	8.5 m	1.6 m	L14:2	3.46	8.1 m	1.6 m	L8:2	8.06	80.4 m	17 m	DPJ67	10.67	81.9 m	3.7 µ (-1382)	L8:2	16.35	87.7 m	3.5 m (8.06)
Radial plate insulation	1	RP 3 – RP 2	0.650	4.3 m	1.6 m	RP 4 – RP 3	0.614	6.0 m	1.6 m	RP 2 – RP 1	0.686	29.8 m	11 m	RP 6 – RP 5	4.81	81.9 m	6.1 µ (442)	RP 2 – RP 1	1.30	87.8 m	3 m (0.61)
	50	RP 4 – RP 3	0.564	76.8 m	1.6 m	RP 4 – RP 3	0.544	5.9 m	2 m	RP 2 – RP 1	0.700	29.1 m	10.3 m	RP 6 – RP 5	4.33	81.9 m	3 µ (-1.4 k)	RP 2 – RP 1	1.31	86.8 m	3 m (0.62)
Conductor insulation	1	terminal 2 – RP 7	0.584	4.5 m	1.5 m	terminal 2 – RP 7	0.539	6.0 m	1.6 m	terminal 2 – RP 7	0.811	23.2 m	8 m	terminal 2 – RP 7	4.25	81.9 m	2 µs (15)	terminal 2 – RP 7	1.41	86.7 m	3 m (0.57)
	50	terminal 2 – RP 7	0.535	5.2 m	1.5 m	terminal 2 – RP 7	0.544	5.9 m	1.7 m	terminal 2 – RP 7	0.815	23.2 m	9 m	Near DPC joint of PC13 – RP 7	3.66	81.9 m	1.4 µ (0)	terminal 2 – RP 7	1.42	86.7 m	3.5 m (0.6)

Tab. 6-1 Overview about all calculated maximum voltages on ITER TF for all types of insulation

6.4 Representative voltages

In conventional high voltage engineering voltages and overvoltages are divided in classes (e. g. fast-front transient). These voltages and overvoltages are then allocated to standard voltage shapes (e. g. standard lightning impulse shape with T_1 = 1.2 µs and T_2 = 50 µs). In most cases standard withstand voltage tests are defined in [IEC60071]. In other cases the standard withstand voltage test is to be specified by the “relevant apparatus committees”.

The standard classis of [IEC60071] are not suitable for the ITER TF fast discharge waveforms and no “relevant apparatus committee” is available for such waveforms. In addition an excitation similar to the appearance to a switching impulse but with longer time to half value may be difficult to perform.

Hence the following representative voltages or overvoltages are proposed.

DC: The DC waveform is proposed due to the equivalent discharge time constant of 11 s, the deformation of the e-function by the PTC behaviour of the resistor, and the simple DC test application combined with the relative low destructive energy. The DC voltage value is selected as the maximum voltage which appears during the discharge. The DC voltage can not be applied between the terminals. Instead the voltage is only applied between one part completely on the same high voltage value and the other part which is grounded (e. g. all conductors and all radial plates on high voltage and the surrounding case on ground potential).

AC: The 50 Hz (or 60 Hz) AC waveform is proposed due to its suitable rise time (few ms), the possibility to perform partial discharge insulation diagnostic in the common known frequency range, the relative good availability of voltage sources and the limited maximum current. The AC waveform should not be applied between the terminals because a ITER TF coil is no transformer. Hence the voltage is only applied between one part completely on the same high voltage value and the other part which is grounded. The AC rms voltage value is selected as the maximum voltage which appears during discharge divided by $\sqrt{2}$.

It may also be possible to test with a series resonance circuit at a somewhat different frequency than 50 Hz if a suitable system is available.

Lightning impulse: Lightning impulse tests are proposed due to the fast rise times which occur during the capacitor discharge in the current commutation process or during earth fault events on some coils. For the impulse test the voltage is applied between the terminals causing the voltage drop along the winding. The impulse crest value is selected as the maximum voltage which appears during the discharge

6.5 Test voltages

In conventional high voltage engineering after determination of the representative voltages and overvoltages the “co-ordination withstand voltages” are determined which have the shape of the representative overvoltages but the values are obtained by a co-ordination factor. This factor considers e. g. the accuracy of the evaluation of the representative overvoltages. Then the “required withstand voltages” are determined by converting the co-ordination withstand voltages to appropriate standard test conditions by multiplying again with a factor. At the end a rated insulation level can be chosen by selection of a set of standard rated withstand voltages.

For ITER such a standard process is not available. Hence in [Fin04] test voltages are proposed which consider the following safety factors and other aspects:

- The selected “usual rule” for voltage tests is proposed to be 2 * U_{fault} + 1 kV. The value is rounded up to integer values (e. g. 2 * 8.1 kV + 1 kV = 17.2 kV => 18 kV).

- The test voltage for values < 5 kV is taken as 5 kV.

- For radial plate and conductor insulation the higher value is taken for both.

- For the impulse test the terminal to ground voltage is selected in a manner that no internal voltage value exceeds the values derived from the “usual rule”.

Tab. 6-2 gives an overview about the proposed test values derived from the two fault cases.

Type of insulation	Fast discharge without fault	Failure of 2 adjacent FDUs		Failure of 2 adjacent FDUs plus earth fault at terminal with maximum voltage to ground		
	Calculated maximum voltage	Calculated maximum voltage	Proposed test voltage for DC and AC tests (peak value)	Calculated maximum voltage	Proposed test voltage for DC and AC tests (peak value)	Proposed test voltage for specific µs impulse tests
Ground insulation	3.5 kV	8.1 kV	18 kV	16.4 kV	34 kV	29.6
Radial plate to radial plate	0.7 kV	0.7 kV	5 kV	4.8 kV	11 kV	(control: U ≤ 11 kV)
Conductor to radial plate	0.6 kV	0.8 kV	5 kV	4.3 kV	11 kV	(control: U ≤ 11 kV)

Tab. 6-2 Calculated voltage and test voltages related to the case with failure of 2 adjacent FDUs and earth fault at terminal with maximum voltage to ground. In case of the specific proposed impulse voltage test with a terminal voltage higher than 29.6 kV the internal voltage to ground is higher than 34 kV on a location which is not accessible for measurement. This value is depending on the test circuit.

For the cases without an earth fault, the only excitation with rise times in the 1 µs range is caused by the discharge of the capacitor bank. Because the voltage of such an excitation is expected to remain in the 1 kV range an impulse test with a rise time in the µs range with a terminal voltage of 5 kV is sufficient although this value is lower than the DC and AC test voltages.

The potential distribution for a specific circuit was calculated for the impulse test. In the examined example it was assumed that a capacitor bank of 150 µF excites the coil. The damping resistor was 0.77 Ω. For other impulse test circuits the distribution must be recalculated.

6.6 Test arrangements

The connection of the helium inlet tap and the radial plate tap must be changed during the high voltage tests. It is therefore recommended to install at least for these cables the current limiting resistors in a panel box after the room temperature instrumentation cable feedthroughs and not at the input of the instrumentation cables. The cables from the double pancake joints are always connected with high voltage and can therefore be closed at the

end with blind plugs during the high voltage tests if they are not connected to the room temperature instrumentation (e. g. during a cold DC test).

6.6.1 Tests on ground insulation (G)

For the ground insulation tests the helium inlet potential is connected directly with the radial plate (Fig. 6-3). Hence it is possible to apply high voltage to the complete conductor and all radial plates and keep the coil case grounded.

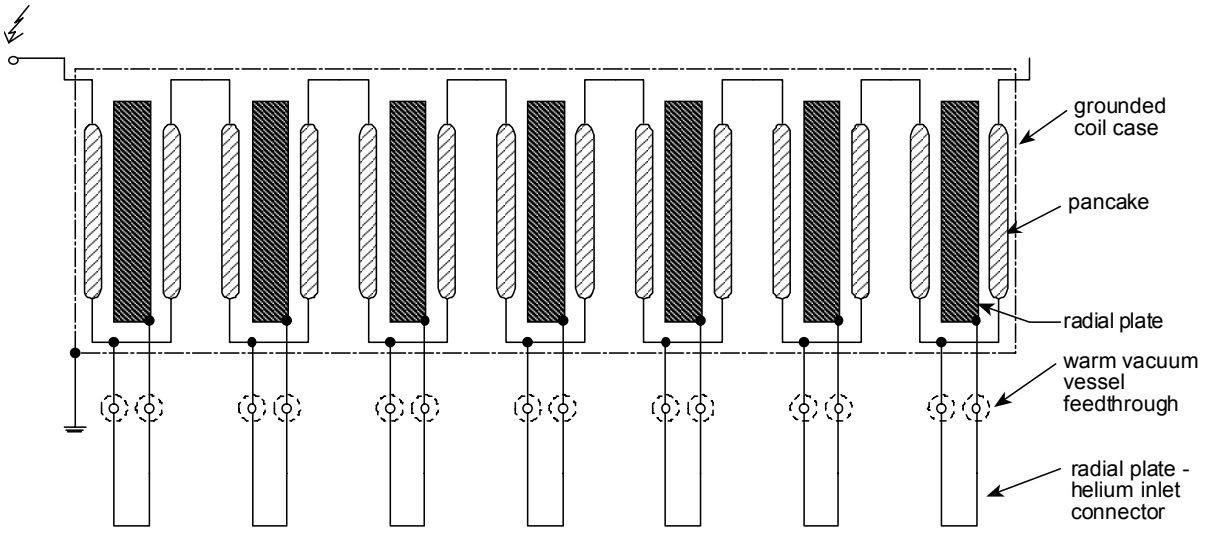

Fig. 6-3 Arrangement G for ground insulation tests. Although the pancakes are within the radial plates they are drawn outside for better visibility.

6.6.2 Tests on radial plate insulation (R)

The radial plates are connected alternately to ground and to inner helium inlet potential for the test on radial plate insulation (Fig. 6-4). The outer radial plates are connected to the helium joint because they are adjacent to the grounded case.

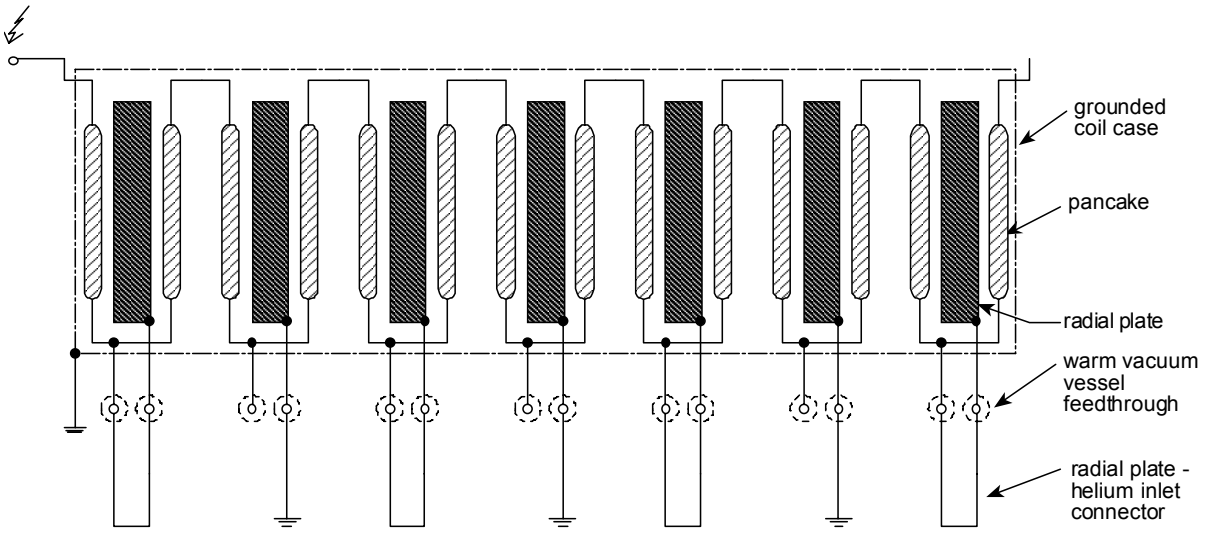

Fig. 6-4 Arrangement R for tests on radial plate insulation.

6.6.3 Tests on conductor insulation (C)

All radial plates are connected to ground for the test of the conductor insulation (Fig. 6-5).

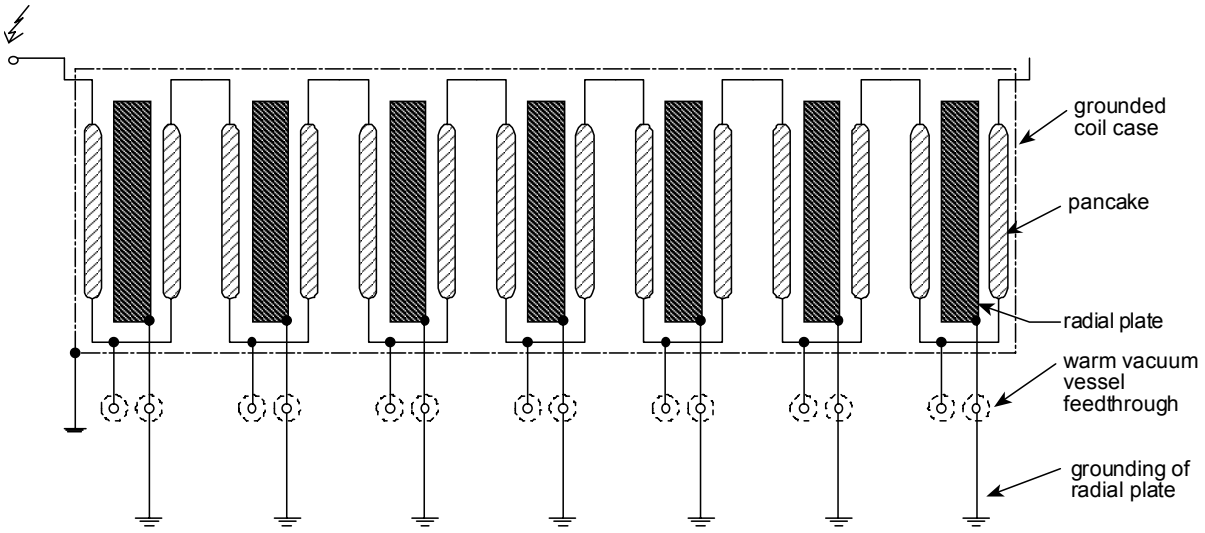

Fig. 6-5 Arrangement C for tests of conductor insulation.

6.6.4 Tests with operation mode arrangement (O)

The complete set of cable lengths are connected to the coil for the test in operation mode arrangement, e. g. for the impulse tests (Fig. 6-6).

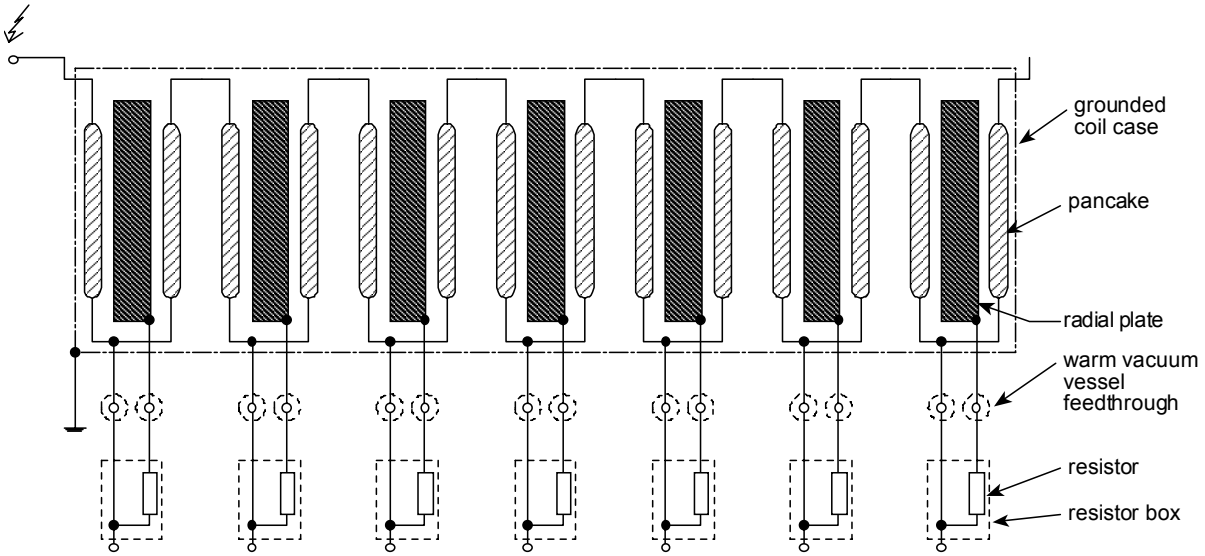

Fig. 6-6 Arrangement O for tests in operation mode arrangement.

6.7 Power supply and high voltage extensions

Different power supplies are connected with the test arrangements (see 6.6). The high voltage output of the power supply is connected with one terminal of the coil. The second coil terminal is left open or the coil is short circuited for AC and DC excitation. The second coil terminal is grounded for impulse tests.

For DC tests the high voltage DC power supplies are usually equipped with internal voltage and current measurement (Fig. 6-7).

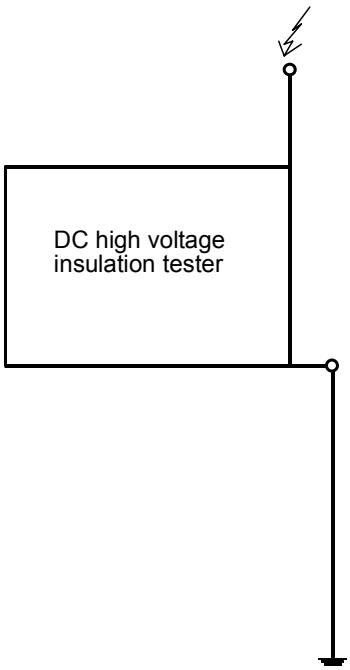

Fig. 6-7 Power supply for DC tests (internal current and voltage indication not shown)

For AC tests external high voltage dividers are used. A possible example of the power supply is shown in Fig. 6-8. A partial discharge measurement is added. The detection impedance is in series to the coupling capacitance C_K. This detection impedance may be put in the grounding path to increase the sensitivity, e. g. for partial discharge measurement of the conductor insulation in one radial plate.

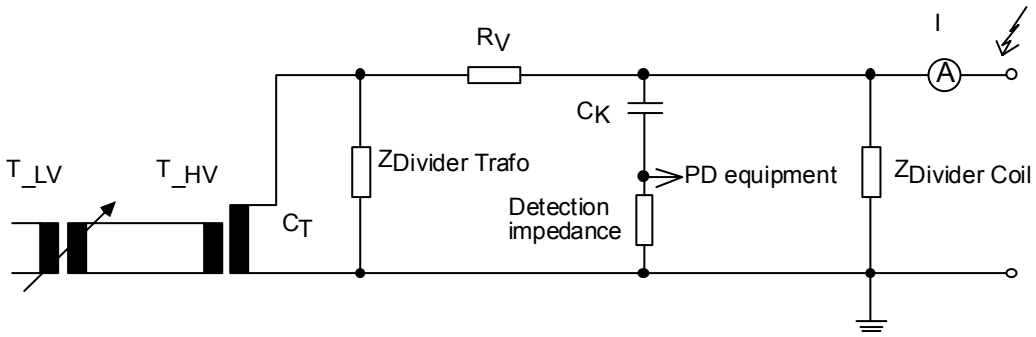

Fig. 6-8 AC power supply (low voltage variable transformer T_LV and high voltage transformer T_HV) with external high voltage dividers for voltage measurements. The detection impedance, coupling capacitance C_K and resistor R_V are added for partial discharge measurement (and in case of R_V for current limitation).

A Schering Bridge is used for the determination of the dissipation factor under AC excitation. One possible example is given in Fig. 6-9. The detailed arrangement of the Schering Bridge will be defined if the boundary conditions are known (type of Schering Bridge, capacitance of standard capacitor, grounding of the coil case, eventually auxiliary branches). The measurement with the Schering Bridge will be probably easier if it is possible to lift the coil case with the bridge to a potential of about 2 V.

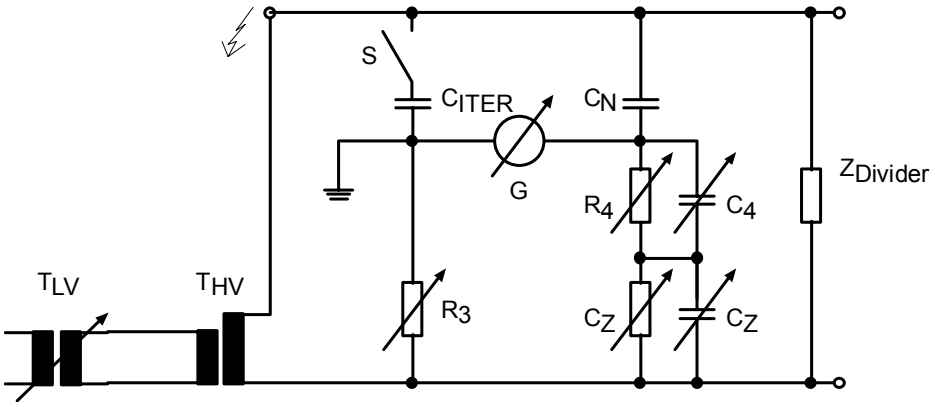

Fig. 6-9 Power supply and Schering Bridge ACS. C_{ITER} represents a TF coil.

An impulse voltage generator is used for the excitation of the coil with impulse voltage rise times (or virtual front times) in the µs range (Fig. 6-10). The detailed settings of the impulse generator will be defined if the specifications of the impulse generator are known (capacitance of the capacitor bank, maximum voltages, internal damping resistors).

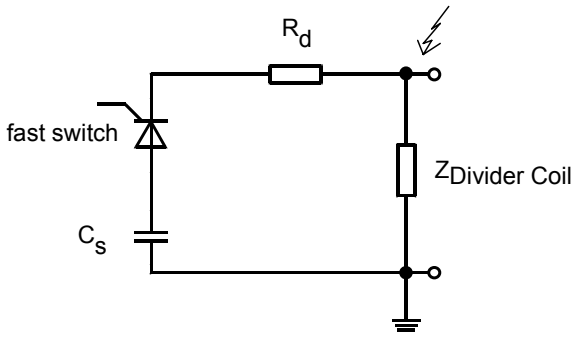

Fig. 6-10 Impulse generator I containing a capacitor bank C_S, a damping resistor R_d and a fast switch (e. g. ignitron, spark gap, thyristor).

6.8 Test criteria and additional information

For each test a criterion must be defined. Some criteria are indispensable. Others may be developed during the tests or taken as additional information, e. g. the partial discharge activity.

6.8.1 Criterion NB: no breakdown

The most important criterion is that no breakdown appears. Hence this criterion is relevant for every test.

6.8.2 Criterion R: insulation resistance

The insulation resistance of all types of insulation must be > 1 GΩ.

For such high insulation resistances and the high capacitance of the coil the charging current is expected to be in the same range (or even higher) as the current caused by the insulation resistance after a test time of 1 min. It may therefore be useful to apply the maximum voltage value for e. g. 15 min for some measurements. In addition it is recommendable to use always the same DC test equipment because the internal resistance of this equipment may be in the range of the coil.

The measured insulation resistance is strongly effected if the coil is connected with additional conductivities (water cooling hoses, measurement equipment, wet room temperature axial breaks, ...). In this case the value is no more related to the coil and the criterion of the insulation resistance value can be skipped.

6.8.3 Criterion IC: constant charging current

The residual leakage current can be neglected compared with the capacitive charging current during AC tests on well insulated and high capacitive samples. A constant charging current is therefore a criterion during a test with constant AC voltage.

6.8.4 Additional information PD: partial discharge activity

The inception voltage, extinction voltage and apparent charge (shape of a partial discharge fingerprint) of the partial discharge measurements can deliver useful information, esp. for the judgement of the insulation quality of a single element within a series production.

6.8.5 Additional information DF: dissipation factor

The measurement of the dissipation factor may deliver useful information, esp. for the insulation diagnostic of a single element within a series production.

6.8.6 Additional information SW: shape of the waveform

The voltage waveform shape during the impulse test may deliver useful information, esp. for the judgement of the insulation quality of one coil within the series production.

6.9 Paschen test

ITER CSMC used vacuum for high voltage insulation. But for a reliable high voltage operation even under vacuum breakdown in the cryostat a complete encapsulation with solid insulation and covering of this insulation with conductive material (e. g. conductive paint) is necessary. Such a “Paschen tight” concept must be verified by a Paschen test where the sample is subjected to a transition of the Paschen curve.

For this test a vacuum vessel is necessary. Every test sample must be prepared to be Paschen tight. Sometimes for superconducting coils an appropriate time of a Paschen test at the manufacturer is to do it after connection of the high voltage instrumentation path. But for ITER TF it makes no sense to install the original warm instrumentation feedthroughs at the manufacturer if it is not possible that these feedthroughs remain on the coil during the assembly in the ITER facility. Hence the room temperature ends of the cables must be either encapsulated in a Paschen tight manner or guided in a Paschen tight manner to the ambient.

Because it is more time consuming to achieve a good vacuum in a large vessel which had been filled with air than filling an “empty” vessel with air under ambient pressure it is proposed to start Paschen testing from vacuum.

One method is to apply permanently the DC test voltage while increasing the pressure continuously from vacuum till ambient pressure. Such a method is e. g. used during a 5 h 49 min Paschen test on 2 warm instrumentation feedthroughs in combination with 50 m instrumentation cables for TOSKA at Forschungszentrum Karlsruhe, Germany.

An other method is to increase the pressure in steps. The steps should be chosen according to a reasonable possible gap length of the fault location in the ground location. Taking into account the minimum thickness of the ITER TF ground insulation (without filler and radial plate insulation) of 6 mm much shorter gap lengths than this value are not very likely. Tab. 6-3 shows a set of interesting pressure values and the belonging gap length for Paschen

Minimum conditions with a Paschen Minimum value in air at room temperature of p * d = 7.3 bar µm:

p / hPa	d / mm
0.001	7300
0.01	730
0.1	73
0.3	24
0.5	15
0.73	10
0.91	8 (≈ radial plate insulation + ground wrap)
1	7.3
5	1.5
10	0.73
100	0.073
1000	0.0073

Tab. 6-3 Proposal of pressure steps for Paschen test of ITER TF by considering the belonging gap lengths in air for reaching Paschen Minimum conditions.

Usually the Paschen tests are performed at room temperature because otherwise the vacuum vessel would need an additional vacuum shield.

6.10 Long-term high voltage testing of conductor and radial plate insulation

Fast discharges are expected to be rare events during ITER operation, e. g. a number of 50 fast discharges is the design value for ITER TF. Equivalent discharge time is some seconds (e. g. 11 s for TF). On this basis 1 min DC testing seems sufficient and 1 min AC test with its 3000 cycles causes a high stress compared with the nominal operation mode of the TF coils. On the other hand test proposals for ITER TF in [Fin04] recommend the continuous applying of DC voltage during a Paschen Minimum test, i. e. during several hours. In addition for partial discharge investigations it is also recommended to avoid a 1 min limitation for AC tests, and a high voltage design which is only optimised for 1 min tests can have major uncertainties for quality assurance control compared to a “long term” design. The test voltages are

listed in Tab. 6-2. Practical investigations are necessary to clarify if these test voltages can cause degradation of the electrical insulation.

6.10.1 Selection of insulation type

It was decided to use the ITER TFMC for a long-term test at room temperature, because the TFMC was not foreseen for other additional experiments after the two test phases described in [Ulb05]. A test time of 10 hours for each voltage step was defined, which is very long compared to the rated high voltage discharge operation of ITER TF.

The known fault in the ground insulation of TFMC makes it not recommendable to test in detail this insulation of TFMC with the value of Tab. 6-1. Instead, the conductor insulation was chosen because it is the most critical part for a well manufactured TF coil. The capacitance of 1.4 µF makes it not possible to examine the complete conductor insulation length because the available AC equipment is not able to produce sufficient reactive power. Therefore only one DP conductor length was tested.

6.10.2 First long term test series

In the first series (sequence in Tab. 6-4) radial plate number 4 was grounded and the conductor and all other radial plates were connected with high voltage (Fig. 6-11, Fig. 6-13).

Waveform	Voltage / kV_{rms}
DC	5.00
AC	3.54
DC	7.07
AC	5.00
DC	11.0
AC	7.78

Tab. 6-4 Test sequence on radial plate number 4.

Hence not only the insulation between conductor and radial plate 4 was tested but also the insulation to the neighboured radial plates number 3 and 5.

The helium piping system was evacuated, filled with 11 bar of nitrogen gas and this pressure value was continuously observed to avoid flashover in the insulation breaks.

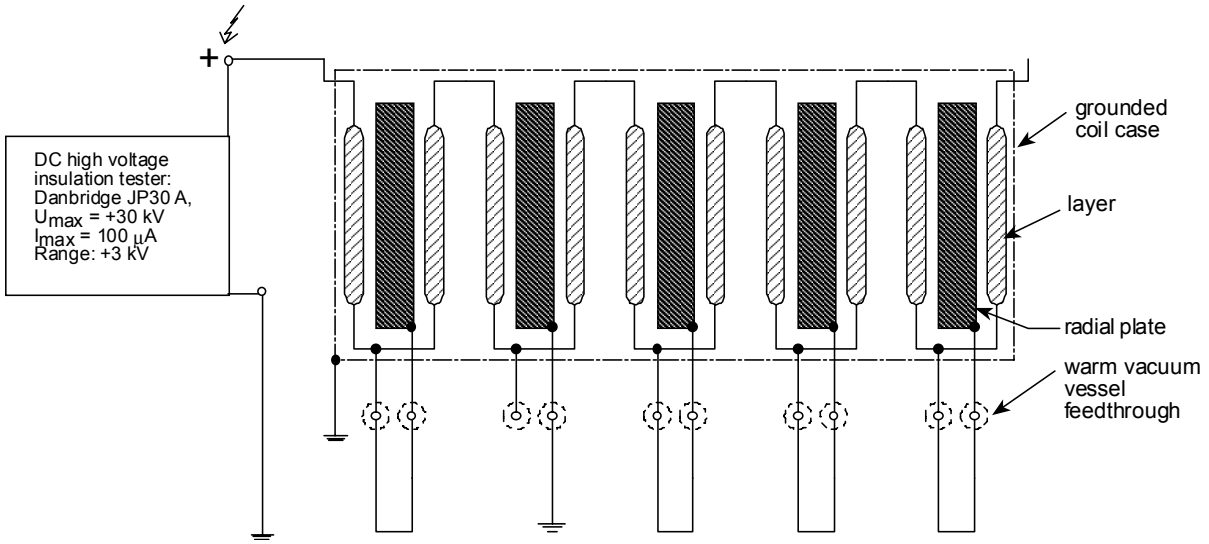

Fig. 6-11 DC test circuit. Only one radial plate is grounded.

The DC tests (Fig. 6-11) were performed in the steps 5 kV, 7.1 kV and 11 kV. For all voltage steps a decreasing of the current with the time was observed. Fig. 6-12 shows the measured current for 11 kV. No degradation was found.

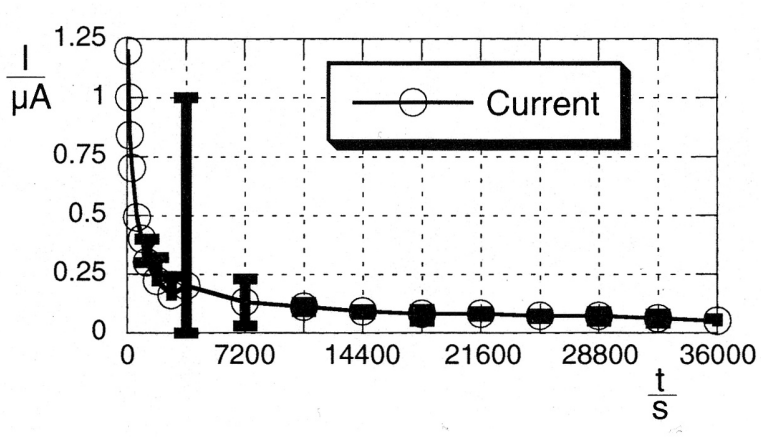

Fig. 6-12 Measured DC current during the 11 kV test depending on the time. The short-term oscillations of the current up to 1 µA at t = 3600 s were caused by the control of the DC power supply. The voltage at the high capacitive sample was not affected by these oscillations within the accuracy of the voltage measurement.

The AC tests (Fig. 6-13) were performed with the steps 3.54 kV, 5.00 kV and 7.78 kV (rms values). The detection impedance for the partial discharge (PD) measurement was connected in series with a coupling capacitor. The PD activity was observed in 1 h periods in an apparent charge vs. time mode. A 1 min PD measurement apparent charge vs. phase angle of the voltage ("PD fingerprint") was carried out after each 1 h period. The current was measured on high voltage side and on primary side of the high voltage transformer.

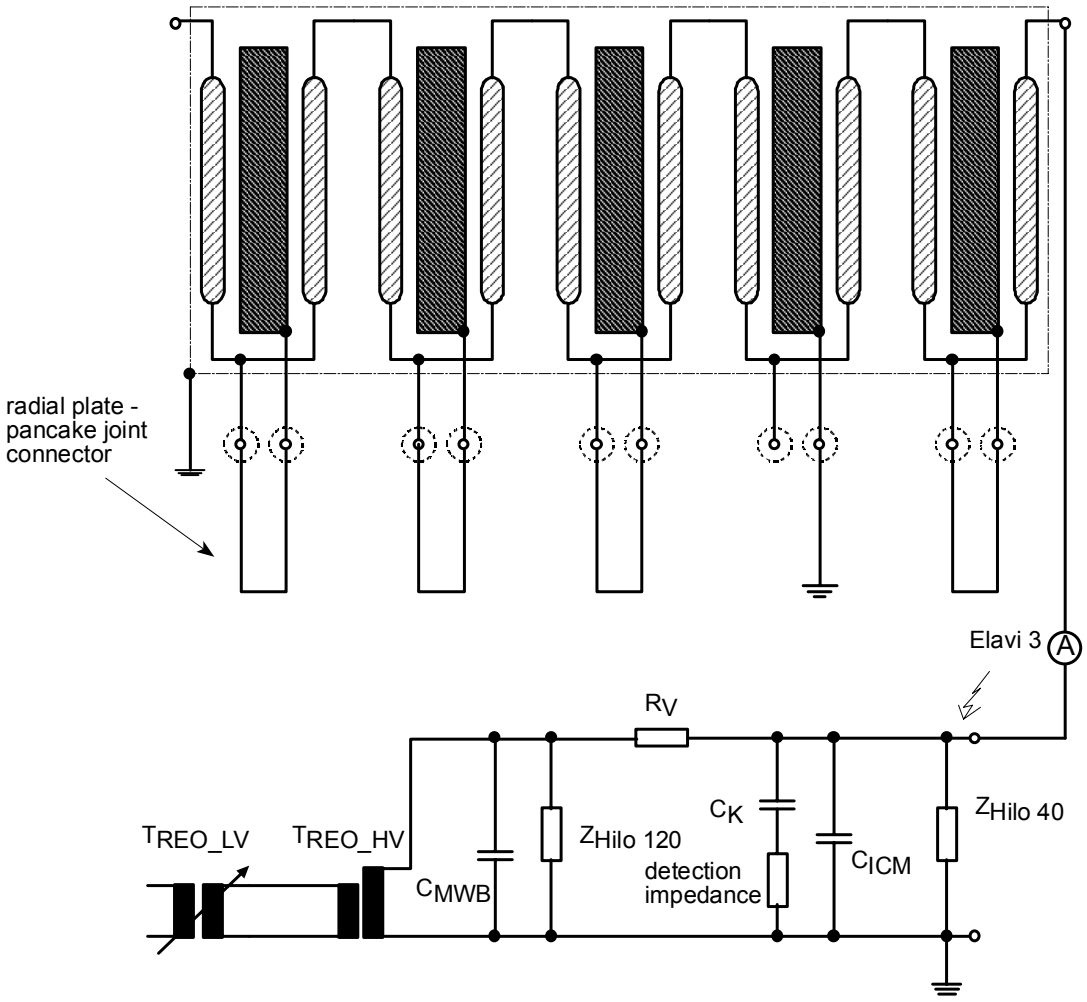

Fig. 6-13 AC test circuit. Only one radial plate is grounded.

During the first and second voltage step all values were in the expected ranges and no breakdown occurred. The fingerprint after 9 hours of 7.78 kV shows no significant change in the PD behaviour – but after about 9 hours 27 min an increase of the apparent charge was observed (Fig. 6-14). A breakdown occurred after 9 hours and 39 min. After this breakdown a permanent degradation of the insulation resistance to 5.6 kΩ was found which makes it impossible to continue with this test.

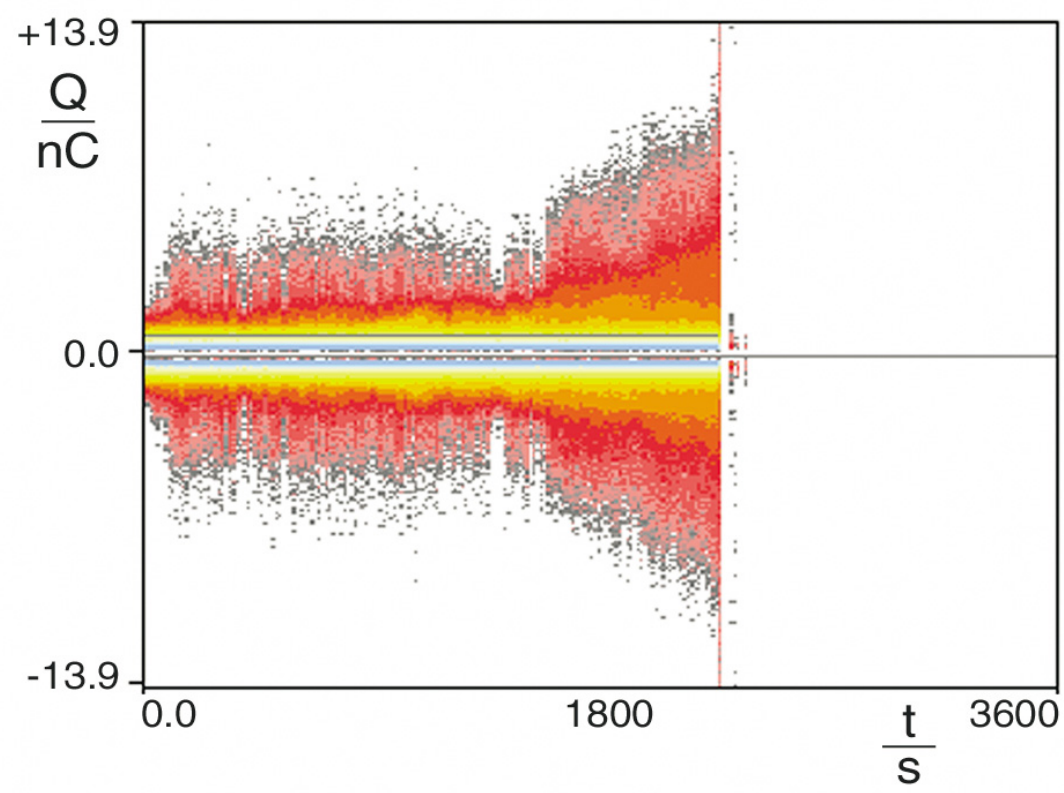

Fig. 6-14 Apparent charge vs. time between hour 9 and 10 of testing with 7.78 kV, i. e. measurement duration for this figure is 1 h and t = 0.0 corresponds to hour 9. The test was stopped after the breakdown (corresponds to 9 h 39 min).

A detailed investigation of the insulation system was performed and finally the fault was localised between radial plate 2 and ground. The conductor and radial plate insulation of radial plate 4 were still fine.

A destruction of the 8 mm ground insulation (combined glass polyimide impregnated with epoxy resin) by a voltage of 7.78 kV is very unlikely, even if some layers are not assembled in a correct way. Hence it was assumed that the fault happened around the path of the wiring which transfers the radial plate potential out of the case. Especially the area, where Tedlar tapes were forgotten to remove during manufacturing, was a good candidate, but a visual determination of the breakdown channel was not possible because the surface in this area is black and rough. The cable screens of all high voltage instrumentation cables are still fine.

6.10.3 Second long term series

It was decided to make a 10 h test with conductor insulation of radial plate 2 as a last test before burn out the fault. In this case the fault location was bridged by connecting radial plate 2 directly with ground and the other radial plates with high voltage. Only the long term tests with the highest voltage values were performed (Tab. 6-5).

Waveform	Voltage / kV_{rms}
DC	11.0
AC	7.78

Tab. 6-5 Test sequence for the grounded radial plate number 2.

The DC test with 11 kV was successfully performed but with higher currents, e. g. after 10 h for the grounded RP4 the value had been $0.05^{+0.01}$ µA and for the grounded RP2 it was $0.38^{\pm 0.02}$ µA.

During AC testing the PD inception starts at 1.7 kV. At the beginning of the voltage step of 7.78 kV the charge was already 12.5 nC which is considerably higher than the measurement before the breakdown with the grounded radial plate 4. Breakdown in this arrangement with the grounded radial plate 2 appeared after a total time of 59 min and 52 s without a prior further increase of charge values.

After the breakdown a resistance of only 85 Ω was detected between conductor (terminal) and ground with the arrangement of the grounded radial plate 2. The resistance between RP 2 and the grounded case was 61 kΩ. The measured values are slightly increasing with the time but remain in the same range.

6.10.4 Burn out

It was tried to burn out the conductor of DP2 to its radial plate although the low resistance value for the conductor insulation fault is far below the specification of the insulation test apparatus. For this purpose the RP 2 was grounded and all other radial plates were connected with the conductor insulation. No light effects were observed during several trials and the protection of the instrument shut down the current very soon. After the trials an insulation resistance of 395 Ω was measured.

Next it was tried to burn out the insulation of RP2 to the grounded case although the resistance value for the fault was below the specification of the insulation test apparatus. For this purpose all radial plates were connected to the conductor. With this method it was clearly visible that the sparks appeared on the second pipe counted from top to bottom at the inner upper slot (Fig. 6-15). This is the high voltage instrumentation cable number 1 which routes the potential of RP2.

Fig. 6-15 Flash above the second tube counted from top at the inner upper slot of the helium inlet tubes.

6.10.5 Conclusion of long-term high voltage test and burn out

10 h testing of ITER TFMC shows that conductor and radial plate insulation can withstand test voltages proposed for ITER in Tab. 6-2. Significant increasing of PD activity before the first breakdown demonstrates that this method can be a valuable tool for monitoring the quality of ITER coil insulation. The first defect appeared in the ground insulation of radial plate 2. Then a fault occurred in the conductor insulation of DP2. Burn out of the ground insulation showed sparks in the upper slot of the helium inlet pipe of DP2. It can be assumed that at least the fault in the insulation between radial plate and the grounded case was caused by the forgotten Tedlar tapes. It is also assumed that this was also the reason for the fault of the conductor insulation.

With these results it is clearly shown that the proposed test voltages cause no relevant degradation even if they are applied for several hours if the insulation is manufactured correctly. Hence a 10 h DC Paschen test and a 5 min AC test with partial discharge measurement can be defined for test duration (1 min PD measurement with charge as function of phase angle of the voltage; 3 min PD measurement with charge as function of time; about 1 min for changing settings).

7 Test sequence and test procedure for ITER TF

This chapter describes the test sequence and preliminary procedure for high voltage testing of ITER TF considering the investigations described in chapter 6. The test sequence should be performed in a way that:

- minimises additional damage in case of an insulation fault,
- minimises assembly work,
- delivers the necessary information.

During the manufacturing process of ITER TF, parts of the coil should already be tested to verify the quality (e. g. DC and AC testing of conductor insulation within one radial plate).

The standard sequence for a completed high voltage apparatus would be DC, AC, impulse in order to minimise the risk of additional destruction at a fault location. For the ITER TF coil the impulse test should be performed after a first DC test because the following DC and AC tests on conductor and radial plate insulation give a detailed information of the insulation status after the impulse test. Making additional DC and AC tests on conductor and radial plate insulation before the impulse test would cause a lot of additional assembly work and is therefore not proposed.

The test voltages must be decided by ITER. Two proposals based on two specific fault scenarios are given in Tab. 6-2.

The increasing of the applied voltage must be performed in defined steps related to the test voltage. The proposal is: 10 %, 30 %, 50 %, 70 %, 90 %, 100 %.

The full set of DC, AC and impulse tests (Tab. 7-1) is relevant for the completed coil.

Test time for DC is up to 10 min to obtain the polarisation index which is the ratio of the insulation resistances at 1 min and 10 min. Test time for AC testing is about 5 min (1 min PD measurement with charge as function of phase angle of the voltage; 3 min PD measurement with charge as function of time; about 1 min for changing settings). Schering Bridge measurement may take also few minutes (about 5 min, depending on the equipment).

Number	Test arrangement – power supply	Test voltage according to fault case 1 / kV	Test voltage according to fault case 2 / kV	Criterion	Addi-tional informa-tion	Test time at 100 % / min
1	O-DC	18.00	34.00	NB, R		1
2	O-I	5.00	29.60	NB	SW	
3	O-DC	18.00	34.00	NB, R		1
4	G-DC	18.00	34.00	NB, R		10
5	G-AC	12.73	24.04	NB, IC	PD	5
6	G-ACS	12.73	24.04	NB	DF	
7	R-DC	5.00	11.00	NB, R		10
8	R-AC	3.54	7.78	NB, IC	PD	5
9	C-DC	5.00	11.00	NB, R		10
10	C-AC	3.54	7.78	NB, IC	PD	5
11	O-DC	18.00	34.00	NB, R		1

Tab. 7-1 Test procedure for a complete acceptance test. AC voltages are given as rms values.
Row 2: O: operation mode, G: ground insulation, R: radial plate insulation, C: conductor insulation, I: impulse, ACS: AC excitation with Schering Bridge measurement. (Test arrangements O, G, R, C are explained in chapter 6.6. Power supplies I, DC, AC, ACS are explained in 6.7) Row 5: NB: no breakdown, R: insulation resistance, IC: constant charging current. (Criterions NB, R, IC are explained in chapter 6.8.) Row 6: PD: partial discharge, DF: dissipation factor, SW: shape of waveform. (Additional information PD, DF, SW are explained in chapter 6.8).

A room temperature test under Paschen Minimum conditions is necessary with G-DC (or O-DC). This test can be done after the DC test under ambient conditions (and before the impulse test).

A full acceptance test is recommended for ITER TF single coils:

- after completion of fabrication under ambient conditions,
- for a cold test,
- after the cold test.

Depending on the boundary conditions of the available equipment (vacuum vessel, impulse generator) it will be defined if these tests are performed on site or by the manufacturer. At least the DC and AC tests should be performed at the manufacturer to reduce the probability of a re-transportation in case of a necessary repair by the manufacturer. At least the test G-DC at full voltage level should be performed on site if all tests are possible at the manufacturer and the transport causes only acceptable mechanical stress. The ITER site must have a high voltage mode which allows a high voltage test with the maximum test voltage level after installation of all coils. A Paschen test on the completed coil system is necessary.

A routine DC check is necessary for the complete coil system before a new current operation period starts.

Depending on the boundary conditions of the switching circuit it may be discussed if a full acceptance test should be performed after installation in the ITER TF system. In this case a second high voltage mode must make it possible to separate each pair of coils from the FDUs. Because each pair of TF coils has a cold connection (in order to decrease the number of current leads) the coils cannot be tested individually in the ITER facility after final assembly. Therefore a two coils impulse test must be investigated by calculation before application.

A reduced test sequence should be performed during manufacturing. Before impregnation with the radial plate insulation the tests C-DC and C-AC should be performed to verify the dielectric strength of the conductor insulation. After insulation of a radial plate the tests R-DC and R-AC should be performed with half of the voltage level. For the simulation of a neighboured radial plate during this test the radial plate is covered with grounded objects e. g. metallic foils.

The tests R-DC and R-AC should be performed with the full maximum voltage after stacking of the radial plate pack (i.e. the 7 radial plates are stacked together) to ensure that the radial plate insulation fulfils the specification.

More detailed test procedures are necessary if more details of the high voltage components, facility and test equipment are known, e. g. containing the pressure values and kind of gas in the axial insulation breaks during room temperature tests. Safety aspects are described in [Fin04].

8 Conclusion

High voltage insulation co-ordination of the superconducting coils is an important issue for a reliable operation of ITER. The results of the calculation of voltage stress within the PF coils will be used to define voltages and procedures for testing of the electrical insulation of the coils. In order to obtain appropriate models for the investigation of the terminal and internal voltages of PF coils the calculation strategy uses the Finite Element Method program Maxwell2D and the network program PSpice. The CS PF system related constituents of this report are:

- The establishing of the simplified Finite Element Method model of the CS PF coil system and the detailed Finite Element Method models of the PF 3 and PF 6 coils. The PF and CS models reflect the status of [DDD06].

- The results of the Finite Element Method calculation, which were taken into network models as lumped elements.

- The establishing of the network model of the CS PF coil system, which includes the power supply, switching network units, fast discharge units, simplified models of the coils and the magnetic coupling of the coil system, which will be used for calculation of voltage excitation on the coil terminals during the normal operation and the fast discharge.

- The establishing of the detailed network models of the PF 3 and PF 6 coils, which were used for calculation in frequency domain and further will be used for calculation of voltage stress within the coils in time domain.

- The resonance frequencies of the PF 3 and PF 6 coils, which were calculated with detailed network models in frequency domain. Additionally the influence of the instrumentation cables and unsymmetrical grounding of the coils were analysed with the detailed network models.

AC, DC and impulse test voltages for ITER TF coils were proposed using the results from previous calculations of two different fault events. A verification of the proposed test voltages for the conductor and radial plate insulation of ITER TF was performed on the ITER TF Model Coil in order to prove that no relevant degradation occurs even if the proposed AC and DC test voltages are applied for several hours. Finally high voltage test procedures were described for ITER TF under special consideration of a Paschen test.

9 References

[aaa00] Dummy

[Bar05] B. Bareyt, Electrical Connections from the CCUs to the Resistors and to the Capacitors (Part of WBS 4.1); June 2005; ITER_D_22J2TY

[Bau98] K. Bauer, S. Fink, G. Friesinger, A. Ulbricht, F. Wüchner, The electircal insulation system of forced flow cooled superconducting (sc) magnet, Cryogenics 38 (1998) pp. 1123-1134

[CDA1] Design Description Document, DDD 1.1 Magnet, 1.2 Component Description, Annex 1: Feeder Design

[CDA3] Design Description Document, DDD 1.1 Magnet, 1.2 Component Description, Annex 3: Control and Instrumentation

[CDA4] Design Description Document, DDD1.1 Magnet, 1.2 Component Description, Annex 4: Electrical Insulation Design and Monitoring

[CDA4a] Design Description Document, DDD1.1 Magnet, 1.2 Component Description, Annex 4: Electrical Insulation Design and Monitoring, Fig. 3-4 p. 16

[Con03] Contract between The European Atomic Energy Community and Euratom / FZK Association, FU06-CT 2003 - 00119, EFDA/03-1055, Brussels, 10th October, 2003

[Dat1] Data sheet, Westcode, Westpack Phase Control Thyristor Type N1174JK200 to N1174JK220, February 2007

[DDD01] Design Description Document DDD 11 Magnet, 1. Engineering Description, 1.1 System Description, 1.2 Component Descriptions, 1.3 Magnet Procurement Packages, N 11 DDD 142 01-07-12 R 0.1

[DDD06] Design Description Document, DDD 1.1 Magnet, Section 1. Engineering Description, October 2006

[DDD06a] Design Description Document, DDD 1.1 Magnet, Section 1. Engineering Description, October 2006, Tab. 1.2.3-5 p. 103, Tab. 1.2.4-1 p. 110

[DDD06b] Design Description Document, DDD 1.1 Magnet, Section 1. Engineering Description, October 2006, Tab. 1.2.4-7 p. 114

[DDD06c] Design Description Document, DDD 1.1 Magnet, Section 1. Engineering Description, October 2006, p. 113

[DDD06d] Design Description Document, DDD 1.1 Magnet, Section 1. Engineering Description, October 2006, p. 115

[DDD06e] Design Description Document, DDD 1.1 Magnet, Section 1. Engineering Description, October 2006, Tab. 1.2.4-8 p. 116

[DDD06f] Design Description Document, DDD 1.1 Magnet, Section 1. Engineering Description, October 2006, p. 102

[DDD06g] Design Description Document, DDD 1.1 Magnet, Section 1. Engineering Description, October 2006, p. 18

[DDD06h] Design Description Document, DDD 1.1 Magnet, Section 1. Engineering Description, October 2006, Tab. 1.2.6-4, p. 123

[DDD06i] Design Description Document, DDD 1.1 Magnet, Section 1. Engineering Description, October 2006, pp. 120 - 125

[DDD06j] Design Description Document, DDD 1.1 Magnet, Section 1. Engineering Description, October 2006, p. 48

[DDDD1] Design Description Documents Drawings, 12.0187.0001

[DDDD2] Design Description Documents Drawings, 12.000438.02, 12.000438.03, 12.000438.04

[DDDD3] Design Description Documents Drawings, 12.000439.01, 12.000439.03, 12.000442.02, 12.000442.06, 12.000380.02, 12.000446.02, 12.000446.05, 13.000373.04, 13.000373.06

[DDDD4] Design Description Documents Drawings, 12.000426.02, 12.000439.02, 12.000439.03, 12.000446.01, 12.000446.02, 12.000446.05, 12.000427.01

[DRG1a] Design Requirements and Guidelines Level 1, Magnet Superconducting and Electrical Design Criteria, N 11 FDR 12 01-07-02 R 0.1, p. 47

[DRGAa] Annex to Design Requirements and Guidelines Level 1, Superconducting Material Database, Article 5. Thermal, Electrical and Mechanical Properties of Materials at Cryogenic Temperatures, p. 3, p. 8

[DRGAb] Annex to Design Requirements and Guidelines Level 1, Superconducting Material Database, Article 5. Thermal, Electrical and Mechanical Properties of Materials at Cryogenic Temperatures, p. 37

[Fas70a] W. G. Fastowski, J. W. Petrowski, A. E. Rowinski, Kryotechnik, Akademie Verlag, Berlin 1970, p. 342

[Fin04] A. Fink, W. H. Fietz, A. M. Miri, X. Quan, A. Ulbricht, Study of the Transient Voltage Behaviour of the Present ITER TF Coil Design for Determination of the Test Voltages and Procedures, Forschungszentrum Karlsruhe, Scientific Report FZKA 7053, 2004

[Gro62] F. W. Grover, Inductance Calculations, Dover Publications, New York, 1962

[IEC60071] IEC 60071-1, Insulation co-ordination, International Electrotechnical commission, Edition 8.0, 2006

[ITER01] www.iter.org

[Max99] Maxwell2D Field Simulator, Ansoft Corporation, Pittsburgh, 1999

[Orc07] OrCAD Capture PSpice 16.0, Cadence Design Systems Inc, 2007

[PAC1] Design Description Document 1.1 Magnet, 2 Performance Analysis, 2.1 Conductor Design and Analysis, N 11 DDD 156 01-07-13 R 0.1

[PAF6A] Design Description Document 1.1 Magnet, 2 Performance Analysis, 2.4 Fault and Safety Analysis, Annex 6A, Assessment of the TF coil circuit behaviour during normal and fault conditions, B. Bareyt, N 41 RI 34 00-11-01 W 0.1

[PAF6Ba] Design Description Document 1.1 Magnet, 2 Performance Analysis, 2.4 Fault and Safety Analysis, Annex 6B, Assessment of the PF coil circuit behaviour during normal and fault conditions, B. Bareyt, N 41 RI 35 00-11-01 W 0.1, pp. 2 - 3

[PAF6Bb] Design Description Document 1.1 Magnet, 2 Performance Analysis, 2.4 Fault and Safety Analysis, Annex 6B, Assessment of the PF coil circuit behaviour during normal and fault conditions, B. Bareyt, N 41 RI 35 00-11-01 W 0.1, Tab. 3.7 p. 13

[PAF6Bc] Design Description Document 1.1 Magnet, 2 Performance Analysis, 2.4 Fault and Safety Analysis, Annex 6B, Assessment of the PF coil circuit behaviour during normal and fault conditions, B. Bareyt, N 41 RI 35 00-11-01 W 0.1, pp. 6-10

[PAF6Bd] Design Description Document 1.1 Magnet, 2 Performance Analysis, 2.4 Fault and Safety Analysis, Annex 6B, Assessment of the PF coil circuit behaviour during normal and fault conditions, B. Bareyt, N 41 RI 35 00-11-01 W 0.1, p. 7

[PPA3] Design Description Document, DDD1.1 Magnet, 1.3 Procurement Packages, Annex 3: Poloidal Field Coils

[PPS1] Design Description Document 4.1, Pulsed Power Supplies, N 41 DDD 16 01-07-06 R 0.3

[PPS1a] Design Description Document 4.1, Pulsed Power Supplies, N 41 DDD 16 01-07-06 R 0.3, p. 19

[PPS1b] Design Description Document 4.1, Pulsed Power Supplies, N 41 DDD 16 01-07-06 R 0.3, Tab. 1.2.2-6 pp. 75 - 76

[PPSA1] Design Description Document 4.1 Pulsed Power Supplies, Appendix A, Equipment List and Technical Data Tables, N 41 DDD 18 01-07-06 R 0.3

[PPSA1a] Design Description Document 4.1 Pulsed Power Supplies, Appendix A, Equipment List and Technical Data Tables, N 41 DDD 18 01-07-06 R 0.3, p. 23

[PPSA1b] Design Description Document 4.1 Pulsed Power Supplies, Appendix A, Equipment List and Technical Data Tables, N 41 DDD 18 01-07-06 R 0.3, pp. 30 - 33

[PPSD1] Pulsed Power Supply Drawings, 41.0024.0001, 41.0025.0001, 41.0026.0001, 41.0027.0001, 41.0028.0001, 41.0029.0001, 41.0030.0001, 41.0031.0001

[PPSD2] Pulsed Power Supply Drawings, 41.0040.0001

[SLBa] Design Description Document, DDD 6.2 Site Layout and Buildings - Introduction, N 62 DDD 22 01-07-18 R 0.1

[SLBD1] Drawings DDD 6.2 Site Layout and Buildings, 62.0377.0001, 62.0333.0001-0015, 62.0357.0001-0004

[Ulb05] A. Ulbricht, et al., The ITER toroidal field model coil project, Fusion Engineering and Design 73 (2005), pp. 189-327

10 IPR

The results obtained within the studies performed under this task did not yield any specific innovation or intellectual property.

This work, supported by the European Communities under the contract of Association between EURATOM and Forschungszentrum Karlsruhe, was carried out within the framework of the European Fusion Development Agreement. The views and opinions expressed herein do not necessarily reflect those of the European Commission.

Annex A Detailed Data of the FEM Models

Annex A.1 FEM Model of CS PF Coil System

Model Definition

Solver: Magnetostatic Symmetry: RZ-Plane

Drawing Size: Z-direction: ±30 m; R-direction: 40 m

Coil Name	Location of the starting point		Model dimensions	
	R-direction (m)	Z-direction (m)	R-direction (m)	Z-direction (m)
CS3U	1.36	4.3	0.719	2.091
CS2U	1.36	2.16	0.719	2.091
CS1U	1.36	0.025	0.719	2.091
CS1L	1.36	-2.11	0.719	2.091
CS2L	1.36	-4.25	0.719	2.091
CS3L	1.36	-6.39	0.719	2.091
PF 1	3.459	7.069	0.968	0.976
PF 2	7.995	6.233	0.649	0.595
PF 3	11.643	2.782	0.708	0.966
PF 4	11.643	-2.726	0.649	0.966
PF 5	7.985	-7.203	0.82	0.945
PF 6	3.447	-8.045	1.633	0.976

Tab. A.1-1 Dimensions of the FEM model for Maxwell 2D of CS PF coil system

Materials

CS and PF coils: Copper with relative permeability = 1

Background: Vacuum with relative permeability = 1

Setup Boundaries and Sources

Current Source All superconducting cables are stranded with 45 kA

Boundary Balloon

Setup Executive Parameters

All coils were chosen into the impedance matrix.

Return path of the current was set to default.

Setup Solution Options

Mesh: Initial mesh

Percent refinement per pass: 5

Number of requested passes: 70

Percent error: 0.1

Convergence Data

Number of complete passes	Number of triangles	Energy Error (%)
70	62561	0.1895

(a) Calculation Results of Simplified FEM Model of CS PF Coil System

	CS3U	CS2U	CS1U	CS1L	CS2L	CS3L
CS3U	2.580E-06					
CS2U	7.998E-07	2.580E-06				
CS1U	1.735E-07	7.999E-07	2.580E-06			

CS1L	5.943E-08	1.735E-07	7.999E-07	2.580E-06		
CS2L	2.644E-08	5.943E-08	1.735E-07	7.999E-07	2.580E-06	
CS3L	1.386E-08	2.643E-08	5.940E-08	1.735E-07	7.996E-07	2.580E-06
PF 1	9.969E-07	4.429E-07	2.053E-07	1.059E-07	6.026E-08	3.703E-08
PF 2	6.977E-07	5.726E-07	4.150E-07	2.846E-07	1.933E-07	1.329E-07
PF 3	4.732E-07	4.953E-07	4.711E-07	4.108E-07	3.356E-07	2.630E-07
PF 4	2.967E-07	3.725E-07	4.437E-07	4.894E-07	4.916E-07	4.491E-07
PF 5	1.298E-07	1.879E-07	2.756E-07	4.011E-07	5.551E-07	6.833E-07
PF 6	4.249E-08	6.845E-08	1.185E-07	2.240E-07	4.628E-07	9.721E-07

Tab. A.1-2 Impedance matrix of the simplified FEM models of CS and PF coils (H)

	PF 1	PF 2	PF 3	PF 4	PF 5	PF 6
PF 1	1.138E-05					
PF 2	3.936E-06	3.635E-05				
PF 3	2.169E-06	1.124E-05	5.342E-05			
PF 4	1.156E-06	5.259E-06	1.434E-05	5.379E-05		
PF 5	4.477E-07	1.886E-06	4.530E-06	9.758E-06	3.310E-05	
PF 6	1.332E-07	5.302E-07	1.187E-06	2.318E-06	4.735E-06	1.116E-05

Tab. A.1-3 Impedance matrix of the simplified FEM models of PF coils (H)

Annex A.2 FEM Models of the PF 3 Coil

(a) FEM Model of the PF 3 Coil for DC

Model Definition

Solver: Magnetostatic Symmetry: RZ-Plane

Drawing Size: Z-direction: ±10 m; R-direction: 20 m

Geometry:

Cooling Tube 1_1: Circle centre: 11672.25 mm; 452.75 mm; Radius: 6 mm

Superconducting cable 1_1: Circle centre: 11672.25 mm; 452.75 mm; Radius: 17.2 mm

Jacket 1_1: First corner: 11646.2 mm; 426.7 mm

Second corner: 11698.3 mm; 478.8 mm

Copy of the conductor 1_1 downwards one time with a distance of 59.5 mm

Copy of the conductor 2_1 downwards one time with a distance of 61.5 mm with consideration of additionally insulation between the double pancakes of 2 mm

Continuing of copy of the conductors downwards with distance depending on the location in the double pancake

Copy of the stack of the 16 first conductors rightwards 12 times with a distance of 59 mm

Materials

Cooling tube	Vacuum, relative permittivity = 1, relative permeability = 1
Superconducting cable	Copper at 4K, relative permittivity = 1, relative permeability = 1, conductivity = 6.4E9 S/m
Stainless steel jacket	Stainless steel at 4K, relative permittivity = 1, relative permeability = 1, conductivity = 1.88e6 S/m
Insulation	Epoxy resin, relative permittivity = 4, relative permeability = 1
Background:	Vacuum, relative permittivity = 1, relative permeability = 1

Setup Boundaries and Sources

Current Source All superconducting cables are stranded with 45 kA

Boundary Balloon

Setup Executive Parameters

All superconducting cables were chosen into the impedance matrix.

Return path of the current was set to default.

Setup Solution Options

Mesh: Manual mesh

Object	Insulation	Cooling Tube	Superconducting cable	Stainless steel jacket	Background
Number of triangles	52124	70	430	750	67290

(b) FEM Model of PF 3 Coil for Frequencies lower than 5 kHz

Model Definition

Solver: Eddy Current Symmetry: RZ-Plane

Drawing Size: Z-direction: +10 m; R-direction: 20 m

Materials

Cooling tube Vacuum, relative permittivity = 1, relative permeability = 1

Superconducting cable Copper at 4K, relative permittivity = 1, relative permeability = 1, conductivity = 6.4E9 S/m

Stainless steel jacket Stainless steel at 4K, relative permittivity = 1, relative permeability = 1, conductivity = 1.88e6 S/m

Insulation Epoxy resin, relative permittivity = 4, relative permeability = 1

Background: Vacuum, relative permittivity = 1, relative permeability = 1

Setup Boundaries and Sources

Current Source All superconducting cables are stranded with 45 kA

Boundary Bottom edge of the model boundary = even symmetry

Other three edges of the model boundary = balloon

Setup Executive Parameters

All superconducting cables were chosen into the impedance matrix.

Return path of the current was set to default.

Setup Solution Options

Mesh: Manual mesh

Object	Insulation	Cooling Tube	Superconducting cable	Stainless steel jacket	Background
Number of triangles	70000	10	48	350	26000

(c) FEM Model of PF 3 Coil for Frequencies higher than 5 kHz

Model Definition

Solver: Eddy Current Symmetry: RZ-Plane

Drawing Size: Z-direction: ±5 m; R-direction: 10 m

Materials

Cooling tube Vacuum, relative permittivity = 1, relative permeability = 1

Superconducting cable Copper at 4K, relative permittivity = 1, relative permeability = 1, conductivity = 6.4E9 S/m

Stainless steel jacket Stainless steel at 4K, relative permittivity = 1, relative permeability = 1, conductivity = 1.88e6 S/m

Insulation Epoxy resin, relative permittivity = 4, relative permeability = 1

Background: Vacuum, relative permittivity = 1, relative permeability = 1

Setup Boundaries and Sources

Current Source All superconducting cables are stranded with 45 kA

Boundary Balloon

Setup Executive Parameters

All superconducting cables were chosen into the impedance matrix.

Return path of the current was set to default.

Setup Solution Options

Mesh: Manual mesh

Object	Insulation	Cooling Tube	Superconducting cable	Stainless steel jacket	Background
Number of triangles	1500	22	150	230	1300

(d) Calculation Results of Detailed FEM Model of the PF 3 Coil

Capacitances of conductors between the layers in one double pancake (F)		Capacitances of conductors between double pancakes(F)		Capacitances between the conductors of one layer (F)	
C_P01_02_C01	1.829E-08	C_P02_03_C01	1.44E-08	C_P01_C01_02	1.97E-08
C_P01_02_C02	1.838E-08	C_P02_03_C02	1.45E-08	C_P01_C02_03	1.98E-08
C_P01_02_C03	1.847E-08	C_P02_03_C03	1.45E-08	C_P01_C03_04	1.99E-08
C_P01_02_C04	1.856E-08	C_P02_03_C04	1.46E-08	C_P01_C04_05	2.00E-08
C_P01_02_C05	1.866E-08	C_P02_03_C05	1.47E-08	C_P01_C05_06	2.01E-08
C_P01_02_C06	1.875E-08	C_P02_03_C06	1.48E-08	C_P01_C06_07	2.02E-08
C_P01_02_C07	1.884E-08	C_P02_03_C07	1.48E-08	C_P01_C07_08	2.03E-08
C_P01_02_C08	1.893E-08	C_P02_03_C08	1.49E-08	C_P01_C08_09	2.04E-08
C_P01_02_C09	1.903E-08	C_P02_03_C09	1.50E-08	C_P01_C09_10	2.05E-08
C_P01_02_C10	1.912E-08	C_P02_03_C10	1.51E-08	C_P01_C10_11	2.06E-08
C_P01_02_C11	1.921E-08	C_P02_03_C11	1.51E-08	C_P01_C11_12	2.07E-08
C_P01_02_C12	1.930E-08	C_P02_03_C12	1.52E-08		

Tab. A.2-1 Calculated capacitances between the conductors of PF 3 coil

Capacitances of the conductors to ground in lowest and uppermost pancakes (F)		Capacitance to ground for outer conductors on the left and right side of the coil (F)		Capacitance to ground for lowest and uppermost outer conductors in Z-direction (F)	
C_P01_E_C01	1.975E-08	C_P02_E_C01	1.02E-08	C_P01_E_C01	9.529E-09
C_P01_E_C02	9.578E-09	C_P02_E_C12	1.05E-08	C_P01_E_C12	1.005E-08
C_P01_E_C03	9.626E-09				
C_P01_E_C04	9.675E-09				
C_P01_E_C05	9.723E-09				
C_P01_E_C06	9.771E-09				
C_P01_E_C07	9.819E-09				
C_P01_E_C08	9.867E-09				
C_P01_E_C09	9.915E-09				
C_P01_E_C10	9.964E-09				
C_P01_E_C11	1.001E-08				
C_P01_E_C12	2.051E-08				

Tab. A.2-2 Calculated capacitances of the outer conductors to ground of PF 3 coil

SC_1_1	8.90E-03	SC_5_1	9.60E-03	SC_9_1	9.79E-03	SC_13_1	9.48E-03
SC_1_2	9.12E-03	SC_5_2	9.90E-03	SC_9_2	1.01E-02	SC_13_2	9.76E-03
SC_1_3	9.31E-03	SC_5_3	1.01E-02	SC_9_3	1.04E-02	SC_13_3	1.00E-02
SC_1_4	9.45E-03	SC_5_4	1.03E-02	SC_9_4	1.06E-02	SC_13_4	1.02E-02
SC_1_5	9.56E-03	SC_5_5	1.05E-02	SC_9_5	1.07E-02	SC_13_5	1.03E-02
SC_1_6	9.63E-03	SC_5_6	1.06E-02	SC_9_6	1.08E-02	SC_13_6	1.04E-02
SC_1_7	9.66E-03	SC_5_7	1.06E-02	SC_9_7	1.08E-02	SC_13_7	1.04E-02
SC_1_8	9.65E-03	SC_5_8	1.06E-02	SC_9_8	1.08E-02	SC_13_8	1.04E-02
SC_1_9	9.61E-03	SC_5_9	1.05E-02	SC_9_9	1.07E-02	SC_13_9	1.03E-02
SC_1_10	9.52E-03	SC_5_10	1.04E-02	SC_9_10	1.06E-02	SC_13_10	1.02E-02
SC_1_11	9.40E-03	SC_5_11	1.02E-02	SC_9_11	1.04E-02	SC_13_11	1.01E-02
SC_1_12	9.23E-03	SC_5_12	9.96E-03	SC_9_12	1.01E-02	SC_13_12	9.82E-03
SC_2_1	9.13E-03	SC_6_1	9.69E-03	SC_10_1	9.76E-03	SC_14_1	9.32E-03
SC_2_2	9.38E-03	SC_6_2	1.00E-02	SC_10_2	1.01E-02	SC_14_2	9.59E-03
SC_2_3	9.58E-03	SC_6_3	1.02E-02	SC_10_3	1.03E-02	SC_14_3	9.81E-03
SC_2_4	9.74E-03	SC_6_4	1.04E-02	SC_10_4	1.05E-02	SC_14_4	9.99E-03
SC_2_5	9.86E-03	SC_6_5	1.06E-02	SC_10_5	1.07E-02	SC_14_5	1.01E-02
SC_2_6	9.93E-03	SC_6_6	1.07E-02	SC_10_6	1.08E-02	SC_14_6	1.02E-02
SC_2_7	9.96E-03	SC_6_7	1.07E-02	SC_10_7	1.08E-02	SC_14_7	1.02E-02
SC_2_8	9.95E-03	SC_6_8	1.07E-02	SC_10_8	1.08E-02	SC_14_8	1.02E-02
SC_2_9	9.90E-03	SC_6_9	1.06E-02	SC_10_9	1.07E-02	SC_14_9	1.02E-02
SC_2_10	9.80E-03	SC_6_10	1.05E-02	SC_10_10	1.06E-02	SC_14_10	1.00E-02
SC_2_11	9.66E-03	SC_6_11	1.03E-02	SC_10_11	1.04E-02	SC_14_11	9.88E-03
SC_2_12	9.46E-03	SC_6_12	1.00E-02	SC_10_12	1.01E-02	SC_14_12	9.66E-03
SC_3_1	9.32E-03	SC_7_1	9.76E-03	SC_11_1	9.69E-03	SC_15_1	9.13E-03
SC_3_2	9.59E-03	SC_7_2	1.01E-02	SC_11_2	1.00E-02	SC_15_2	9.38E-03
SC_3_3	9.81E-03	SC_7_3	1.03E-02	SC_11_3	1.02E-02	SC_15_3	9.58E-03
SC_3_4	9.99E-03	SC_7_4	1.05E-02	SC_11_4	1.04E-02	SC_15_4	9.74E-03
SC_3_5	1.01E-02	SC_7_5	1.07E-02	SC_11_5	1.06E-02	SC_15_5	9.86E-03
SC_3_6	1.02E-02	SC_7_6	1.08E-02	SC_11_6	1.07E-02	SC_15_6	9.93E-03
SC_3_7	1.02E-02	SC_7_7	1.08E-02	SC_11_7	1.07E-02	SC_15_7	9.96E-03
SC_3_8	1.02E-02	SC_7_8	1.08E-02	SC_11_8	1.07E-02	SC_15_8	9.95E-03
SC_3_9	1.02E-02	SC_7_9	1.07E-02	SC_11_9	1.06E-02	SC_15_9	9.90E-03
SC_3_10	1.00E-02	SC_7_10	1.06E-02	SC_11_10	1.05E-02	SC_15_10	9.80E-03
SC_3_11	9.88E-03	SC_7_11	1.04E-02	SC_11_11	1.03E-02	SC_15_11	9.66E-03
SC_3_12	9.66E-03	SC_7_12	1.01E-02	SC_11_12	1.00E-02	SC_15_12	9.46E-03
SC_4_1	9.48E-03	SC_8_1	9.79E-03	SC_12_1	9.60E-03	SC_16_1	8.90E-03
SC_4_2	9.76E-03	SC_8_2	1.01E-02	SC_12_2	9.90E-03	SC_16_2	9.12E-03
SC_4_3	1.00E-02	SC_8_3	1.04E-02	SC_12_3	1.01E-02	SC_16_3	9.31E-03
SC_4_4	1.02E-02	SC_8_4	1.06E-02	SC_12_4	1.03E-02	SC_16_4	9.45E-03
SC_4_5	1.03E-02	SC_8_5	1.07E-02	SC_12_5	1.05E-02	SC_16_5	9.56E-03
SC_4_6	1.04E-02	SC_8_6	1.08E-02	SC_12_6	1.06E-02	SC_16_6	9.63E-03
SC_4_7	1.04E-02	SC_8_7	1.08E-02	SC_12_7	1.06E-02	SC_16_7	9.66E-03
SC_4_8	1.04E-02	SC_8_8	1.08E-02	SC_12_8	1.06E-02	SC_16_8	9.65E-03
SC_4_9	1.03E-02	SC_8_9	1.07E-02	SC_12_9	1.05E-02	SC_16_9	9.61E-03
SC_4_10	1.02E-02	SC_8_10	1.06E-02	SC_12_10	1.04E-02	SC_16_10	9.52E-03
SC_4_11	1.01E-02	SC_8_11	1.04E-02	SC_12_11	1.02E-02	SC_16_11	9.40E-03
SC_4_12	9.82E-03	SC_8_12	1.01E-02	SC_12_12	9.96E-03	SC_16_12	9.23E-03

Tab. A.2-3 Cumulative inductances for each conductor of PF 3 coil at DC (H)

SC_1_1	1.19E-05	SC_5_1	1.19E-05	SC_9_1	1.19E-05	SC_13_1	1.19E-05
SC_1_2	1.36E-05	SC_5_2	1.36E-05	SC_9_2	1.36E-05	SC_13_2	1.36E-05
SC_1_3	1.37E-05	SC_5_3	1.37E-05	SC_9_3	1.37E-05	SC_13_3	1.37E-05
SC_1_4	1.38E-05	SC_5_4	1.38E-05	SC_9_4	1.38E-05	SC_13_4	1.38E-05
SC_1_5	1.39E-05	SC_5_5	1.39E-05	SC_9_5	1.39E-05	SC_13_5	1.39E-05
SC_1_6	1.39E-05	SC_5_6	1.39E-05	SC_9_6	1.39E-05	SC_13_6	1.39E-05
SC_1_7	1.40E-05	SC_5_7	1.40E-05	SC_9_7	1.40E-05	SC_13_7	1.40E-05
SC_1_8	1.41E-05	SC_5_8	1.41E-05	SC_9_8	1.41E-05	SC_13_8	1.41E-05
SC_1_9	1.41E-05	SC_5_9	1.41E-05	SC_9_9	1.41E-05	SC_13_9	1.41E-05
SC_1_10	1.42E-05	SC_5_10	1.42E-05	SC_9_10	1.42E-05	SC_13_10	1.42E-05
SC_1_11	1.42E-05	SC_5_11	1.42E-05	SC_9_11	1.42E-05	SC_13_11	1.42E-05
SC_1_12	1.26E-05	SC_5_12	1.26E-05	SC_9_12	1.26E-05	SC_13_12	1.26E-05
SC_2_1	1.19E-05	SC_6_1	1.19E-05	SC_10_1	1.19E-05	SC_14_1	1.19E-05
SC_2_2	1.36E-05	SC_6_2	1.36E-05	SC_10_2	1.36E-05	SC_14_2	1.36E-05
SC_2_3	1.37E-05	SC_6_3	1.37E-05	SC_10_3	1.37E-05	SC_14_3	1.37E-05
SC_2_4	1.38E-05	SC_6_4	1.38E-05	SC_10_4	1.38E-05	SC_14_4	1.38E-05
SC_2_5	1.39E-05	SC_6_5	1.39E-05	SC_10_5	1.39E-05	SC_14_5	1.39E-05
SC_2_6	1.39E-05	SC_6_6	1.39E-05	SC_10_6	1.39E-05	SC_14_6	1.39E-05
SC_2_7	1.40E-05	SC_6_7	1.40E-05	SC_10_7	1.40E-05	SC_14_7	1.40E-05
SC_2_8	1.41E-05	SC_6_8	1.41E-05	SC_10_8	1.41E-05	SC_14_8	1.41E-05
SC_2_9	1.41E-05	SC_6_9	1.41E-05	SC_10_9	1.41E-05	SC_14_9	1.41E-05
SC_2_10	1.42E-05	SC_6_10	1.42E-05	SC_10_10	1.42E-05	SC_14_10	1.42E-05
SC_2_11	1.42E-05	SC_6_11	1.42E-05	SC_10_11	1.42E-05	SC_14_11	1.42E-05
SC_2_12	1.26E-05	SC_6_12	1.26E-05	SC_10_12	1.26E-05	SC_14_12	1.26E-05
SC_3_1	1.19E-05	SC_7_1	1.19E-05	SC_11_1	1.19E-05	SC_15_1	1.19E-05
SC_3_2	1.36E-05	SC_7_2	1.36E-05	SC_11_2	1.36E-05	SC_15_2	1.36E-05
SC_3_3	1.37E-05	SC_7_3	1.37E-05	SC_11_3	1.37E-05	SC_15_3	1.37E-05
SC_3_4	1.38E-05	SC_7_4	1.38E-05	SC_11_4	1.38E-05	SC_15_4	1.38E-05
SC_3_5	1.39E-05	SC_7_5	1.39E-05	SC_11_5	1.39E-05	SC_15_5	1.39E-05
SC_3_6	1.39E-05	SC_7_6	1.39E-05	SC_11_6	1.39E-05	SC_15_6	1.39E-05
SC_3_7	1.40E-05	SC_7_7	1.40E-05	SC_11_7	1.40E-05	SC_15_7	1.40E-05
SC_3_8	1.41E-05	SC_7_8	1.41E-05	SC_11_8	1.41E-05	SC_15_8	1.41E-05
SC_3_9	1.41E-05	SC_7_9	1.41E-05	SC_11_9	1.41E-05	SC_15_9	1.41E-05
SC_3_10	1.42E-05	SC_7_10	1.42E-05	SC_11_10	1.42E-05	SC_15_10	1.42E-05
SC_3_11	1.42E-05	SC_7_11	1.42E-05	SC_11_11	1.42E-05	SC_15_11	1.42E-05
SC_3_12	1.26E-05	SC_7_12	1.26E-05	SC_11_12	1.26E-05	SC_15_12	1.26E-05
SC_4_1	1.19E-05	SC_8_1	1.19E-05	SC_12_1	1.19E-05	SC_16_1	1.19E-05
SC_4_2	1.36E-05	SC_8_2	1.36E-05	SC_12_2	1.36E-05	SC_16_2	1.36E-05
SC_4_3	1.37E-05	SC_8_3	1.37E-05	SC_12_3	1.37E-05	SC_16_3	1.37E-05
SC_4_4	1.38E-05	SC_8_4	1.38E-05	SC_12_4	1.38E-05	SC_16_4	1.38E-05
SC_4_5	1.39E-05	SC_8_5	1.39E-05	SC_12_5	1.39E-05	SC_16_5	1.39E-05
SC_4_6	1.39E-05	SC_8_6	1.39E-05	SC_12_6	1.39E-05	SC_16_6	1.39E-05
SC_4_7	1.40E-05	SC_8_7	1.40E-05	SC_12_7	1.40E-05	SC_16_7	1.40E-05
SC_4_8	1.41E-05	SC_8_8	1.41E-05	SC_12_8	1.41E-05	SC_16_8	1.41E-05
SC_4_9	1.41E-05	SC_8_9	1.41E-05	SC_12_9	1.41E-05	SC_16_9	1.41E-05
SC_4_10	1.42E-05	SC_8_10	1.42E-05	SC_12_10	1.42E-05	SC_16_10	1.42E-05
SC_4_11	1.42E-05	SC_8_11	1.42E-05	SC_12_11	1.42E-05	SC_16_11	1.42E-05
SC_4_12	1.26E-05	SC_8_12	1.26E-05	SC_12_12	1.26E-05	SC_16_12	1.26E-05

Tab. A.2-4 Cumulative inductances for each conductor of PF 3 coil at 354 Hz (H)

SC_1_1	1.07E-05	SC_5_1	1.07E-05	SC_9_1	1.07E-05	SC_13_1	1.07E-05
SC_1_2	1.23E-05	SC_5_2	1.23E-05	SC_9_2	1.23E-05	SC_13_2	1.23E-05
SC_1_3	1.24E-05	SC_5_3	1.24E-05	SC_9_3	1.24E-05	SC_13_3	1.24E-05
SC_1_4	1.25E-05	SC_5_4	1.25E-05	SC_9_4	1.25E-05	SC_13_4	1.25E-05
SC_1_5	1.25E-05	SC_5_5	1.25E-05	SC_9_5	1.25E-05	SC_13_5	1.25E-05
SC_1_6	1.26E-05	SC_5_6	1.26E-05	SC_9_6	1.26E-05	SC_13_6	1.26E-05
SC_1_7	1.27E-05	SC_5_7	1.27E-05	SC_9_7	1.27E-05	SC_13_7	1.27E-05
SC_1_8	1.27E-05	SC_5_8	1.27E-05	SC_9_8	1.27E-05	SC_13_8	1.27E-05
SC_1_9	1.28E-05	SC_5_9	1.28E-05	SC_9_9	1.28E-05	SC_13_9	1.28E-05
SC_1_10	1.28E-05	SC_5_10	1.28E-05	SC_9_10	1.28E-05	SC_13_10	1.28E-05
SC_1_11	1.29E-05	SC_5_11	1.29E-05	SC_9_11	1.29E-05	SC_13_11	1.29E-05
SC_1_12	1.12E-05	SC_5_12	1.12E-05	SC_9_12	1.12E-05	SC_13_12	1.12E-05
SC_2_1	1.07E-05	SC_6_1	1.07E-05	SC_10_1	1.07E-05	SC_14_1	1.07E-05
SC_2_2	1.23E-05	SC_6_2	1.23E-05	SC_10_2	1.23E-05	SC_14_2	1.23E-05
SC_2_3	1.24E-05	SC_6_3	1.24E-05	SC_10_3	1.24E-05	SC_14_3	1.24E-05
SC_2_4	1.25E-05	SC_6_4	1.25E-05	SC_10_4	1.25E-05	SC_14_4	1.25E-05
SC_2_5	1.25E-05	SC_6_5	1.25E-05	SC_10_5	1.25E-05	SC_14_5	1.25E-05
SC_2_6	1.26E-05	SC_6_6	1.26E-05	SC_10_6	1.26E-05	SC_14_6	1.26E-05
SC_2_7	1.27E-05	SC_6_7	1.27E-05	SC_10_7	1.27E-05	SC_14_7	1.27E-05
SC_2_8	1.27E-05	SC_6_8	1.27E-05	SC_10_8	1.27E-05	SC_14_8	1.27E-05
SC_2_9	1.28E-05	SC_6_9	1.28E-05	SC_10_9	1.28E-05	SC_14_9	1.28E-05
SC_2_10	1.28E-05	SC_6_10	1.28E-05	SC_10_10	1.28E-05	SC_14_10	1.28E-05
SC_2_11	1.29E-05	SC_6_11	1.29E-05	SC_10_11	1.29E-05	SC_14_11	1.29E-05
SC_2_12	1.12E-05	SC_6_12	1.12E-05	SC_10_12	1.12E-05	SC_14_12	1.12E-05
SC_3_1	1.07E-05	SC_7_1	1.07E-05	SC_11_1	1.07E-05	SC_15_1	1.07E-05
SC_3_2	1.23E-05	SC_7_2	1.23E-05	SC_11_2	1.23E-05	SC_15_2	1.23E-05
SC_3_3	1.24E-05	SC_7_3	1.24E-05	SC_11_3	1.24E-05	SC_15_3	1.24E-05
SC_3_4	1.25E-05	SC_7_4	1.25E-05	SC_11_4	1.25E-05	SC_15_4	1.25E-05
SC_3_5	1.25E-05	SC_7_5	1.25E-05	SC_11_5	1.25E-05	SC_15_5	1.25E-05
SC_3_6	1.26E-05	SC_7_6	1.26E-05	SC_11_6	1.26E-05	SC_15_6	1.26E-05
SC_3_7	1.27E-05	SC_7_7	1.27E-05	SC_11_7	1.27E-05	SC_15_7	1.27E-05
SC_3_8	1.27E-05	SC_7_8	1.27E-05	SC_11_8	1.27E-05	SC_15_8	1.27E-05
SC_3_9	1.28E-05	SC_7_9	1.28E-05	SC_11_9	1.28E-05	SC_15_9	1.28E-05
SC_3_10	1.28E-05	SC_7_10	1.28E-05	SC_11_10	1.28E-05	SC_15_10	1.28E-05
SC_3_11	1.29E-05	SC_7_11	1.29E-05	SC_11_11	1.29E-05	SC_15_11	1.29E-05
SC_3_12	1.12E-05	SC_7_12	1.12E-05	SC_11_12	1.12E-05	SC_15_12	1.12E-05
SC_4_1	1.07E-05	SC_8_1	1.07E-05	SC_12_1	1.07E-05	SC_16_1	1.07E-05
SC_4_2	1.23E-05	SC_8_2	1.23E-05	SC_12_2	1.23E-05	SC_16_2	1.23E-05
SC_4_3	1.24E-05	SC_8_3	1.24E-05	SC_12_3	1.24E-05	SC_16_3	1.24E-05
SC_4_4	1.25E-05	SC_8_4	1.25E-05	SC_12_4	1.25E-05	SC_16_4	1.25E-05
SC_4_5	1.25E-05	SC_8_5	1.25E-05	SC_12_5	1.25E-05	SC_16_5	1.25E-05
SC_4_6	1.26E-05	SC_8_6	1.26E-05	SC_12_6	1.26E-05	SC_16_6	1.26E-05
SC_4_7	1.27E-05	SC_8_7	1.27E-05	SC_12_7	1.27E-05	SC_16_7	1.27E-05
SC_4_8	1.27E-05	SC_8_8	1.27E-05	SC_12_8	1.27E-05	SC_16_8	1.27E-05
SC_4_9	1.28E-05	SC_8_9	1.28E-05	SC_12_9	1.28E-05	SC_16_9	1.28E-05
SC_4_10	1.28E-05	SC_8_10	1.28E-05	SC_12_10	1.28E-05	SC_16_10	1.28E-05
SC_4_11	1.29E-05	SC_8_11	1.29E-05	SC_12_11	1.29E-05	SC_16_11	1.29E-05
SC_4_12	1.12E-05	SC_8_12	1.12E-05	SC_12_12	1.12E-05	SC_16_12	1.12E-05

Tab. A.2-5 Cumulative inductances for each conductor of PF 3 coil at 422 Hz (H)

SC_1_1	4.54E-06	SC_5_1	4.54E-06	SC_9_1	4.54E-06	SC_13_1	4.54E-06
SC_1_2	4.56E-06	SC_5_2	4.56E-06	SC_9_2	4.56E-06	SC_13_2	4.56E-06
SC_1_3	4.59E-06	SC_5_3	4.59E-06	SC_9_3	4.59E-06	SC_13_3	4.59E-06
SC_1_4	4.61E-06	SC_5_4	4.61E-06	SC_9_4	4.61E-06	SC_13_4	4.61E-06
SC_1_5	4.63E-06	SC_5_5	4.63E-06	SC_9_5	4.63E-06	SC_13_5	4.63E-06
SC_1_6	4.66E-06	SC_5_6	4.66E-06	SC_9_6	4.66E-06	SC_13_6	4.66E-06
SC_1_7	4.68E-06	SC_5_7	4.68E-06	SC_9_7	4.68E-06	SC_13_7	4.68E-06
SC_1_8	4.70E-06	SC_5_8	4.70E-06	SC_9_8	4.70E-06	SC_13_8	4.70E-06
SC_1_9	4.73E-06	SC_5_9	4.73E-06	SC_9_9	4.73E-06	SC_13_9	4.73E-06
SC_1_10	4.75E-06	SC_5_10	4.75E-06	SC_9_10	4.75E-06	SC_13_10	4.75E-06
SC_1_11	4.77E-06	SC_5_11	4.77E-06	SC_9_11	4.77E-06	SC_13_11	4.77E-06
SC_1_12	4.80E-06	SC_5_12	4.80E-06	SC_9_12	4.80E-06	SC_13_12	4.80E-06
SC_2_1	4.54E-06	SC_6_1	4.54E-06	SC_10_1	4.54E-06	SC_14_1	4.54E-06
SC_2_2	4.56E-06	SC_6_2	4.56E-06	SC_10_2	4.56E-06	SC_14_2	4.56E-06
SC_2_3	4.59E-06	SC_6_3	4.59E-06	SC_10_3	4.59E-06	SC_14_3	4.59E-06
SC_2_4	4.61E-06	SC_6_4	4.61E-06	SC_10_4	4.61E-06	SC_14_4	4.61E-06
SC_2_5	4.63E-06	SC_6_5	4.63E-06	SC_10_5	4.63E-06	SC_14_5	4.63E-06
SC_2_6	4.66E-06	SC_6_6	4.66E-06	SC_10_6	4.66E-06	SC_14_6	4.66E-06
SC_2_7	4.68E-06	SC_6_7	4.68E-06	SC_10_7	4.68E-06	SC_14_7	4.68E-06
SC_2_8	4.70E-06	SC_6_8	4.70E-06	SC_10_8	4.70E-06	SC_14_8	4.70E-06
SC_2_9	4.73E-06	SC_6_9	4.73E-06	SC_10_9	4.73E-06	SC_14_9	4.73E-06
SC_2_10	4.75E-06	SC_6_10	4.75E-06	SC_10_10	4.75E-06	SC_14_10	4.75E-06
SC_2_11	4.77E-06	SC_6_11	4.77E-06	SC_10_11	4.77E-06	SC_14_11	4.77E-06
SC_2_12	4.80E-06	SC_6_12	4.80E-06	SC_10_12	4.80E-06	SC_14_12	4.80E-06
SC_3_1	4.54E-06	SC_7_1	4.54E-06	SC_11_1	4.54E-06	SC_15_1	4.54E-06
SC_3_2	4.56E-06	SC_7_2	4.56E-06	SC_11_2	4.56E-06	SC_15_2	4.56E-06
SC_3_3	4.59E-06	SC_7_3	4.59E-06	SC_11_3	4.59E-06	SC_15_3	4.59E-06
SC_3_4	4.61E-06	SC_7_4	4.61E-06	SC_11_4	4.61E-06	SC_15_4	4.61E-06
SC_3_5	4.63E-06	SC_7_5	4.63E-06	SC_11_5	4.63E-06	SC_15_5	4.63E-06
SC_3_6	4.66E-06	SC_7_6	4.66E-06	SC_11_6	4.66E-06	SC_15_6	4.66E-06
SC_3_7	4.68E-06	SC_7_7	4.68E-06	SC_11_7	4.68E-06	SC_15_7	4.68E-06
SC_3_8	4.70E-06	SC_7_8	4.70E-06	SC_11_8	4.70E-06	SC_15_8	4.70E-06
SC_3_9	4.73E-06	SC_7_9	4.73E-06	SC_11_9	4.73E-06	SC_15_9	4.73E-06
SC_3_10	4.75E-06	SC_7_10	4.75E-06	SC_11_10	4.75E-06	SC_15_10	4.75E-06
SC_3_11	4.77E-06	SC_7_11	4.77E-06	SC_11_11	4.77E-06	SC_15_11	4.77E-06
SC_3_12	4.80E-06	SC_7_12	4.80E-06	SC_11_12	4.80E-06	SC_15_12	4.80E-06
SC_4_1	4.54E-06	SC_8_1	4.54E-06	SC_12_1	4.54E-06	SC_16_1	4.54E-06
SC_4_2	4.56E-06	SC_8_2	4.56E-06	SC_12_2	4.56E-06	SC_16_2	4.56E-06
SC_4_3	4.59E-06	SC_8_3	4.59E-06	SC_12_3	4.59E-06	SC_16_3	4.59E-06
SC_4_4	4.61E-06	SC_8_4	4.61E-06	SC_12_4	4.61E-06	SC_16_4	4.61E-06
SC_4_5	4.63E-06	SC_8_5	4.63E-06	SC_12_5	4.63E-06	SC_16_5	4.63E-06
SC_4_6	4.66E-06	SC_8_6	4.66E-06	SC_12_6	4.66E-06	SC_16_6	4.66E-06
SC_4_7	4.68E-06	SC_8_7	4.68E-06	SC_12_7	4.68E-06	SC_16_7	4.68E-06
SC_4_8	4.70E-06	SC_8_8	4.70E-06	SC_12_8	4.70E-06	SC_16_8	4.70E-06
SC_4_9	4.73E-06	SC_8_9	4.73E-06	SC_12_9	4.73E-06	SC_16_9	4.73E-06
SC_4_10	4.75E-06	SC_8_10	4.75E-06	SC_12_10	4.75E-06	SC_16_10	4.75E-06
SC_4_11	4.77E-06	SC_8_11	4.77E-06	SC_12_11	4.77E-06	SC_16_11	4.77E-06
SC_4_12	4.80E-06	SC_8_12	4.80E-06	SC_12_12	4.80E-06	SC_16_12	4.80E-06

Tab. A.2-6 Cumulative inductances for each conductor of PF 3 coil at 9.5 kHz (H)

SC_1_1	4.37E-06	SC_5_1	4.37E-06	SC_9_1	4.37E-06	SC_13_1	4.37E-06
SC_1_2	4.40E-06	SC_5_2	4.40E-06	SC_9_2	4.40E-06	SC_13_2	4.40E-06
SC_1_3	4.42E-06	SC_5_3	4.42E-06	SC_9_3	4.42E-06	SC_13_3	4.42E-06
SC_1_4	4.44E-06	SC_5_4	4.44E-06	SC_9_4	4.44E-06	SC_13_4	4.44E-06
SC_1_5	4.46E-06	SC_5_5	4.46E-06	SC_9_5	4.46E-06	SC_13_5	4.46E-06
SC_1_6	4.48E-06	SC_5_6	4.48E-06	SC_9_6	4.48E-06	SC_13_6	4.48E-06
SC_1_7	4.51E-06	SC_5_7	4.51E-06	SC_9_7	4.51E-06	SC_13_7	4.51E-06
SC_1_8	4.53E-06	SC_5_8	4.53E-06	SC_9_8	4.53E-06	SC_13_8	4.53E-06
SC_1_9	4.55E-06	SC_5_9	4.55E-06	SC_9_9	4.55E-06	SC_13_9	4.55E-06
SC_1_10	4.57E-06	SC_5_10	4.57E-06	SC_9_10	4.57E-06	SC_13_10	4.57E-06
SC_1_11	4.59E-06	SC_5_11	4.59E-06	SC_9_11	4.59E-06	SC_13_11	4.59E-06
SC_1_12	4.62E-06	SC_5_12	4.62E-06	SC_9_12	4.62E-06	SC_13_12	4.62E-06
SC_2_1	4.37E-06	SC_6_1	4.37E-06	SC_10_1	4.37E-06	SC_14_1	4.37E-06
SC_2_2	4.40E-06	SC_6_2	4.40E-06	SC_10_2	4.40E-06	SC_14_2	4.40E-06
SC_2_3	4.42E-06	SC_6_3	4.42E-06	SC_10_3	4.42E-06	SC_14_3	4.42E-06
SC_2_4	4.44E-06	SC_6_4	4.44E-06	SC_10_4	4.44E-06	SC_14_4	4.44E-06
SC_2_5	4.46E-06	SC_6_5	4.46E-06	SC_10_5	4.46E-06	SC_14_5	4.46E-06
SC_2_6	4.48E-06	SC_6_6	4.48E-06	SC_10_6	4.48E-06	SC_14_6	4.48E-06
SC_2_7	4.51E-06	SC_6_7	4.51E-06	SC_10_7	4.51E-06	SC_14_7	4.51E-06
SC_2_8	4.53E-06	SC_6_8	4.53E-06	SC_10_8	4.53E-06	SC_14_8	4.53E-06
SC_2_9	4.55E-06	SC_6_9	4.55E-06	SC_10_9	4.55E-06	SC_14_9	4.55E-06
SC_2_10	4.57E-06	SC_6_10	4.57E-06	SC_10_10	4.57E-06	SC_14_10	4.57E-06
SC_2_11	4.59E-06	SC_6_11	4.59E-06	SC_10_11	4.59E-06	SC_14_11	4.59E-06
SC_2_12	4.62E-06	SC_6_12	4.62E-06	SC_10_12	4.62E-06	SC_14_12	4.62E-06
SC_3_1	4.37E-06	SC_7_1	4.37E-06	SC_11_1	4.37E-06	SC_15_1	4.37E-06
SC_3_2	4.40E-06	SC_7_2	4.40E-06	SC_11_2	4.40E-06	SC_15_2	4.40E-06
SC_3_3	4.42E-06	SC_7_3	4.42E-06	SC_11_3	4.42E-06	SC_15_3	4.42E-06
SC_3_4	4.44E-06	SC_7_4	4.44E-06	SC_11_4	4.44E-06	SC_15_4	4.44E-06
SC_3_5	4.46E-06	SC_7_5	4.46E-06	SC_11_5	4.46E-06	SC_15_5	4.46E-06
SC_3_6	4.48E-06	SC_7_6	4.48E-06	SC_11_6	4.48E-06	SC_15_6	4.48E-06
SC_3_7	4.51E-06	SC_7_7	4.51E-06	SC_11_7	4.51E-06	SC_15_7	4.51E-06
SC_3_8	4.53E-06	SC_7_8	4.53E-06	SC_11_8	4.53E-06	SC_15_8	4.53E-06
SC_3_9	4.55E-06	SC_7_9	4.55E-06	SC_11_9	4.55E-06	SC_15_9	4.55E-06
SC_3_10	4.57E-06	SC_7_10	4.57E-06	SC_11_10	4.57E-06	SC_15_10	4.57E-06
SC_3_11	4.59E-06	SC_7_11	4.59E-06	SC_11_11	4.59E-06	SC_15_11	4.59E-06
SC_3_12	4.62E-06	SC_7_12	4.62E-06	SC_11_12	4.62E-06	SC_15_12	4.62E-06
SC_4_1	4.37E-06	SC_8_1	4.37E-06	SC_12_1	4.37E-06	SC_16_1	4.37E-06
SC_4_2	4.40E-06	SC_8_2	4.40E-06	SC_12_2	4.40E-06	SC_16_2	4.40E-06
SC_4_3	4.42E-06	SC_8_3	4.42E-06	SC_12_3	4.42E-06	SC_16_3	4.42E-06
SC_4_4	4.44E-06	SC_8_4	4.44E-06	SC_12_4	4.44E-06	SC_16_4	4.44E-06
SC_4_5	4.46E-06	SC_8_5	4.46E-06	SC_12_5	4.46E-06	SC_16_5	4.46E-06
SC_4_6	4.48E-06	SC_8_6	4.48E-06	SC_12_6	4.48E-06	SC_16_6	4.48E-06
SC_4_7	4.51E-06	SC_8_7	4.51E-06	SC_12_7	4.51E-06	SC_16_7	4.51E-06
SC_4_8	4.53E-06	SC_8_8	4.53E-06	SC_12_8	4.53E-06	SC_16_8	4.53E-06
SC_4_9	4.55E-06	SC_8_9	4.55E-06	SC_12_9	4.55E-06	SC_16_9	4.55E-06
SC_4_10	4.57E-06	SC_8_10	4.57E-06	SC_12_10	4.57E-06	SC_16_10	4.57E-06
SC_4_11	4.59E-06	SC_8_11	4.59E-06	SC_12_11	4.59E-06	SC_16_11	4.59E-06
SC_4_12	4.62E-06	SC_8_12	4.62E-06	SC_12_12	4.62E-06	SC_16_12	4.62E-06

Tab. A.2-7 Cumulative inductances for each conductor of PF 3 coil at 11.9 kHz (H)

SC_1_1	4.17E-06	SC_5_1	4.17E-06	SC_9_1	4.17E-06	SC_13_1	4.17E-06
SC_1_2	4.19E-06	SC_5_2	4.19E-06	SC_9_2	4.19E-06	SC_13_2	4.19E-06
SC_1_3	4.21E-06	SC_5_3	4.21E-06	SC_9_3	4.21E-06	SC_13_3	4.21E-06
SC_1_4	4.23E-06	SC_5_4	4.23E-06	SC_9_4	4.23E-06	SC_13_4	4.23E-06
SC_1_5	4.25E-06	SC_5_5	4.25E-06	SC_9_5	4.25E-06	SC_13_5	4.25E-06
SC_1_6	4.28E-06	SC_5_6	4.28E-06	SC_9_6	4.28E-06	SC_13_6	4.28E-06
SC_1_7	4.30E-06	SC_5_7	4.30E-06	SC_9_7	4.30E-06	SC_13_7	4.30E-06
SC_1_8	4.32E-06	SC_5_8	4.32E-06	SC_9_8	4.32E-06	SC_13_8	4.32E-06
SC_1_9	4.34E-06	SC_5_9	4.34E-06	SC_9_9	4.34E-06	SC_13_9	4.34E-06
SC_1_10	4.36E-06	SC_5_10	4.36E-06	SC_9_10	4.36E-06	SC_13_10	4.36E-06
SC_1_11	4.38E-06	SC_5_11	4.38E-06	SC_9_11	4.38E-06	SC_13_11	4.38E-06
SC_1_12	4.40E-06	SC_5_12	4.40E-06	SC_9_12	4.40E-06	SC_13_12	4.40E-06
SC_2_1	4.17E-06	SC_6_1	4.17E-06	SC_10_1	4.17E-06	SC_14_1	4.17E-06
SC_2_2	4.19E-06	SC_6_2	4.19E-06	SC_10_2	4.19E-06	SC_14_2	4.19E-06
SC_2_3	4.21E-06	SC_6_3	4.21E-06	SC_10_3	4.21E-06	SC_14_3	4.21E-06
SC_2_4	4.23E-06	SC_6_4	4.23E-06	SC_10_4	4.23E-06	SC_14_4	4.23E-06
SC_2_5	4.25E-06	SC_6_5	4.25E-06	SC_10_5	4.25E-06	SC_14_5	4.25E-06
SC_2_6	4.28E-06	SC_6_6	4.28E-06	SC_10_6	4.28E-06	SC_14_6	4.28E-06
SC_2_7	4.30E-06	SC_6_7	4.30E-06	SC_10_7	4.30E-06	SC_14_7	4.30E-06
SC_2_8	4.32E-06	SC_6_8	4.32E-06	SC_10_8	4.32E-06	SC_14_8	4.32E-06
SC_2_9	4.34E-06	SC_6_9	4.34E-06	SC_10_9	4.34E-06	SC_14_9	4.34E-06
SC_2_10	4.36E-06	SC_6_10	4.36E-06	SC_10_10	4.36E-06	SC_14_10	4.36E-06
SC_2_11	4.38E-06	SC_6_11	4.38E-06	SC_10_11	4.38E-06	SC_14_11	4.38E-06
SC_2_12	4.40E-06	SC_6_12	4.40E-06	SC_10_12	4.40E-06	SC_14_12	4.40E-06
SC_3_1	4.17E-06	SC_7_1	4.17E-06	SC_11_1	4.17E-06	SC_15_1	4.17E-06
SC_3_2	4.19E-06	SC_7_2	4.19E-06	SC_11_2	4.19E-06	SC_15_2	4.19E-06
SC_3_3	4.21E-06	SC_7_3	4.21E-06	SC_11_3	4.21E-06	SC_15_3	4.21E-06
SC_3_4	4.23E-06	SC_7_4	4.23E-06	SC_11_4	4.23E-06	SC_15_4	4.23E-06
SC_3_5	4.25E-06	SC_7_5	4.25E-06	SC_11_5	4.25E-06	SC_15_5	4.25E-06
SC_3_6	4.28E-06	SC_7_6	4.28E-06	SC_11_6	4.28E-06	SC_15_6	4.28E-06
SC_3_7	4.30E-06	SC_7_7	4.30E-06	SC_11_7	4.30E-06	SC_15_7	4.30E-06
SC_3_8	4.32E-06	SC_7_8	4.32E-06	SC_11_8	4.32E-06	SC_15_8	4.32E-06
SC_3_9	4.34E-06	SC_7_9	4.34E-06	SC_11_9	4.34E-06	SC_15_9	4.34E-06
SC_3_10	4.36E-06	SC_7_10	4.36E-06	SC_11_10	4.36E-06	SC_15_10	4.36E-06
SC_3_11	4.38E-06	SC_7_11	4.38E-06	SC_11_11	4.38E-06	SC_15_11	4.38E-06
SC_3_12	4.40E-06	SC_7_12	4.40E-06	SC_11_12	4.40E-06	SC_15_12	4.40E-06
SC_4_1	4.17E-06	SC_8_1	4.17E-06	SC_12_1	4.17E-06	SC_16_1	4.17E-06
SC_4_2	4.19E-06	SC_8_2	4.19E-06	SC_12_2	4.19E-06	SC_16_2	4.19E-06
SC_4_3	4.21E-06	SC_8_3	4.21E-06	SC_12_3	4.21E-06	SC_16_3	4.21E-06
SC_4_4	4.23E-06	SC_8_4	4.23E-06	SC_12_4	4.23E-06	SC_16_4	4.23E-06
SC_4_5	4.25E-06	SC_8_5	4.25E-06	SC_12_5	4.25E-06	SC_16_5	4.25E-06
SC_4_6	4.28E-06	SC_8_6	4.28E-06	SC_12_6	4.28E-06	SC_16_6	4.28E-06
SC_4_7	4.30E-06	SC_8_7	4.30E-06	SC_12_7	4.30E-06	SC_16_7	4.30E-06
SC_4_8	4.32E-06	SC_8_8	4.32E-06	SC_12_8	4.32E-06	SC_16_8	4.32E-06
SC_4_9	4.34E-06	SC_8_9	4.34E-06	SC_12_9	4.34E-06	SC_16_9	4.34E-06
SC_4_10	4.36E-06	SC_8_10	4.36E-06	SC_12_10	4.36E-06	SC_16_10	4.36E-06
SC_4_11	4.38E-06	SC_8_11	4.38E-06	SC_12_11	4.38E-06	SC_16_11	4.38E-06
SC_4_12	4.40E-06	SC_8_12	4.40E-06	SC_12_12	4.40E-06	SC_16_12	4.40E-06

Tab. A.2-8 Cumulative inductances for each conductor of PF 3 coil at 16.3 kHz (H)

SC_1_1	4.15E-06	SC_5_1	4.15E-06	SC_9_1	4.15E-06	SC_13_1	4.15E-06
SC_1_2	4.17E-06	SC_5_2	4.17E-06	SC_9_2	4.17E-06	SC_13_2	4.17E-06
SC_1_3	4.19E-06	SC_5_3	4.19E-06	SC_9_3	4.19E-06	SC_13_3	4.19E-06
SC_1_4	4.21E-06	SC_5_4	4.21E-06	SC_9_4	4.21E-06	SC_13_4	4.21E-06
SC_1_5	4.23E-06	SC_5_5	4.23E-06	SC_9_5	4.23E-06	SC_13_5	4.23E-06
SC_1_6	4.25E-06	SC_5_6	4.25E-06	SC_9_6	4.25E-06	SC_13_6	4.25E-06
SC_1_7	4.27E-06	SC_5_7	4.27E-06	SC_9_7	4.27E-06	SC_13_7	4.27E-06
SC_1_8	4.29E-06	SC_5_8	4.29E-06	SC_9_8	4.29E-06	SC_13_8	4.29E-06
SC_1_9	4.31E-06	SC_5_9	4.31E-06	SC_9_9	4.31E-06	SC_13_9	4.31E-06
SC_1_10	4.34E-06	SC_5_10	4.34E-06	SC_9_10	4.34E-06	SC_13_10	4.34E-06
SC_1_11	4.36E-06	SC_5_11	4.36E-06	SC_9_11	4.36E-06	SC_13_11	4.36E-06
SC_1_12	4.38E-06	SC_5_12	4.38E-06	SC_9_12	4.38E-06	SC_13_12	4.38E-06
SC_2_1	4.15E-06	SC_6_1	4.15E-06	SC_10_1	4.15E-06	SC_14_1	4.15E-06
SC_2_2	4.17E-06	SC_6_2	4.17E-06	SC_10_2	4.17E-06	SC_14_2	4.17E-06
SC_2_3	4.19E-06	SC_6_3	4.19E-06	SC_10_3	4.19E-06	SC_14_3	4.19E-06
SC_2_4	4.21E-06	SC_6_4	4.21E-06	SC_10_4	4.21E-06	SC_14_4	4.21E-06
SC_2_5	4.23E-06	SC_6_5	4.23E-06	SC_10_5	4.23E-06	SC_14_5	4.23E-06
SC_2_6	4.25E-06	SC_6_6	4.25E-06	SC_10_6	4.25E-06	SC_14_6	4.25E-06
SC_2_7	4.27E-06	SC_6_7	4.27E-06	SC_10_7	4.27E-06	SC_14_7	4.27E-06
SC_2_8	4.29E-06	SC_6_8	4.29E-06	SC_10_8	4.29E-06	SC_14_8	4.29E-06
SC_2_9	4.31E-06	SC_6_9	4.31E-06	SC_10_9	4.31E-06	SC_14_9	4.31E-06
SC_2_10	4.34E-06	SC_6_10	4.34E-06	SC_10_10	4.34E-06	SC_14_10	4.34E-06
SC_2_11	4.36E-06	SC_6_11	4.36E-06	SC_10_11	4.36E-06	SC_14_11	4.36E-06
SC_2_12	4.38E-06	SC_6_12	4.38E-06	SC_10_12	4.38E-06	SC_14_12	4.38E-06
SC_3_1	4.15E-06	SC_7_1	4.15E-06	SC_11_1	4.15E-06	SC_15_1	4.15E-06
SC_3_2	4.17E-06	SC_7_2	4.17E-06	SC_11_2	4.17E-06	SC_15_2	4.17E-06
SC_3_3	4.19E-06	SC_7_3	4.19E-06	SC_11_3	4.19E-06	SC_15_3	4.19E-06
SC_3_4	4.21E-06	SC_7_4	4.21E-06	SC_11_4	4.21E-06	SC_15_4	4.21E-06
SC_3_5	4.23E-06	SC_7_5	4.23E-06	SC_11_5	4.23E-06	SC_15_5	4.23E-06
SC_3_6	4.25E-06	SC_7_6	4.25E-06	SC_11_6	4.25E-06	SC_15_6	4.25E-06
SC_3_7	4.27E-06	SC_7_7	4.27E-06	SC_11_7	4.27E-06	SC_15_7	4.27E-06
SC_3_8	4.29E-06	SC_7_8	4.29E-06	SC_11_8	4.29E-06	SC_15_8	4.29E-06
SC_3_9	4.31E-06	SC_7_9	4.31E-06	SC_11_9	4.31E-06	SC_15_9	4.31E-06
SC_3_10	4.34E-06	SC_7_10	4.34E-06	SC_11_10	4.34E-06	SC_15_10	4.34E-06
SC_3_11	4.36E-06	SC_7_11	4.36E-06	SC_11_11	4.36E-06	SC_15_11	4.36E-06
SC_3_12	4.38E-06	SC_7_12	4.38E-06	SC_11_12	4.38E-06	SC_15_12	4.38E-06
SC_4_1	4.15E-06	SC_8_1	4.15E-06	SC_12_1	4.15E-06	SC_16_1	4.15E-06
SC_4_2	4.17E-06	SC_8_2	4.17E-06	SC_12_2	4.17E-06	SC_16_2	4.17E-06
SC_4_3	4.19E-06	SC_8_3	4.19E-06	SC_12_3	4.19E-06	SC_16_3	4.19E-06
SC_4_4	4.21E-06	SC_8_4	4.21E-06	SC_12_4	4.21E-06	SC_16_4	4.21E-06
SC_4_5	4.23E-06	SC_8_5	4.23E-06	SC_12_5	4.23E-06	SC_16_5	4.23E-06
SC_4_6	4.25E-06	SC_8_6	4.25E-06	SC_12_6	4.25E-06	SC_16_6	4.25E-06
SC_4_7	4.27E-06	SC_8_7	4.27E-06	SC_12_7	4.27E-06	SC_16_7	4.27E-06
SC_4_8	4.29E-06	SC_8_8	4.29E-06	SC_12_8	4.29E-06	SC_16_8	4.29E-06
SC_4_9	4.31E-06	SC_8_9	4.31E-06	SC_12_9	4.31E-06	SC_16_9	4.31E-06
SC_4_10	4.34E-06	SC_8_10	4.34E-06	SC_12_10	4.34E-06	SC_16_10	4.34E-06
SC_4_11	4.36E-06	SC_8_11	4.36E-06	SC_12_11	4.36E-06	SC_16_11	4.36E-06
SC_4_12	4.38E-06	SC_8_12	4.38E-06	SC_12_12	4.38E-06	SC_16_12	4.38E-06

Tab. A.2-9 Cumulative inductances for each conductor of PF 3 coil at 17.0 kHz (H)

SC_1_1	4.06E-06	SC_5_1	4.06E-06	SC_9_1	4.06E-06	SC_13_1	4.06E-06
SC_1_2	4.08E-06	SC_5_2	4.08E-06	SC_9_2	4.08E-06	SC_13_2	4.08E-06
SC_1_3	4.10E-06	SC_5_3	4.10E-06	SC_9_3	4.10E-06	SC_13_3	4.10E-06
SC_1_4	4.12E-06	SC_5_4	4.12E-06	SC_9_4	4.12E-06	SC_13_4	4.12E-06
SC_1_5	4.14E-06	SC_5_5	4.14E-06	SC_9_5	4.14E-06	SC_13_5	4.14E-06
SC_1_6	4.16E-06	SC_5_6	4.16E-06	SC_9_6	4.16E-06	SC_13_6	4.16E-06
SC_1_7	4.18E-06	SC_5_7	4.18E-06	SC_9_7	4.18E-06	SC_13_7	4.18E-06
SC_1_8	4.20E-06	SC_5_8	4.20E-06	SC_9_8	4.20E-06	SC_13_8	4.20E-06
SC_1_9	4.22E-06	SC_5_9	4.22E-06	SC_9_9	4.22E-06	SC_13_9	4.22E-06
SC_1_10	4.24E-06	SC_5_10	4.24E-06	SC_9_10	4.24E-06	SC_13_10	4.24E-06
SC_1_11	4.26E-06	SC_5_11	4.26E-06	SC_9_11	4.26E-06	SC_13_11	4.26E-06
SC_1_12	4.28E-06	SC_5_12	4.28E-06	SC_9_12	4.28E-06	SC_13_12	4.28E-06
SC_2_1	4.06E-06	SC_6_1	4.06E-06	SC_10_1	4.06E-06	SC_14_1	4.06E-06
SC_2_2	4.08E-06	SC_6_2	4.08E-06	SC_10_2	4.08E-06	SC_14_2	4.08E-06
SC_2_3	4.10E-06	SC_6_3	4.10E-06	SC_10_3	4.10E-06	SC_14_3	4.10E-06
SC_2_4	4.12E-06	SC_6_4	4.12E-06	SC_10_4	4.12E-06	SC_14_4	4.12E-06
SC_2_5	4.14E-06	SC_6_5	4.14E-06	SC_10_5	4.14E-06	SC_14_5	4.14E-06
SC_2_6	4.16E-06	SC_6_6	4.16E-06	SC_10_6	4.16E-06	SC_14_6	4.16E-06
SC_2_7	4.18E-06	SC_6_7	4.18E-06	SC_10_7	4.18E-06	SC_14_7	4.18E-06
SC_2_8	4.20E-06	SC_6_8	4.20E-06	SC_10_8	4.20E-06	SC_14_8	4.20E-06
SC_2_9	4.22E-06	SC_6_9	4.22E-06	SC_10_9	4.22E-06	SC_14_9	4.22E-06
SC_2_10	4.24E-06	SC_6_10	4.24E-06	SC_10_10	4.24E-06	SC_14_10	4.24E-06
SC_2_11	4.26E-06	SC_6_11	4.26E-06	SC_10_11	4.26E-06	SC_14_11	4.26E-06
SC_2_12	4.28E-06	SC_6_12	4.28E-06	SC_10_12	4.28E-06	SC_14_12	4.28E-06
SC_3_1	4.06E-06	SC_7_1	4.06E-06	SC_11_1	4.06E-06	SC_15_1	4.06E-06
SC_3_2	4.08E-06	SC_7_2	4.08E-06	SC_11_2	4.08E-06	SC_15_2	4.08E-06
SC_3_3	4.10E-06	SC_7_3	4.10E-06	SC_11_3	4.10E-06	SC_15_3	4.10E-06
SC_3_4	4.12E-06	SC_7_4	4.12E-06	SC_11_4	4.12E-06	SC_15_4	4.12E-06
SC_3_5	4.14E-06	SC_7_5	4.14E-06	SC_11_5	4.14E-06	SC_15_5	4.14E-06
SC_3_6	4.16E-06	SC_7_6	4.16E-06	SC_11_6	4.16E-06	SC_15_6	4.16E-06
SC_3_7	4.18E-06	SC_7_7	4.18E-06	SC_11_7	4.18E-06	SC_15_7	4.18E-06
SC_3_8	4.20E-06	SC_7_8	4.20E-06	SC_11_8	4.20E-06	SC_15_8	4.20E-06
SC_3_9	4.22E-06	SC_7_9	4.22E-06	SC_11_9	4.22E-06	SC_15_9	4.22E-06
SC_3_10	4.24E-06	SC_7_10	4.24E-06	SC_11_10	4.24E-06	SC_15_10	4.24E-06
SC_3_11	4.26E-06	SC_7_11	4.26E-06	SC_11_11	4.26E-06	SC_15_11	4.26E-06
SC_3_12	4.28E-06	SC_7_12	4.28E-06	SC_11_12	4.28E-06	SC_15_12	4.28E-06
SC_4_1	4.06E-06	SC_8_1	4.06E-06	SC_12_1	4.06E-06	SC_16_1	4.06E-06
SC_4_2	4.08E-06	SC_8_2	4.08E-06	SC_12_2	4.08E-06	SC_16_2	4.08E-06
SC_4_3	4.10E-06	SC_8_3	4.10E-06	SC_12_3	4.10E-06	SC_16_3	4.10E-06
SC_4_4	4.12E-06	SC_8_4	4.12E-06	SC_12_4	4.12E-06	SC_16_4	4.12E-06
SC_4_5	4.14E-06	SC_8_5	4.14E-06	SC_12_5	4.14E-06	SC_16_5	4.14E-06
SC_4_6	4.16E-06	SC_8_6	4.16E-06	SC_12_6	4.16E-06	SC_16_6	4.16E-06
SC_4_7	4.18E-06	SC_8_7	4.18E-06	SC_12_7	4.18E-06	SC_16_7	4.18E-06
SC_4_8	4.20E-06	SC_8_8	4.20E-06	SC_12_8	4.20E-06	SC_16_8	4.20E-06
SC_4_9	4.22E-06	SC_8_9	4.22E-06	SC_12_9	4.22E-06	SC_16_9	4.22E-06
SC_4_10	4.24E-06	SC_8_10	4.24E-06	SC_12_10	4.24E-06	SC_16_10	4.24E-06
SC_4_11	4.26E-06	SC_8_11	4.26E-06	SC_12_11	4.26E-06	SC_16_11	4.26E-06
SC_4_12	4.28E-06	SC_8_12	4.28E-06	SC_12_12	4.28E-06	SC_16_12	4.28E-06

Tab. A.2-10 Cumulative inductances for each conductor of PF 3 coil at 19.8 kHz (H)

SC_1_1	4.04E-06	SC_5_1	4.04E-06	SC_9_1	4.04E-06	SC_13_1	4.04E-06
SC_1_2	4.06E-06	SC_5_2	4.06E-06	SC_9_2	4.06E-06	SC_13_2	4.06E-06
SC_1_3	4.08E-06	SC_5_3	4.08E-06	SC_9_3	4.08E-06	SC_13_3	4.08E-06
SC_1_4	4.10E-06	SC_5_4	4.10E-06	SC_9_4	4.10E-06	SC_13_4	4.10E-06
SC_1_5	4.12E-06	SC_5_5	4.12E-06	SC_9_5	4.12E-06	SC_13_5	4.12E-06
SC_1_6	4.14E-06	SC_5_6	4.14E-06	SC_9_6	4.14E-06	SC_13_6	4.14E-06
SC_1_7	4.16E-06	SC_5_7	4.16E-06	SC_9_7	4.16E-06	SC_13_7	4.16E-06
SC_1_8	4.18E-06	SC_5_8	4.18E-06	SC_9_8	4.18E-06	SC_13_8	4.18E-06
SC_1_9	4.20E-06	SC_5_9	4.20E-06	SC_9_9	4.20E-06	SC_13_9	4.20E-06
SC_1_10	4.22E-06	SC_5_10	4.22E-06	SC_9_10	4.22E-06	SC_13_10	4.22E-06
SC_1_11	4.24E-06	SC_5_11	4.24E-06	SC_9_11	4.24E-06	SC_13_11	4.24E-06
SC_1_12	4.26E-06	SC_5_12	4.26E-06	SC_9_12	4.26E-06	SC_13_12	4.26E-06
SC_2_1	4.04E-06	SC_6_1	4.04E-06	SC_10_1	4.04E-06	SC_14_1	4.04E-06
SC_2_2	4.06E-06	SC_6_2	4.06E-06	SC_10_2	4.06E-06	SC_14_2	4.06E-06
SC_2_3	4.08E-06	SC_6_3	4.08E-06	SC_10_3	4.08E-06	SC_14_3	4.08E-06
SC_2_4	4.10E-06	SC_6_4	4.10E-06	SC_10_4	4.10E-06	SC_14_4	4.10E-06
SC_2_5	4.12E-06	SC_6_5	4.12E-06	SC_10_5	4.12E-06	SC_14_5	4.12E-06
SC_2_6	4.14E-06	SC_6_6	4.14E-06	SC_10_6	4.14E-06	SC_14_6	4.14E-06
SC_2_7	4.16E-06	SC_6_7	4.16E-06	SC_10_7	4.16E-06	SC_14_7	4.16E-06
SC_2_8	4.18E-06	SC_6_8	4.18E-06	SC_10_8	4.18E-06	SC_14_8	4.18E-06
SC_2_9	4.20E-06	SC_6_9	4.20E-06	SC_10_9	4.20E-06	SC_14_9	4.20E-06
SC_2_10	4.22E-06	SC_6_10	4.22E-06	SC_10_10	4.22E-06	SC_14_10	4.22E-06
SC_2_11	4.24E-06	SC_6_11	4.24E-06	SC_10_11	4.24E-06	SC_14_11	4.24E-06
SC_2_12	4.26E-06	SC_6_12	4.26E-06	SC_10_12	4.26E-06	SC_14_12	4.26E-06
SC_3_1	4.04E-06	SC_7_1	4.04E-06	SC_11_1	4.04E-06	SC_15_1	4.04E-06
SC_3_2	4.06E-06	SC_7_2	4.06E-06	SC_11_2	4.06E-06	SC_15_2	4.06E-06
SC_3_3	4.08E-06	SC_7_3	4.08E-06	SC_11_3	4.08E-06	SC_15_3	4.08E-06
SC_3_4	4.10E-06	SC_7_4	4.10E-06	SC_11_4	4.10E-06	SC_15_4	4.10E-06
SC_3_5	4.12E-06	SC_7_5	4.12E-06	SC_11_5	4.12E-06	SC_15_5	4.12E-06
SC_3_6	4.14E-06	SC_7_6	4.14E-06	SC_11_6	4.14E-06	SC_15_6	4.14E-06
SC_3_7	4.16E-06	SC_7_7	4.16E-06	SC_11_7	4.16E-06	SC_15_7	4.16E-06
SC_3_8	4.18E-06	SC_7_8	4.18E-06	SC_11_8	4.18E-06	SC_15_8	4.18E-06
SC_3_9	4.20E-06	SC_7_9	4.20E-06	SC_11_9	4.20E-06	SC_15_9	4.20E-06
SC_3_10	4.22E-06	SC_7_10	4.22E-06	SC_11_10	4.22E-06	SC_15_10	4.22E-06
SC_3_11	4.24E-06	SC_7_11	4.24E-06	SC_11_11	4.24E-06	SC_15_11	4.24E-06
SC_3_12	4.26E-06	SC_7_12	4.26E-06	SC_11_12	4.26E-06	SC_15_12	4.26E-06
SC_4_1	4.04E-06	SC_8_1	4.04E-06	SC_12_1	4.04E-06	SC_16_1	4.04E-06
SC_4_2	4.06E-06	SC_8_2	4.06E-06	SC_12_2	4.06E-06	SC_16_2	4.06E-06
SC_4_3	4.08E-06	SC_8_3	4.08E-06	SC_12_3	4.08E-06	SC_16_3	4.08E-06
SC_4_4	4.10E-06	SC_8_4	4.10E-06	SC_12_4	4.10E-06	SC_16_4	4.10E-06
SC_4_5	4.12E-06	SC_8_5	4.12E-06	SC_12_5	4.12E-06	SC_16_5	4.12E-06
SC_4_6	4.14E-06	SC_8_6	4.14E-06	SC_12_6	4.14E-06	SC_16_6	4.14E-06
SC_4_7	4.16E-06	SC_8_7	4.16E-06	SC_12_7	4.16E-06	SC_16_7	4.16E-06
SC_4_8	4.18E-06	SC_8_8	4.18E-06	SC_12_8	4.18E-06	SC_16_8	4.18E-06
SC_4_9	4.20E-06	SC_8_9	4.20E-06	SC_12_9	4.20E-06	SC_16_9	4.20E-06
SC_4_10	4.22E-06	SC_8_10	4.22E-06	SC_12_10	4.22E-06	SC_16_10	4.22E-06
SC_4_11	4.24E-06	SC_8_11	4.24E-06	SC_12_11	4.24E-06	SC_16_11	4.24E-06
SC_4_12	4.26E-06	SC_8_12	4.26E-06	SC_12_12	4.26E-06	SC_16_12	4.26E-06

Tab. A.2-11 Cumulative inductances for each conductor of PF 3 coil at 20.6 kHz (H)

SC_1_1	4.04E-06	SC_5_1	4.04E-06	SC_9_1	4.04E-06	SC_13_1	4.04E-06
SC_1_2	4.06E-06	SC_5_2	4.06E-06	SC_9_2	4.06E-06	SC_13_2	4.06E-06
SC_1_3	4.08E-06	SC_5_3	4.08E-06	SC_9_3	4.08E-06	SC_13_3	4.08E-06
SC_1_4	4.10E-06	SC_5_4	4.10E-06	SC_9_4	4.10E-06	SC_13_4	4.10E-06
SC_1_5	4.12E-06	SC_5_5	4.12E-06	SC_9_5	4.12E-06	SC_13_5	4.12E-06
SC_1_6	4.14E-06	SC_5_6	4.14E-06	SC_9_6	4.14E-06	SC_13_6	4.14E-06
SC_1_7	4.16E-06	SC_5_7	4.16E-06	SC_9_7	4.16E-06	SC_13_7	4.16E-06
SC_1_8	4.18E-06	SC_5_8	4.18E-06	SC_9_8	4.18E-06	SC_13_8	4.18E-06
SC_1_9	4.20E-06	SC_5_9	4.20E-06	SC_9_9	4.20E-06	SC_13_9	4.20E-06
SC_1_10	4.22E-06	SC_5_10	4.22E-06	SC_9_10	4.22E-06	SC_13_10	4.22E-06
SC_1_11	4.24E-06	SC_5_11	4.24E-06	SC_9_11	4.24E-06	SC_13_11	4.24E-06
SC_1_12	4.26E-06	SC_5_12	4.26E-06	SC_9_12	4.26E-06	SC_13_12	4.26E-06
SC_2_1	4.04E-06	SC_6_1	4.04E-06	SC_10_1	4.04E-06	SC_14_1	4.04E-06
SC_2_2	4.06E-06	SC_6_2	4.06E-06	SC_10_2	4.06E-06	SC_14_2	4.06E-06
SC_2_3	4.08E-06	SC_6_3	4.08E-06	SC_10_3	4.08E-06	SC_14_3	4.08E-06
SC_2_4	4.10E-06	SC_6_4	4.10E-06	SC_10_4	4.10E-06	SC_14_4	4.10E-06
SC_2_5	4.12E-06	SC_6_5	4.12E-06	SC_10_5	4.12E-06	SC_14_5	4.12E-06
SC_2_6	4.14E-06	SC_6_6	4.14E-06	SC_10_6	4.14E-06	SC_14_6	4.14E-06
SC_2_7	4.16E-06	SC_6_7	4.16E-06	SC_10_7	4.16E-06	SC_14_7	4.16E-06
SC_2_8	4.18E-06	SC_6_8	4.18E-06	SC_10_8	4.18E-06	SC_14_8	4.18E-06
SC_2_9	4.20E-06	SC_6_9	4.20E-06	SC_10_9	4.20E-06	SC_14_9	4.20E-06
SC_2_10	4.22E-06	SC_6_10	4.22E-06	SC_10_10	4.22E-06	SC_14_10	4.22E-06
SC_2_11	4.24E-06	SC_6_11	4.24E-06	SC_10_11	4.24E-06	SC_14_11	4.24E-06
SC_2_12	4.26E-06	SC_6_12	4.26E-06	SC_10_12	4.26E-06	SC_14_12	4.26E-06
SC_3_1	4.04E-06	SC_7_1	4.04E-06	SC_11_1	4.04E-06	SC_15_1	4.04E-06
SC_3_2	4.06E-06	SC_7_2	4.06E-06	SC_11_2	4.06E-06	SC_15_2	4.06E-06
SC_3_3	4.08E-06	SC_7_3	4.08E-06	SC_11_3	4.08E-06	SC_15_3	4.08E-06
SC_3_4	4.10E-06	SC_7_4	4.10E-06	SC_11_4	4.10E-06	SC_15_4	4.10E-06
SC_3_5	4.12E-06	SC_7_5	4.12E-06	SC_11_5	4.12E-06	SC_15_5	4.12E-06
SC_3_6	4.14E-06	SC_7_6	4.14E-06	SC_11_6	4.14E-06	SC_15_6	4.14E-06
SC_3_7	4.16E-06	SC_7_7	4.16E-06	SC_11_7	4.16E-06	SC_15_7	4.16E-06
SC_3_8	4.18E-06	SC_7_8	4.18E-06	SC_11_8	4.18E-06	SC_15_8	4.18E-06
SC_3_9	4.20E-06	SC_7_9	4.20E-06	SC_11_9	4.20E-06	SC_15_9	4.20E-06
SC_3_10	4.22E-06	SC_7_10	4.22E-06	SC_11_10	4.22E-06	SC_15_10	4.22E-06
SC_3_11	4.24E-06	SC_7_11	4.24E-06	SC_11_11	4.24E-06	SC_15_11	4.24E-06
SC_3_12	4.26E-06	SC_7_12	4.26E-06	SC_11_12	4.26E-06	SC_15_12	4.26E-06
SC_4_1	4.04E-06	SC_8_1	4.04E-06	SC_12_1	4.04E-06	SC_16_1	4.04E-06
SC_4_2	4.06E-06	SC_8_2	4.06E-06	SC_12_2	4.06E-06	SC_16_2	4.06E-06
SC_4_3	4.08E-06	SC_8_3	4.08E-06	SC_12_3	4.08E-06	SC_16_3	4.08E-06
SC_4_4	4.10E-06	SC_8_4	4.10E-06	SC_12_4	4.10E-06	SC_16_4	4.10E-06
SC_4_5	4.12E-06	SC_8_5	4.12E-06	SC_12_5	4.12E-06	SC_16_5	4.12E-06
SC_4_6	4.14E-06	SC_8_6	4.14E-06	SC_12_6	4.14E-06	SC_16_6	4.14E-06
SC_4_7	4.16E-06	SC_8_7	4.16E-06	SC_12_7	4.16E-06	SC_16_7	4.16E-06
SC_4_8	4.18E-06	SC_8_8	4.18E-06	SC_12_8	4.18E-06	SC_16_8	4.18E-06
SC_4_9	4.20E-06	SC_8_9	4.20E-06	SC_12_9	4.20E-06	SC_16_9	4.20E-06
SC_4_10	4.22E-06	SC_8_10	4.22E-06	SC_12_10	4.22E-06	SC_16_10	4.22E-06
SC_4_11	4.24E-06	SC_8_11	4.24E-06	SC_12_11	4.24E-06	SC_16_11	4.24E-06
SC_4_12	4.26E-06	SC_8_12	4.26E-06	SC_12_12	4.26E-06	SC_16_12	4.26E-06

Tab. A.2-12 Cumulative inductances for each conductor of PF 3 coil at 20.66 kHz (H)

SC_1_1	4.03E-06	SC_5_1	4.03E-06	SC_9_1	4.03E-06	SC_13_1	4.03E-06
SC_1_2	4.06E-06	SC_5_2	4.06E-06	SC_9_2	4.06E-06	SC_13_2	4.06E-06
SC_1_3	4.08E-06	SC_5_3	4.08E-06	SC_9_3	4.08E-06	SC_13_3	4.08E-06
SC_1_4	4.10E-06	SC_5_4	4.10E-06	SC_9_4	4.10E-06	SC_13_4	4.10E-06
SC_1_5	4.12E-06	SC_5_5	4.12E-06	SC_9_5	4.12E-06	SC_13_5	4.12E-06
SC_1_6	4.14E-06	SC_5_6	4.14E-06	SC_9_6	4.14E-06	SC_13_6	4.14E-06
SC_1_7	4.16E-06	SC_5_7	4.16E-06	SC_9_7	4.16E-06	SC_13_7	4.16E-06
SC_1_8	4.18E-06	SC_5_8	4.18E-06	SC_9_8	4.18E-06	SC_13_8	4.18E-06
SC_1_9	4.20E-06	SC_5_9	4.20E-06	SC_9_9	4.20E-06	SC_13_9	4.20E-06
SC_1_10	4.22E-06	SC_5_10	4.22E-06	SC_9_10	4.22E-06	SC_13_10	4.22E-06
SC_1_11	4.24E-06	SC_5_11	4.24E-06	SC_9_11	4.24E-06	SC_13_11	4.24E-06
SC_1_12	4.26E-06	SC_5_12	4.26E-06	SC_9_12	4.26E-06	SC_13_12	4.26E-06
SC_2_1	4.03E-06	SC_6_1	4.03E-06	SC_10_1	4.03E-06	SC_14_1	4.03E-06
SC_2_2	4.06E-06	SC_6_2	4.06E-06	SC_10_2	4.06E-06	SC_14_2	4.06E-06
SC_2_3	4.08E-06	SC_6_3	4.08E-06	SC_10_3	4.08E-06	SC_14_3	4.08E-06
SC_2_4	4.10E-06	SC_6_4	4.10E-06	SC_10_4	4.10E-06	SC_14_4	4.10E-06
SC_2_5	4.12E-06	SC_6_5	4.12E-06	SC_10_5	4.12E-06	SC_14_5	4.12E-06
SC_2_6	4.14E-06	SC_6_6	4.14E-06	SC_10_6	4.14E-06	SC_14_6	4.14E-06
SC_2_7	4.16E-06	SC_6_7	4.16E-06	SC_10_7	4.16E-06	SC_14_7	4.16E-06
SC_2_8	4.18E-06	SC_6_8	4.18E-06	SC_10_8	4.18E-06	SC_14_8	4.18E-06
SC_2_9	4.20E-06	SC_6_9	4.20E-06	SC_10_9	4.20E-06	SC_14_9	4.20E-06
SC_2_10	4.22E-06	SC_6_10	4.22E-06	SC_10_10	4.22E-06	SC_14_10	4.22E-06
SC_2_11	4.24E-06	SC_6_11	4.24E-06	SC_10_11	4.24E-06	SC_14_11	4.24E-06
SC_2_12	4.26E-06	SC_6_12	4.26E-06	SC_10_12	4.26E-06	SC_14_12	4.26E-06
SC_3_1	4.03E-06	SC_7_1	4.03E-06	SC_11_1	4.03E-06	SC_15_1	4.03E-06
SC_3_2	4.06E-06	SC_7_2	4.06E-06	SC_11_2	4.06E-06	SC_15_2	4.06E-06
SC_3_3	4.08E-06	SC_7_3	4.08E-06	SC_11_3	4.08E-06	SC_15_3	4.08E-06
SC_3_4	4.10E-06	SC_7_4	4.10E-06	SC_11_4	4.10E-06	SC_15_4	4.10E-06
SC_3_5	4.12E-06	SC_7_5	4.12E-06	SC_11_5	4.12E-06	SC_15_5	4.12E-06
SC_3_6	4.14E-06	SC_7_6	4.14E-06	SC_11_6	4.14E-06	SC_15_6	4.14E-06
SC_3_7	4.16E-06	SC_7_7	4.16E-06	SC_11_7	4.16E-06	SC_15_7	4.16E-06
SC_3_8	4.18E-06	SC_7_8	4.18E-06	SC_11_8	4.18E-06	SC_15_8	4.18E-06
SC_3_9	4.20E-06	SC_7_9	4.20E-06	SC_11_9	4.20E-06	SC_15_9	4.20E-06
SC_3_10	4.22E-06	SC_7_10	4.22E-06	SC_11_10	4.22E-06	SC_15_10	4.22E-06
SC_3_11	4.24E-06	SC_7_11	4.24E-06	SC_11_11	4.24E-06	SC_15_11	4.24E-06
SC_3_12	4.26E-06	SC_7_12	4.26E-06	SC_11_12	4.26E-06	SC_15_12	4.26E-06
SC_4_1	4.03E-06	SC_8_1	4.03E-06	SC_12_1	4.03E-06	SC_16_1	4.03E-06
SC_4_2	4.06E-06	SC_8_2	4.06E-06	SC_12_2	4.06E-06	SC_16_2	4.06E-06
SC_4_3	4.08E-06	SC_8_3	4.08E-06	SC_12_3	4.08E-06	SC_16_3	4.08E-06
SC_4_4	4.10E-06	SC_8_4	4.10E-06	SC_12_4	4.10E-06	SC_16_4	4.10E-06
SC_4_5	4.12E-06	SC_8_5	4.12E-06	SC_12_5	4.12E-06	SC_16_5	4.12E-06
SC_4_6	4.14E-06	SC_8_6	4.14E-06	SC_12_6	4.14E-06	SC_16_6	4.14E-06
SC_4_7	4.16E-06	SC_8_7	4.16E-06	SC_12_7	4.16E-06	SC_16_7	4.16E-06
SC_4_8	4.18E-06	SC_8_8	4.18E-06	SC_12_8	4.18E-06	SC_16_8	4.18E-06
SC_4_9	4.20E-06	SC_8_9	4.20E-06	SC_12_9	4.20E-06	SC_16_9	4.20E-06
SC_4_10	4.22E-06	SC_8_10	4.22E-06	SC_12_10	4.22E-06	SC_16_10	4.22E-06
SC_4_11	4.24E-06	SC_8_11	4.24E-06	SC_12_11	4.24E-06	SC_16_11	4.24E-06
SC_4_12	4.26E-06	SC_8_12	4.26E-06	SC_12_12	4.26E-06	SC_16_12	4.26E-06

Tab. A.2-13 Cumulative inductances for each conductor of PF 3 coil at 20.8 kHz (H)

SC_1_1	3.99E-06	SC_5_1	3.99E-06	SC_9_1	3.99E-06	SC_13_1	3.99E-06
SC_1_2	4.01E-06	SC_5_2	4.01E-06	SC_9_2	4.01E-06	SC_13_2	4.01E-06
SC_1_3	4.03E-06	SC_5_3	4.03E-06	SC_9_3	4.03E-06	SC_13_3	4.03E-06
SC_1_4	4.05E-06	SC_5_4	4.05E-06	SC_9_4	4.05E-06	SC_13_4	4.05E-06
SC_1_5	4.07E-06	SC_5_5	4.07E-06	SC_9_5	4.07E-06	SC_13_5	4.07E-06
SC_1_6	4.09E-06	SC_5_6	4.09E-06	SC_9_6	4.09E-06	SC_13_6	4.09E-06
SC_1_7	4.11E-06	SC_5_7	4.11E-06	SC_9_7	4.11E-06	SC_13_7	4.11E-06
SC_1_8	4.13E-06	SC_5_8	4.13E-06	SC_9_8	4.13E-06	SC_13_8	4.13E-06
SC_1_9	4.15E-06	SC_5_9	4.15E-06	SC_9_9	4.15E-06	SC_13_9	4.15E-06
SC_1_10	4.17E-06	SC_5_10	4.17E-06	SC_9_10	4.17E-06	SC_13_10	4.17E-06
SC_1_11	4.19E-06	SC_5_11	4.19E-06	SC_9_11	4.19E-06	SC_13_11	4.19E-06
SC_1_12	4.21E-06	SC_5_12	4.21E-06	SC_9_12	4.21E-06	SC_13_12	4.21E-06
SC_2_1	3.99E-06	SC_6_1	3.99E-06	SC_10_1	3.99E-06	SC_14_1	3.99E-06
SC_2_2	4.01E-06	SC_6_2	4.01E-06	SC_10_2	4.01E-06	SC_14_2	4.01E-06
SC_2_3	4.03E-06	SC_6_3	4.03E-06	SC_10_3	4.03E-06	SC_14_3	4.03E-06
SC_2_4	4.05E-06	SC_6_4	4.05E-06	SC_10_4	4.05E-06	SC_14_4	4.05E-06
SC_2_5	4.07E-06	SC_6_5	4.07E-06	SC_10_5	4.07E-06	SC_14_5	4.07E-06
SC_2_6	4.09E-06	SC_6_6	4.09E-06	SC_10_6	4.09E-06	SC_14_6	4.09E-06
SC_2_7	4.11E-06	SC_6_7	4.11E-06	SC_10_7	4.11E-06	SC_14_7	4.11E-06
SC_2_8	4.13E-06	SC_6_8	4.13E-06	SC_10_8	4.13E-06	SC_14_8	4.13E-06
SC_2_9	4.15E-06	SC_6_9	4.15E-06	SC_10_9	4.15E-06	SC_14_9	4.15E-06
SC_2_10	4.17E-06	SC_6_10	4.17E-06	SC_10_10	4.17E-06	SC_14_10	4.17E-06
SC_2_11	4.19E-06	SC_6_11	4.19E-06	SC_10_11	4.19E-06	SC_14_11	4.19E-06
SC_2_12	4.21E-06	SC_6_12	4.21E-06	SC_10_12	4.21E-06	SC_14_12	4.21E-06
SC_3_1	3.99E-06	SC_7_1	3.99E-06	SC_11_1	3.99E-06	SC_15_1	3.99E-06
SC_3_2	4.01E-06	SC_7_2	4.01E-06	SC_11_2	4.01E-06	SC_15_2	4.01E-06
SC_3_3	4.03E-06	SC_7_3	4.03E-06	SC_11_3	4.03E-06	SC_15_3	4.03E-06
SC_3_4	4.05E-06	SC_7_4	4.05E-06	SC_11_4	4.05E-06	SC_15_4	4.05E-06
SC_3_5	4.07E-06	SC_7_5	4.07E-06	SC_11_5	4.07E-06	SC_15_5	4.07E-06
SC_3_6	4.09E-06	SC_7_6	4.09E-06	SC_11_6	4.09E-06	SC_15_6	4.09E-06
SC_3_7	4.11E-06	SC_7_7	4.11E-06	SC_11_7	4.11E-06	SC_15_7	4.11E-06
SC_3_8	4.13E-06	SC_7_8	4.13E-06	SC_11_8	4.13E-06	SC_15_8	4.13E-06
SC_3_9	4.15E-06	SC_7_9	4.15E-06	SC_11_9	4.15E-06	SC_15_9	4.15E-06
SC_3_10	4.17E-06	SC_7_10	4.17E-06	SC_11_10	4.17E-06	SC_15_10	4.17E-06
SC_3_11	4.19E-06	SC_7_11	4.19E-06	SC_11_11	4.19E-06	SC_15_11	4.19E-06
SC_3_12	4.21E-06	SC_7_12	4.21E-06	SC_11_12	4.21E-06	SC_15_12	4.21E-06
SC_4_1	3.99E-06	SC_8_1	3.99E-06	SC_12_1	3.99E-06	SC_16_1	3.99E-06
SC_4_2	4.01E-06	SC_8_2	4.01E-06	SC_12_2	4.01E-06	SC_16_2	4.01E-06
SC_4_3	4.03E-06	SC_8_3	4.03E-06	SC_12_3	4.03E-06	SC_16_3	4.03E-06
SC_4_4	4.05E-06	SC_8_4	4.05E-06	SC_12_4	4.05E-06	SC_16_4	4.05E-06
SC_4_5	4.07E-06	SC_8_5	4.07E-06	SC_12_5	4.07E-06	SC_16_5	4.07E-06
SC_4_6	4.09E-06	SC_8_6	4.09E-06	SC_12_6	4.09E-06	SC_16_6	4.09E-06
SC_4_7	4.11E-06	SC_8_7	4.11E-06	SC_12_7	4.11E-06	SC_16_7	4.11E-06
SC_4_8	4.13E-06	SC_8_8	4.13E-06	SC_12_8	4.13E-06	SC_16_8	4.13E-06
SC_4_9	4.15E-06	SC_8_9	4.15E-06	SC_12_9	4.15E-06	SC_16_9	4.15E-06
SC_4_10	4.17E-06	SC_8_10	4.17E-06	SC_12_10	4.17E-06	SC_16_10	4.17E-06
SC_4_11	4.19E-06	SC_8_11	4.19E-06	SC_12_11	4.19E-06	SC_16_11	4.19E-06
SC_4_12	4.21E-06	SC_8_12	4.21E-06	SC_12_12	4.21E-06	SC_16_12	4.21E-06

Tab. A.2-14 Cumulative inductances for each conductor of PF 3 coil at 22.8 kHz (H)

SC_1_1	3.32E-06	SC_5_1	3.32E-06	SC_9_1	3.32E-06	SC_13_1	3.32E-06
SC_1_2	3.33E-06	SC_5_2	3.33E-06	SC_9_2	3.33E-06	SC_13_2	3.33E-06
SC_1_3	3.35E-06	SC_5_3	3.35E-06	SC_9_3	3.35E-06	SC_13_3	3.35E-06
SC_1_4	3.37E-06	SC_5_4	3.37E-06	SC_9_4	3.37E-06	SC_13_4	3.37E-06
SC_1_5	3.38E-06	SC_5_5	3.38E-06	SC_9_5	3.38E-06	SC_13_5	3.38E-06
SC_1_6	3.40E-06	SC_5_6	3.40E-06	SC_9_6	3.40E-06	SC_13_6	3.40E-06
SC_1_7	3.42E-06	SC_5_7	3.42E-06	SC_9_7	3.42E-06	SC_13_7	3.42E-06
SC_1_8	3.43E-06	SC_5_8	3.43E-06	SC_9_8	3.43E-06	SC_13_8	3.43E-06
SC_1_9	3.45E-06	SC_5_9	3.45E-06	SC_9_9	3.45E-06	SC_13_9	3.45E-06
SC_1_10	3.47E-06	SC_5_10	3.47E-06	SC_9_10	3.47E-06	SC_13_10	3.47E-06
SC_1_11	3.48E-06	SC_5_11	3.48E-06	SC_9_11	3.48E-06	SC_13_11	3.48E-06
SC_1_12	3.50E-06	SC_5_12	3.50E-06	SC_9_12	3.50E-06	SC_13_12	3.50E-06
SC_2_1	3.32E-06	SC_6_1	3.32E-06	SC_10_1	3.32E-06	SC_14_1	3.32E-06
SC_2_2	3.33E-06	SC_6_2	3.33E-06	SC_10_2	3.33E-06	SC_14_2	3.33E-06
SC_2_3	3.35E-06	SC_6_3	3.35E-06	SC_10_3	3.35E-06	SC_14_3	3.35E-06
SC_2_4	3.37E-06	SC_6_4	3.37E-06	SC_10_4	3.37E-06	SC_14_4	3.37E-06
SC_2_5	3.38E-06	SC_6_5	3.38E-06	SC_10_5	3.38E-06	SC_14_5	3.38E-06
SC_2_6	3.40E-06	SC_6_6	3.40E-06	SC_10_6	3.40E-06	SC_14_6	3.40E-06
SC_2_7	3.42E-06	SC_6_7	3.42E-06	SC_10_7	3.42E-06	SC_14_7	3.42E-06
SC_2_8	3.43E-06	SC_6_8	3.43E-06	SC_10_8	3.43E-06	SC_14_8	3.43E-06
SC_2_9	3.45E-06	SC_6_9	3.45E-06	SC_10_9	3.45E-06	SC_14_9	3.45E-06
SC_2_10	3.47E-06	SC_6_10	3.47E-06	SC_10_10	3.47E-06	SC_14_10	3.47E-06
SC_2_11	3.48E-06	SC_6_11	3.48E-06	SC_10_11	3.48E-06	SC_14_11	3.48E-06
SC_2_12	3.50E-06	SC_6_12	3.50E-06	SC_10_12	3.50E-06	SC_14_12	3.50E-06
SC_3_1	3.32E-06	SC_7_1	3.32E-06	SC_11_1	3.32E-06	SC_15_1	3.32E-06
SC_3_2	3.33E-06	SC_7_2	3.33E-06	SC_11_2	3.33E-06	SC_15_2	3.33E-06
SC_3_3	3.35E-06	SC_7_3	3.35E-06	SC_11_3	3.35E-06	SC_15_3	3.35E-06
SC_3_4	3.37E-06	SC_7_4	3.37E-06	SC_11_4	3.37E-06	SC_15_4	3.37E-06
SC_3_5	3.38E-06	SC_7_5	3.38E-06	SC_11_5	3.38E-06	SC_15_5	3.38E-06
SC_3_6	3.40E-06	SC_7_6	3.40E-06	SC_11_6	3.40E-06	SC_15_6	3.40E-06
SC_3_7	3.42E-06	SC_7_7	3.42E-06	SC_11_7	3.42E-06	SC_15_7	3.42E-06
SC_3_8	3.43E-06	SC_7_8	3.43E-06	SC_11_8	3.43E-06	SC_15_8	3.43E-06
SC_3_9	3.45E-06	SC_7_9	3.45E-06	SC_11_9	3.45E-06	SC_15_9	3.45E-06
SC_3_10	3.47E-06	SC_7_10	3.47E-06	SC_11_10	3.47E-06	SC_15_10	3.47E-06
SC_3_11	3.48E-06	SC_7_11	3.48E-06	SC_11_11	3.48E-06	SC_15_11	3.48E-06
SC_3_12	3.50E-06	SC_7_12	3.50E-06	SC_11_12	3.50E-06	SC_15_12	3.50E-06
SC_4_1	3.32E-06	SC_8_1	3.32E-06	SC_12_1	3.32E-06	SC_16_1	3.32E-06
SC_4_2	3.33E-06	SC_8_2	3.33E-06	SC_12_2	3.33E-06	SC_16_2	3.33E-06
SC_4_3	3.35E-06	SC_8_3	3.35E-06	SC_12_3	3.35E-06	SC_16_3	3.35E-06
SC_4_4	3.37E-06	SC_8_4	3.37E-06	SC_12_4	3.37E-06	SC_16_4	3.37E-06
SC_4_5	3.38E-06	SC_8_5	3.38E-06	SC_12_5	3.38E-06	SC_16_5	3.38E-06
SC_4_6	3.40E-06	SC_8_6	3.40E-06	SC_12_6	3.40E-06	SC_16_6	3.40E-06
SC_4_7	3.42E-06	SC_8_7	3.42E-06	SC_12_7	3.42E-06	SC_16_7	3.42E-06
SC_4_8	3.43E-06	SC_8_8	3.43E-06	SC_12_8	3.43E-06	SC_16_8	3.43E-06
SC_4_9	3.45E-06	SC_8_9	3.45E-06	SC_12_9	3.45E-06	SC_16_9	3.45E-06
SC_4_10	3.47E-06	SC_8_10	3.47E-06	SC_12_10	3.47E-06	SC_16_10	3.47E-06
SC_4_11	3.48E-06	SC_8_11	3.48E-06	SC_12_11	3.48E-06	SC_16_11	3.48E-06
SC_4_12	3.50E-06	SC_8_12	3.50E-06	SC_12_12	3.50E-06	SC_16_12	3.50E-06

Tab. A.2-15 Cumulative inductances for each conductor of PF 3 coil at 200 kHz (H)

SC_1_1	3.26E-06	SC_5_1	3.26E-06	SC_9_1	3.26E-06	SC_13_1	3.26E-06
SC_1_2	3.27E-06	SC_5_2	3.27E-06	SC_9_2	3.27E-06	SC_13_2	3.27E-06
SC_1_3	3.29E-06	SC_5_3	3.29E-06	SC_9_3	3.29E-06	SC_13_3	3.29E-06
SC_1_4	3.30E-06	SC_5_4	3.30E-06	SC_9_4	3.30E-06	SC_13_4	3.30E-06
SC_1_5	3.32E-06	SC_5_5	3.32E-06	SC_9_5	3.32E-06	SC_13_5	3.32E-06
SC_1_6	3.34E-06	SC_5_6	3.34E-06	SC_9_6	3.34E-06	SC_13_6	3.34E-06
SC_1_7	3.35E-06	SC_5_7	3.35E-06	SC_9_7	3.35E-06	SC_13_7	3.35E-06
SC_1_8	3.37E-06	SC_5_8	3.37E-06	SC_9_8	3.37E-06	SC_13_8	3.37E-06
SC_1_9	3.39E-06	SC_5_9	3.39E-06	SC_9_9	3.39E-06	SC_13_9	3.39E-06
SC_1_10	3.40E-06	SC_5_10	3.40E-06	SC_9_10	3.40E-06	SC_13_10	3.40E-06
SC_1_11	3.42E-06	SC_5_11	3.42E-06	SC_9_11	3.42E-06	SC_13_11	3.42E-06
SC_1_12	3.44E-06	SC_5_12	3.44E-06	SC_9_12	3.44E-06	SC_13_12	3.44E-06
SC_2_1	3.26E-06	SC_6_1	3.26E-06	SC_10_1	3.26E-06	SC_14_1	3.26E-06
SC_2_2	3.27E-06	SC_6_2	3.27E-06	SC_10_2	3.27E-06	SC_14_2	3.27E-06
SC_2_3	3.29E-06	SC_6_3	3.29E-06	SC_10_3	3.29E-06	SC_14_3	3.29E-06
SC_2_4	3.30E-06	SC_6_4	3.30E-06	SC_10_4	3.30E-06	SC_14_4	3.30E-06
SC_2_5	3.32E-06	SC_6_5	3.32E-06	SC_10_5	3.32E-06	SC_14_5	3.32E-06
SC_2_6	3.34E-06	SC_6_6	3.34E-06	SC_10_6	3.34E-06	SC_14_6	3.34E-06
SC_2_7	3.35E-06	SC_6_7	3.35E-06	SC_10_7	3.35E-06	SC_14_7	3.35E-06
SC_2_8	3.37E-06	SC_6_8	3.37E-06	SC_10_8	3.37E-06	SC_14_8	3.37E-06
SC_2_9	3.39E-06	SC_6_9	3.39E-06	SC_10_9	3.39E-06	SC_14_9	3.39E-06
SC_2_10	3.40E-06	SC_6_10	3.40E-06	SC_10_10	3.40E-06	SC_14_10	3.40E-06
SC_2_11	3.42E-06	SC_6_11	3.42E-06	SC_10_11	3.42E-06	SC_14_11	3.42E-06
SC_2_12	3.44E-06	SC_6_12	3.44E-06	SC_10_12	3.44E-06	SC_14_12	3.44E-06
SC_3_1	3.26E-06	SC_7_1	3.26E-06	SC_11_1	3.26E-06	SC_15_1	3.26E-06
SC_3_2	3.27E-06	SC_7_2	3.27E-06	SC_11_2	3.27E-06	SC_15_2	3.27E-06
SC_3_3	3.29E-06	SC_7_3	3.29E-06	SC_11_3	3.29E-06	SC_15_3	3.29E-06
SC_3_4	3.30E-06	SC_7_4	3.30E-06	SC_11_4	3.30E-06	SC_15_4	3.30E-06
SC_3_5	3.32E-06	SC_7_5	3.32E-06	SC_11_5	3.32E-06	SC_15_5	3.32E-06
SC_3_6	3.34E-06	SC_7_6	3.34E-06	SC_11_6	3.34E-06	SC_15_6	3.34E-06
SC_3_7	3.35E-06	SC_7_7	3.35E-06	SC_11_7	3.35E-06	SC_15_7	3.35E-06
SC_3_8	3.37E-06	SC_7_8	3.37E-06	SC_11_8	3.37E-06	SC_15_8	3.37E-06
SC_3_9	3.39E-06	SC_7_9	3.39E-06	SC_11_9	3.39E-06	SC_15_9	3.39E-06
SC_3_10	3.40E-06	SC_7_10	3.40E-06	SC_11_10	3.40E-06	SC_15_10	3.40E-06
SC_3_11	3.42E-06	SC_7_11	3.42E-06	SC_11_11	3.42E-06	SC_15_11	3.42E-06
SC_3_12	3.44E-06	SC_7_12	3.44E-06	SC_11_12	3.44E-06	SC_15_12	3.44E-06
SC_4_1	3.26E-06	SC_8_1	3.26E-06	SC_12_1	3.26E-06	SC_16_1	3.26E-06
SC_4_2	3.27E-06	SC_8_2	3.27E-06	SC_12_2	3.27E-06	SC_16_2	3.27E-06
SC_4_3	3.29E-06	SC_8_3	3.29E-06	SC_12_3	3.29E-06	SC_16_3	3.29E-06
SC_4_4	3.30E-06	SC_8_4	3.30E-06	SC_12_4	3.30E-06	SC_16_4	3.30E-06
SC_4_5	3.32E-06	SC_8_5	3.32E-06	SC_12_5	3.32E-06	SC_16_5	3.32E-06
SC_4_6	3.34E-06	SC_8_6	3.34E-06	SC_12_6	3.34E-06	SC_16_6	3.34E-06
SC_4_7	3.35E-06	SC_8_7	3.35E-06	SC_12_7	3.35E-06	SC_16_7	3.35E-06
SC_4_8	3.37E-06	SC_8_8	3.37E-06	SC_12_8	3.37E-06	SC_16_8	3.37E-06
SC_4_9	3.39E-06	SC_8_9	3.39E-06	SC_12_9	3.39E-06	SC_16_9	3.39E-06
SC_4_10	3.40E-06	SC_8_10	3.40E-06	SC_12_10	3.40E-06	SC_16_10	3.40E-06
SC_4_11	3.42E-06	SC_8_11	3.42E-06	SC_12_11	3.42E-06	SC_16_11	3.42E-06
SC_4_12	3.44E-06	SC_8_12	3.44E-06	SC_12_12	3.44E-06	SC_16_12	3.44E-06

Tab. A.2-16 Cumulative inductances for each conductor of PF 3 coil at 295 kHz (H)

Annex A.3 FEM Models of the PF 6 Coil

(a) FEM Model of the PF 6 Coil for DC

Model Definition

Solver: Magnetostatic Symmetry: RZ-Plane

Drawing Size: Z-direction: ±5 m; R-direction: 10 m

Geometry:

Cooling Tube 1_1: Circle centre: 3476.25 mm; 458 mm; Radius: 6 mm

Superconducting cable 1_1: Circle centre: 3476.25 mm; 458 mm; Radius: 19 mm

Jacket 1_1: First corner: 3449.45 mm; 431.2 mm

Second corner: 3503.05 mm; 484.8 mm

Copy of the conductor 1_1 downwards one time with a distance of 60.7 mm

Copy of the conductor 2_1 downwards one time with a distance of 60.7 mm with consideration of additionally insulation between the double pancakes of 1 mm

Continuing of copy of the conductors downwards with distance depending on the location in the double pancake

Copy of the stack of the 16 first conductors rightwards 27 times with a distance of 60.5 mm

Materials

Cooling tube	Vacuum, relative permittivity = 1, relative permeability = 1
Superconducting cable	Copper at 4K, relative permittivity = 1, relative permeability = 1, conductivity = 6.4E9 S/m
Stainless steel jacket	Stainless steel at 4K, relative permittivity = 1, relative permeability = 1, conductivity = 1.88e6 S/m
Insulation	Epoxy resin, relative permittivity = 4, relative permeability = 1
Background:	Vacuum, relative permittivity = 1, relative permeability = 1

Setup Boundaries and Sources

Current Source All superconducting cables are stranded with 45 kA

Boundary Balloon

Setup Executive Parameters

All superconducting cables were chosen into the impedance matrix.

Return path of the current was set to default.

Setup Solution Options

Mesh: Manual mesh

Object	Insulation	Cooling Tube	Superconducting cable	Stainless steel jacket	Background
Number of triangles	10000	34	72	45	11400

(b) FEM Model of the PF 6 Coil for Frequencies Lower than 5 kHz

Model Definition

Solver: Eddy Current Symmetry: RZ-Plane

Drawing Size: Z-direction: +5 m; R-direction: 10 m

Materials

Cooling tube Vacuum, relative permittivity = 1, relative permeability = 1

Superconducting cable Copper at 4K, relative permittivity = 1, relative permeability = 1, conductivity = 6.4E9 S/m

Stainless steel jacket Stainless steel at 4K, relative permittivity = 1, relative permeability = 1, conductivity = 1.88e6 S/m

Insulation Epoxy resin, relative permittivity = 4, relative permeability = 1

Background: Vacuum, relative permittivity = 1, relative permeability = 1

Setup Boundaries and Sources

Current Source All superconducting cables are stranded with 45 kA

Boundary Balloon

Setup Executive Parameters

All superconducting cables were chosen into the impedance matrix.

Return path of the current was set to default.

Setup Solution Options

Mesh: Manual mesh

Object	Insulation	Cooling Tube	Superconducting cable	Stainless steel jacket	Background
Number of triangles	70000	34	72	302	5000

(c) FEM Model of the PF 6 Coil for Frequencies Higher than 5 kHz

Model Definition

Solver: Eddy Current Symmetry: RZ-Plane

Drawing Size: Z-direction: ±5 m; R-direction: 10 m

Materials

Cooling tube Vacuum, relative permittivity = 1, relative permeability = 1

Superconducting cable Copper at 4K, relative permittivity = 1, relative permeability = 1, conductivity = 6.4E9 S/m

Stainless steel jacket Stainless steel at 4K, relative permittivity = 1, relative permeability = 1, conductivity = 1.88e6 S/m

Insulation Epoxy resin, relative permittivity = 4, relative permeability = 1

Background: Vacuum, relative permittivity = 1, relative permeability = 1

Setup Boundaries and Sources

Current Source All superconducting cables are stranded with 45 kA

Boundary Balloon

Setup Executive Parameters

All superconducting cables were chosen into the impedance matrix.

Return path of the current was set to default.

Setup Solution Options

Mesh: Manual mesh

Object	Insulation	Cooling Tube	Superconducting cable	Stainless steel jacket	Background
Number of triangles	3600	34	1200	2600	1200

(d) Calculation Results of Detailed FEM Model of PF 6 Coil

Capacitances of conductors between the layers in one double pancake (F)		Capacitances of conductors between double pancakes(F)		Capacitances between the conductors of one layer (F)	
C_P01_02_C01	5.84E-09	C_P02_03_C01	5.12E-09	C_P01_C01_02	6.06E-09
C_P01_02_C02	5.94E-09	C_P02_03_C02	5.21E-09	C_P01_C02_03	6.17E-09
C_P01_02_C03	6.04E-09	C_P02_03_C03	5.30E-09	C_P01_C03_04	6.27E-09
C_P01_02_C04	6.14E-09	C_P02_03_C04	5.39E-09	C_P01_C04_05	6.38E-09
C_P01_02_C05	6.25E-09	C_P02_03_C05	5.48E-09	C_P01_C05_06	6.48E-09
C_P01_02_C06	6.35E-09	C_P02_03_C06	5.56E-09	C_P01_C06_07	6.58E-09
C_P01_02_C07	6.45E-09	C_P02_03_C07	5.65E-09	C_P01_C07_08	6.69E-09
C_P01_02_C08	6.55E-09	C_P02_03_C08	5.74E-09	C_P01_C08_09	6.79E-09
C_P01_02_C09	6.65E-09	C_P02_03_C09	5.83E-09	C_P01_C09_10	6.90E-09
C_P01_02_C10	6.75E-09	C_P02_03_C10	5.92E-09	C_P01_C10_11	7.00E-09
C_P01_02_C11	6.86E-09	C_P02_03_C11	6.01E-09	C_P01_C11_12	7.11E-09
C_P01_02_C12	6.96E-09	C_P02_03_C12	6.10E-09	C_P01_C12_13	7.21E-09
C_P01_02_C13	7.06E-09	C_P02_03_C13	6.19E-09	C_P01_C13_14	7.32E-09
C_P01_02_C14	7.16E-09	C_P02_03_C14	6.28E-09	C_P01_C14_15	7.42E-09
C_P01_02_C15	7.26E-09	C_P02_03_C15	6.37E-09	C_P01_C15_16	7.53E-09
C_P01_02_C16	7.36E-09	C_P02_03_C16	6.46E-09	C_P01_C16_17	7.63E-09
C_P01_02_C17	7.47E-09	C_P02_03_C17	6.54E-09	C_P01_C17_18	7.73E-09
C_P01_02_C18	7.57E-09	C_P02_03_C18	6.63E-09	C_P01_C18_19	7.84E-09
C_P01_02_C19	7.67E-09	C_P02_03_C19	6.72E-09	C_P01_C19_20	7.94E-09
C_P01_02_C20	7.77E-09	C_P02_03_C20	6.81E-09	C_P01_C20_21	8.05E-09
C_P01_02_C21	7.87E-09	C_P02_03_C21	6.90E-09	C_P01_C21_22	8.15E-09
C_P01_02_C22	7.97E-09	C_P02_03_C22	6.99E-09	C_P01_C22_23	8.26E-09
C_P01_02_C23	8.08E-09	C_P02_03_C23	7.08E-09	C_P01_C23_24	8.36E-09
C_P01_02_C24	8.18E-09	C_P02_03_C24	7.17E-09	C_P01_C24_25	8.47E-09
C_P01_02_C25	8.28E-09	C_P02_03_C25	7.26E-09	C_P01_C25_26	8.57E-09
C_P01_02_C26	8.38E-09	C_P02_03_C26	7.35E-09	C_P01_C26_27	8.68E-09
C_P01_02_C27	8.48E-09	C_P02_03_C27	7.44E-09		

Tab. A.3-1 Calculated capacitances between the conductors of PF 6 coil

Capacitances of the conductors to ground in lowest and upper-most pancakes (F)		Capacitance to ground for outer conductors on the left and right side of the coil (F)		Capacitance to ground for lowest and uppermost outer conductors in Z-direction (F)	
C_P01_E_C01	6.25E-09	C_P02_E_C01	3.11E-09	C_P01_E_C01	3.14E-09
C_P01_E_C02	3.20E-09	C_P02_E_C27	4.43E-09	C_P01_E_C27	4.56E-09
C_P01_E_C03	3.25E-09				
C_P01_E_C04	3.31E-09				
C_P01_E_C05	3.36E-09				
C_P01_E_C06	3.41E-09				
C_P01_E_C07	3.47E-09				
C_P01_E_C08	3.52E-09				
C_P01_E_C09	3.58E-09				
C_P01_E_C10	3.63E-09				
C_P01_E_C11	3.69E-09				
C_P01_E_C12	3.74E-09				
C_P01_E_C13	3.80E-09				
C_P01_E_C14	3.85E-09				
C_P01_E_C15	3.91E-09				
C_P01_E_C16	3.96E-09				
C_P01_E_C17	4.02E-09				
C_P01_E_C18	4.07E-09				
C_P01_E_C19	4.13E-09				
C_P01_E_C20	4.18E-09				
C_P01_E_C21	4.23E-09				
C_P01_E_C22	4.29E-09				
C_P01_E_C23	4.34E-09				
C_P01_E_C24	4.40E-09				
C_P01_E_C25	4.45E-09				
C_P01_E_C26	4.51E-09				
C_P01_E_C27	8.99E-09				

Tab. A.3-2 Calculated capacitances of the outer conductors to ground of PF 6 coil

SC_1_1	3.29E-03	SC_5_1	3.55E-03	SC_9_1	3.63E-03	SC_13_1	3.51E-03
SC_1_2	3.44E-03	SC_5_2	3.74E-03	SC_9_2	3.82E-03	SC_13_2	3.69E-03
SC_1_3	3.59E-03	SC_5_3	3.92E-03	SC_9_3	4.00E-03	SC_13_3	3.86E-03
SC_1_4	3.73E-03	SC_5_4	4.08E-03	SC_9_4	4.18E-03	SC_13_4	4.02E-03
SC_1_5	3.86E-03	SC_5_5	4.24E-03	SC_9_5	4.34E-03	SC_13_5	4.17E-03
SC_1_6	3.99E-03	SC_5_6	4.38E-03	SC_9_6	4.49E-03	SC_13_6	4.31E-03
SC_1_7	4.11E-03	SC_5_7	4.52E-03	SC_9_7	4.63E-03	SC_13_7	4.45E-03
SC_1_8	4.22E-03	SC_5_8	4.65E-03	SC_9_8	4.76E-03	SC_13_8	4.57E-03
SC_1_9	4.32E-03	SC_5_9	4.76E-03	SC_9_9	4.88E-03	SC_13_9	4.68E-03
SC_1_10	4.42E-03	SC_5_10	4.87E-03	SC_9_10	4.99E-03	SC_13_10	4.79E-03
SC_1_11	4.50E-03	SC_5_11	4.97E-03	SC_9_11	5.09E-03	SC_13_11	4.88E-03
SC_1_12	4.58E-03	SC_5_12	5.06E-03	SC_9_12	5.18E-03	SC_13_12	4.97E-03
SC_1_13	4.65E-03	SC_5_13	5.13E-03	SC_9_13	5.26E-03	SC_13_13	5.05E-03
SC_1_14	4.71E-03	SC_5_14	5.20E-03	SC_9_14	5.33E-03	SC_13_14	5.11E-03
SC_1_15	4.76E-03	SC_5_15	5.26E-03	SC_9_15	5.39E-03	SC_13_15	5.17E-03
SC_1_16	4.81E-03	SC_5_16	5.30E-03	SC_9_16	5.44E-03	SC_13_16	5.21E-03
SC_1_17	4.84E-03	SC_5_17	5.34E-03	SC_9_17	5.47E-03	SC_13_17	5.25E-03
SC_1_18	4.86E-03	SC_5_18	5.36E-03	SC_9_18	5.49E-03	SC_13_18	5.27E-03
SC_1_19	4.87E-03	SC_5_19	5.37E-03	SC_9_19	5.50E-03	SC_13_19	5.28E-03
SC_1_20	4.87E-03	SC_5_20	5.37E-03	SC_9_20	5.50E-03	SC_13_20	5.28E-03
SC_1_21	4.86E-03	SC_5_21	5.35E-03	SC_9_21	5.48E-03	SC_13_21	5.26E-03
SC_1_22	4.84E-03	SC_5_22	5.31E-03	SC_9_22	5.44E-03	SC_13_22	5.23E-03
SC_1_23	4.80E-03	SC_5_23	5.26E-03	SC_9_23	5.38E-03	SC_13_23	5.18E-03
SC_1_24	4.75E-03	SC_5_24	5.20E-03	SC_9_24	5.31E-03	SC_13_24	5.12E-03
SC_1_25	4.69E-03	SC_5_25	5.11E-03	SC_9_25	5.22E-03	SC_13_25	5.03E-03
SC_1_26	4.61E-03	SC_5_26	5.00E-03	SC_9_26	5.10E-03	SC_13_26	4.93E-03
SC_1_27	4.51E-03	SC_5_27	4.87E-03	SC_9_27	4.97E-03	SC_13_27	4.81E-03
SC_2_1	3.37E-03	SC_6_1	3.59E-03	SC_10_1	3.61E-03	SC_14_1	3.45E-03
SC_2_2	3.54E-03	SC_6_2	3.78E-03	SC_10_2	3.81E-03	SC_14_2	3.62E-03
SC_2_3	3.70E-03	SC_6_3	3.96E-03	SC_10_3	3.99E-03	SC_14_3	3.79E-03
SC_2_4	3.84E-03	SC_6_4	4.13E-03	SC_10_4	4.16E-03	SC_14_4	3.94E-03
SC_2_5	3.98E-03	SC_6_5	4.29E-03	SC_10_5	4.32E-03	SC_14_5	4.09E-03
SC_2_6	4.12E-03	SC_6_6	4.44E-03	SC_10_6	4.47E-03	SC_14_6	4.23E-03
SC_2_7	4.24E-03	SC_6_7	4.58E-03	SC_10_7	4.61E-03	SC_14_7	4.36E-03
SC_2_8	4.36E-03	SC_6_8	4.70E-03	SC_10_8	4.74E-03	SC_14_8	4.47E-03
SC_2_9	4.46E-03	SC_6_9	4.82E-03	SC_10_9	4.86E-03	SC_14_9	4.59E-03
SC_2_10	4.56E-03	SC_6_10	4.93E-03	SC_10_10	4.97E-03	SC_14_10	4.69E-03
SC_2_11	4.65E-03	SC_6_11	5.03E-03	SC_10_11	5.07E-03	SC_14_11	4.78E-03
SC_2_12	4.73E-03	SC_6_12	5.12E-03	SC_10_12	5.16E-03	SC_14_12	4.86E-03
SC_2_13	4.81E-03	SC_6_13	5.20E-03	SC_10_13	5.24E-03	SC_14_13	4.94E-03
SC_2_14	4.87E-03	SC_6_14	5.27E-03	SC_10_14	5.31E-03	SC_14_14	5.00E-03
SC_2_15	4.92E-03	SC_6_15	5.32E-03	SC_10_15	5.37E-03	SC_14_15	5.06E-03
SC_2_16	4.97E-03	SC_6_16	5.37E-03	SC_10_16	5.42E-03	SC_14_16	5.10E-03
SC_2_17	5.00E-03	SC_6_17	5.40E-03	SC_10_17	5.45E-03	SC_14_17	5.14E-03
SC_2_18	5.02E-03	SC_6_18	5.43E-03	SC_10_18	5.47E-03	SC_14_18	5.16E-03
SC_2_19	5.03E-03	SC_6_19	5.44E-03	SC_10_19	5.48E-03	SC_14_19	5.17E-03
SC_2_20	5.03E-03	SC_6_20	5.43E-03	SC_10_20	5.48E-03	SC_14_20	5.17E-03
SC_2_21	5.02E-03	SC_6_21	5.41E-03	SC_10_21	5.45E-03	SC_14_21	5.15E-03
SC_2_22	4.99E-03	SC_6_22	5.38E-03	SC_10_22	5.42E-03	SC_14_22	5.12E-03
SC_2_23	4.95E-03	SC_6_23	5.32E-03	SC_10_23	5.37E-03	SC_14_23	5.08E-03
SC_2_24	4.90E-03	SC_6_24	5.25E-03	SC_10_24	5.29E-03	SC_14_24	5.02E-03
SC_2_25	4.82E-03	SC_6_25	5.16E-03	SC_10_25	5.20E-03	SC_14_25	4.94E-03
SC_2_26	4.74E-03	SC_6_26	5.05E-03	SC_10_26	5.09E-03	SC_14_26	4.84E-03
SC_2_27	4.63E-03	SC_6_27	4.92E-03	SC_10_27	4.95E-03	SC_14_27	4.73E-03
SC_3_1	3.45E-03	SC_7_1	3.61E-03	SC_11_1	3.59E-03	SC_15_1	3.37E-03

SC_3_2	3.62E-03	SC_7_2	3.81E-03	SC_11_2	3.78E-03	SC_15_2	3.54E-03
SC_3_3	3.79E-03	SC_7_3	3.99E-03	SC_11_3	3.96E-03	SC_15_3	3.70E-03
SC_3_4	3.94E-03	SC_7_4	4.16E-03	SC_11_4	4.13E-03	SC_15_4	3.85E-03
SC_3_5	4.09E-03	SC_7_5	4.32E-03	SC_11_5	4.29E-03	SC_15_5	3.99E-03
SC_3_6	4.23E-03	SC_7_6	4.47E-03	SC_11_6	4.44E-03	SC_15_6	4.12E-03
SC_3_7	4.35E-03	SC_7_7	4.61E-03	SC_11_7	4.58E-03	SC_15_7	4.24E-03
SC_3_8	4.47E-03	SC_7_8	4.74E-03	SC_11_8	4.70E-03	SC_15_8	4.36E-03
SC_3_9	4.58E-03	SC_7_9	4.86E-03	SC_11_9	4.82E-03	SC_15_9	4.46E-03
SC_3_10	4.69E-03	SC_7_10	4.97E-03	SC_11_10	4.93E-03	SC_15_10	4.56E-03
SC_3_11	4.78E-03	SC_7_11	5.07E-03	SC_11_11	5.03E-03	SC_15_11	4.65E-03
SC_3_12	4.86E-03	SC_7_12	5.16E-03	SC_11_12	5.12E-03	SC_15_12	4.73E-03
SC_3_13	4.94E-03	SC_7_13	5.24E-03	SC_11_13	5.20E-03	SC_15_13	4.81E-03
SC_3_14	5.00E-03	SC_7_14	5.31E-03	SC_11_14	5.27E-03	SC_15_14	4.87E-03
SC_3_15	5.06E-03	SC_7_15	5.37E-03	SC_11_15	5.32E-03	SC_15_15	4.92E-03
SC_3_16	5.10E-03	SC_7_16	5.41E-03	SC_11_16	5.37E-03	SC_15_16	4.97E-03
SC_3_17	5.14E-03	SC_7_17	5.45E-03	SC_11_17	5.41E-03	SC_15_17	5.00E-03
SC_3_18	5.16E-03	SC_7_18	5.47E-03	SC_11_18	5.43E-03	SC_15_18	5.02E-03
SC_3_19	5.17E-03	SC_7_19	5.48E-03	SC_11_19	5.44E-03	SC_15_19	5.03E-03
SC_3_20	5.17E-03	SC_7_20	5.47E-03	SC_11_20	5.43E-03	SC_15_20	5.03E-03
SC_3_21	5.15E-03	SC_7_21	5.45E-03	SC_11_21	5.41E-03	SC_15_21	5.02E-03
SC_3_22	5.12E-03	SC_7_22	5.42E-03	SC_11_22	5.38E-03	SC_15_22	4.99E-03
SC_3_23	5.08E-03	SC_7_23	5.36E-03	SC_11_23	5.32E-03	SC_15_23	4.95E-03
SC_3_24	5.02E-03	SC_7_24	5.29E-03	SC_11_24	5.25E-03	SC_15_24	4.90E-03
SC_3_25	4.94E-03	SC_7_25	5.20E-03	SC_11_25	5.16E-03	SC_15_25	4.83E-03
SC_3_26	4.84E-03	SC_7_26	5.09E-03	SC_11_26	5.05E-03	SC_15_26	4.74E-03
SC_3_27	4.72E-03	SC_7_27	4.95E-03	SC_11_27	4.92E-03	SC_15_27	4.63E-03
SC_4_1	3.51E-03	SC_8_1	3.63E-03	SC_12_1	3.55E-03	SC_16_1	3.29E-03
SC_4_2	3.69E-03	SC_8_2	3.82E-03	SC_12_2	3.74E-03	SC_16_2	3.44E-03
SC_4_3	3.86E-03	SC_8_3	4.00E-03	SC_12_3	3.92E-03	SC_16_3	3.59E-03
SC_4_4	4.02E-03	SC_8_4	4.18E-03	SC_12_4	4.08E-03	SC_16_4	3.73E-03
SC_4_5	4.17E-03	SC_8_5	4.34E-03	SC_12_5	4.24E-03	SC_16_5	3.87E-03
SC_4_6	4.31E-03	SC_8_6	4.49E-03	SC_12_6	4.39E-03	SC_16_6	3.99E-03
SC_4_7	4.45E-03	SC_8_7	4.63E-03	SC_12_7	4.52E-03	SC_16_7	4.11E-03
SC_4_8	4.57E-03	SC_8_8	4.76E-03	SC_12_8	4.65E-03	SC_16_8	4.22E-03
SC_4_9	4.68E-03	SC_8_9	4.88E-03	SC_12_9	4.76E-03	SC_16_9	4.32E-03
SC_4_10	4.79E-03	SC_8_10	4.99E-03	SC_12_10	4.87E-03	SC_16_10	4.42E-03
SC_4_11	4.88E-03	SC_8_11	5.09E-03	SC_12_11	4.97E-03	SC_16_11	4.51E-03
SC_4_12	4.97E-03	SC_8_12	5.18E-03	SC_12_12	5.06E-03	SC_16_12	4.58E-03
SC_4_13	5.05E-03	SC_8_13	5.26E-03	SC_12_13	5.13E-03	SC_16_13	4.65E-03
SC_4_14	5.11E-03	SC_8_14	5.33E-03	SC_12_14	5.20E-03	SC_16_14	4.71E-03
SC_4_15	5.17E-03	SC_8_15	5.39E-03	SC_12_15	5.26E-03	SC_16_15	4.77E-03
SC_4_16	5.21E-03	SC_8_16	5.44E-03	SC_12_16	5.30E-03	SC_16_16	4.81E-03
SC_4_17	5.25E-03	SC_8_17	5.47E-03	SC_12_17	5.34E-03	SC_16_17	4.84E-03
SC_4_18	5.27E-03	SC_8_18	5.49E-03	SC_12_18	5.36E-03	SC_16_18	4.86E-03
SC_4_19	5.28E-03	SC_8_19	5.50E-03	SC_12_19	5.37E-03	SC_16_19	4.87E-03
SC_4_20	5.28E-03	SC_8_20	5.50E-03	SC_12_20	5.37E-03	SC_16_20	4.87E-03
SC_4_21	5.26E-03	SC_8_21	5.48E-03	SC_12_21	5.35E-03	SC_16_21	4.86E-03
SC_4_22	5.23E-03	SC_8_22	5.44E-03	SC_12_22	5.31E-03	SC_16_22	4.84E-03
SC_4_23	5.18E-03	SC_8_23	5.38E-03	SC_12_23	5.26E-03	SC_16_23	4.80E-03
SC_4_24	5.12E-03	SC_8_24	5.31E-03	SC_12_24	5.20E-03	SC_16_24	4.75E-03
SC_4_25	5.03E-03	SC_8_25	5.22E-03	SC_12_25	5.11E-03	SC_16_25	4.69E-03
SC_4_26	4.93E-03	SC_8_26	5.10E-03	SC_12_26	5.00E-03	SC_16_26	4.61E-03
SC_4_27	4.80E-03	SC_8_27	4.96E-03	SC_12_27	4.87E-03	SC_16_27	4.51E-03

Tab. A.3-3 Cumulative inductances for each conductor of PF 6 coil at DC (H)

SC_1_1	3.19E-06	SC_5_1	3.19E-06	SC_9_1	3.19E-06	SC_13_1	3.19E-06
SC_1_2	3.68E-06	SC_5_2	3.68E-06	SC_9_2	3.68E-06	SC_13_2	3.68E-06
SC_1_3	3.76E-06	SC_5_3	3.76E-06	SC_9_3	3.76E-06	SC_13_3	3.76E-06
SC_1_4	3.82E-06	SC_5_4	3.82E-06	SC_9_4	3.82E-06	SC_13_4	3.82E-06
SC_1_5	3.89E-06	SC_5_5	3.89E-06	SC_9_5	3.89E-06	SC_13_5	3.89E-06
SC_1_6	3.95E-06	SC_5_6	3.95E-06	SC_9_6	3.95E-06	SC_13_6	3.95E-06
SC_1_7	4.02E-06	SC_5_7	4.02E-06	SC_9_7	4.02E-06	SC_13_7	4.02E-06
SC_1_8	4.08E-06	SC_5_8	4.08E-06	SC_9_8	4.08E-06	SC_13_8	4.08E-06
SC_1_9	4.15E-06	SC_5_9	4.15E-06	SC_9_9	4.15E-06	SC_13_9	4.15E-06
SC_1_10	4.21E-06	SC_5_10	4.21E-06	SC_9_10	4.21E-06	SC_13_10	4.21E-06
SC_1_11	4.27E-06	SC_5_11	4.27E-06	SC_9_11	4.27E-06	SC_13_11	4.27E-06
SC_1_12	4.34E-06	SC_5_12	4.34E-06	SC_9_12	4.34E-06	SC_13_12	4.34E-06
SC_1_13	4.40E-06	SC_5_13	4.40E-06	SC_9_13	4.40E-06	SC_13_13	4.40E-06
SC_1_14	4.47E-06	SC_5_14	4.47E-06	SC_9_14	4.47E-06	SC_13_14	4.47E-06
SC_1_15	4.53E-06	SC_5_15	4.53E-06	SC_9_15	4.53E-06	SC_13_15	4.53E-06
SC_1_16	4.60E-06	SC_5_16	4.60E-06	SC_9_16	4.60E-06	SC_13_16	4.60E-06
SC_1_17	4.66E-06	SC_5_17	4.66E-06	SC_9_17	4.66E-06	SC_13_17	4.66E-06
SC_1_18	4.73E-06	SC_5_18	4.73E-06	SC_9_18	4.73E-06	SC_13_18	4.73E-06
SC_1_19	4.79E-06	SC_5_19	4.79E-06	SC_9_19	4.79E-06	SC_13_19	4.79E-06
SC_1_20	4.86E-06	SC_5_20	4.86E-06	SC_9_20	4.86E-06	SC_13_20	4.86E-06
SC_1_21	4.93E-06	SC_5_21	4.93E-06	SC_9_21	4.93E-06	SC_13_21	4.93E-06
SC_1_22	5.01E-06	SC_5_22	5.01E-06	SC_9_22	5.01E-06	SC_13_22	5.01E-06
SC_1_23	5.14E-06	SC_5_23	5.14E-06	SC_9_23	5.14E-06	SC_13_23	5.14E-06
SC_1_24	5.32E-06	SC_5_24	5.32E-06	SC_9_24	5.32E-06	SC_13_24	5.32E-06
SC_1_25	6.76E-06	SC_5_25	6.76E-06	SC_9_25	6.76E-06	SC_13_25	6.76E-06
SC_1_26	6.62E-06	SC_5_26	6.62E-06	SC_9_26	6.62E-06	SC_13_26	6.62E-06
SC_1_27	6.61E-06	SC_5_27	6.61E-06	SC_9_27	6.61E-06	SC_13_27	6.61E-06
SC_2_1	3.19E-06	SC_6_1	3.19E-06	SC_10_1	3.19E-06	SC_14_1	3.19E-06
SC_2_2	3.68E-06	SC_6_2	3.68E-06	SC_10_2	3.68E-06	SC_14_2	3.68E-06
SC_2_3	3.76E-06	SC_6_3	3.76E-06	SC_10_3	3.76E-06	SC_14_3	3.76E-06
SC_2_4	3.82E-06	SC_6_4	3.82E-06	SC_10_4	3.82E-06	SC_14_4	3.82E-06
SC_2_5	3.89E-06	SC_6_5	3.89E-06	SC_10_5	3.89E-06	SC_14_5	3.89E-06
SC_2_6	3.95E-06	SC_6_6	3.95E-06	SC_10_6	3.95E-06	SC_14_6	3.95E-06
SC_2_7	4.02E-06	SC_6_7	4.02E-06	SC_10_7	4.02E-06	SC_14_7	4.02E-06
SC_2_8	4.08E-06	SC_6_8	4.08E-06	SC_10_8	4.08E-06	SC_14_8	4.08E-06
SC_2_9	4.15E-06	SC_6_9	4.15E-06	SC_10_9	4.15E-06	SC_14_9	4.15E-06
SC_2_10	4.21E-06	SC_6_10	4.21E-06	SC_10_10	4.21E-06	SC_14_10	4.21E-06
SC_2_11	4.27E-06	SC_6_11	4.27E-06	SC_10_11	4.27E-06	SC_14_11	4.27E-06
SC_2_12	4.34E-06	SC_6_12	4.34E-06	SC_10_12	4.34E-06	SC_14_12	4.34E-06
SC_2_13	4.40E-06	SC_6_13	4.40E-06	SC_10_13	4.40E-06	SC_14_13	4.40E-06
SC_2_14	4.47E-06	SC_6_14	4.47E-06	SC_10_14	4.47E-06	SC_14_14	4.47E-06
SC_2_15	4.53E-06	SC_6_15	4.53E-06	SC_10_15	4.53E-06	SC_14_15	4.53E-06
SC_2_16	4.60E-06	SC_6_16	4.60E-06	SC_10_16	4.60E-06	SC_14_16	4.60E-06
SC_2_17	4.66E-06	SC_6_17	4.66E-06	SC_10_17	4.66E-06	SC_14_17	4.66E-06
SC_2_18	4.73E-06	SC_6_18	4.73E-06	SC_10_18	4.73E-06	SC_14_18	4.73E-06
SC_2_19	4.79E-06	SC_6_19	4.79E-06	SC_10_19	4.79E-06	SC_14_19	4.79E-06
SC_2_20	4.86E-06	SC_6_20	4.86E-06	SC_10_20	4.86E-06	SC_14_20	4.86E-06
SC_2_21	4.93E-06	SC_6_21	4.93E-06	SC_10_21	4.93E-06	SC_14_21	4.93E-06
SC_2_22	5.01E-06	SC_6_22	5.01E-06	SC_10_22	5.01E-06	SC_14_22	5.01E-06
SC_2_23	5.14E-06	SC_6_23	5.14E-06	SC_10_23	5.14E-06	SC_14_23	5.14E-06
SC_2_24	5.32E-06	SC_6_24	5.32E-06	SC_10_24	5.32E-06	SC_14_24	5.32E-06
SC_2_25	6.76E-06	SC_6_25	6.76E-06	SC_10_25	6.76E-06	SC_14_25	6.76E-06
SC_2_26	6.62E-06	SC_6_26	6.62E-06	SC_10_26	6.62E-06	SC_14_26	6.62E-06
SC_2_27	6.61E-06	SC_6_27	6.61E-06	SC_10_27	6.61E-06	SC_14_27	6.61E-06
SC_3_1	3.19E-06	SC_7_1	3.19E-06	SC_11_1	3.19E-06	SC_15_1	3.19E-06

SC_3_2	3.68E-06	SC_7_2	3.68E-06	SC_11_2	3.68E-06	SC_15_2	3.68E-06
SC_3_3	3.76E-06	SC_7_3	3.76E-06	SC_11_3	3.76E-06	SC_15_3	3.76E-06
SC_3_4	3.82E-06	SC_7_4	3.82E-06	SC_11_4	3.82E-06	SC_15_4	3.82E-06
SC_3_5	3.89E-06	SC_7_5	3.89E-06	SC_11_5	3.89E-06	SC_15_5	3.89E-06
SC_3_6	3.95E-06	SC_7_6	3.95E-06	SC_11_6	3.95E-06	SC_15_6	3.95E-06
SC_3_7	4.02E-06	SC_7_7	4.02E-06	SC_11_7	4.02E-06	SC_15_7	4.02E-06
SC_3_8	4.08E-06	SC_7_8	4.08E-06	SC_11_8	4.08E-06	SC_15_8	4.08E-06
SC_3_9	4.15E-06	SC_7_9	4.15E-06	SC_11_9	4.15E-06	SC_15_9	4.15E-06
SC_3_10	4.21E-06	SC_7_10	4.21E-06	SC_11_10	4.21E-06	SC_15_10	4.21E-06
SC_3_11	4.27E-06	SC_7_11	4.27E-06	SC_11_11	4.27E-06	SC_15_11	4.27E-06
SC_3_12	4.34E-06	SC_7_12	4.34E-06	SC_11_12	4.34E-06	SC_15_12	4.34E-06
SC_3_13	4.40E-06	SC_7_13	4.40E-06	SC_11_13	4.40E-06	SC_15_13	4.40E-06
SC_3_14	4.47E-06	SC_7_14	4.47E-06	SC_11_14	4.47E-06	SC_15_14	4.47E-06
SC_3_15	4.53E-06	SC_7_15	4.53E-06	SC_11_15	4.53E-06	SC_15_15	4.53E-06
SC_3_16	4.60E-06	SC_7_16	4.60E-06	SC_11_16	4.60E-06	SC_15_16	4.60E-06
SC_3_17	4.66E-06	SC_7_17	4.66E-06	SC_11_17	4.66E-06	SC_15_17	4.66E-06
SC_3_18	4.73E-06	SC_7_18	4.73E-06	SC_11_18	4.73E-06	SC_15_18	4.73E-06
SC_3_19	4.79E-06	SC_7_19	4.79E-06	SC_11_19	4.79E-06	SC_15_19	4.79E-06
SC_3_20	4.86E-06	SC_7_20	4.86E-06	SC_11_20	4.86E-06	SC_15_20	4.86E-06
SC_3_21	4.93E-06	SC_7_21	4.93E-06	SC_11_21	4.93E-06	SC_15_21	4.93E-06
SC_3_22	5.01E-06	SC_7_22	5.01E-06	SC_11_22	5.01E-06	SC_15_22	5.01E-06
SC_3_23	5.14E-06	SC_7_23	5.14E-06	SC_11_23	5.14E-06	SC_15_23	5.14E-06
SC_3_24	5.32E-06	SC_7_24	5.32E-06	SC_11_24	5.32E-06	SC_15_24	5.32E-06
SC_3_25	6.76E-06	SC_7_25	6.76E-06	SC_11_25	6.76E-06	SC_15_25	6.76E-06
SC_3_26	6.62E-06	SC_7_26	6.62E-06	SC_11_26	6.62E-06	SC_15_26	6.62E-06
SC_3_27	6.61E-06	SC_7_27	6.61E-06	SC_11_27	6.61E-06	SC_15_27	6.61E-06
SC_4_1	3.19E-06	SC_8_1	3.19E-06	SC_12_1	3.19E-06	SC_16_1	3.19E-06
SC_4_2	3.68E-06	SC_8_2	3.68E-06	SC_12_2	3.68E-06	SC_16_2	3.68E-06
SC_4_3	3.76E-06	SC_8_3	3.76E-06	SC_12_3	3.76E-06	SC_16_3	3.76E-06
SC_4_4	3.82E-06	SC_8_4	3.82E-06	SC_12_4	3.82E-06	SC_16_4	3.82E-06
SC_4_5	3.89E-06	SC_8_5	3.89E-06	SC_12_5	3.89E-06	SC_16_5	3.89E-06
SC_4_6	3.95E-06	SC_8_6	3.95E-06	SC_12_6	3.95E-06	SC_16_6	3.95E-06
SC_4_7	4.02E-06	SC_8_7	4.02E-06	SC_12_7	4.02E-06	SC_16_7	4.02E-06
SC_4_8	4.08E-06	SC_8_8	4.08E-06	SC_12_8	4.08E-06	SC_16_8	4.08E-06
SC_4_9	4.15E-06	SC_8_9	4.15E-06	SC_12_9	4.15E-06	SC_16_9	4.15E-06
SC_4_10	4.21E-06	SC_8_10	4.21E-06	SC_12_10	4.21E-06	SC_16_10	4.21E-06
SC_4_11	4.27E-06	SC_8_11	4.27E-06	SC_12_11	4.27E-06	SC_16_11	4.27E-06
SC_4_12	4.34E-06	SC_8_12	4.34E-06	SC_12_12	4.34E-06	SC_16_12	4.34E-06
SC_4_13	4.40E-06	SC_8_13	4.40E-06	SC_12_13	4.40E-06	SC_16_13	4.40E-06
SC_4_14	4.47E-06	SC_8_14	4.47E-06	SC_12_14	4.47E-06	SC_16_14	4.47E-06
SC_4_15	4.53E-06	SC_8_15	4.53E-06	SC_12_15	4.53E-06	SC_16_15	4.53E-06
SC_4_16	4.60E-06	SC_8_16	4.60E-06	SC_12_16	4.60E-06	SC_16_16	4.60E-06
SC_4_17	4.66E-06	SC_8_17	4.66E-06	SC_12_17	4.66E-06	SC_16_17	4.66E-06
SC_4_18	4.73E-06	SC_8_18	4.73E-06	SC_12_18	4.73E-06	SC_16_18	4.73E-06
SC_4_19	4.79E-06	SC_8_19	4.79E-06	SC_12_19	4.79E-06	SC_16_19	4.79E-06
SC_4_20	4.86E-06	SC_8_20	4.86E-06	SC_12_20	4.86E-06	SC_16_20	4.86E-06
SC_4_21	4.93E-06	SC_8_21	4.93E-06	SC_12_21	4.93E-06	SC_16_21	4.93E-06
SC_4_22	5.01E-06	SC_8_22	5.01E-06	SC_12_22	5.01E-06	SC_16_22	5.01E-06
SC_4_23	5.14E-06	SC_8_23	5.14E-06	SC_12_23	5.14E-06	SC_16_23	5.14E-06
SC_4_24	5.32E-06	SC_8_24	5.32E-06	SC_12_24	5.32E-06	SC_16_24	5.32E-06
SC_4_25	6.76E-06	SC_8_25	6.76E-06	SC_12_25	6.76E-06	SC_16_25	6.76E-06
SC_4_26	6.62E-06	SC_8_26	6.62E-06	SC_12_26	6.62E-06	SC_16_26	6.62E-06
SC_4_27	6.61E-06	SC_8_27	6.61E-06	SC_12_27	6.61E-06	SC_16_27	6.61E-06

Tab. A.3-4 Cumulative inductances for each conductor of PF 6 coil at 406 Hz (H)

SC_1_1	2.81E-06	SC_5_1	2.81E-06	SC_9_1	2.81E-06	SC_13_1	2.81E-06
SC_1_2	3.29E-06	SC_5_2	3.29E-06	SC_9_2	3.29E-06	SC_13_2	3.29E-06
SC_1_3	3.35E-06	SC_5_3	3.35E-06	SC_9_3	3.35E-06	SC_13_3	3.35E-06
SC_1_4	3.41E-06	SC_5_4	3.41E-06	SC_9_4	3.41E-06	SC_13_4	3.41E-06
SC_1_5	3.46E-06	SC_5_5	3.46E-06	SC_9_5	3.46E-06	SC_13_5	3.46E-06
SC_1_6	3.52E-06	SC_5_6	3.52E-06	SC_9_6	3.52E-06	SC_13_6	3.52E-06
SC_1_7	3.58E-06	SC_5_7	3.58E-06	SC_9_7	3.58E-06	SC_13_7	3.58E-06
SC_1_8	3.64E-06	SC_5_8	3.64E-06	SC_9_8	3.64E-06	SC_13_8	3.64E-06
SC_1_9	3.69E-06	SC_5_9	3.69E-06	SC_9_9	3.69E-06	SC_13_9	3.69E-06
SC_1_10	3.75E-06	SC_5_10	3.75E-06	SC_9_10	3.75E-06	SC_13_10	3.75E-06
SC_1_11	3.81E-06	SC_5_11	3.81E-06	SC_9_11	3.81E-06	SC_13_11	3.81E-06
SC_1_12	3.86E-06	SC_5_12	3.86E-06	SC_9_12	3.86E-06	SC_13_12	3.86E-06
SC_1_13	3.92E-06	SC_5_13	3.92E-06	SC_9_13	3.92E-06	SC_13_13	3.92E-06
SC_1_14	3.98E-06	SC_5_14	3.98E-06	SC_9_14	3.98E-06	SC_13_14	3.98E-06
SC_1_15	4.03E-06	SC_5_15	4.03E-06	SC_9_15	4.03E-06	SC_13_15	4.03E-06
SC_1_16	4.09E-06	SC_5_16	4.09E-06	SC_9_16	4.09E-06	SC_13_16	4.09E-06
SC_1_17	4.15E-06	SC_5_17	4.15E-06	SC_9_17	4.15E-06	SC_13_17	4.15E-06
SC_1_18	4.21E-06	SC_5_18	4.21E-06	SC_9_18	4.21E-06	SC_13_18	4.21E-06
SC_1_19	4.26E-06	SC_5_19	4.26E-06	SC_9_19	4.26E-06	SC_13_19	4.26E-06
SC_1_20	4.32E-06	SC_5_20	4.32E-06	SC_9_20	4.32E-06	SC_13_20	4.32E-06
SC_1_21	4.38E-06	SC_5_21	4.38E-06	SC_9_21	4.38E-06	SC_13_21	4.38E-06
SC_1_22	4.45E-06	SC_5_22	4.45E-06	SC_9_22	4.45E-06	SC_13_22	4.45E-06
SC_1_23	4.55E-06	SC_5_23	4.55E-06	SC_9_23	4.55E-06	SC_13_23	4.55E-06
SC_1_24	4.70E-06	SC_5_24	4.70E-06	SC_9_24	4.70E-06	SC_13_24	4.70E-06
SC_1_25	6.07E-06	SC_5_25	6.07E-06	SC_9_25	6.07E-06	SC_13_25	6.07E-06
SC_1_26	6.05E-06	SC_5_26	6.05E-06	SC_9_26	6.05E-06	SC_13_26	6.05E-06
SC_1_27	5.72E-06	SC_5_27	5.72E-06	SC_9_27	5.72E-06	SC_13_27	5.72E-06
SC_2_1	2.81E-06	SC_6_1	2.81E-06	SC_10_1	2.81E-06	SC_14_1	2.81E-06
SC_2_2	3.29E-06	SC_6_2	3.29E-06	SC_10_2	3.29E-06	SC_14_2	3.29E-06
SC_2_3	3.35E-06	SC_6_3	3.35E-06	SC_10_3	3.35E-06	SC_14_3	3.35E-06
SC_2_4	3.41E-06	SC_6_4	3.41E-06	SC_10_4	3.41E-06	SC_14_4	3.41E-06
SC_2_5	3.46E-06	SC_6_5	3.46E-06	SC_10_5	3.46E-06	SC_14_5	3.46E-06
SC_2_6	3.52E-06	SC_6_6	3.52E-06	SC_10_6	3.52E-06	SC_14_6	3.52E-06
SC_2_7	3.58E-06	SC_6_7	3.58E-06	SC_10_7	3.58E-06	SC_14_7	3.58E-06
SC_2_8	3.64E-06	SC_6_8	3.64E-06	SC_10_8	3.64E-06	SC_14_8	3.64E-06
SC_2_9	3.69E-06	SC_6_9	3.69E-06	SC_10_9	3.69E-06	SC_14_9	3.69E-06
SC_2_10	3.75E-06	SC_6_10	3.75E-06	SC_10_10	3.75E-06	SC_14_10	3.75E-06
SC_2_11	3.81E-06	SC_6_11	3.81E-06	SC_10_11	3.81E-06	SC_14_11	3.81E-06
SC_2_12	3.86E-06	SC_6_12	3.86E-06	SC_10_12	3.86E-06	SC_14_12	3.86E-06
SC_2_13	3.92E-06	SC_6_13	3.92E-06	SC_10_13	3.92E-06	SC_14_13	3.92E-06
SC_2_14	3.98E-06	SC_6_14	3.98E-06	SC_10_14	3.98E-06	SC_14_14	3.98E-06
SC_2_15	4.03E-06	SC_6_15	4.03E-06	SC_10_15	4.03E-06	SC_14_15	4.03E-06
SC_2_16	4.09E-06	SC_6_16	4.09E-06	SC_10_16	4.09E-06	SC_14_16	4.09E-06
SC_2_17	4.15E-06	SC_6_17	4.15E-06	SC_10_17	4.15E-06	SC_14_17	4.15E-06
SC_2_18	4.21E-06	SC_6_18	4.21E-06	SC_10_18	4.21E-06	SC_14_18	4.21E-06
SC_2_19	4.26E-06	SC_6_19	4.26E-06	SC_10_19	4.26E-06	SC_14_19	4.26E-06
SC_2_20	4.32E-06	SC_6_20	4.32E-06	SC_10_20	4.32E-06	SC_14_20	4.32E-06
SC_2_21	4.38E-06	SC_6_21	4.38E-06	SC_10_21	4.38E-06	SC_14_21	4.38E-06
SC_2_22	4.45E-06	SC_6_22	4.45E-06	SC_10_22	4.45E-06	SC_14_22	4.45E-06
SC_2_23	4.55E-06	SC_6_23	4.55E-06	SC_10_23	4.55E-06	SC_14_23	4.55E-06
SC_2_24	4.70E-06	SC_6_24	4.70E-06	SC_10_24	4.70E-06	SC_14_24	4.70E-06
SC_2_25	6.07E-06	SC_6_25	6.07E-06	SC_10_25	6.07E-06	SC_14_25	6.07E-06
SC_2_26	6.05E-06	SC_6_26	6.05E-06	SC_10_26	6.05E-06	SC_14_26	6.05E-06
SC_2_27	5.72E-06	SC_6_27	5.72E-06	SC_10_27	5.72E-06	SC_14_27	5.72E-06
SC_3_1	2.81E-06	SC_7_1	2.81E-06	SC_11_1	2.81E-06	SC_15_1	2.81E-06

SC_3_2	3.29E-06	SC_7_2	3.29E-06	SC_11_2	3.29E-06	SC_15_2	3.29E-06
SC_3_3	3.35E-06	SC_7_3	3.35E-06	SC_11_3	3.35E-06	SC_15_3	3.35E-06
SC_3_4	3.41E-06	SC_7_4	3.41E-06	SC_11_4	3.41E-06	SC_15_4	3.41E-06
SC_3_5	3.46E-06	SC_7_5	3.46E-06	SC_11_5	3.46E-06	SC_15_5	3.46E-06
SC_3_6	3.52E-06	SC_7_6	3.52E-06	SC_11_6	3.52E-06	SC_15_6	3.52E-06
SC_3_7	3.58E-06	SC_7_7	3.58E-06	SC_11_7	3.58E-06	SC_15_7	3.58E-06
SC_3_8	3.64E-06	SC_7_8	3.64E-06	SC_11_8	3.64E-06	SC_15_8	3.64E-06
SC_3_9	3.69E-06	SC_7_9	3.69E-06	SC_11_9	3.69E-06	SC_15_9	3.69E-06
SC_3_10	3.75E-06	SC_7_10	3.75E-06	SC_11_10	3.75E-06	SC_15_10	3.75E-06
SC_3_11	3.81E-06	SC_7_11	3.81E-06	SC_11_11	3.81E-06	SC_15_11	3.81E-06
SC_3_12	3.86E-06	SC_7_12	3.86E-06	SC_11_12	3.86E-06	SC_15_12	3.86E-06
SC_3_13	3.92E-06	SC_7_13	3.92E-06	SC_11_13	3.92E-06	SC_15_13	3.92E-06
SC_3_14	3.98E-06	SC_7_14	3.98E-06	SC_11_14	3.98E-06	SC_15_14	3.98E-06
SC_3_15	4.03E-06	SC_7_15	4.03E-06	SC_11_15	4.03E-06	SC_15_15	4.03E-06
SC_3_16	4.09E-06	SC_7_16	4.09E-06	SC_11_16	4.09E-06	SC_15_16	4.09E-06
SC_3_17	4.15E-06	SC_7_17	4.15E-06	SC_11_17	4.15E-06	SC_15_17	4.15E-06
SC_3_18	4.21E-06	SC_7_18	4.21E-06	SC_11_18	4.21E-06	SC_15_18	4.21E-06
SC_3_19	4.26E-06	SC_7_19	4.26E-06	SC_11_19	4.26E-06	SC_15_19	4.26E-06
SC_3_20	4.32E-06	SC_7_20	4.32E-06	SC_11_20	4.32E-06	SC_15_20	4.32E-06
SC_3_21	4.38E-06	SC_7_21	4.38E-06	SC_11_21	4.38E-06	SC_15_21	4.38E-06
SC_3_22	4.45E-06	SC_7_22	4.45E-06	SC_11_22	4.45E-06	SC_15_22	4.45E-06
SC_3_23	4.55E-06	SC_7_23	4.55E-06	SC_11_23	4.55E-06	SC_15_23	4.55E-06
SC_3_24	4.70E-06	SC_7_24	4.70E-06	SC_11_24	4.70E-06	SC_15_24	4.70E-06
SC_3_25	6.07E-06	SC_7_25	6.07E-06	SC_11_25	6.07E-06	SC_15_25	6.07E-06
SC_3_26	6.05E-06	SC_7_26	6.05E-06	SC_11_26	6.05E-06	SC_15_26	6.05E-06
SC_3_27	5.72E-06	SC_7_27	5.72E-06	SC_11_27	5.72E-06	SC_15_27	5.72E-06
SC_4_1	2.81E-06	SC_8_1	2.81E-06	SC_12_1	2.81E-06	SC_16_1	2.81E-06
SC_4_2	3.29E-06	SC_8_2	3.29E-06	SC_12_2	3.29E-06	SC_16_2	3.29E-06
SC_4_3	3.35E-06	SC_8_3	3.35E-06	SC_12_3	3.35E-06	SC_16_3	3.35E-06
SC_4_4	3.41E-06	SC_8_4	3.41E-06	SC_12_4	3.41E-06	SC_16_4	3.41E-06
SC_4_5	3.46E-06	SC_8_5	3.46E-06	SC_12_5	3.46E-06	SC_16_5	3.46E-06
SC_4_6	3.52E-06	SC_8_6	3.52E-06	SC_12_6	3.52E-06	SC_16_6	3.52E-06
SC_4_7	3.58E-06	SC_8_7	3.58E-06	SC_12_7	3.58E-06	SC_16_7	3.58E-06
SC_4_8	3.64E-06	SC_8_8	3.64E-06	SC_12_8	3.64E-06	SC_16_8	3.64E-06
SC_4_9	3.69E-06	SC_8_9	3.69E-06	SC_12_9	3.69E-06	SC_16_9	3.69E-06
SC_4_10	3.75E-06	SC_8_10	3.75E-06	SC_12_10	3.75E-06	SC_16_10	3.75E-06
SC_4_11	3.81E-06	SC_8_11	3.81E-06	SC_12_11	3.81E-06	SC_16_11	3.81E-06
SC_4_12	3.86E-06	SC_8_12	3.86E-06	SC_12_12	3.86E-06	SC_16_12	3.86E-06
SC_4_13	3.92E-06	SC_8_13	3.92E-06	SC_12_13	3.92E-06	SC_16_13	3.92E-06
SC_4_14	3.98E-06	SC_8_14	3.98E-06	SC_12_14	3.98E-06	SC_16_14	3.98E-06
SC_4_15	4.03E-06	SC_8_15	4.03E-06	SC_12_15	4.03E-06	SC_16_15	4.03E-06
SC_4_16	4.09E-06	SC_8_16	4.09E-06	SC_12_16	4.09E-06	SC_16_16	4.09E-06
SC_4_17	4.15E-06	SC_8_17	4.15E-06	SC_12_17	4.15E-06	SC_16_17	4.15E-06
SC_4_18	4.21E-06	SC_8_18	4.21E-06	SC_12_18	4.21E-06	SC_16_18	4.21E-06
SC_4_19	4.26E-06	SC_8_19	4.26E-06	SC_12_19	4.26E-06	SC_16_19	4.26E-06
SC_4_20	4.32E-06	SC_8_20	4.32E-06	SC_12_20	4.32E-06	SC_16_20	4.32E-06
SC_4_21	4.38E-06	SC_8_21	4.38E-06	SC_12_21	4.38E-06	SC_16_21	4.38E-06
SC_4_22	4.45E-06	SC_8_22	4.45E-06	SC_12_22	4.45E-06	SC_16_22	4.45E-06
SC_4_23	4.55E-06	SC_8_23	4.55E-06	SC_12_23	4.55E-06	SC_16_23	4.55E-06
SC_4_24	4.70E-06	SC_8_24	4.70E-06	SC_12_24	4.70E-06	SC_16_24	4.70E-06
SC_4_25	6.07E-06	SC_8_25	6.07E-06	SC_12_25	6.07E-06	SC_16_25	6.07E-06
SC_4_26	6.05E-06	SC_8_26	6.05E-06	SC_12_26	6.05E-06	SC_16_26	6.05E-06
SC_4_27	5.72E-06	SC_8_27	5.72E-06	SC_12_27	5.72E-06	SC_16_27	5.72E-06

Tab. A.3-5 Cumulative inductances for each conductor of PF 6 coil at 500 Hz (H)

SC_1_1	2.22E-06	SC_5_1	2.22E-06	SC_9_1	2.22E-06	SC_13_1	2.22E-06
SC_1_2	2.53E-06	SC_5_2	2.53E-06	SC_9_2	2.53E-06	SC_13_2	2.53E-06
SC_1_3	2.58E-06	SC_5_3	2.58E-06	SC_9_3	2.58E-06	SC_13_3	2.58E-06
SC_1_4	2.62E-06	SC_5_4	2.62E-06	SC_9_4	2.62E-06	SC_13_4	2.62E-06
SC_1_5	2.66E-06	SC_5_5	2.66E-06	SC_9_5	2.66E-06	SC_13_5	2.66E-06
SC_1_6	2.71E-06	SC_5_6	2.71E-06	SC_9_6	2.71E-06	SC_13_6	2.71E-06
SC_1_7	2.75E-06	SC_5_7	2.75E-06	SC_9_7	2.75E-06	SC_13_7	2.75E-06
SC_1_8	2.79E-06	SC_5_8	2.79E-06	SC_9_8	2.79E-06	SC_13_8	2.79E-06
SC_1_9	2.84E-06	SC_5_9	2.84E-06	SC_9_9	2.84E-06	SC_13_9	2.84E-06
SC_1_10	2.88E-06	SC_5_10	2.88E-06	SC_9_10	2.88E-06	SC_13_10	2.88E-06
SC_1_11	2.92E-06	SC_5_11	2.92E-06	SC_9_11	2.92E-06	SC_13_11	2.92E-06
SC_1_12	2.97E-06	SC_5_12	2.97E-06	SC_9_12	2.97E-06	SC_13_12	2.97E-06
SC_1_13	3.01E-06	SC_5_13	3.01E-06	SC_9_13	3.01E-06	SC_13_13	3.01E-06
SC_1_14	3.05E-06	SC_5_14	3.05E-06	SC_9_14	3.05E-06	SC_13_14	3.05E-06
SC_1_15	3.10E-06	SC_5_15	3.10E-06	SC_9_15	3.10E-06	SC_13_15	3.10E-06
SC_1_16	3.14E-06	SC_5_16	3.14E-06	SC_9_16	3.14E-06	SC_13_16	3.14E-06
SC_1_17	3.19E-06	SC_5_17	3.19E-06	SC_9_17	3.19E-06	SC_13_17	3.19E-06
SC_1_18	3.23E-06	SC_5_18	3.23E-06	SC_9_18	3.23E-06	SC_13_18	3.23E-06
SC_1_19	3.27E-06	SC_5_19	3.27E-06	SC_9_19	3.27E-06	SC_13_19	3.27E-06
SC_1_20	3.32E-06	SC_5_20	3.32E-06	SC_9_20	3.32E-06	SC_13_20	3.32E-06
SC_1_21	3.36E-06	SC_5_21	3.36E-06	SC_9_21	3.36E-06	SC_13_21	3.36E-06
SC_1_22	3.41E-06	SC_5_22	3.41E-06	SC_9_22	3.41E-06	SC_13_22	3.41E-06
SC_1_23	3.46E-06	SC_5_23	3.46E-06	SC_9_23	3.46E-06	SC_13_23	3.46E-06
SC_1_24	3.58E-06	SC_5_24	3.58E-06	SC_9_24	3.58E-06	SC_13_24	3.58E-06
SC_1_25	4.63E-06	SC_5_25	4.63E-06	SC_9_25	4.63E-06	SC_13_25	4.63E-06
SC_1_26	4.73E-06	SC_5_26	4.73E-06	SC_9_26	4.73E-06	SC_13_26	4.73E-06
SC_1_27	4.15E-06	SC_5_27	4.15E-06	SC_9_27	4.15E-06	SC_13_27	4.15E-06
SC_2_1	2.22E-06	SC_6_1	2.22E-06	SC_10_1	2.22E-06	SC_14_1	2.22E-06
SC_2_2	2.53E-06	SC_6_2	2.53E-06	SC_10_2	2.53E-06	SC_14_2	2.53E-06
SC_2_3	2.58E-06	SC_6_3	2.58E-06	SC_10_3	2.58E-06	SC_14_3	2.58E-06
SC_2_4	2.62E-06	SC_6_4	2.62E-06	SC_10_4	2.62E-06	SC_14_4	2.62E-06
SC_2_5	2.66E-06	SC_6_5	2.66E-06	SC_10_5	2.66E-06	SC_14_5	2.66E-06
SC_2_6	2.71E-06	SC_6_6	2.71E-06	SC_10_6	2.71E-06	SC_14_6	2.71E-06
SC_2_7	2.75E-06	SC_6_7	2.75E-06	SC_10_7	2.75E-06	SC_14_7	2.75E-06
SC_2_8	2.79E-06	SC_6_8	2.79E-06	SC_10_8	2.79E-06	SC_14_8	2.79E-06
SC_2_9	2.84E-06	SC_6_9	2.84E-06	SC_10_9	2.84E-06	SC_14_9	2.84E-06
SC_2_10	2.88E-06	SC_6_10	2.88E-06	SC_10_10	2.88E-06	SC_14_10	2.88E-06
SC_2_11	2.92E-06	SC_6_11	2.92E-06	SC_10_11	2.92E-06	SC_14_11	2.92E-06
SC_2_12	2.97E-06	SC_6_12	2.97E-06	SC_10_12	2.97E-06	SC_14_12	2.97E-06
SC_2_13	3.01E-06	SC_6_13	3.01E-06	SC_10_13	3.01E-06	SC_14_13	3.01E-06
SC_2_14	3.05E-06	SC_6_14	3.05E-06	SC_10_14	3.05E-06	SC_14_14	3.05E-06
SC_2_15	3.10E-06	SC_6_15	3.10E-06	SC_10_15	3.10E-06	SC_14_15	3.10E-06
SC_2_16	3.14E-06	SC_6_16	3.14E-06	SC_10_16	3.14E-06	SC_14_16	3.14E-06
SC_2_17	3.19E-06	SC_6_17	3.19E-06	SC_10_17	3.19E-06	SC_14_17	3.19E-06
SC_2_18	3.23E-06	SC_6_18	3.23E-06	SC_10_18	3.23E-06	SC_14_18	3.23E-06
SC_2_19	3.27E-06	SC_6_19	3.27E-06	SC_10_19	3.27E-06	SC_14_19	3.27E-06
SC_2_20	3.32E-06	SC_6_20	3.32E-06	SC_10_20	3.32E-06	SC_14_20	3.32E-06
SC_2_21	3.36E-06	SC_6_21	3.36E-06	SC_10_21	3.36E-06	SC_14_21	3.36E-06
SC_2_22	3.41E-06	SC_6_22	3.41E-06	SC_10_22	3.41E-06	SC_14_22	3.41E-06
SC_2_23	3.46E-06	SC_6_23	3.46E-06	SC_10_23	3.46E-06	SC_14_23	3.46E-06
SC_2_24	3.58E-06	SC_6_24	3.58E-06	SC_10_24	3.58E-06	SC_14_24	3.58E-06
SC_2_25	4.63E-06	SC_6_25	4.63E-06	SC_10_25	4.63E-06	SC_14_25	4.63E-06
SC_2_26	4.73E-06	SC_6_26	4.73E-06	SC_10_26	4.73E-06	SC_14_26	4.73E-06
SC_2_27	4.15E-06	SC_6_27	4.15E-06	SC_10_27	4.15E-06	SC_14_27	4.15E-06
SC_3_1	2.22E-06	SC_7_1	2.22E-06	SC_11_1	2.22E-06	SC_15_1	2.22E-06

SC_3_2	2.53E-06	SC_7_2	2.53E-06	SC_11_2	2.53E-06	SC_15_2	2.53E-06
SC_3_3	2.58E-06	SC_7_3	2.58E-06	SC_11_3	2.58E-06	SC_15_3	2.58E-06
SC_3_4	2.62E-06	SC_7_4	2.62E-06	SC_11_4	2.62E-06	SC_15_4	2.62E-06
SC_3_5	2.66E-06	SC_7_5	2.66E-06	SC_11_5	2.66E-06	SC_15_5	2.66E-06
SC_3_6	2.71E-06	SC_7_6	2.71E-06	SC_11_6	2.71E-06	SC_15_6	2.71E-06
SC_3_7	2.75E-06	SC_7_7	2.75E-06	SC_11_7	2.75E-06	SC_15_7	2.75E-06
SC_3_8	2.79E-06	SC_7_8	2.79E-06	SC_11_8	2.79E-06	SC_15_8	2.79E-06
SC_3_9	2.84E-06	SC_7_9	2.84E-06	SC_11_9	2.84E-06	SC_15_9	2.84E-06
SC_3_10	2.88E-06	SC_7_10	2.88E-06	SC_11_10	2.88E-06	SC_15_10	2.88E-06
SC_3_11	2.92E-06	SC_7_11	2.92E-06	SC_11_11	2.92E-06	SC_15_11	2.92E-06
SC_3_12	2.97E-06	SC_7_12	2.97E-06	SC_11_12	2.97E-06	SC_15_12	2.97E-06
SC_3_13	3.01E-06	SC_7_13	3.01E-06	SC_11_13	3.01E-06	SC_15_13	3.01E-06
SC_3_14	3.05E-06	SC_7_14	3.05E-06	SC_11_14	3.05E-06	SC_15_14	3.05E-06
SC_3_15	3.10E-06	SC_7_15	3.10E-06	SC_11_15	3.10E-06	SC_15_15	3.10E-06
SC_3_16	3.14E-06	SC_7_16	3.14E-06	SC_11_16	3.14E-06	SC_15_16	3.14E-06
SC_3_17	3.19E-06	SC_7_17	3.19E-06	SC_11_17	3.19E-06	SC_15_17	3.19E-06
SC_3_18	3.23E-06	SC_7_18	3.23E-06	SC_11_18	3.23E-06	SC_15_18	3.23E-06
SC_3_19	3.27E-06	SC_7_19	3.27E-06	SC_11_19	3.27E-06	SC_15_19	3.27E-06
SC_3_20	3.32E-06	SC_7_20	3.32E-06	SC_11_20	3.32E-06	SC_15_20	3.32E-06
SC_3_21	3.36E-06	SC_7_21	3.36E-06	SC_11_21	3.36E-06	SC_15_21	3.36E-06
SC_3_22	3.41E-06	SC_7_22	3.41E-06	SC_11_22	3.41E-06	SC_15_22	3.41E-06
SC_3_23	3.46E-06	SC_7_23	3.46E-06	SC_11_23	3.46E-06	SC_15_23	3.46E-06
SC_3_24	3.58E-06	SC_7_24	3.58E-06	SC_11_24	3.58E-06	SC_15_24	3.58E-06
SC_3_25	4.63E-06	SC_7_25	4.63E-06	SC_11_25	4.63E-06	SC_15_25	4.63E-06
SC_3_26	4.73E-06	SC_7_26	4.73E-06	SC_11_26	4.73E-06	SC_15_26	4.73E-06
SC_3_27	4.15E-06	SC_7_27	4.15E-06	SC_11_27	4.15E-06	SC_15_27	4.15E-06
SC_4_1	2.22E-06	SC_8_1	2.22E-06	SC_12_1	2.22E-06	SC_16_1	2.22E-06
SC_4_2	2.53E-06	SC_8_2	2.53E-06	SC_12_2	2.53E-06	SC_16_2	2.53E-06
SC_4_3	2.58E-06	SC_8_3	2.58E-06	SC_12_3	2.58E-06	SC_16_3	2.58E-06
SC_4_4	2.62E-06	SC_8_4	2.62E-06	SC_12_4	2.62E-06	SC_16_4	2.62E-06
SC_4_5	2.66E-06	SC_8_5	2.66E-06	SC_12_5	2.66E-06	SC_16_5	2.66E-06
SC_4_6	2.71E-06	SC_8_6	2.71E-06	SC_12_6	2.71E-06	SC_16_6	2.71E-06
SC_4_7	2.75E-06	SC_8_7	2.75E-06	SC_12_7	2.75E-06	SC_16_7	2.75E-06
SC_4_8	2.79E-06	SC_8_8	2.79E-06	SC_12_8	2.79E-06	SC_16_8	2.79E-06
SC_4_9	2.84E-06	SC_8_9	2.84E-06	SC_12_9	2.84E-06	SC_16_9	2.84E-06
SC_4_10	2.88E-06	SC_8_10	2.88E-06	SC_12_10	2.88E-06	SC_16_10	2.88E-06
SC_4_11	2.92E-06	SC_8_11	2.92E-06	SC_12_11	2.92E-06	SC_16_11	2.92E-06
SC_4_12	2.97E-06	SC_8_12	2.97E-06	SC_12_12	2.97E-06	SC_16_12	2.97E-06
SC_4_13	3.01E-06	SC_8_13	3.01E-06	SC_12_13	3.01E-06	SC_16_13	3.01E-06
SC_4_14	3.05E-06	SC_8_14	3.05E-06	SC_12_14	3.05E-06	SC_16_14	3.05E-06
SC_4_15	3.10E-06	SC_8_15	3.10E-06	SC_12_15	3.10E-06	SC_16_15	3.10E-06
SC_4_16	3.14E-06	SC_8_16	3.14E-06	SC_12_16	3.14E-06	SC_16_16	3.14E-06
SC_4_17	3.19E-06	SC_8_17	3.19E-06	SC_12_17	3.19E-06	SC_16_17	3.19E-06
SC_4_18	3.23E-06	SC_8_18	3.23E-06	SC_12_18	3.23E-06	SC_16_18	3.23E-06
SC_4_19	3.27E-06	SC_8_19	3.27E-06	SC_12_19	3.27E-06	SC_16_19	3.27E-06
SC_4_20	3.32E-06	SC_8_20	3.32E-06	SC_12_20	3.32E-06	SC_16_20	3.32E-06
SC_4_21	3.36E-06	SC_8_21	3.36E-06	SC_12_21	3.36E-06	SC_16_21	3.36E-06
SC_4_22	3.41E-06	SC_8_22	3.41E-06	SC_12_22	3.41E-06	SC_16_22	3.41E-06
SC_4_23	3.46E-06	SC_8_23	3.46E-06	SC_12_23	3.46E-06	SC_16_23	3.46E-06
SC_4_24	3.58E-06	SC_8_24	3.58E-06	SC_12_24	3.58E-06	SC_16_24	3.58E-06
SC_4_25	4.63E-06	SC_8_25	4.63E-06	SC_12_25	4.63E-06	SC_16_25	4.63E-06
SC_4_26	4.73E-06	SC_8_26	4.73E-06	SC_12_26	4.73E-06	SC_16_26	4.73E-06
SC_4_27	4.15E-06	SC_8_27	4.15E-06	SC_12_27	4.15E-06	SC_16_27	4.15E-06

Tab. A.3-6 Cumulative inductances for each conductor of PF 6 coil at 814 Hz (H)

SC_1_1	1.28E-06	SC_5_1	1.28E-06	SC_9_1	1.28E-06	SC_13_1	1.28E-06
SC_1_2	1.30E-06	SC_5_2	1.30E-06	SC_9_2	1.30E-06	SC_13_2	1.30E-06
SC_1_3	1.32E-06	SC_5_3	1.32E-06	SC_9_3	1.32E-06	SC_13_3	1.32E-06
SC_1_4	1.34E-06	SC_5_4	1.34E-06	SC_9_4	1.34E-06	SC_13_4	1.34E-06
SC_1_5	1.36E-06	SC_5_5	1.36E-06	SC_9_5	1.36E-06	SC_13_5	1.36E-06
SC_1_6	1.39E-06	SC_5_6	1.39E-06	SC_9_6	1.39E-06	SC_13_6	1.39E-06
SC_1_7	1.41E-06	SC_5_7	1.41E-06	SC_9_7	1.41E-06	SC_13_7	1.41E-06
SC_1_8	1.43E-06	SC_5_8	1.43E-06	SC_9_8	1.43E-06	SC_13_8	1.43E-06
SC_1_9	1.45E-06	SC_5_9	1.45E-06	SC_9_9	1.45E-06	SC_13_9	1.45E-06
SC_1_10	1.48E-06	SC_5_10	1.48E-06	SC_9_10	1.48E-06	SC_13_10	1.48E-06
SC_1_11	1.50E-06	SC_5_11	1.50E-06	SC_9_11	1.50E-06	SC_13_11	1.50E-06
SC_1_12	1.52E-06	SC_5_12	1.52E-06	SC_9_12	1.52E-06	SC_13_12	1.52E-06
SC_1_13	1.54E-06	SC_5_13	1.54E-06	SC_9_13	1.54E-06	SC_13_13	1.54E-06
SC_1_14	1.56E-06	SC_5_14	1.56E-06	SC_9_14	1.56E-06	SC_13_14	1.56E-06
SC_1_15	1.59E-06	SC_5_15	1.59E-06	SC_9_15	1.59E-06	SC_13_15	1.59E-06
SC_1_16	1.61E-06	SC_5_16	1.61E-06	SC_9_16	1.61E-06	SC_13_16	1.61E-06
SC_1_17	1.63E-06	SC_5_17	1.63E-06	SC_9_17	1.63E-06	SC_13_17	1.63E-06
SC_1_18	1.65E-06	SC_5_18	1.65E-06	SC_9_18	1.65E-06	SC_13_18	1.65E-06
SC_1_19	1.68E-06	SC_5_19	1.68E-06	SC_9_19	1.68E-06	SC_13_19	1.68E-06
SC_1_20	1.70E-06	SC_5_20	1.70E-06	SC_9_20	1.70E-06	SC_13_20	1.70E-06
SC_1_21	1.72E-06	SC_5_21	1.72E-06	SC_9_21	1.72E-06	SC_13_21	1.72E-06
SC_1_22	1.74E-06	SC_5_22	1.74E-06	SC_9_22	1.74E-06	SC_13_22	1.74E-06
SC_1_23	1.76E-06	SC_5_23	1.76E-06	SC_9_23	1.76E-06	SC_13_23	1.76E-06
SC_1_24	1.79E-06	SC_5_24	1.79E-06	SC_9_24	1.79E-06	SC_13_24	1.79E-06
SC_1_25	1.97E-06	SC_5_25	1.97E-06	SC_9_25	1.97E-06	SC_13_25	1.97E-06
SC_1_26	2.00E-06	SC_5_26	2.00E-06	SC_9_26	2.00E-06	SC_13_26	2.00E-06
SC_1_27	2.02E-06	SC_5_27	2.02E-06	SC_9_27	2.02E-06	SC_13_27	2.02E-06
SC_2_1	1.28E-06	SC_6_1	1.28E-06	SC_10_1	1.28E-06	SC_14_1	1.28E-06
SC_2_2	1.30E-06	SC_6_2	1.30E-06	SC_10_2	1.30E-06	SC_14_2	1.30E-06
SC_2_3	1.32E-06	SC_6_3	1.32E-06	SC_10_3	1.32E-06	SC_14_3	1.32E-06
SC_2_4	1.34E-06	SC_6_4	1.34E-06	SC_10_4	1.34E-06	SC_14_4	1.34E-06
SC_2_5	1.36E-06	SC_6_5	1.36E-06	SC_10_5	1.36E-06	SC_14_5	1.36E-06
SC_2_6	1.39E-06	SC_6_6	1.39E-06	SC_10_6	1.39E-06	SC_14_6	1.39E-06
SC_2_7	1.41E-06	SC_6_7	1.41E-06	SC_10_7	1.41E-06	SC_14_7	1.41E-06
SC_2_8	1.43E-06	SC_6_8	1.43E-06	SC_10_8	1.43E-06	SC_14_8	1.43E-06
SC_2_9	1.45E-06	SC_6_9	1.45E-06	SC_10_9	1.45E-06	SC_14_9	1.45E-06
SC_2_10	1.48E-06	SC_6_10	1.48E-06	SC_10_10	1.48E-06	SC_14_10	1.48E-06
SC_2_11	1.50E-06	SC_6_11	1.50E-06	SC_10_11	1.50E-06	SC_14_11	1.50E-06
SC_2_12	1.52E-06	SC_6_12	1.52E-06	SC_10_12	1.52E-06	SC_14_12	1.52E-06
SC_2_13	1.54E-06	SC_6_13	1.54E-06	SC_10_13	1.54E-06	SC_14_13	1.54E-06
SC_2_14	1.56E-06	SC_6_14	1.56E-06	SC_10_14	1.56E-06	SC_14_14	1.56E-06
SC_2_15	1.59E-06	SC_6_15	1.59E-06	SC_10_15	1.59E-06	SC_14_15	1.59E-06
SC_2_16	1.61E-06	SC_6_16	1.61E-06	SC_10_16	1.61E-06	SC_14_16	1.61E-06
SC_2_17	1.63E-06	SC_6_17	1.63E-06	SC_10_17	1.63E-06	SC_14_17	1.63E-06
SC_2_18	1.65E-06	SC_6_18	1.65E-06	SC_10_18	1.65E-06	SC_14_18	1.65E-06
SC_2_19	1.68E-06	SC_6_19	1.68E-06	SC_10_19	1.68E-06	SC_14_19	1.68E-06
SC_2_20	1.70E-06	SC_6_20	1.70E-06	SC_10_20	1.70E-06	SC_14_20	1.70E-06
SC_2_21	1.72E-06	SC_6_21	1.72E-06	SC_10_21	1.72E-06	SC_14_21	1.72E-06
SC_2_22	1.74E-06	SC_6_22	1.74E-06	SC_10_22	1.74E-06	SC_14_22	1.74E-06
SC_2_23	1.76E-06	SC_6_23	1.76E-06	SC_10_23	1.76E-06	SC_14_23	1.76E-06
SC_2_24	1.79E-06	SC_6_24	1.79E-06	SC_10_24	1.79E-06	SC_14_24	1.79E-06
SC_2_25	1.97E-06	SC_6_25	1.97E-06	SC_10_25	1.97E-06	SC_14_25	1.97E-06
SC_2_26	2.00E-06	SC_6_26	2.00E-06	SC_10_26	2.00E-06	SC_14_26	2.00E-06
SC_2_27	2.02E-06	SC_6_27	2.02E-06	SC_10_27	2.02E-06	SC_14_27	2.02E-06
SC_3_1	1.28E-06	SC_7_1	1.28E-06	SC_11_1	1.28E-06	SC_15_1	1.28E-06

SC_3_2	1.30E-06	SC_7_2	1.30E-06	SC_11_2	1.30E-06	SC_15_2	1.30E-06
SC_3_3	1.32E-06	SC_7_3	1.32E-06	SC_11_3	1.32E-06	SC_15_3	1.32E-06
SC_3_4	1.34E-06	SC_7_4	1.34E-06	SC_11_4	1.34E-06	SC_15_4	1.34E-06
SC_3_5	1.36E-06	SC_7_5	1.36E-06	SC_11_5	1.36E-06	SC_15_5	1.36E-06
SC_3_6	1.39E-06	SC_7_6	1.39E-06	SC_11_6	1.39E-06	SC_15_6	1.39E-06
SC_3_7	1.41E-06	SC_7_7	1.41E-06	SC_11_7	1.41E-06	SC_15_7	1.41E-06
SC_3_8	1.43E-06	SC_7_8	1.43E-06	SC_11_8	1.43E-06	SC_15_8	1.43E-06
SC_3_9	1.45E-06	SC_7_9	1.45E-06	SC_11_9	1.45E-06	SC_15_9	1.45E-06
SC_3_10	1.48E-06	SC_7_10	1.48E-06	SC_11_10	1.48E-06	SC_15_10	1.48E-06
SC_3_11	1.50E-06	SC_7_11	1.50E-06	SC_11_11	1.50E-06	SC_15_11	1.50E-06
SC_3_12	1.52E-06	SC_7_12	1.52E-06	SC_11_12	1.52E-06	SC_15_12	1.52E-06
SC_3_13	1.54E-06	SC_7_13	1.54E-06	SC_11_13	1.54E-06	SC_15_13	1.54E-06
SC_3_14	1.56E-06	SC_7_14	1.56E-06	SC_11_14	1.56E-06	SC_15_14	1.56E-06
SC_3_15	1.59E-06	SC_7_15	1.59E-06	SC_11_15	1.59E-06	SC_15_15	1.59E-06
SC_3_16	1.61E-06	SC_7_16	1.61E-06	SC_11_16	1.61E-06	SC_15_16	1.61E-06
SC_3_17	1.63E-06	SC_7_17	1.63E-06	SC_11_17	1.63E-06	SC_15_17	1.63E-06
SC_3_18	1.65E-06	SC_7_18	1.65E-06	SC_11_18	1.65E-06	SC_15_18	1.65E-06
SC_3_19	1.68E-06	SC_7_19	1.68E-06	SC_11_19	1.68E-06	SC_15_19	1.68E-06
SC_3_20	1.70E-06	SC_7_20	1.70E-06	SC_11_20	1.70E-06	SC_15_20	1.70E-06
SC_3_21	1.72E-06	SC_7_21	1.72E-06	SC_11_21	1.72E-06	SC_15_21	1.72E-06
SC_3_22	1.74E-06	SC_7_22	1.74E-06	SC_11_22	1.74E-06	SC_15_22	1.74E-06
SC_3_23	1.76E-06	SC_7_23	1.76E-06	SC_11_23	1.76E-06	SC_15_23	1.76E-06
SC_3_24	1.79E-06	SC_7_24	1.79E-06	SC_11_24	1.79E-06	SC_15_24	1.79E-06
SC_3_25	1.97E-06	SC_7_25	1.97E-06	SC_11_25	1.97E-06	SC_15_25	1.97E-06
SC_3_26	2.00E-06	SC_7_26	2.00E-06	SC_11_26	2.00E-06	SC_15_26	2.00E-06
SC_3_27	2.02E-06	SC_7_27	2.02E-06	SC_11_27	2.02E-06	SC_15_27	2.02E-06
SC_4_1	1.28E-06	SC_8_1	1.28E-06	SC_12_1	1.28E-06	SC_16_1	1.28E-06
SC_4_2	1.30E-06	SC_8_2	1.30E-06	SC_12_2	1.30E-06	SC_16_2	1.30E-06
SC_4_3	1.32E-06	SC_8_3	1.32E-06	SC_12_3	1.32E-06	SC_16_3	1.32E-06
SC_4_4	1.34E-06	SC_8_4	1.34E-06	SC_12_4	1.34E-06	SC_16_4	1.34E-06
SC_4_5	1.36E-06	SC_8_5	1.36E-06	SC_12_5	1.36E-06	SC_16_5	1.36E-06
SC_4_6	1.39E-06	SC_8_6	1.39E-06	SC_12_6	1.39E-06	SC_16_6	1.39E-06
SC_4_7	1.41E-06	SC_8_7	1.41E-06	SC_12_7	1.41E-06	SC_16_7	1.41E-06
SC_4_8	1.43E-06	SC_8_8	1.43E-06	SC_12_8	1.43E-06	SC_16_8	1.43E-06
SC_4_9	1.45E-06	SC_8_9	1.45E-06	SC_12_9	1.45E-06	SC_16_9	1.45E-06
SC_4_10	1.48E-06	SC_8_10	1.48E-06	SC_12_10	1.48E-06	SC_16_10	1.48E-06
SC_4_11	1.50E-06	SC_8_11	1.50E-06	SC_12_11	1.50E-06	SC_16_11	1.50E-06
SC_4_12	1.52E-06	SC_8_12	1.52E-06	SC_12_12	1.52E-06	SC_16_12	1.52E-06
SC_4_13	1.54E-06	SC_8_13	1.54E-06	SC_12_13	1.54E-06	SC_16_13	1.54E-06
SC_4_14	1.56E-06	SC_8_14	1.56E-06	SC_12_14	1.56E-06	SC_16_14	1.56E-06
SC_4_15	1.59E-06	SC_8_15	1.59E-06	SC_12_15	1.59E-06	SC_16_15	1.59E-06
SC_4_16	1.61E-06	SC_8_16	1.61E-06	SC_12_16	1.61E-06	SC_16_16	1.61E-06
SC_4_17	1.63E-06	SC_8_17	1.63E-06	SC_12_17	1.63E-06	SC_16_17	1.63E-06
SC_4_18	1.65E-06	SC_8_18	1.65E-06	SC_12_18	1.65E-06	SC_16_18	1.65E-06
SC_4_19	1.68E-06	SC_8_19	1.68E-06	SC_12_19	1.68E-06	SC_16_19	1.68E-06
SC_4_20	1.70E-06	SC_8_20	1.70E-06	SC_12_20	1.70E-06	SC_16_20	1.70E-06
SC_4_21	1.72E-06	SC_8_21	1.72E-06	SC_12_21	1.72E-06	SC_16_21	1.72E-06
SC_4_22	1.74E-06	SC_8_22	1.74E-06	SC_12_22	1.74E-06	SC_16_22	1.74E-06
SC_4_23	1.76E-06	SC_8_23	1.76E-06	SC_12_23	1.76E-06	SC_16_23	1.76E-06
SC_4_24	1.79E-06	SC_8_24	1.79E-06	SC_12_24	1.79E-06	SC_16_24	1.79E-06
SC_4_25	1.97E-06	SC_8_25	1.97E-06	SC_12_25	1.97E-06	SC_16_25	1.97E-06
SC_4_26	2.00E-06	SC_8_26	2.00E-06	SC_12_26	2.00E-06	SC_16_26	2.00E-06
SC_4_27	2.02E-06	SC_8_27	2.02E-06	SC_12_27	2.02E-06	SC_16_27	2.02E-06

Tab. A.3-7 Cumulative inductances for each conductor of PF 6 coil at 12.9 kHz (H)

SC_1_1	1.23E-06	SC_5_1	1.23E-06	SC_9_1	1.23E-06	SC_13_1	1.23E-06
SC_1_2	1.25E-06	SC_5_2	1.25E-06	SC_9_2	1.25E-06	SC_13_2	1.25E-06
SC_1_3	1.27E-06	SC_5_3	1.27E-06	SC_9_3	1.27E-06	SC_13_3	1.27E-06
SC_1_4	1.29E-06	SC_5_4	1.29E-06	SC_9_4	1.29E-06	SC_13_4	1.29E-06
SC_1_5	1.32E-06	SC_5_5	1.32E-06	SC_9_5	1.32E-06	SC_13_5	1.32E-06
SC_1_6	1.34E-06	SC_5_6	1.34E-06	SC_9_6	1.34E-06	SC_13_6	1.34E-06
SC_1_7	1.36E-06	SC_5_7	1.36E-06	SC_9_7	1.36E-06	SC_13_7	1.36E-06
SC_1_8	1.38E-06	SC_5_8	1.38E-06	SC_9_8	1.38E-06	SC_13_8	1.38E-06
SC_1_9	1.40E-06	SC_5_9	1.40E-06	SC_9_9	1.40E-06	SC_13_9	1.40E-06
SC_1_10	1.42E-06	SC_5_10	1.42E-06	SC_9_10	1.42E-06	SC_13_10	1.42E-06
SC_1_11	1.44E-06	SC_5_11	1.44E-06	SC_9_11	1.44E-06	SC_13_11	1.44E-06
SC_1_12	1.47E-06	SC_5_12	1.47E-06	SC_9_12	1.47E-06	SC_13_12	1.47E-06
SC_1_13	1.49E-06	SC_5_13	1.49E-06	SC_9_13	1.49E-06	SC_13_13	1.49E-06
SC_1_14	1.51E-06	SC_5_14	1.51E-06	SC_9_14	1.51E-06	SC_13_14	1.51E-06
SC_1_15	1.53E-06	SC_5_15	1.53E-06	SC_9_15	1.53E-06	SC_13_15	1.53E-06
SC_1_16	1.55E-06	SC_5_16	1.55E-06	SC_9_16	1.55E-06	SC_13_16	1.55E-06
SC_1_17	1.57E-06	SC_5_17	1.57E-06	SC_9_17	1.57E-06	SC_13_17	1.57E-06
SC_1_18	1.59E-06	SC_5_18	1.59E-06	SC_9_18	1.59E-06	SC_13_18	1.59E-06
SC_1_19	1.62E-06	SC_5_19	1.62E-06	SC_9_19	1.62E-06	SC_13_19	1.62E-06
SC_1_20	1.64E-06	SC_5_20	1.64E-06	SC_9_20	1.64E-06	SC_13_20	1.64E-06
SC_1_21	1.66E-06	SC_5_21	1.66E-06	SC_9_21	1.66E-06	SC_13_21	1.66E-06
SC_1_22	1.68E-06	SC_5_22	1.68E-06	SC_9_22	1.68E-06	SC_13_22	1.68E-06
SC_1_23	1.70E-06	SC_5_23	1.70E-06	SC_9_23	1.70E-06	SC_13_23	1.70E-06
SC_1_24	1.72E-06	SC_5_24	1.72E-06	SC_9_24	1.72E-06	SC_13_24	1.72E-06
SC_1_25	1.89E-06	SC_5_25	1.89E-06	SC_9_25	1.89E-06	SC_13_25	1.89E-06
SC_1_26	1.92E-06	SC_5_26	1.92E-06	SC_9_26	1.92E-06	SC_13_26	1.92E-06
SC_1_27	1.94E-06	SC_5_27	1.94E-06	SC_9_27	1.94E-06	SC_13_27	1.94E-06
SC_2_1	1.23E-06	SC_6_1	1.23E-06	SC_10_1	1.23E-06	SC_14_1	1.23E-06
SC_2_2	1.25E-06	SC_6_2	1.25E-06	SC_10_2	1.25E-06	SC_14_2	1.25E-06
SC_2_3	1.27E-06	SC_6_3	1.27E-06	SC_10_3	1.27E-06	SC_14_3	1.27E-06
SC_2_4	1.29E-06	SC_6_4	1.29E-06	SC_10_4	1.29E-06	SC_14_4	1.29E-06
SC_2_5	1.32E-06	SC_6_5	1.32E-06	SC_10_5	1.32E-06	SC_14_5	1.32E-06
SC_2_6	1.34E-06	SC_6_6	1.34E-06	SC_10_6	1.34E-06	SC_14_6	1.34E-06
SC_2_7	1.36E-06	SC_6_7	1.36E-06	SC_10_7	1.36E-06	SC_14_7	1.36E-06
SC_2_8	1.38E-06	SC_6_8	1.38E-06	SC_10_8	1.38E-06	SC_14_8	1.38E-06
SC_2_9	1.40E-06	SC_6_9	1.40E-06	SC_10_9	1.40E-06	SC_14_9	1.40E-06
SC_2_10	1.42E-06	SC_6_10	1.42E-06	SC_10_10	1.42E-06	SC_14_10	1.42E-06
SC_2_11	1.44E-06	SC_6_11	1.44E-06	SC_10_11	1.44E-06	SC_14_11	1.44E-06
SC_2_12	1.47E-06	SC_6_12	1.47E-06	SC_10_12	1.47E-06	SC_14_12	1.47E-06
SC_2_13	1.49E-06	SC_6_13	1.49E-06	SC_10_13	1.49E-06	SC_14_13	1.49E-06
SC_2_14	1.51E-06	SC_6_14	1.51E-06	SC_10_14	1.51E-06	SC_14_14	1.51E-06
SC_2_15	1.53E-06	SC_6_15	1.53E-06	SC_10_15	1.53E-06	SC_14_15	1.53E-06
SC_2_16	1.55E-06	SC_6_16	1.55E-06	SC_10_16	1.55E-06	SC_14_16	1.55E-06
SC_2_17	1.57E-06	SC_6_17	1.57E-06	SC_10_17	1.57E-06	SC_14_17	1.57E-06
SC_2_18	1.59E-06	SC_6_18	1.59E-06	SC_10_18	1.59E-06	SC_14_18	1.59E-06
SC_2_19	1.62E-06	SC_6_19	1.62E-06	SC_10_19	1.62E-06	SC_14_19	1.62E-06
SC_2_20	1.64E-06	SC_6_20	1.64E-06	SC_10_20	1.64E-06	SC_14_20	1.64E-06
SC_2_21	1.66E-06	SC_6_21	1.66E-06	SC_10_21	1.66E-06	SC_14_21	1.66E-06
SC_2_22	1.68E-06	SC_6_22	1.68E-06	SC_10_22	1.68E-06	SC_14_22	1.68E-06
SC_2_23	1.70E-06	SC_6_23	1.70E-06	SC_10_23	1.70E-06	SC_14_23	1.70E-06
SC_2_24	1.72E-06	SC_6_24	1.72E-06	SC_10_24	1.72E-06	SC_14_24	1.72E-06
SC_2_25	1.89E-06	SC_6_25	1.89E-06	SC_10_25	1.89E-06	SC_14_25	1.89E-06
SC_2_26	1.92E-06	SC_6_26	1.92E-06	SC_10_26	1.92E-06	SC_14_26	1.92E-06
SC_2_27	1.94E-06	SC_6_27	1.94E-06	SC_10_27	1.94E-06	SC_14_27	1.94E-06
SC_3_1	1.23E-06	SC_7_1	1.23E-06	SC_11_1	1.23E-06	SC_15_1	1.23E-06

SC_3_2	1.25E-06	SC_7_2	1.25E-06	SC_11_2	1.25E-06	SC_15_2	1.25E-06
SC_3_3	1.27E-06	SC_7_3	1.27E-06	SC_11_3	1.27E-06	SC_15_3	1.27E-06
SC_3_4	1.29E-06	SC_7_4	1.29E-06	SC_11_4	1.29E-06	SC_15_4	1.29E-06
SC_3_5	1.32E-06	SC_7_5	1.32E-06	SC_11_5	1.32E-06	SC_15_5	1.32E-06
SC_3_6	1.34E-06	SC_7_6	1.34E-06	SC_11_6	1.34E-06	SC_15_6	1.34E-06
SC_3_7	1.36E-06	SC_7_7	1.36E-06	SC_11_7	1.36E-06	SC_15_7	1.36E-06
SC_3_8	1.38E-06	SC_7_8	1.38E-06	SC_11_8	1.38E-06	SC_15_8	1.38E-06
SC_3_9	1.40E-06	SC_7_9	1.40E-06	SC_11_9	1.40E-06	SC_15_9	1.40E-06
SC_3_10	1.42E-06	SC_7_10	1.42E-06	SC_11_10	1.42E-06	SC_15_10	1.42E-06
SC_3_11	1.44E-06	SC_7_11	1.44E-06	SC_11_11	1.44E-06	SC_15_11	1.44E-06
SC_3_12	1.47E-06	SC_7_12	1.47E-06	SC_11_12	1.47E-06	SC_15_12	1.47E-06
SC_3_13	1.49E-06	SC_7_13	1.49E-06	SC_11_13	1.49E-06	SC_15_13	1.49E-06
SC_3_14	1.51E-06	SC_7_14	1.51E-06	SC_11_14	1.51E-06	SC_15_14	1.51E-06
SC_3_15	1.53E-06	SC_7_15	1.53E-06	SC_11_15	1.53E-06	SC_15_15	1.53E-06
SC_3_16	1.55E-06	SC_7_16	1.55E-06	SC_11_16	1.55E-06	SC_15_16	1.55E-06
SC_3_17	1.57E-06	SC_7_17	1.57E-06	SC_11_17	1.57E-06	SC_15_17	1.57E-06
SC_3_18	1.59E-06	SC_7_18	1.59E-06	SC_11_18	1.59E-06	SC_15_18	1.59E-06
SC_3_19	1.62E-06	SC_7_19	1.62E-06	SC_11_19	1.62E-06	SC_15_19	1.62E-06
SC_3_20	1.64E-06	SC_7_20	1.64E-06	SC_11_20	1.64E-06	SC_15_20	1.64E-06
SC_3_21	1.66E-06	SC_7_21	1.66E-06	SC_11_21	1.66E-06	SC_15_21	1.66E-06
SC_3_22	1.68E-06	SC_7_22	1.68E-06	SC_11_22	1.68E-06	SC_15_22	1.68E-06
SC_3_23	1.70E-06	SC_7_23	1.70E-06	SC_11_23	1.70E-06	SC_15_23	1.70E-06
SC_3_24	1.72E-06	SC_7_24	1.72E-06	SC_11_24	1.72E-06	SC_15_24	1.72E-06
SC_3_25	1.89E-06	SC_7_25	1.89E-06	SC_11_25	1.89E-06	SC_15_25	1.89E-06
SC_3_26	1.92E-06	SC_7_26	1.92E-06	SC_11_26	1.92E-06	SC_15_26	1.92E-06
SC_3_27	1.94E-06	SC_7_27	1.94E-06	SC_11_27	1.94E-06	SC_15_27	1.94E-06
SC_4_1	1.23E-06	SC_8_1	1.23E-06	SC_12_1	1.23E-06	SC_16_1	1.23E-06
SC_4_2	1.25E-06	SC_8_2	1.25E-06	SC_12_2	1.25E-06	SC_16_2	1.25E-06
SC_4_3	1.27E-06	SC_8_3	1.27E-06	SC_12_3	1.27E-06	SC_16_3	1.27E-06
SC_4_4	1.29E-06	SC_8_4	1.29E-06	SC_12_4	1.29E-06	SC_16_4	1.29E-06
SC_4_5	1.32E-06	SC_8_5	1.32E-06	SC_12_5	1.32E-06	SC_16_5	1.32E-06
SC_4_6	1.34E-06	SC_8_6	1.34E-06	SC_12_6	1.34E-06	SC_16_6	1.34E-06
SC_4_7	1.36E-06	SC_8_7	1.36E-06	SC_12_7	1.36E-06	SC_16_7	1.36E-06
SC_4_8	1.38E-06	SC_8_8	1.38E-06	SC_12_8	1.38E-06	SC_16_8	1.38E-06
SC_4_9	1.40E-06	SC_8_9	1.40E-06	SC_12_9	1.40E-06	SC_16_9	1.40E-06
SC_4_10	1.42E-06	SC_8_10	1.42E-06	SC_12_10	1.42E-06	SC_16_10	1.42E-06
SC_4_11	1.44E-06	SC_8_11	1.44E-06	SC_12_11	1.44E-06	SC_16_11	1.44E-06
SC_4_12	1.47E-06	SC_8_12	1.47E-06	SC_12_12	1.47E-06	SC_16_12	1.47E-06
SC_4_13	1.49E-06	SC_8_13	1.49E-06	SC_12_13	1.49E-06	SC_16_13	1.49E-06
SC_4_14	1.51E-06	SC_8_14	1.51E-06	SC_12_14	1.51E-06	SC_16_14	1.51E-06
SC_4_15	1.53E-06	SC_8_15	1.53E-06	SC_12_15	1.53E-06	SC_16_15	1.53E-06
SC_4_16	1.55E-06	SC_8_16	1.55E-06	SC_12_16	1.55E-06	SC_16_16	1.55E-06
SC_4_17	1.57E-06	SC_8_17	1.57E-06	SC_12_17	1.57E-06	SC_16_17	1.57E-06
SC_4_18	1.59E-06	SC_8_18	1.59E-06	SC_12_18	1.59E-06	SC_16_18	1.59E-06
SC_4_19	1.62E-06	SC_8_19	1.62E-06	SC_12_19	1.62E-06	SC_16_19	1.62E-06
SC_4_20	1.64E-06	SC_8_20	1.64E-06	SC_12_20	1.64E-06	SC_16_20	1.64E-06
SC_4_21	1.66E-06	SC_8_21	1.66E-06	SC_12_21	1.66E-06	SC_16_21	1.66E-06
SC_4_22	1.68E-06	SC_8_22	1.68E-06	SC_12_22	1.68E-06	SC_16_22	1.68E-06
SC_4_23	1.70E-06	SC_8_23	1.70E-06	SC_12_23	1.70E-06	SC_16_23	1.70E-06
SC_4_24	1.72E-06	SC_8_24	1.72E-06	SC_12_24	1.72E-06	SC_16_24	1.72E-06
SC_4_25	1.89E-06	SC_8_25	1.89E-06	SC_12_25	1.89E-06	SC_16_25	1.89E-06
SC_4_26	1.92E-06	SC_8_26	1.92E-06	SC_12_26	1.92E-06	SC_16_26	1.92E-06
SC_4_27	1.94E-06	SC_8_27	1.94E-06	SC_12_27	1.94E-06	SC_16_27	1.94E-06

Tab. A.3-8 Cumulative inductances for each conductor of PF 6 coil at 16.8 kHz (H)

SC_1_1	1.19E-06	SC_5_1	1.19E-06	SC_9_1	1.19E-06	SC_13_1	1.19E-06
SC_1_2	1.21E-06	SC_5_2	1.21E-06	SC_9_2	1.21E-06	SC_13_2	1.21E-06
SC_1_3	1.23E-06	SC_5_3	1.23E-06	SC_9_3	1.23E-06	SC_13_3	1.23E-06
SC_1_4	1.25E-06	SC_5_4	1.25E-06	SC_9_4	1.25E-06	SC_13_4	1.25E-06
SC_1_5	1.27E-06	SC_5_5	1.27E-06	SC_9_5	1.27E-06	SC_13_5	1.27E-06
SC_1_6	1.29E-06	SC_5_6	1.29E-06	SC_9_6	1.29E-06	SC_13_6	1.29E-06
SC_1_7	1.31E-06	SC_5_7	1.31E-06	SC_9_7	1.31E-06	SC_13_7	1.31E-06
SC_1_8	1.33E-06	SC_5_8	1.33E-06	SC_9_8	1.33E-06	SC_13_8	1.33E-06
SC_1_9	1.36E-06	SC_5_9	1.36E-06	SC_9_9	1.36E-06	SC_13_9	1.36E-06
SC_1_10	1.38E-06	SC_5_10	1.38E-06	SC_9_10	1.38E-06	SC_13_10	1.38E-06
SC_1_11	1.40E-06	SC_5_11	1.40E-06	SC_9_11	1.40E-06	SC_13_11	1.40E-06
SC_1_12	1.42E-06	SC_5_12	1.42E-06	SC_9_12	1.42E-06	SC_13_12	1.42E-06
SC_1_13	1.44E-06	SC_5_13	1.44E-06	SC_9_13	1.44E-06	SC_13_13	1.44E-06
SC_1_14	1.46E-06	SC_5_14	1.46E-06	SC_9_14	1.46E-06	SC_13_14	1.46E-06
SC_1_15	1.48E-06	SC_5_15	1.48E-06	SC_9_15	1.48E-06	SC_13_15	1.48E-06
SC_1_16	1.50E-06	SC_5_16	1.50E-06	SC_9_16	1.50E-06	SC_13_16	1.50E-06
SC_1_17	1.52E-06	SC_5_17	1.52E-06	SC_9_17	1.52E-06	SC_13_17	1.52E-06
SC_1_18	1.54E-06	SC_5_18	1.54E-06	SC_9_18	1.54E-06	SC_13_18	1.54E-06
SC_1_19	1.56E-06	SC_5_19	1.56E-06	SC_9_19	1.56E-06	SC_13_19	1.56E-06
SC_1_20	1.58E-06	SC_5_20	1.58E-06	SC_9_20	1.58E-06	SC_13_20	1.58E-06
SC_1_21	1.60E-06	SC_5_21	1.60E-06	SC_9_21	1.60E-06	SC_13_21	1.60E-06
SC_1_22	1.62E-06	SC_5_22	1.62E-06	SC_9_22	1.62E-06	SC_13_22	1.62E-06
SC_1_23	1.65E-06	SC_5_23	1.65E-06	SC_9_23	1.65E-06	SC_13_23	1.65E-06
SC_1_24	1.67E-06	SC_5_24	1.67E-06	SC_9_24	1.67E-06	SC_13_24	1.67E-06
SC_1_25	1.82E-06	SC_5_25	1.82E-06	SC_9_25	1.82E-06	SC_13_25	1.82E-06
SC_1_26	1.84E-06	SC_5_26	1.84E-06	SC_9_26	1.84E-06	SC_13_26	1.84E-06
SC_1_27	1.86E-06	SC_5_27	1.86E-06	SC_9_27	1.86E-06	SC_13_27	1.86E-06
SC_2_1	1.19E-06	SC_6_1	1.19E-06	SC_10_1	1.19E-06	SC_14_1	1.19E-06
SC_2_2	1.21E-06	SC_6_2	1.21E-06	SC_10_2	1.21E-06	SC_14_2	1.21E-06
SC_2_3	1.23E-06	SC_6_3	1.23E-06	SC_10_3	1.23E-06	SC_14_3	1.23E-06
SC_2_4	1.25E-06	SC_6_4	1.25E-06	SC_10_4	1.25E-06	SC_14_4	1.25E-06
SC_2_5	1.27E-06	SC_6_5	1.27E-06	SC_10_5	1.27E-06	SC_14_5	1.27E-06
SC_2_6	1.29E-06	SC_6_6	1.29E-06	SC_10_6	1.29E-06	SC_14_6	1.29E-06
SC_2_7	1.31E-06	SC_6_7	1.31E-06	SC_10_7	1.31E-06	SC_14_7	1.31E-06
SC_2_8	1.33E-06	SC_6_8	1.33E-06	SC_10_8	1.33E-06	SC_14_8	1.33E-06
SC_2_9	1.36E-06	SC_6_9	1.36E-06	SC_10_9	1.36E-06	SC_14_9	1.36E-06
SC_2_10	1.38E-06	SC_6_10	1.38E-06	SC_10_10	1.38E-06	SC_14_10	1.38E-06
SC_2_11	1.40E-06	SC_6_11	1.40E-06	SC_10_11	1.40E-06	SC_14_11	1.40E-06
SC_2_12	1.42E-06	SC_6_12	1.42E-06	SC_10_12	1.42E-06	SC_14_12	1.42E-06
SC_2_13	1.44E-06	SC_6_13	1.44E-06	SC_10_13	1.44E-06	SC_14_13	1.44E-06
SC_2_14	1.46E-06	SC_6_14	1.46E-06	SC_10_14	1.46E-06	SC_14_14	1.46E-06
SC_2_15	1.48E-06	SC_6_15	1.48E-06	SC_10_15	1.48E-06	SC_14_15	1.48E-06
SC_2_16	1.50E-06	SC_6_16	1.50E-06	SC_10_16	1.50E-06	SC_14_16	1.50E-06
SC_2_17	1.52E-06	SC_6_17	1.52E-06	SC_10_17	1.52E-06	SC_14_17	1.52E-06
SC_2_18	1.54E-06	SC_6_18	1.54E-06	SC_10_18	1.54E-06	SC_14_18	1.54E-06
SC_2_19	1.56E-06	SC_6_19	1.56E-06	SC_10_19	1.56E-06	SC_14_19	1.56E-06
SC_2_20	1.58E-06	SC_6_20	1.58E-06	SC_10_20	1.58E-06	SC_14_20	1.58E-06
SC_2_21	1.60E-06	SC_6_21	1.60E-06	SC_10_21	1.60E-06	SC_14_21	1.60E-06
SC_2_22	1.62E-06	SC_6_22	1.62E-06	SC_10_22	1.62E-06	SC_14_22	1.62E-06
SC_2_23	1.65E-06	SC_6_23	1.65E-06	SC_10_23	1.65E-06	SC_14_23	1.65E-06
SC_2_24	1.67E-06	SC_6_24	1.67E-06	SC_10_24	1.67E-06	SC_14_24	1.67E-06
SC_2_25	1.82E-06	SC_6_25	1.82E-06	SC_10_25	1.82E-06	SC_14_25	1.82E-06
SC_2_26	1.84E-06	SC_6_26	1.84E-06	SC_10_26	1.84E-06	SC_14_26	1.84E-06
SC_2_27	1.86E-06	SC_6_27	1.86E-06	SC_10_27	1.86E-06	SC_14_27	1.86E-06
SC_3_1	1.19E-06	SC_7_1	1.19E-06	SC_11_1	1.19E-06	SC_15_1	1.19E-06

SC_3_2	1.21E-06	SC_7_2	1.21E-06	SC_11_2	1.21E-06	SC_15_2	1.21E-06
SC_3_3	1.23E-06	SC_7_3	1.23E-06	SC_11_3	1.23E-06	SC_15_3	1.23E-06
SC_3_4	1.25E-06	SC_7_4	1.25E-06	SC_11_4	1.25E-06	SC_15_4	1.25E-06
SC_3_5	1.27E-06	SC_7_5	1.27E-06	SC_11_5	1.27E-06	SC_15_5	1.27E-06
SC_3_6	1.29E-06	SC_7_6	1.29E-06	SC_11_6	1.29E-06	SC_15_6	1.29E-06
SC_3_7	1.31E-06	SC_7_7	1.31E-06	SC_11_7	1.31E-06	SC_15_7	1.31E-06
SC_3_8	1.33E-06	SC_7_8	1.33E-06	SC_11_8	1.33E-06	SC_15_8	1.33E-06
SC_3_9	1.36E-06	SC_7_9	1.36E-06	SC_11_9	1.36E-06	SC_15_9	1.36E-06
SC_3_10	1.38E-06	SC_7_10	1.38E-06	SC_11_10	1.38E-06	SC_15_10	1.38E-06
SC_3_11	1.40E-06	SC_7_11	1.40E-06	SC_11_11	1.40E-06	SC_15_11	1.40E-06
SC_3_12	1.42E-06	SC_7_12	1.42E-06	SC_11_12	1.42E-06	SC_15_12	1.42E-06
SC_3_13	1.44E-06	SC_7_13	1.44E-06	SC_11_13	1.44E-06	SC_15_13	1.44E-06
SC_3_14	1.46E-06	SC_7_14	1.46E-06	SC_11_14	1.46E-06	SC_15_14	1.46E-06
SC_3_15	1.48E-06	SC_7_15	1.48E-06	SC_11_15	1.48E-06	SC_15_15	1.48E-06
SC_3_16	1.50E-06	SC_7_16	1.50E-06	SC_11_16	1.50E-06	SC_15_16	1.50E-06
SC_3_17	1.52E-06	SC_7_17	1.52E-06	SC_11_17	1.52E-06	SC_15_17	1.52E-06
SC_3_18	1.54E-06	SC_7_18	1.54E-06	SC_11_18	1.54E-06	SC_15_18	1.54E-06
SC_3_19	1.56E-06	SC_7_19	1.56E-06	SC_11_19	1.56E-06	SC_15_19	1.56E-06
SC_3_20	1.58E-06	SC_7_20	1.58E-06	SC_11_20	1.58E-06	SC_15_20	1.58E-06
SC_3_21	1.60E-06	SC_7_21	1.60E-06	SC_11_21	1.60E-06	SC_15_21	1.60E-06
SC_3_22	1.62E-06	SC_7_22	1.62E-06	SC_11_22	1.62E-06	SC_15_22	1.62E-06
SC_3_23	1.65E-06	SC_7_23	1.65E-06	SC_11_23	1.65E-06	SC_15_23	1.65E-06
SC_3_24	1.67E-06	SC_7_24	1.67E-06	SC_11_24	1.67E-06	SC_15_24	1.67E-06
SC_3_25	1.82E-06	SC_7_25	1.82E-06	SC_11_25	1.82E-06	SC_15_25	1.82E-06
SC_3_26	1.84E-06	SC_7_26	1.84E-06	SC_11_26	1.84E-06	SC_15_26	1.84E-06
SC_3_27	1.86E-06	SC_7_27	1.86E-06	SC_11_27	1.86E-06	SC_15_27	1.86E-06
SC_4_1	1.19E-06	SC_8_1	1.19E-06	SC_12_1	1.19E-06	SC_16_1	1.19E-06
SC_4_2	1.21E-06	SC_8_2	1.21E-06	SC_12_2	1.21E-06	SC_16_2	1.21E-06
SC_4_3	1.23E-06	SC_8_3	1.23E-06	SC_12_3	1.23E-06	SC_16_3	1.23E-06
SC_4_4	1.25E-06	SC_8_4	1.25E-06	SC_12_4	1.25E-06	SC_16_4	1.25E-06
SC_4_5	1.27E-06	SC_8_5	1.27E-06	SC_12_5	1.27E-06	SC_16_5	1.27E-06
SC_4_6	1.29E-06	SC_8_6	1.29E-06	SC_12_6	1.29E-06	SC_16_6	1.29E-06
SC_4_7	1.31E-06	SC_8_7	1.31E-06	SC_12_7	1.31E-06	SC_16_7	1.31E-06
SC_4_8	1.33E-06	SC_8_8	1.33E-06	SC_12_8	1.33E-06	SC_16_8	1.33E-06
SC_4_9	1.36E-06	SC_8_9	1.36E-06	SC_12_9	1.36E-06	SC_16_9	1.36E-06
SC_4_10	1.38E-06	SC_8_10	1.38E-06	SC_12_10	1.38E-06	SC_16_10	1.38E-06
SC_4_11	1.40E-06	SC_8_11	1.40E-06	SC_12_11	1.40E-06	SC_16_11	1.40E-06
SC_4_12	1.42E-06	SC_8_12	1.42E-06	SC_12_12	1.42E-06	SC_16_12	1.42E-06
SC_4_13	1.44E-06	SC_8_13	1.44E-06	SC_12_13	1.44E-06	SC_16_13	1.44E-06
SC_4_14	1.46E-06	SC_8_14	1.46E-06	SC_12_14	1.46E-06	SC_16_14	1.46E-06
SC_4_15	1.48E-06	SC_8_15	1.48E-06	SC_12_15	1.48E-06	SC_16_15	1.48E-06
SC_4_16	1.50E-06	SC_8_16	1.50E-06	SC_12_16	1.50E-06	SC_16_16	1.50E-06
SC_4_17	1.52E-06	SC_8_17	1.52E-06	SC_12_17	1.52E-06	SC_16_17	1.52E-06
SC_4_18	1.54E-06	SC_8_18	1.54E-06	SC_12_18	1.54E-06	SC_16_18	1.54E-06
SC_4_19	1.56E-06	SC_8_19	1.56E-06	SC_12_19	1.56E-06	SC_16_19	1.56E-06
SC_4_20	1.58E-06	SC_8_20	1.58E-06	SC_12_20	1.58E-06	SC_16_20	1.58E-06
SC_4_21	1.60E-06	SC_8_21	1.60E-06	SC_12_21	1.60E-06	SC_16_21	1.60E-06
SC_4_22	1.62E-06	SC_8_22	1.62E-06	SC_12_22	1.62E-06	SC_16_22	1.62E-06
SC_4_23	1.65E-06	SC_8_23	1.65E-06	SC_12_23	1.65E-06	SC_16_23	1.65E-06
SC_4_24	1.67E-06	SC_8_24	1.67E-06	SC_12_24	1.67E-06	SC_16_24	1.67E-06
SC_4_25	1.82E-06	SC_8_25	1.82E-06	SC_12_25	1.82E-06	SC_16_25	1.82E-06
SC_4_26	1.84E-06	SC_8_26	1.84E-06	SC_12_26	1.84E-06	SC_16_26	1.84E-06
SC_4_27	1.86E-06	SC_8_27	1.86E-06	SC_12_27	1.86E-06	SC_16_27	1.86E-06

Tab. A.3-9 Cumulative inductances for each conductor of PF 6 coil at 22.1 kHz (H)

SC_1_1	1.19E-06	SC_5_1	1.19E-06	SC_9_1	1.19E-06	SC_13_1	1.19E-06
SC_1_2	1.21E-06	SC_5_2	1.21E-06	SC_9_2	1.21E-06	SC_13_2	1.21E-06
SC_1_3	1.23E-06	SC_5_3	1.23E-06	SC_9_3	1.23E-06	SC_13_3	1.23E-06
SC_1_4	1.25E-06	SC_5_4	1.25E-06	SC_9_4	1.25E-06	SC_13_4	1.25E-06
SC_1_5	1.27E-06	SC_5_5	1.27E-06	SC_9_5	1.27E-06	SC_13_5	1.27E-06
SC_1_6	1.29E-06	SC_5_6	1.29E-06	SC_9_6	1.29E-06	SC_13_6	1.29E-06
SC_1_7	1.31E-06	SC_5_7	1.31E-06	SC_9_7	1.31E-06	SC_13_7	1.31E-06
SC_1_8	1.33E-06	SC_5_8	1.33E-06	SC_9_8	1.33E-06	SC_13_8	1.33E-06
SC_1_9	1.35E-06	SC_5_9	1.35E-06	SC_9_9	1.35E-06	SC_13_9	1.35E-06
SC_1_10	1.37E-06	SC_5_10	1.37E-06	SC_9_10	1.37E-06	SC_13_10	1.37E-06
SC_1_11	1.39E-06	SC_5_11	1.39E-06	SC_9_11	1.39E-06	SC_13_11	1.39E-06
SC_1_12	1.41E-06	SC_5_12	1.41E-06	SC_9_12	1.41E-06	SC_13_12	1.41E-06
SC_1_13	1.43E-06	SC_5_13	1.43E-06	SC_9_13	1.43E-06	SC_13_13	1.43E-06
SC_1_14	1.45E-06	SC_5_14	1.45E-06	SC_9_14	1.45E-06	SC_13_14	1.45E-06
SC_1_15	1.47E-06	SC_5_15	1.47E-06	SC_9_15	1.47E-06	SC_13_15	1.47E-06
SC_1_16	1.49E-06	SC_5_16	1.49E-06	SC_9_16	1.49E-06	SC_13_16	1.49E-06
SC_1_17	1.52E-06	SC_5_17	1.52E-06	SC_9_17	1.52E-06	SC_13_17	1.52E-06
SC_1_18	1.54E-06	SC_5_18	1.54E-06	SC_9_18	1.54E-06	SC_13_18	1.54E-06
SC_1_19	1.56E-06	SC_5_19	1.56E-06	SC_9_19	1.56E-06	SC_13_19	1.56E-06
SC_1_20	1.58E-06	SC_5_20	1.58E-06	SC_9_20	1.58E-06	SC_13_20	1.58E-06
SC_1_21	1.60E-06	SC_5_21	1.60E-06	SC_9_21	1.60E-06	SC_13_21	1.60E-06
SC_1_22	1.62E-06	SC_5_22	1.62E-06	SC_9_22	1.62E-06	SC_13_22	1.62E-06
SC_1_23	1.64E-06	SC_5_23	1.64E-06	SC_9_23	1.64E-06	SC_13_23	1.64E-06
SC_1_24	1.66E-06	SC_5_24	1.66E-06	SC_9_24	1.66E-06	SC_13_24	1.66E-06
SC_1_25	1.81E-06	SC_5_25	1.81E-06	SC_9_25	1.81E-06	SC_13_25	1.81E-06
SC_1_26	1.83E-06	SC_5_26	1.83E-06	SC_9_26	1.83E-06	SC_13_26	1.83E-06
SC_1_27	1.85E-06	SC_5_27	1.85E-06	SC_9_27	1.85E-06	SC_13_27	1.85E-06
SC_2_1	1.19E-06	SC_6_1	1.19E-06	SC_10_1	1.19E-06	SC_14_1	1.19E-06
SC_2_2	1.21E-06	SC_6_2	1.21E-06	SC_10_2	1.21E-06	SC_14_2	1.21E-06
SC_2_3	1.23E-06	SC_6_3	1.23E-06	SC_10_3	1.23E-06	SC_14_3	1.23E-06
SC_2_4	1.25E-06	SC_6_4	1.25E-06	SC_10_4	1.25E-06	SC_14_4	1.25E-06
SC_2_5	1.27E-06	SC_6_5	1.27E-06	SC_10_5	1.27E-06	SC_14_5	1.27E-06
SC_2_6	1.29E-06	SC_6_6	1.29E-06	SC_10_6	1.29E-06	SC_14_6	1.29E-06
SC_2_7	1.31E-06	SC_6_7	1.31E-06	SC_10_7	1.31E-06	SC_14_7	1.31E-06
SC_2_8	1.33E-06	SC_6_8	1.33E-06	SC_10_8	1.33E-06	SC_14_8	1.33E-06
SC_2_9	1.35E-06	SC_6_9	1.35E-06	SC_10_9	1.35E-06	SC_14_9	1.35E-06
SC_2_10	1.37E-06	SC_6_10	1.37E-06	SC_10_10	1.37E-06	SC_14_10	1.37E-06
SC_2_11	1.39E-06	SC_6_11	1.39E-06	SC_10_11	1.39E-06	SC_14_11	1.39E-06
SC_2_12	1.41E-06	SC_6_12	1.41E-06	SC_10_12	1.41E-06	SC_14_12	1.41E-06
SC_2_13	1.43E-06	SC_6_13	1.43E-06	SC_10_13	1.43E-06	SC_14_13	1.43E-06
SC_2_14	1.45E-06	SC_6_14	1.45E-06	SC_10_14	1.45E-06	SC_14_14	1.45E-06
SC_2_15	1.47E-06	SC_6_15	1.47E-06	SC_10_15	1.47E-06	SC_14_15	1.47E-06
SC_2_16	1.49E-06	SC_6_16	1.49E-06	SC_10_16	1.49E-06	SC_14_16	1.49E-06
SC_2_17	1.52E-06	SC_6_17	1.52E-06	SC_10_17	1.52E-06	SC_14_17	1.52E-06
SC_2_18	1.54E-06	SC_6_18	1.54E-06	SC_10_18	1.54E-06	SC_14_18	1.54E-06
SC_2_19	1.56E-06	SC_6_19	1.56E-06	SC_10_19	1.56E-06	SC_14_19	1.56E-06
SC_2_20	1.58E-06	SC_6_20	1.58E-06	SC_10_20	1.58E-06	SC_14_20	1.58E-06
SC_2_21	1.60E-06	SC_6_21	1.60E-06	SC_10_21	1.60E-06	SC_14_21	1.60E-06
SC_2_22	1.62E-06	SC_6_22	1.62E-06	SC_10_22	1.62E-06	SC_14_22	1.62E-06
SC_2_23	1.64E-06	SC_6_23	1.64E-06	SC_10_23	1.64E-06	SC_14_23	1.64E-06
SC_2_24	1.66E-06	SC_6_24	1.66E-06	SC_10_24	1.66E-06	SC_14_24	1.66E-06
SC_2_25	1.81E-06	SC_6_25	1.81E-06	SC_10_25	1.81E-06	SC_14_25	1.81E-06
SC_2_26	1.83E-06	SC_6_26	1.83E-06	SC_10_26	1.83E-06	SC_14_26	1.83E-06
SC_2_27	1.85E-06	SC_6_27	1.85E-06	SC_10_27	1.85E-06	SC_14_27	1.85E-06
SC_3_1	1.19E-06	SC_7_1	1.19E-06	SC_11_1	1.19E-06	SC_15_1	1.19E-06

SC_3_2	1.21E-06	SC_7_2	1.21E-06	SC_11_2	1.21E-06	SC_15_2	1.21E-06
SC_3_3	1.23E-06	SC_7_3	1.23E-06	SC_11_3	1.23E-06	SC_15_3	1.23E-06
SC_3_4	1.25E-06	SC_7_4	1.25E-06	SC_11_4	1.25E-06	SC_15_4	1.25E-06
SC_3_5	1.27E-06	SC_7_5	1.27E-06	SC_11_5	1.27E-06	SC_15_5	1.27E-06
SC_3_6	1.29E-06	SC_7_6	1.29E-06	SC_11_6	1.29E-06	SC_15_6	1.29E-06
SC_3_7	1.31E-06	SC_7_7	1.31E-06	SC_11_7	1.31E-06	SC_15_7	1.31E-06
SC_3_8	1.33E-06	SC_7_8	1.33E-06	SC_11_8	1.33E-06	SC_15_8	1.33E-06
SC_3_9	1.35E-06	SC_7_9	1.35E-06	SC_11_9	1.35E-06	SC_15_9	1.35E-06
SC_3_10	1.37E-06	SC_7_10	1.37E-06	SC_11_10	1.37E-06	SC_15_10	1.37E-06
SC_3_11	1.39E-06	SC_7_11	1.39E-06	SC_11_11	1.39E-06	SC_15_11	1.39E-06
SC_3_12	1.41E-06	SC_7_12	1.41E-06	SC_11_12	1.41E-06	SC_15_12	1.41E-06
SC_3_13	1.43E-06	SC_7_13	1.43E-06	SC_11_13	1.43E-06	SC_15_13	1.43E-06
SC_3_14	1.45E-06	SC_7_14	1.45E-06	SC_11_14	1.45E-06	SC_15_14	1.45E-06
SC_3_15	1.47E-06	SC_7_15	1.47E-06	SC_11_15	1.47E-06	SC_15_15	1.47E-06
SC_3_16	1.49E-06	SC_7_16	1.49E-06	SC_11_16	1.49E-06	SC_15_16	1.49E-06
SC_3_17	1.52E-06	SC_7_17	1.52E-06	SC_11_17	1.52E-06	SC_15_17	1.52E-06
SC_3_18	1.54E-06	SC_7_18	1.54E-06	SC_11_18	1.54E-06	SC_15_18	1.54E-06
SC_3_19	1.56E-06	SC_7_19	1.56E-06	SC_11_19	1.56E-06	SC_15_19	1.56E-06
SC_3_20	1.58E-06	SC_7_20	1.58E-06	SC_11_20	1.58E-06	SC_15_20	1.58E-06
SC_3_21	1.60E-06	SC_7_21	1.60E-06	SC_11_21	1.60E-06	SC_15_21	1.60E-06
SC_3_22	1.62E-06	SC_7_22	1.62E-06	SC_11_22	1.62E-06	SC_15_22	1.62E-06
SC_3_23	1.64E-06	SC_7_23	1.64E-06	SC_11_23	1.64E-06	SC_15_23	1.64E-06
SC_3_24	1.66E-06	SC_7_24	1.66E-06	SC_11_24	1.66E-06	SC_15_24	1.66E-06
SC_3_25	1.81E-06	SC_7_25	1.81E-06	SC_11_25	1.81E-06	SC_15_25	1.81E-06
SC_3_26	1.83E-06	SC_7_26	1.83E-06	SC_11_26	1.83E-06	SC_15_26	1.83E-06
SC_3_27	1.85E-06	SC_7_27	1.85E-06	SC_11_27	1.85E-06	SC_15_27	1.85E-06
SC_4_1	1.19E-06	SC_8_1	1.19E-06	SC_12_1	1.19E-06	SC_16_1	1.19E-06
SC_4_2	1.21E-06	SC_8_2	1.21E-06	SC_12_2	1.21E-06	SC_16_2	1.21E-06
SC_4_3	1.23E-06	SC_8_3	1.23E-06	SC_12_3	1.23E-06	SC_16_3	1.23E-06
SC_4_4	1.25E-06	SC_8_4	1.25E-06	SC_12_4	1.25E-06	SC_16_4	1.25E-06
SC_4_5	1.27E-06	SC_8_5	1.27E-06	SC_12_5	1.27E-06	SC_16_5	1.27E-06
SC_4_6	1.29E-06	SC_8_6	1.29E-06	SC_12_6	1.29E-06	SC_16_6	1.29E-06
SC_4_7	1.31E-06	SC_8_7	1.31E-06	SC_12_7	1.31E-06	SC_16_7	1.31E-06
SC_4_8	1.33E-06	SC_8_8	1.33E-06	SC_12_8	1.33E-06	SC_16_8	1.33E-06
SC_4_9	1.35E-06	SC_8_9	1.35E-06	SC_12_9	1.35E-06	SC_16_9	1.35E-06
SC_4_10	1.37E-06	SC_8_10	1.37E-06	SC_12_10	1.37E-06	SC_16_10	1.37E-06
SC_4_11	1.39E-06	SC_8_11	1.39E-06	SC_12_11	1.39E-06	SC_16_11	1.39E-06
SC_4_12	1.41E-06	SC_8_12	1.41E-06	SC_12_12	1.41E-06	SC_16_12	1.41E-06
SC_4_13	1.43E-06	SC_8_13	1.43E-06	SC_12_13	1.43E-06	SC_16_13	1.43E-06
SC_4_14	1.45E-06	SC_8_14	1.45E-06	SC_12_14	1.45E-06	SC_16_14	1.45E-06
SC_4_15	1.47E-06	SC_8_15	1.47E-06	SC_12_15	1.47E-06	SC_16_15	1.47E-06
SC_4_16	1.49E-06	SC_8_16	1.49E-06	SC_12_16	1.49E-06	SC_16_16	1.49E-06
SC_4_17	1.52E-06	SC_8_17	1.52E-06	SC_12_17	1.52E-06	SC_16_17	1.52E-06
SC_4_18	1.54E-06	SC_8_18	1.54E-06	SC_12_18	1.54E-06	SC_16_18	1.54E-06
SC_4_19	1.56E-06	SC_8_19	1.56E-06	SC_12_19	1.56E-06	SC_16_19	1.56E-06
SC_4_20	1.58E-06	SC_8_20	1.58E-06	SC_12_20	1.58E-06	SC_16_20	1.58E-06
SC_4_21	1.60E-06	SC_8_21	1.60E-06	SC_12_21	1.60E-06	SC_16_21	1.60E-06
SC_4_22	1.62E-06	SC_8_22	1.62E-06	SC_12_22	1.62E-06	SC_16_22	1.62E-06
SC_4_23	1.64E-06	SC_8_23	1.64E-06	SC_12_23	1.64E-06	SC_16_23	1.64E-06
SC_4_24	1.66E-06	SC_8_24	1.66E-06	SC_12_24	1.66E-06	SC_16_24	1.66E-06
SC_4_25	1.81E-06	SC_8_25	1.81E-06	SC_12_25	1.81E-06	SC_16_25	1.81E-06
SC_4_26	1.83E-06	SC_8_26	1.83E-06	SC_12_26	1.83E-06	SC_16_26	1.83E-06
SC_4_27	1.85E-06	SC_8_27	1.85E-06	SC_12_27	1.85E-06	SC_16_27	1.85E-06

Tab. A.3-10 Cumulative inductances for each conductor of PF 6 coil at 22.9 kHz (H)

SC_1_1	1.16E-06	SC_5_1	1.16E-06	SC_9_1	1.16E-06	SC_13_1	1.16E-06
SC_1_2	1.18E-06	SC_5_2	1.18E-06	SC_9_2	1.18E-06	SC_13_2	1.18E-06
SC_1_3	1.20E-06	SC_5_3	1.20E-06	SC_9_3	1.20E-06	SC_13_3	1.20E-06
SC_1_4	1.22E-06	SC_5_4	1.22E-06	SC_9_4	1.22E-06	SC_13_4	1.22E-06
SC_1_5	1.24E-06	SC_5_5	1.24E-06	SC_9_5	1.24E-06	SC_13_5	1.24E-06
SC_1_6	1.26E-06	SC_5_6	1.26E-06	SC_9_6	1.26E-06	SC_13_6	1.26E-06
SC_1_7	1.28E-06	SC_5_7	1.28E-06	SC_9_7	1.28E-06	SC_13_7	1.28E-06
SC_1_8	1.30E-06	SC_5_8	1.30E-06	SC_9_8	1.30E-06	SC_13_8	1.30E-06
SC_1_9	1.32E-06	SC_5_9	1.32E-06	SC_9_9	1.32E-06	SC_13_9	1.32E-06
SC_1_10	1.34E-06	SC_5_10	1.34E-06	SC_9_10	1.34E-06	SC_13_10	1.34E-06
SC_1_11	1.36E-06	SC_5_11	1.36E-06	SC_9_11	1.36E-06	SC_13_11	1.36E-06
SC_1_12	1.38E-06	SC_5_12	1.38E-06	SC_9_12	1.38E-06	SC_13_12	1.38E-06
SC_1_13	1.40E-06	SC_5_13	1.40E-06	SC_9_13	1.40E-06	SC_13_13	1.40E-06
SC_1_14	1.42E-06	SC_5_14	1.42E-06	SC_9_14	1.42E-06	SC_13_14	1.42E-06
SC_1_15	1.44E-06	SC_5_15	1.44E-06	SC_9_15	1.44E-06	SC_13_15	1.44E-06
SC_1_16	1.46E-06	SC_5_16	1.46E-06	SC_9_16	1.46E-06	SC_13_16	1.46E-06
SC_1_17	1.48E-06	SC_5_17	1.48E-06	SC_9_17	1.48E-06	SC_13_17	1.48E-06
SC_1_18	1.50E-06	SC_5_18	1.50E-06	SC_9_18	1.50E-06	SC_13_18	1.50E-06
SC_1_19	1.52E-06	SC_5_19	1.52E-06	SC_9_19	1.52E-06	SC_13_19	1.52E-06
SC_1_20	1.54E-06	SC_5_20	1.54E-06	SC_9_20	1.54E-06	SC_13_20	1.54E-06
SC_1_21	1.56E-06	SC_5_21	1.56E-06	SC_9_21	1.56E-06	SC_13_21	1.56E-06
SC_1_22	1.58E-06	SC_5_22	1.58E-06	SC_9_22	1.58E-06	SC_13_22	1.58E-06
SC_1_23	1.60E-06	SC_5_23	1.60E-06	SC_9_23	1.60E-06	SC_13_23	1.60E-06
SC_1_24	1.62E-06	SC_5_24	1.62E-06	SC_9_24	1.62E-06	SC_13_24	1.62E-06
SC_1_25	1.76E-06	SC_5_25	1.76E-06	SC_9_25	1.76E-06	SC_13_25	1.76E-06
SC_1_26	1.78E-06	SC_5_26	1.78E-06	SC_9_26	1.78E-06	SC_13_26	1.78E-06
SC_1_27	1.81E-06	SC_5_27	1.81E-06	SC_9_27	1.81E-06	SC_13_27	1.81E-06
SC_2_1	1.16E-06	SC_6_1	1.16E-06	SC_10_1	1.16E-06	SC_14_1	1.16E-06
SC_2_2	1.18E-06	SC_6_2	1.18E-06	SC_10_2	1.18E-06	SC_14_2	1.18E-06
SC_2_3	1.20E-06	SC_6_3	1.20E-06	SC_10_3	1.20E-06	SC_14_3	1.20E-06
SC_2_4	1.22E-06	SC_6_4	1.22E-06	SC_10_4	1.22E-06	SC_14_4	1.22E-06
SC_2_5	1.24E-06	SC_6_5	1.24E-06	SC_10_5	1.24E-06	SC_14_5	1.24E-06
SC_2_6	1.26E-06	SC_6_6	1.26E-06	SC_10_6	1.26E-06	SC_14_6	1.26E-06
SC_2_7	1.28E-06	SC_6_7	1.28E-06	SC_10_7	1.28E-06	SC_14_7	1.28E-06
SC_2_8	1.30E-06	SC_6_8	1.30E-06	SC_10_8	1.30E-06	SC_14_8	1.30E-06
SC_2_9	1.32E-06	SC_6_9	1.32E-06	SC_10_9	1.32E-06	SC_14_9	1.32E-06
SC_2_10	1.34E-06	SC_6_10	1.34E-06	SC_10_10	1.34E-06	SC_14_10	1.34E-06
SC_2_11	1.36E-06	SC_6_11	1.36E-06	SC_10_11	1.36E-06	SC_14_11	1.36E-06
SC_2_12	1.38E-06	SC_6_12	1.38E-06	SC_10_12	1.38E-06	SC_14_12	1.38E-06
SC_2_13	1.40E-06	SC_6_13	1.40E-06	SC_10_13	1.40E-06	SC_14_13	1.40E-06
SC_2_14	1.42E-06	SC_6_14	1.42E-06	SC_10_14	1.42E-06	SC_14_14	1.42E-06
SC_2_15	1.44E-06	SC_6_15	1.44E-06	SC_10_15	1.44E-06	SC_14_15	1.44E-06
SC_2_16	1.46E-06	SC_6_16	1.46E-06	SC_10_16	1.46E-06	SC_14_16	1.46E-06
SC_2_17	1.48E-06	SC_6_17	1.48E-06	SC_10_17	1.48E-06	SC_14_17	1.48E-06
SC_2_18	1.50E-06	SC_6_18	1.50E-06	SC_10_18	1.50E-06	SC_14_18	1.50E-06
SC_2_19	1.52E-06	SC_6_19	1.52E-06	SC_10_19	1.52E-06	SC_14_19	1.52E-06
SC_2_20	1.54E-06	SC_6_20	1.54E-06	SC_10_20	1.54E-06	SC_14_20	1.54E-06
SC_2_21	1.56E-06	SC_6_21	1.56E-06	SC_10_21	1.56E-06	SC_14_21	1.56E-06
SC_2_22	1.58E-06	SC_6_22	1.58E-06	SC_10_22	1.58E-06	SC_14_22	1.58E-06
SC_2_23	1.60E-06	SC_6_23	1.60E-06	SC_10_23	1.60E-06	SC_14_23	1.60E-06
SC_2_24	1.62E-06	SC_6_24	1.62E-06	SC_10_24	1.62E-06	SC_14_24	1.62E-06
SC_2_25	1.76E-06	SC_6_25	1.76E-06	SC_10_25	1.76E-06	SC_14_25	1.76E-06
SC_2_26	1.78E-06	SC_6_26	1.78E-06	SC_10_26	1.78E-06	SC_14_26	1.78E-06
SC_2_27	1.81E-06	SC_6_27	1.81E-06	SC_10_27	1.81E-06	SC_14_27	1.81E-06
SC_3_1	1.16E-06	SC_7_1	1.16E-06	SC_11_1	1.16E-06	SC_15_1	1.16E-06

SC_3_2	1.18E-06	SC_7_2	1.18E-06	SC_11_2	1.18E-06	SC_15_2	1.18E-06
SC_3_3	1.20E-06	SC_7_3	1.20E-06	SC_11_3	1.20E-06	SC_15_3	1.20E-06
SC_3_4	1.22E-06	SC_7_4	1.22E-06	SC_11_4	1.22E-06	SC_15_4	1.22E-06
SC_3_5	1.24E-06	SC_7_5	1.24E-06	SC_11_5	1.24E-06	SC_15_5	1.24E-06
SC_3_6	1.26E-06	SC_7_6	1.26E-06	SC_11_6	1.26E-06	SC_15_6	1.26E-06
SC_3_7	1.28E-06	SC_7_7	1.28E-06	SC_11_7	1.28E-06	SC_15_7	1.28E-06
SC_3_8	1.30E-06	SC_7_8	1.30E-06	SC_11_8	1.30E-06	SC_15_8	1.30E-06
SC_3_9	1.32E-06	SC_7_9	1.32E-06	SC_11_9	1.32E-06	SC_15_9	1.32E-06
SC_3_10	1.34E-06	SC_7_10	1.34E-06	SC_11_10	1.34E-06	SC_15_10	1.34E-06
SC_3_11	1.36E-06	SC_7_11	1.36E-06	SC_11_11	1.36E-06	SC_15_11	1.36E-06
SC_3_12	1.38E-06	SC_7_12	1.38E-06	SC_11_12	1.38E-06	SC_15_12	1.38E-06
SC_3_13	1.40E-06	SC_7_13	1.40E-06	SC_11_13	1.40E-06	SC_15_13	1.40E-06
SC_3_14	1.42E-06	SC_7_14	1.42E-06	SC_11_14	1.42E-06	SC_15_14	1.42E-06
SC_3_15	1.44E-06	SC_7_15	1.44E-06	SC_11_15	1.44E-06	SC_15_15	1.44E-06
SC_3_16	1.46E-06	SC_7_16	1.46E-06	SC_11_16	1.46E-06	SC_15_16	1.46E-06
SC_3_17	1.48E-06	SC_7_17	1.48E-06	SC_11_17	1.48E-06	SC_15_17	1.48E-06
SC_3_18	1.50E-06	SC_7_18	1.50E-06	SC_11_18	1.50E-06	SC_15_18	1.50E-06
SC_3_19	1.52E-06	SC_7_19	1.52E-06	SC_11_19	1.52E-06	SC_15_19	1.52E-06
SC_3_20	1.54E-06	SC_7_20	1.54E-06	SC_11_20	1.54E-06	SC_15_20	1.54E-06
SC_3_21	1.56E-06	SC_7_21	1.56E-06	SC_11_21	1.56E-06	SC_15_21	1.56E-06
SC_3_22	1.58E-06	SC_7_22	1.58E-06	SC_11_22	1.58E-06	SC_15_22	1.58E-06
SC_3_23	1.60E-06	SC_7_23	1.60E-06	SC_11_23	1.60E-06	SC_15_23	1.60E-06
SC_3_24	1.62E-06	SC_7_24	1.62E-06	SC_11_24	1.62E-06	SC_15_24	1.62E-06
SC_3_25	1.76E-06	SC_7_25	1.76E-06	SC_11_25	1.76E-06	SC_15_25	1.76E-06
SC_3_26	1.78E-06	SC_7_26	1.78E-06	SC_11_26	1.78E-06	SC_15_26	1.78E-06
SC_3_27	1.81E-06	SC_7_27	1.81E-06	SC_11_27	1.81E-06	SC_15_27	1.81E-06
SC_4_1	1.16E-06	SC_8_1	1.16E-06	SC_12_1	1.16E-06	SC_16_1	1.16E-06
SC_4_2	1.18E-06	SC_8_2	1.18E-06	SC_12_2	1.18E-06	SC_16_2	1.18E-06
SC_4_3	1.20E-06	SC_8_3	1.20E-06	SC_12_3	1.20E-06	SC_16_3	1.20E-06
SC_4_4	1.22E-06	SC_8_4	1.22E-06	SC_12_4	1.22E-06	SC_16_4	1.22E-06
SC_4_5	1.24E-06	SC_8_5	1.24E-06	SC_12_5	1.24E-06	SC_16_5	1.24E-06
SC_4_6	1.26E-06	SC_8_6	1.26E-06	SC_12_6	1.26E-06	SC_16_6	1.26E-06
SC_4_7	1.28E-06	SC_8_7	1.28E-06	SC_12_7	1.28E-06	SC_16_7	1.28E-06
SC_4_8	1.30E-06	SC_8_8	1.30E-06	SC_12_8	1.30E-06	SC_16_8	1.30E-06
SC_4_9	1.32E-06	SC_8_9	1.32E-06	SC_12_9	1.32E-06	SC_16_9	1.32E-06
SC_4_10	1.34E-06	SC_8_10	1.34E-06	SC_12_10	1.34E-06	SC_16_10	1.34E-06
SC_4_11	1.36E-06	SC_8_11	1.36E-06	SC_12_11	1.36E-06	SC_16_11	1.36E-06
SC_4_12	1.38E-06	SC_8_12	1.38E-06	SC_12_12	1.38E-06	SC_16_12	1.38E-06
SC_4_13	1.40E-06	SC_8_13	1.40E-06	SC_12_13	1.40E-06	SC_16_13	1.40E-06
SC_4_14	1.42E-06	SC_8_14	1.42E-06	SC_12_14	1.42E-06	SC_16_14	1.42E-06
SC_4_15	1.44E-06	SC_8_15	1.44E-06	SC_12_15	1.44E-06	SC_16_15	1.44E-06
SC_4_16	1.46E-06	SC_8_16	1.46E-06	SC_12_16	1.46E-06	SC_16_16	1.46E-06
SC_4_17	1.48E-06	SC_8_17	1.48E-06	SC_12_17	1.48E-06	SC_16_17	1.48E-06
SC_4_18	1.50E-06	SC_8_18	1.50E-06	SC_12_18	1.50E-06	SC_16_18	1.50E-06
SC_4_19	1.52E-06	SC_8_19	1.52E-06	SC_12_19	1.52E-06	SC_16_19	1.52E-06
SC_4_20	1.54E-06	SC_8_20	1.54E-06	SC_12_20	1.54E-06	SC_16_20	1.54E-06
SC_4_21	1.56E-06	SC_8_21	1.56E-06	SC_12_21	1.56E-06	SC_16_21	1.56E-06
SC_4_22	1.58E-06	SC_8_22	1.58E-06	SC_12_22	1.58E-06	SC_16_22	1.58E-06
SC_4_23	1.60E-06	SC_8_23	1.60E-06	SC_12_23	1.60E-06	SC_16_23	1.60E-06
SC_4_24	1.62E-06	SC_8_24	1.62E-06	SC_12_24	1.62E-06	SC_16_24	1.62E-06
SC_4_25	1.76E-06	SC_8_25	1.76E-06	SC_12_25	1.76E-06	SC_16_25	1.76E-06
SC_4_26	1.78E-06	SC_8_26	1.78E-06	SC_12_26	1.78E-06	SC_16_26	1.78E-06
SC_4_27	1.81E-06	SC_8_27	1.81E-06	SC_12_27	1.81E-06	SC_16_27	1.81E-06

Tab. A.3-11 Cumulative inductances for each conductor of PF 6 coil at 27.7 kHz (H)

SC_1_1	1.16E-06	SC_5_1	1.16E-06	SC_9_1	1.16E-06	SC_13_1	1.16E-06
SC_1_2	1.18E-06	SC_5_2	1.18E-06	SC_9_2	1.18E-06	SC_13_2	1.18E-06
SC_1_3	1.20E-06	SC_5_3	1.20E-06	SC_9_3	1.20E-06	SC_13_3	1.20E-06
SC_1_4	1.22E-06	SC_5_4	1.22E-06	SC_9_4	1.22E-06	SC_13_4	1.22E-06
SC_1_5	1.24E-06	SC_5_5	1.24E-06	SC_9_5	1.24E-06	SC_13_5	1.24E-06
SC_1_6	1.26E-06	SC_5_6	1.26E-06	SC_9_6	1.26E-06	SC_13_6	1.26E-06
SC_1_7	1.28E-06	SC_5_7	1.28E-06	SC_9_7	1.28E-06	SC_13_7	1.28E-06
SC_1_8	1.30E-06	SC_5_8	1.30E-06	SC_9_8	1.30E-06	SC_13_8	1.30E-06
SC_1_9	1.32E-06	SC_5_9	1.32E-06	SC_9_9	1.32E-06	SC_13_9	1.32E-06
SC_1_10	1.34E-06	SC_5_10	1.34E-06	SC_9_10	1.34E-06	SC_13_10	1.34E-06
SC_1_11	1.36E-06	SC_5_11	1.36E-06	SC_9_11	1.36E-06	SC_13_11	1.36E-06
SC_1_12	1.38E-06	SC_5_12	1.38E-06	SC_9_12	1.38E-06	SC_13_12	1.38E-06
SC_1_13	1.40E-06	SC_5_13	1.40E-06	SC_9_13	1.40E-06	SC_13_13	1.40E-06
SC_1_14	1.42E-06	SC_5_14	1.42E-06	SC_9_14	1.42E-06	SC_13_14	1.42E-06
SC_1_15	1.44E-06	SC_5_15	1.44E-06	SC_9_15	1.44E-06	SC_13_15	1.44E-06
SC_1_16	1.46E-06	SC_5_16	1.46E-06	SC_9_16	1.46E-06	SC_13_16	1.46E-06
SC_1_17	1.48E-06	SC_5_17	1.48E-06	SC_9_17	1.48E-06	SC_13_17	1.48E-06
SC_1_18	1.50E-06	SC_5_18	1.50E-06	SC_9_18	1.50E-06	SC_13_18	1.50E-06
SC_1_19	1.52E-06	SC_5_19	1.52E-06	SC_9_19	1.52E-06	SC_13_19	1.52E-06
SC_1_20	1.54E-06	SC_5_20	1.54E-06	SC_9_20	1.54E-06	SC_13_20	1.54E-06
SC_1_21	1.56E-06	SC_5_21	1.56E-06	SC_9_21	1.56E-06	SC_13_21	1.56E-06
SC_1_22	1.58E-06	SC_5_22	1.58E-06	SC_9_22	1.58E-06	SC_13_22	1.58E-06
SC_1_23	1.60E-06	SC_5_23	1.60E-06	SC_9_23	1.60E-06	SC_13_23	1.60E-06
SC_1_24	1.62E-06	SC_5_24	1.62E-06	SC_9_24	1.62E-06	SC_13_24	1.62E-06
SC_1_25	1.76E-06	SC_5_25	1.76E-06	SC_9_25	1.76E-06	SC_13_25	1.76E-06
SC_1_26	1.78E-06	SC_5_26	1.78E-06	SC_9_26	1.78E-06	SC_13_26	1.78E-06
SC_1_27	1.80E-06	SC_5_27	1.80E-06	SC_9_27	1.80E-06	SC_13_27	1.80E-06
SC_2_1	1.16E-06	SC_6_1	1.16E-06	SC_10_1	1.16E-06	SC_14_1	1.16E-06
SC_2_2	1.18E-06	SC_6_2	1.18E-06	SC_10_2	1.18E-06	SC_14_2	1.18E-06
SC_2_3	1.20E-06	SC_6_3	1.20E-06	SC_10_3	1.20E-06	SC_14_3	1.20E-06
SC_2_4	1.22E-06	SC_6_4	1.22E-06	SC_10_4	1.22E-06	SC_14_4	1.22E-06
SC_2_5	1.24E-06	SC_6_5	1.24E-06	SC_10_5	1.24E-06	SC_14_5	1.24E-06
SC_2_6	1.26E-06	SC_6_6	1.26E-06	SC_10_6	1.26E-06	SC_14_6	1.26E-06
SC_2_7	1.28E-06	SC_6_7	1.28E-06	SC_10_7	1.28E-06	SC_14_7	1.28E-06
SC_2_8	1.30E-06	SC_6_8	1.30E-06	SC_10_8	1.30E-06	SC_14_8	1.30E-06
SC_2_9	1.32E-06	SC_6_9	1.32E-06	SC_10_9	1.32E-06	SC_14_9	1.32E-06
SC_2_10	1.34E-06	SC_6_10	1.34E-06	SC_10_10	1.34E-06	SC_14_10	1.34E-06
SC_2_11	1.36E-06	SC_6_11	1.36E-06	SC_10_11	1.36E-06	SC_14_11	1.36E-06
SC_2_12	1.38E-06	SC_6_12	1.38E-06	SC_10_12	1.38E-06	SC_14_12	1.38E-06
SC_2_13	1.40E-06	SC_6_13	1.40E-06	SC_10_13	1.40E-06	SC_14_13	1.40E-06
SC_2_14	1.42E-06	SC_6_14	1.42E-06	SC_10_14	1.42E-06	SC_14_14	1.42E-06
SC_2_15	1.44E-06	SC_6_15	1.44E-06	SC_10_15	1.44E-06	SC_14_15	1.44E-06
SC_2_16	1.46E-06	SC_6_16	1.46E-06	SC_10_16	1.46E-06	SC_14_16	1.46E-06
SC_2_17	1.48E-06	SC_6_17	1.48E-06	SC_10_17	1.48E-06	SC_14_17	1.48E-06
SC_2_18	1.50E-06	SC_6_18	1.50E-06	SC_10_18	1.50E-06	SC_14_18	1.50E-06
SC_2_19	1.52E-06	SC_6_19	1.52E-06	SC_10_19	1.52E-06	SC_14_19	1.52E-06
SC_2_20	1.54E-06	SC_6_20	1.54E-06	SC_10_20	1.54E-06	SC_14_20	1.54E-06
SC_2_21	1.56E-06	SC_6_21	1.56E-06	SC_10_21	1.56E-06	SC_14_21	1.56E-06
SC_2_22	1.58E-06	SC_6_22	1.58E-06	SC_10_22	1.58E-06	SC_14_22	1.58E-06
SC_2_23	1.60E-06	SC_6_23	1.60E-06	SC_10_23	1.60E-06	SC_14_23	1.60E-06
SC_2_24	1.62E-06	SC_6_24	1.62E-06	SC_10_24	1.62E-06	SC_14_24	1.62E-06
SC_2_25	1.76E-06	SC_6_25	1.76E-06	SC_10_25	1.76E-06	SC_14_25	1.76E-06
SC_2_26	1.78E-06	SC_6_26	1.78E-06	SC_10_26	1.78E-06	SC_14_26	1.78E-06
SC_2_27	1.80E-06	SC_6_27	1.80E-06	SC_10_27	1.80E-06	SC_14_27	1.80E-06
SC_3_1	1.16E-06	SC_7_1	1.16E-06	SC_11_1	1.16E-06	SC_15_1	1.16E-06

SC_3_2	1.18E-06	SC_7_2	1.18E-06	SC_11_2	1.18E-06	SC_15_2	1.18E-06
SC_3_3	1.20E-06	SC_7_3	1.20E-06	SC_11_3	1.20E-06	SC_15_3	1.20E-06
SC_3_4	1.22E-06	SC_7_4	1.22E-06	SC_11_4	1.22E-06	SC_15_4	1.22E-06
SC_3_5	1.24E-06	SC_7_5	1.24E-06	SC_11_5	1.24E-06	SC_15_5	1.24E-06
SC_3_6	1.26E-06	SC_7_6	1.26E-06	SC_11_6	1.26E-06	SC_15_6	1.26E-06
SC_3_7	1.28E-06	SC_7_7	1.28E-06	SC_11_7	1.28E-06	SC_15_7	1.28E-06
SC_3_8	1.30E-06	SC_7_8	1.30E-06	SC_11_8	1.30E-06	SC_15_8	1.30E-06
SC_3_9	1.32E-06	SC_7_9	1.32E-06	SC_11_9	1.32E-06	SC_15_9	1.32E-06
SC_3_10	1.34E-06	SC_7_10	1.34E-06	SC_11_10	1.34E-06	SC_15_10	1.34E-06
SC_3_11	1.36E-06	SC_7_11	1.36E-06	SC_11_11	1.36E-06	SC_15_11	1.36E-06
SC_3_12	1.38E-06	SC_7_12	1.38E-06	SC_11_12	1.38E-06	SC_15_12	1.38E-06
SC_3_13	1.40E-06	SC_7_13	1.40E-06	SC_11_13	1.40E-06	SC_15_13	1.40E-06
SC_3_14	1.42E-06	SC_7_14	1.42E-06	SC_11_14	1.42E-06	SC_15_14	1.42E-06
SC_3_15	1.44E-06	SC_7_15	1.44E-06	SC_11_15	1.44E-06	SC_15_15	1.44E-06
SC_3_16	1.46E-06	SC_7_16	1.46E-06	SC_11_16	1.46E-06	SC_15_16	1.46E-06
SC_3_17	1.48E-06	SC_7_17	1.48E-06	SC_11_17	1.48E-06	SC_15_17	1.48E-06
SC_3_18	1.50E-06	SC_7_18	1.50E-06	SC_11_18	1.50E-06	SC_15_18	1.50E-06
SC_3_19	1.52E-06	SC_7_19	1.52E-06	SC_11_19	1.52E-06	SC_15_19	1.52E-06
SC_3_20	1.54E-06	SC_7_20	1.54E-06	SC_11_20	1.54E-06	SC_15_20	1.54E-06
SC_3_21	1.56E-06	SC_7_21	1.56E-06	SC_11_21	1.56E-06	SC_15_21	1.56E-06
SC_3_22	1.58E-06	SC_7_22	1.58E-06	SC_11_22	1.58E-06	SC_15_22	1.58E-06
SC_3_23	1.60E-06	SC_7_23	1.60E-06	SC_11_23	1.60E-06	SC_15_23	1.60E-06
SC_3_24	1.62E-06	SC_7_24	1.62E-06	SC_11_24	1.62E-06	SC_15_24	1.62E-06
SC_3_25	1.76E-06	SC_7_25	1.76E-06	SC_11_25	1.76E-06	SC_15_25	1.76E-06
SC_3_26	1.78E-06	SC_7_26	1.78E-06	SC_11_26	1.78E-06	SC_15_26	1.78E-06
SC_3_27	1.80E-06	SC_7_27	1.80E-06	SC_11_27	1.80E-06	SC_15_27	1.80E-06
SC_4_1	1.16E-06	SC_8_1	1.16E-06	SC_12_1	1.16E-06	SC_16_1	1.16E-06
SC_4_2	1.18E-06	SC_8_2	1.18E-06	SC_12_2	1.18E-06	SC_16_2	1.18E-06
SC_4_3	1.20E-06	SC_8_3	1.20E-06	SC_12_3	1.20E-06	SC_16_3	1.20E-06
SC_4_4	1.22E-06	SC_8_4	1.22E-06	SC_12_4	1.22E-06	SC_16_4	1.22E-06
SC_4_5	1.24E-06	SC_8_5	1.24E-06	SC_12_5	1.24E-06	SC_16_5	1.24E-06
SC_4_6	1.26E-06	SC_8_6	1.26E-06	SC_12_6	1.26E-06	SC_16_6	1.26E-06
SC_4_7	1.28E-06	SC_8_7	1.28E-06	SC_12_7	1.28E-06	SC_16_7	1.28E-06
SC_4_8	1.30E-06	SC_8_8	1.30E-06	SC_12_8	1.30E-06	SC_16_8	1.30E-06
SC_4_9	1.32E-06	SC_8_9	1.32E-06	SC_12_9	1.32E-06	SC_16_9	1.32E-06
SC_4_10	1.34E-06	SC_8_10	1.34E-06	SC_12_10	1.34E-06	SC_16_10	1.34E-06
SC_4_11	1.36E-06	SC_8_11	1.36E-06	SC_12_11	1.36E-06	SC_16_11	1.36E-06
SC_4_12	1.38E-06	SC_8_12	1.38E-06	SC_12_12	1.38E-06	SC_16_12	1.38E-06
SC_4_13	1.40E-06	SC_8_13	1.40E-06	SC_12_13	1.40E-06	SC_16_13	1.40E-06
SC_4_14	1.42E-06	SC_8_14	1.42E-06	SC_12_14	1.42E-06	SC_16_14	1.42E-06
SC_4_15	1.44E-06	SC_8_15	1.44E-06	SC_12_15	1.44E-06	SC_16_15	1.44E-06
SC_4_16	1.46E-06	SC_8_16	1.46E-06	SC_12_16	1.46E-06	SC_16_16	1.46E-06
SC_4_17	1.48E-06	SC_8_17	1.48E-06	SC_12_17	1.48E-06	SC_16_17	1.48E-06
SC_4_18	1.50E-06	SC_8_18	1.50E-06	SC_12_18	1.50E-06	SC_16_18	1.50E-06
SC_4_19	1.52E-06	SC_8_19	1.52E-06	SC_12_19	1.52E-06	SC_16_19	1.52E-06
SC_4_20	1.54E-06	SC_8_20	1.54E-06	SC_12_20	1.54E-06	SC_16_20	1.54E-06
SC_4_21	1.56E-06	SC_8_21	1.56E-06	SC_12_21	1.56E-06	SC_16_21	1.56E-06
SC_4_22	1.58E-06	SC_8_22	1.58E-06	SC_12_22	1.58E-06	SC_16_22	1.58E-06
SC_4_23	1.60E-06	SC_8_23	1.60E-06	SC_12_23	1.60E-06	SC_16_23	1.60E-06
SC_4_24	1.62E-06	SC_8_24	1.62E-06	SC_12_24	1.62E-06	SC_16_24	1.62E-06
SC_4_25	1.76E-06	SC_8_25	1.76E-06	SC_12_25	1.76E-06	SC_16_25	1.76E-06
SC_4_26	1.78E-06	SC_8_26	1.78E-06	SC_12_26	1.78E-06	SC_16_26	1.78E-06
SC_4_27	1.80E-06	SC_8_27	1.80E-06	SC_12_27	1.80E-06	SC_16_27	1.80E-06

Tab. A.3-12 Cumulative inductances for each conductor of PF 6 coil at 28.6 kHz (H)

SC_1_1	1.16E-06	SC_5_1	1.16E-06	SC_9_1	1.16E-06	SC_13_1	1.16E-06
SC_1_2	1.18E-06	SC_5_2	1.18E-06	SC_9_2	1.18E-06	SC_13_2	1.18E-06
SC_1_3	1.20E-06	SC_5_3	1.20E-06	SC_9_3	1.20E-06	SC_13_3	1.20E-06
SC_1_4	1.22E-06	SC_5_4	1.22E-06	SC_9_4	1.22E-06	SC_13_4	1.22E-06
SC_1_5	1.24E-06	SC_5_5	1.24E-06	SC_9_5	1.24E-06	SC_13_5	1.24E-06
SC_1_6	1.26E-06	SC_5_6	1.26E-06	SC_9_6	1.26E-06	SC_13_6	1.26E-06
SC_1_7	1.28E-06	SC_5_7	1.28E-06	SC_9_7	1.28E-06	SC_13_7	1.28E-06
SC_1_8	1.30E-06	SC_5_8	1.30E-06	SC_9_8	1.30E-06	SC_13_8	1.30E-06
SC_1_9	1.32E-06	SC_5_9	1.32E-06	SC_9_9	1.32E-06	SC_13_9	1.32E-06
SC_1_10	1.34E-06	SC_5_10	1.34E-06	SC_9_10	1.34E-06	SC_13_10	1.34E-06
SC_1_11	1.36E-06	SC_5_11	1.36E-06	SC_9_11	1.36E-06	SC_13_11	1.36E-06
SC_1_12	1.38E-06	SC_5_12	1.38E-06	SC_9_12	1.38E-06	SC_13_12	1.38E-06
SC_1_13	1.40E-06	SC_5_13	1.40E-06	SC_9_13	1.40E-06	SC_13_13	1.40E-06
SC_1_14	1.42E-06	SC_5_14	1.42E-06	SC_9_14	1.42E-06	SC_13_14	1.42E-06
SC_1_15	1.44E-06	SC_5_15	1.44E-06	SC_9_15	1.44E-06	SC_13_15	1.44E-06
SC_1_16	1.46E-06	SC_5_16	1.46E-06	SC_9_16	1.46E-06	SC_13_16	1.46E-06
SC_1_17	1.48E-06	SC_5_17	1.48E-06	SC_9_17	1.48E-06	SC_13_17	1.48E-06
SC_1_18	1.50E-06	SC_5_18	1.50E-06	SC_9_18	1.50E-06	SC_13_18	1.50E-06
SC_1_19	1.52E-06	SC_5_19	1.52E-06	SC_9_19	1.52E-06	SC_13_19	1.52E-06
SC_1_20	1.54E-06	SC_5_20	1.54E-06	SC_9_20	1.54E-06	SC_13_20	1.54E-06
SC_1_21	1.56E-06	SC_5_21	1.56E-06	SC_9_21	1.56E-06	SC_13_21	1.56E-06
SC_1_22	1.58E-06	SC_5_22	1.58E-06	SC_9_22	1.58E-06	SC_13_22	1.58E-06
SC_1_23	1.60E-06	SC_5_23	1.60E-06	SC_9_23	1.60E-06	SC_13_23	1.60E-06
SC_1_24	1.62E-06	SC_5_24	1.62E-06	SC_9_24	1.62E-06	SC_13_24	1.62E-06
SC_1_25	1.76E-06	SC_5_25	1.76E-06	SC_9_25	1.76E-06	SC_13_25	1.76E-06
SC_1_26	1.78E-06	SC_5_26	1.78E-06	SC_9_26	1.78E-06	SC_13_26	1.78E-06
SC_1_27	1.80E-06	SC_5_27	1.80E-06	SC_9_27	1.80E-06	SC_13_27	1.80E-06
SC_2_1	1.16E-06	SC_6_1	1.16E-06	SC_10_1	1.16E-06	SC_14_1	1.16E-06
SC_2_2	1.18E-06	SC_6_2	1.18E-06	SC_10_2	1.18E-06	SC_14_2	1.18E-06
SC_2_3	1.20E-06	SC_6_3	1.20E-06	SC_10_3	1.20E-06	SC_14_3	1.20E-06
SC_2_4	1.22E-06	SC_6_4	1.22E-06	SC_10_4	1.22E-06	SC_14_4	1.22E-06
SC_2_5	1.24E-06	SC_6_5	1.24E-06	SC_10_5	1.24E-06	SC_14_5	1.24E-06
SC_2_6	1.26E-06	SC_6_6	1.26E-06	SC_10_6	1.26E-06	SC_14_6	1.26E-06
SC_2_7	1.28E-06	SC_6_7	1.28E-06	SC_10_7	1.28E-06	SC_14_7	1.28E-06
SC_2_8	1.30E-06	SC_6_8	1.30E-06	SC_10_8	1.30E-06	SC_14_8	1.30E-06
SC_2_9	1.32E-06	SC_6_9	1.32E-06	SC_10_9	1.32E-06	SC_14_9	1.32E-06
SC_2_10	1.34E-06	SC_6_10	1.34E-06	SC_10_10	1.34E-06	SC_14_10	1.34E-06
SC_2_11	1.36E-06	SC_6_11	1.36E-06	SC_10_11	1.36E-06	SC_14_11	1.36E-06
SC_2_12	1.38E-06	SC_6_12	1.38E-06	SC_10_12	1.38E-06	SC_14_12	1.38E-06
SC_2_13	1.40E-06	SC_6_13	1.40E-06	SC_10_13	1.40E-06	SC_14_13	1.40E-06
SC_2_14	1.42E-06	SC_6_14	1.42E-06	SC_10_14	1.42E-06	SC_14_14	1.42E-06
SC_2_15	1.44E-06	SC_6_15	1.44E-06	SC_10_15	1.44E-06	SC_14_15	1.44E-06
SC_2_16	1.46E-06	SC_6_16	1.46E-06	SC_10_16	1.46E-06	SC_14_16	1.46E-06
SC_2_17	1.48E-06	SC_6_17	1.48E-06	SC_10_17	1.48E-06	SC_14_17	1.48E-06
SC_2_18	1.50E-06	SC_6_18	1.50E-06	SC_10_18	1.50E-06	SC_14_18	1.50E-06
SC_2_19	1.52E-06	SC_6_19	1.52E-06	SC_10_19	1.52E-06	SC_14_19	1.52E-06
SC_2_20	1.54E-06	SC_6_20	1.54E-06	SC_10_20	1.54E-06	SC_14_20	1.54E-06
SC_2_21	1.56E-06	SC_6_21	1.56E-06	SC_10_21	1.56E-06	SC_14_21	1.56E-06
SC_2_22	1.58E-06	SC_6_22	1.58E-06	SC_10_22	1.58E-06	SC_14_22	1.58E-06
SC_2_23	1.60E-06	SC_6_23	1.60E-06	SC_10_23	1.60E-06	SC_14_23	1.60E-06
SC_2_24	1.62E-06	SC_6_24	1.62E-06	SC_10_24	1.62E-06	SC_14_24	1.62E-06
SC_2_25	1.76E-06	SC_6_25	1.76E-06	SC_10_25	1.76E-06	SC_14_25	1.76E-06
SC_2_26	1.78E-06	SC_6_26	1.78E-06	SC_10_26	1.78E-06	SC_14_26	1.78E-06
SC_2_27	1.80E-06	SC_6_27	1.80E-06	SC_10_27	1.80E-06	SC_14_27	1.80E-06
SC_3_1	1.16E-06	SC_7_1	1.16E-06	SC_11_1	1.16E-06	SC_15_1	1.16E-06

SC_3_2	1.18E-06	SC_7_2	1.18E-06	SC_11_2	1.18E-06	SC_15_2	1.18E-06
SC_3_3	1.20E-06	SC_7_3	1.20E-06	SC_11_3	1.20E-06	SC_15_3	1.20E-06
SC_3_4	1.22E-06	SC_7_4	1.22E-06	SC_11_4	1.22E-06	SC_15_4	1.22E-06
SC_3_5	1.24E-06	SC_7_5	1.24E-06	SC_11_5	1.24E-06	SC_15_5	1.24E-06
SC_3_6	1.26E-06	SC_7_6	1.26E-06	SC_11_6	1.26E-06	SC_15_6	1.26E-06
SC_3_7	1.28E-06	SC_7_7	1.28E-06	SC_11_7	1.28E-06	SC_15_7	1.28E-06
SC_3_8	1.30E-06	SC_7_8	1.30E-06	SC_11_8	1.30E-06	SC_15_8	1.30E-06
SC_3_9	1.32E-06	SC_7_9	1.32E-06	SC_11_9	1.32E-06	SC_15_9	1.32E-06
SC_3_10	1.34E-06	SC_7_10	1.34E-06	SC_11_10	1.34E-06	SC_15_10	1.34E-06
SC_3_11	1.36E-06	SC_7_11	1.36E-06	SC_11_11	1.36E-06	SC_15_11	1.36E-06
SC_3_12	1.38E-06	SC_7_12	1.38E-06	SC_11_12	1.38E-06	SC_15_12	1.38E-06
SC_3_13	1.40E-06	SC_7_13	1.40E-06	SC_11_13	1.40E-06	SC_15_13	1.40E-06
SC_3_14	1.42E-06	SC_7_14	1.42E-06	SC_11_14	1.42E-06	SC_15_14	1.42E-06
SC_3_15	1.44E-06	SC_7_15	1.44E-06	SC_11_15	1.44E-06	SC_15_15	1.44E-06
SC_3_16	1.46E-06	SC_7_16	1.46E-06	SC_11_16	1.46E-06	SC_15_16	1.46E-06
SC_3_17	1.48E-06	SC_7_17	1.48E-06	SC_11_17	1.48E-06	SC_15_17	1.48E-06
SC_3_18	1.50E-06	SC_7_18	1.50E-06	SC_11_18	1.50E-06	SC_15_18	1.50E-06
SC_3_19	1.52E-06	SC_7_19	1.52E-06	SC_11_19	1.52E-06	SC_15_19	1.52E-06
SC_3_20	1.54E-06	SC_7_20	1.54E-06	SC_11_20	1.54E-06	SC_15_20	1.54E-06
SC_3_21	1.56E-06	SC_7_21	1.56E-06	SC_11_21	1.56E-06	SC_15_21	1.56E-06
SC_3_22	1.58E-06	SC_7_22	1.58E-06	SC_11_22	1.58E-06	SC_15_22	1.58E-06
SC_3_23	1.60E-06	SC_7_23	1.60E-06	SC_11_23	1.60E-06	SC_15_23	1.60E-06
SC_3_24	1.62E-06	SC_7_24	1.62E-06	SC_11_24	1.62E-06	SC_15_24	1.62E-06
SC_3_25	1.76E-06	SC_7_25	1.76E-06	SC_11_25	1.76E-06	SC_15_25	1.76E-06
SC_3_26	1.78E-06	SC_7_26	1.78E-06	SC_11_26	1.78E-06	SC_15_26	1.78E-06
SC_3_27	1.80E-06	SC_7_27	1.80E-06	SC_11_27	1.80E-06	SC_15_27	1.80E-06
SC_4_1	1.16E-06	SC_8_1	1.16E-06	SC_12_1	1.16E-06	SC_16_1	1.16E-06
SC_4_2	1.18E-06	SC_8_2	1.18E-06	SC_12_2	1.18E-06	SC_16_2	1.18E-06
SC_4_3	1.20E-06	SC_8_3	1.20E-06	SC_12_3	1.20E-06	SC_16_3	1.20E-06
SC_4_4	1.22E-06	SC_8_4	1.22E-06	SC_12_4	1.22E-06	SC_16_4	1.22E-06
SC_4_5	1.24E-06	SC_8_5	1.24E-06	SC_12_5	1.24E-06	SC_16_5	1.24E-06
SC_4_6	1.26E-06	SC_8_6	1.26E-06	SC_12_6	1.26E-06	SC_16_6	1.26E-06
SC_4_7	1.28E-06	SC_8_7	1.28E-06	SC_12_7	1.28E-06	SC_16_7	1.28E-06
SC_4_8	1.30E-06	SC_8_8	1.30E-06	SC_12_8	1.30E-06	SC_16_8	1.30E-06
SC_4_9	1.32E-06	SC_8_9	1.32E-06	SC_12_9	1.32E-06	SC_16_9	1.32E-06
SC_4_10	1.34E-06	SC_8_10	1.34E-06	SC_12_10	1.34E-06	SC_16_10	1.34E-06
SC_4_11	1.36E-06	SC_8_11	1.36E-06	SC_12_11	1.36E-06	SC_16_11	1.36E-06
SC_4_12	1.38E-06	SC_8_12	1.38E-06	SC_12_12	1.38E-06	SC_16_12	1.38E-06
SC_4_13	1.40E-06	SC_8_13	1.40E-06	SC_12_13	1.40E-06	SC_16_13	1.40E-06
SC_4_14	1.42E-06	SC_8_14	1.42E-06	SC_12_14	1.42E-06	SC_16_14	1.42E-06
SC_4_15	1.44E-06	SC_8_15	1.44E-06	SC_12_15	1.44E-06	SC_16_15	1.44E-06
SC_4_16	1.46E-06	SC_8_16	1.46E-06	SC_12_16	1.46E-06	SC_16_16	1.46E-06
SC_4_17	1.48E-06	SC_8_17	1.48E-06	SC_12_17	1.48E-06	SC_16_17	1.48E-06
SC_4_18	1.50E-06	SC_8_18	1.50E-06	SC_12_18	1.50E-06	SC_16_18	1.50E-06
SC_4_19	1.52E-06	SC_8_19	1.52E-06	SC_12_19	1.52E-06	SC_16_19	1.52E-06
SC_4_20	1.54E-06	SC_8_20	1.54E-06	SC_12_20	1.54E-06	SC_16_20	1.54E-06
SC_4_21	1.56E-06	SC_8_21	1.56E-06	SC_12_21	1.56E-06	SC_16_21	1.56E-06
SC_4_22	1.58E-06	SC_8_22	1.58E-06	SC_12_22	1.58E-06	SC_16_22	1.58E-06
SC_4_23	1.60E-06	SC_8_23	1.60E-06	SC_12_23	1.60E-06	SC_16_23	1.60E-06
SC_4_24	1.62E-06	SC_8_24	1.62E-06	SC_12_24	1.62E-06	SC_16_24	1.62E-06
SC_4_25	1.76E-06	SC_8_25	1.76E-06	SC_12_25	1.76E-06	SC_16_25	1.76E-06
SC_4_26	1.78E-06	SC_8_26	1.78E-06	SC_12_26	1.78E-06	SC_16_26	1.78E-06
SC_4_27	1.80E-06	SC_8_27	1.80E-06	SC_12_27	1.80E-06	SC_16_27	1.80E-06

Tab. A.3-13 Cumulative inductances for each conductor of PF 6 coil at 28.7 kHz (H)

SC_1_1	1.15E-06	SC_5_1	1.15E-06	SC_9_1	1.15E-06	SC_13_1	1.15E-06
SC_1_2	1.17E-06	SC_5_2	1.17E-06	SC_9_2	1.17E-06	SC_13_2	1.17E-06
SC_1_3	1.19E-06	SC_5_3	1.19E-06	SC_9_3	1.19E-06	SC_13_3	1.19E-06
SC_1_4	1.21E-06	SC_5_4	1.21E-06	SC_9_4	1.21E-06	SC_13_4	1.21E-06
SC_1_5	1.23E-06	SC_5_5	1.23E-06	SC_9_5	1.23E-06	SC_13_5	1.23E-06
SC_1_6	1.25E-06	SC_5_6	1.25E-06	SC_9_6	1.25E-06	SC_13_6	1.25E-06
SC_1_7	1.27E-06	SC_5_7	1.27E-06	SC_9_7	1.27E-06	SC_13_7	1.27E-06
SC_1_8	1.29E-06	SC_5_8	1.29E-06	SC_9_8	1.29E-06	SC_13_8	1.29E-06
SC_1_9	1.31E-06	SC_5_9	1.31E-06	SC_9_9	1.31E-06	SC_13_9	1.31E-06
SC_1_10	1.33E-06	SC_5_10	1.33E-06	SC_9_10	1.33E-06	SC_13_10	1.33E-06
SC_1_11	1.35E-06	SC_5_11	1.35E-06	SC_9_11	1.35E-06	SC_13_11	1.35E-06
SC_1_12	1.37E-06	SC_5_12	1.37E-06	SC_9_12	1.37E-06	SC_13_12	1.37E-06
SC_1_13	1.39E-06	SC_5_13	1.39E-06	SC_9_13	1.39E-06	SC_13_13	1.39E-06
SC_1_14	1.41E-06	SC_5_14	1.41E-06	SC_9_14	1.41E-06	SC_13_14	1.41E-06
SC_1_15	1.43E-06	SC_5_15	1.43E-06	SC_9_15	1.43E-06	SC_13_15	1.43E-06
SC_1_16	1.45E-06	SC_5_16	1.45E-06	SC_9_16	1.45E-06	SC_13_16	1.45E-06
SC_1_17	1.47E-06	SC_5_17	1.47E-06	SC_9_17	1.47E-06	SC_13_17	1.47E-06
SC_1_18	1.49E-06	SC_5_18	1.49E-06	SC_9_18	1.49E-06	SC_13_18	1.49E-06
SC_1_19	1.51E-06	SC_5_19	1.51E-06	SC_9_19	1.51E-06	SC_13_19	1.51E-06
SC_1_20	1.53E-06	SC_5_20	1.53E-06	SC_9_20	1.53E-06	SC_13_20	1.53E-06
SC_1_21	1.55E-06	SC_5_21	1.55E-06	SC_9_21	1.55E-06	SC_13_21	1.55E-06
SC_1_22	1.57E-06	SC_5_22	1.57E-06	SC_9_22	1.57E-06	SC_13_22	1.57E-06
SC_1_23	1.59E-06	SC_5_23	1.59E-06	SC_9_23	1.59E-06	SC_13_23	1.59E-06
SC_1_24	1.61E-06	SC_5_24	1.61E-06	SC_9_24	1.61E-06	SC_13_24	1.61E-06
SC_1_25	1.74E-06	SC_5_25	1.74E-06	SC_9_25	1.74E-06	SC_13_25	1.74E-06
SC_1_26	1.76E-06	SC_5_26	1.76E-06	SC_9_26	1.76E-06	SC_13_26	1.76E-06
SC_1_27	1.78E-06	SC_5_27	1.78E-06	SC_9_27	1.78E-06	SC_13_27	1.78E-06
SC_2_1	1.15E-06	SC_6_1	1.15E-06	SC_10_1	1.15E-06	SC_14_1	1.15E-06
SC_2_2	1.17E-06	SC_6_2	1.17E-06	SC_10_2	1.17E-06	SC_14_2	1.17E-06
SC_2_3	1.19E-06	SC_6_3	1.19E-06	SC_10_3	1.19E-06	SC_14_3	1.19E-06
SC_2_4	1.21E-06	SC_6_4	1.21E-06	SC_10_4	1.21E-06	SC_14_4	1.21E-06
SC_2_5	1.23E-06	SC_6_5	1.23E-06	SC_10_5	1.23E-06	SC_14_5	1.23E-06
SC_2_6	1.25E-06	SC_6_6	1.25E-06	SC_10_6	1.25E-06	SC_14_6	1.25E-06
SC_2_7	1.27E-06	SC_6_7	1.27E-06	SC_10_7	1.27E-06	SC_14_7	1.27E-06
SC_2_8	1.29E-06	SC_6_8	1.29E-06	SC_10_8	1.29E-06	SC_14_8	1.29E-06
SC_2_9	1.31E-06	SC_6_9	1.31E-06	SC_10_9	1.31E-06	SC_14_9	1.31E-06
SC_2_10	1.33E-06	SC_6_10	1.33E-06	SC_10_10	1.33E-06	SC_14_10	1.33E-06
SC_2_11	1.35E-06	SC_6_11	1.35E-06	SC_10_11	1.35E-06	SC_14_11	1.35E-06
SC_2_12	1.37E-06	SC_6_12	1.37E-06	SC_10_12	1.37E-06	SC_14_12	1.37E-06
SC_2_13	1.39E-06	SC_6_13	1.39E-06	SC_10_13	1.39E-06	SC_14_13	1.39E-06
SC_2_14	1.41E-06	SC_6_14	1.41E-06	SC_10_14	1.41E-06	SC_14_14	1.41E-06
SC_2_15	1.43E-06	SC_6_15	1.43E-06	SC_10_15	1.43E-06	SC_14_15	1.43E-06
SC_2_16	1.45E-06	SC_6_16	1.45E-06	SC_10_16	1.45E-06	SC_14_16	1.45E-06
SC_2_17	1.47E-06	SC_6_17	1.47E-06	SC_10_17	1.47E-06	SC_14_17	1.47E-06
SC_2_18	1.49E-06	SC_6_18	1.49E-06	SC_10_18	1.49E-06	SC_14_18	1.49E-06
SC_2_19	1.51E-06	SC_6_19	1.51E-06	SC_10_19	1.51E-06	SC_14_19	1.51E-06
SC_2_20	1.53E-06	SC_6_20	1.53E-06	SC_10_20	1.53E-06	SC_14_20	1.53E-06
SC_2_21	1.55E-06	SC_6_21	1.55E-06	SC_10_21	1.55E-06	SC_14_21	1.55E-06
SC_2_22	1.57E-06	SC_6_22	1.57E-06	SC_10_22	1.57E-06	SC_14_22	1.57E-06
SC_2_23	1.59E-06	SC_6_23	1.59E-06	SC_10_23	1.59E-06	SC_14_23	1.59E-06
SC_2_24	1.61E-06	SC_6_24	1.61E-06	SC_10_24	1.61E-06	SC_14_24	1.61E-06
SC_2_25	1.74E-06	SC_6_25	1.74E-06	SC_10_25	1.74E-06	SC_14_25	1.74E-06
SC_2_26	1.76E-06	SC_6_26	1.76E-06	SC_10_26	1.76E-06	SC_14_26	1.76E-06
SC_2_27	1.78E-06	SC_6_27	1.78E-06	SC_10_27	1.78E-06	SC_14_27	1.78E-06
SC_3_1	1.15E-06	SC_7_1	1.15E-06	SC_11_1	1.15E-06	SC_15_1	1.15E-06

SC_3_2	1.17E-06	SC_7_2	1.17E-06	SC_11_2	1.17E-06	SC_15_2	1.17E-06
SC_3_3	1.19E-06	SC_7_3	1.19E-06	SC_11_3	1.19E-06	SC_15_3	1.19E-06
SC_3_4	1.21E-06	SC_7_4	1.21E-06	SC_11_4	1.21E-06	SC_15_4	1.21E-06
SC_3_5	1.23E-06	SC_7_5	1.23E-06	SC_11_5	1.23E-06	SC_15_5	1.23E-06
SC_3_6	1.25E-06	SC_7_6	1.25E-06	SC_11_6	1.25E-06	SC_15_6	1.25E-06
SC_3_7	1.27E-06	SC_7_7	1.27E-06	SC_11_7	1.27E-06	SC_15_7	1.27E-06
SC_3_8	1.29E-06	SC_7_8	1.29E-06	SC_11_8	1.29E-06	SC_15_8	1.29E-06
SC_3_9	1.31E-06	SC_7_9	1.31E-06	SC_11_9	1.31E-06	SC_15_9	1.31E-06
SC_3_10	1.33E-06	SC_7_10	1.33E-06	SC_11_10	1.33E-06	SC_15_10	1.33E-06
SC_3_11	1.35E-06	SC_7_11	1.35E-06	SC_11_11	1.35E-06	SC_15_11	1.35E-06
SC_3_12	1.37E-06	SC_7_12	1.37E-06	SC_11_12	1.37E-06	SC_15_12	1.37E-06
SC_3_13	1.39E-06	SC_7_13	1.39E-06	SC_11_13	1.39E-06	SC_15_13	1.39E-06
SC_3_14	1.41E-06	SC_7_14	1.41E-06	SC_11_14	1.41E-06	SC_15_14	1.41E-06
SC_3_15	1.43E-06	SC_7_15	1.43E-06	SC_11_15	1.43E-06	SC_15_15	1.43E-06
SC_3_16	1.45E-06	SC_7_16	1.45E-06	SC_11_16	1.45E-06	SC_15_16	1.45E-06
SC_3_17	1.47E-06	SC_7_17	1.47E-06	SC_11_17	1.47E-06	SC_15_17	1.47E-06
SC_3_18	1.49E-06	SC_7_18	1.49E-06	SC_11_18	1.49E-06	SC_15_18	1.49E-06
SC_3_19	1.51E-06	SC_7_19	1.51E-06	SC_11_19	1.51E-06	SC_15_19	1.51E-06
SC_3_20	1.53E-06	SC_7_20	1.53E-06	SC_11_20	1.53E-06	SC_15_20	1.53E-06
SC_3_21	1.55E-06	SC_7_21	1.55E-06	SC_11_21	1.55E-06	SC_15_21	1.55E-06
SC_3_22	1.57E-06	SC_7_22	1.57E-06	SC_11_22	1.57E-06	SC_15_22	1.57E-06
SC_3_23	1.59E-06	SC_7_23	1.59E-06	SC_11_23	1.59E-06	SC_15_23	1.59E-06
SC_3_24	1.61E-06	SC_7_24	1.61E-06	SC_11_24	1.61E-06	SC_15_24	1.61E-06
SC_3_25	1.74E-06	SC_7_25	1.74E-06	SC_11_25	1.74E-06	SC_15_25	1.74E-06
SC_3_26	1.76E-06	SC_7_26	1.76E-06	SC_11_26	1.76E-06	SC_15_26	1.76E-06
SC_3_27	1.78E-06	SC_7_27	1.78E-06	SC_11_27	1.78E-06	SC_15_27	1.78E-06
SC_4_1	1.15E-06	SC_8_1	1.15E-06	SC_12_1	1.15E-06	SC_16_1	1.15E-06
SC_4_2	1.17E-06	SC_8_2	1.17E-06	SC_12_2	1.17E-06	SC_16_2	1.17E-06
SC_4_3	1.19E-06	SC_8_3	1.19E-06	SC_12_3	1.19E-06	SC_16_3	1.19E-06
SC_4_4	1.21E-06	SC_8_4	1.21E-06	SC_12_4	1.21E-06	SC_16_4	1.21E-06
SC_4_5	1.23E-06	SC_8_5	1.23E-06	SC_12_5	1.23E-06	SC_16_5	1.23E-06
SC_4_6	1.25E-06	SC_8_6	1.25E-06	SC_12_6	1.25E-06	SC_16_6	1.25E-06
SC_4_7	1.27E-06	SC_8_7	1.27E-06	SC_12_7	1.27E-06	SC_16_7	1.27E-06
SC_4_8	1.29E-06	SC_8_8	1.29E-06	SC_12_8	1.29E-06	SC_16_8	1.29E-06
SC_4_9	1.31E-06	SC_8_9	1.31E-06	SC_12_9	1.31E-06	SC_16_9	1.31E-06
SC_4_10	1.33E-06	SC_8_10	1.33E-06	SC_12_10	1.33E-06	SC_16_10	1.33E-06
SC_4_11	1.35E-06	SC_8_11	1.35E-06	SC_12_11	1.35E-06	SC_16_11	1.35E-06
SC_4_12	1.37E-06	SC_8_12	1.37E-06	SC_12_12	1.37E-06	SC_16_12	1.37E-06
SC_4_13	1.39E-06	SC_8_13	1.39E-06	SC_12_13	1.39E-06	SC_16_13	1.39E-06
SC_4_14	1.41E-06	SC_8_14	1.41E-06	SC_12_14	1.41E-06	SC_16_14	1.41E-06
SC_4_15	1.43E-06	SC_8_15	1.43E-06	SC_12_15	1.43E-06	SC_16_15	1.43E-06
SC_4_16	1.45E-06	SC_8_16	1.45E-06	SC_12_16	1.45E-06	SC_16_16	1.45E-06
SC_4_17	1.47E-06	SC_8_17	1.47E-06	SC_12_17	1.47E-06	SC_16_17	1.47E-06
SC_4_18	1.49E-06	SC_8_18	1.49E-06	SC_12_18	1.49E-06	SC_16_18	1.49E-06
SC_4_19	1.51E-06	SC_8_19	1.51E-06	SC_12_19	1.51E-06	SC_16_19	1.51E-06
SC_4_20	1.53E-06	SC_8_20	1.53E-06	SC_12_20	1.53E-06	SC_16_20	1.53E-06
SC_4_21	1.55E-06	SC_8_21	1.55E-06	SC_12_21	1.55E-06	SC_16_21	1.55E-06
SC_4_22	1.57E-06	SC_8_22	1.57E-06	SC_12_22	1.57E-06	SC_16_22	1.57E-06
SC_4_23	1.59E-06	SC_8_23	1.59E-06	SC_12_23	1.59E-06	SC_16_23	1.59E-06
SC_4_24	1.61E-06	SC_8_24	1.61E-06	SC_12_24	1.61E-06	SC_16_24	1.61E-06
SC_4_25	1.74E-06	SC_8_25	1.74E-06	SC_12_25	1.74E-06	SC_16_25	1.74E-06
SC_4_26	1.76E-06	SC_8_26	1.76E-06	SC_12_26	1.76E-06	SC_16_26	1.76E-06
SC_4_27	1.78E-06	SC_8_27	1.78E-06	SC_12_27	1.78E-06	SC_16_27	1.78E-06

Tab. A.3-14 Cumulative inductances for each conductor of PF 6 coil at 30.8 kHz (H)

SC_1_1	1.00E-06	SC_5_1	1.00E-06	SC_9_1	1.00E-06	SC_13_1	1.00E-06
SC_1_2	1.02E-06	SC_5_2	1.02E-06	SC_9_2	1.02E-06	SC_13_2	1.02E-06
SC_1_3	1.04E-06	SC_5_3	1.04E-06	SC_9_3	1.04E-06	SC_13_3	1.04E-06
SC_1_4	1.06E-06	SC_5_4	1.06E-06	SC_9_4	1.06E-06	SC_13_4	1.06E-06
SC_1_5	1.07E-06	SC_5_5	1.07E-06	SC_9_5	1.07E-06	SC_13_5	1.07E-06
SC_1_6	1.09E-06	SC_5_6	1.09E-06	SC_9_6	1.09E-06	SC_13_6	1.09E-06
SC_1_7	1.11E-06	SC_5_7	1.11E-06	SC_9_7	1.11E-06	SC_13_7	1.11E-06
SC_1_8	1.13E-06	SC_5_8	1.13E-06	SC_9_8	1.13E-06	SC_13_8	1.13E-06
SC_1_9	1.14E-06	SC_5_9	1.14E-06	SC_9_9	1.14E-06	SC_13_9	1.14E-06
SC_1_10	1.16E-06	SC_5_10	1.16E-06	SC_9_10	1.16E-06	SC_13_10	1.16E-06
SC_1_11	1.18E-06	SC_5_11	1.18E-06	SC_9_11	1.18E-06	SC_13_11	1.18E-06
SC_1_12	1.20E-06	SC_5_12	1.20E-06	SC_9_12	1.20E-06	SC_13_12	1.20E-06
SC_1_13	1.21E-06	SC_5_13	1.21E-06	SC_9_13	1.21E-06	SC_13_13	1.21E-06
SC_1_14	1.23E-06	SC_5_14	1.23E-06	SC_9_14	1.23E-06	SC_13_14	1.23E-06
SC_1_15	1.25E-06	SC_5_15	1.25E-06	SC_9_15	1.25E-06	SC_13_15	1.25E-06
SC_1_16	1.27E-06	SC_5_16	1.27E-06	SC_9_16	1.27E-06	SC_13_16	1.27E-06
SC_1_17	1.28E-06	SC_5_17	1.28E-06	SC_9_17	1.28E-06	SC_13_17	1.28E-06
SC_1_18	1.30E-06	SC_5_18	1.30E-06	SC_9_18	1.30E-06	SC_13_18	1.30E-06
SC_1_19	1.32E-06	SC_5_19	1.32E-06	SC_9_19	1.32E-06	SC_13_19	1.32E-06
SC_1_20	1.34E-06	SC_5_20	1.34E-06	SC_9_20	1.34E-06	SC_13_20	1.34E-06
SC_1_21	1.35E-06	SC_5_21	1.35E-06	SC_9_21	1.35E-06	SC_13_21	1.35E-06
SC_1_22	1.37E-06	SC_5_22	1.37E-06	SC_9_22	1.37E-06	SC_13_22	1.37E-06
SC_1_23	1.39E-06	SC_5_23	1.39E-06	SC_9_23	1.39E-06	SC_13_23	1.39E-06
SC_1_24	1.41E-06	SC_5_24	1.41E-06	SC_9_24	1.41E-06	SC_13_24	1.41E-06
SC_1_25	1.47E-06	SC_5_25	1.47E-06	SC_9_25	1.47E-06	SC_13_25	1.47E-06
SC_1_26	1.49E-06	SC_5_26	1.49E-06	SC_9_26	1.49E-06	SC_13_26	1.49E-06
SC_1_27	1.50E-06	SC_5_27	1.50E-06	SC_9_27	1.50E-06	SC_13_27	1.50E-06
SC_2_1	1.00E-06	SC_6_1	1.00E-06	SC_10_1	1.00E-06	SC_14_1	1.00E-06
SC_2_2	1.02E-06	SC_6_2	1.02E-06	SC_10_2	1.02E-06	SC_14_2	1.02E-06
SC_2_3	1.04E-06	SC_6_3	1.04E-06	SC_10_3	1.04E-06	SC_14_3	1.04E-06
SC_2_4	1.06E-06	SC_6_4	1.06E-06	SC_10_4	1.06E-06	SC_14_4	1.06E-06
SC_2_5	1.07E-06	SC_6_5	1.07E-06	SC_10_5	1.07E-06	SC_14_5	1.07E-06
SC_2_6	1.09E-06	SC_6_6	1.09E-06	SC_10_6	1.09E-06	SC_14_6	1.09E-06
SC_2_7	1.11E-06	SC_6_7	1.11E-06	SC_10_7	1.11E-06	SC_14_7	1.11E-06
SC_2_8	1.13E-06	SC_6_8	1.13E-06	SC_10_8	1.13E-06	SC_14_8	1.13E-06
SC_2_9	1.14E-06	SC_6_9	1.14E-06	SC_10_9	1.14E-06	SC_14_9	1.14E-06
SC_2_10	1.16E-06	SC_6_10	1.16E-06	SC_10_10	1.16E-06	SC_14_10	1.16E-06
SC_2_11	1.18E-06	SC_6_11	1.18E-06	SC_10_11	1.18E-06	SC_14_11	1.18E-06
SC_2_12	1.20E-06	SC_6_12	1.20E-06	SC_10_12	1.20E-06	SC_14_12	1.20E-06
SC_2_13	1.21E-06	SC_6_13	1.21E-06	SC_10_13	1.21E-06	SC_14_13	1.21E-06
SC_2_14	1.23E-06	SC_6_14	1.23E-06	SC_10_14	1.23E-06	SC_14_14	1.23E-06
SC_2_15	1.25E-06	SC_6_15	1.25E-06	SC_10_15	1.25E-06	SC_14_15	1.25E-06
SC_2_16	1.27E-06	SC_6_16	1.27E-06	SC_10_16	1.27E-06	SC_14_16	1.27E-06
SC_2_17	1.28E-06	SC_6_17	1.28E-06	SC_10_17	1.28E-06	SC_14_17	1.28E-06
SC_2_18	1.30E-06	SC_6_18	1.30E-06	SC_10_18	1.30E-06	SC_14_18	1.30E-06
SC_2_19	1.32E-06	SC_6_19	1.32E-06	SC_10_19	1.32E-06	SC_14_19	1.32E-06
SC_2_20	1.34E-06	SC_6_20	1.34E-06	SC_10_20	1.34E-06	SC_14_20	1.34E-06
SC_2_21	1.35E-06	SC_6_21	1.35E-06	SC_10_21	1.35E-06	SC_14_21	1.35E-06
SC_2_22	1.37E-06	SC_6_22	1.37E-06	SC_10_22	1.37E-06	SC_14_22	1.37E-06
SC_2_23	1.39E-06	SC_6_23	1.39E-06	SC_10_23	1.39E-06	SC_14_23	1.39E-06
SC_2_24	1.41E-06	SC_6_24	1.41E-06	SC_10_24	1.41E-06	SC_14_24	1.41E-06
SC_2_25	1.47E-06	SC_6_25	1.47E-06	SC_10_25	1.47E-06	SC_14_25	1.47E-06
SC_2_26	1.49E-06	SC_6_26	1.49E-06	SC_10_26	1.49E-06	SC_14_26	1.49E-06
SC_2_27	1.50E-06	SC_6_27	1.50E-06	SC_10_27	1.50E-06	SC_14_27	1.50E-06
SC_3_1	1.00E-06	SC_7_1	1.00E-06	SC_11_1	1.00E-06	SC_15_1	1.00E-06

SC_3_2	1.02E-06	SC_7_2	1.02E-06	SC_11_2	1.02E-06	SC_15_2	1.02E-06
SC_3_3	1.04E-06	SC_7_3	1.04E-06	SC_11_3	1.04E-06	SC_15_3	1.04E-06
SC_3_4	1.06E-06	SC_7_4	1.06E-06	SC_11_4	1.06E-06	SC_15_4	1.06E-06
SC_3_5	1.07E-06	SC_7_5	1.07E-06	SC_11_5	1.07E-06	SC_15_5	1.07E-06
SC_3_6	1.09E-06	SC_7_6	1.09E-06	SC_11_6	1.09E-06	SC_15_6	1.09E-06
SC_3_7	1.11E-06	SC_7_7	1.11E-06	SC_11_7	1.11E-06	SC_15_7	1.11E-06
SC_3_8	1.13E-06	SC_7_8	1.13E-06	SC_11_8	1.13E-06	SC_15_8	1.13E-06
SC_3_9	1.14E-06	SC_7_9	1.14E-06	SC_11_9	1.14E-06	SC_15_9	1.14E-06
SC_3_10	1.16E-06	SC_7_10	1.16E-06	SC_11_10	1.16E-06	SC_15_10	1.16E-06
SC_3_11	1.18E-06	SC_7_11	1.18E-06	SC_11_11	1.18E-06	SC_15_11	1.18E-06
SC_3_12	1.20E-06	SC_7_12	1.20E-06	SC_11_12	1.20E-06	SC_15_12	1.20E-06
SC_3_13	1.21E-06	SC_7_13	1.21E-06	SC_11_13	1.21E-06	SC_15_13	1.21E-06
SC_3_14	1.23E-06	SC_7_14	1.23E-06	SC_11_14	1.23E-06	SC_15_14	1.23E-06
SC_3_15	1.25E-06	SC_7_15	1.25E-06	SC_11_15	1.25E-06	SC_15_15	1.25E-06
SC_3_16	1.27E-06	SC_7_16	1.27E-06	SC_11_16	1.27E-06	SC_15_16	1.27E-06
SC_3_17	1.28E-06	SC_7_17	1.28E-06	SC_11_17	1.28E-06	SC_15_17	1.28E-06
SC_3_18	1.30E-06	SC_7_18	1.30E-06	SC_11_18	1.30E-06	SC_15_18	1.30E-06
SC_3_19	1.32E-06	SC_7_19	1.32E-06	SC_11_19	1.32E-06	SC_15_19	1.32E-06
SC_3_20	1.34E-06	SC_7_20	1.34E-06	SC_11_20	1.34E-06	SC_15_20	1.34E-06
SC_3_21	1.35E-06	SC_7_21	1.35E-06	SC_11_21	1.35E-06	SC_15_21	1.35E-06
SC_3_22	1.37E-06	SC_7_22	1.37E-06	SC_11_22	1.37E-06	SC_15_22	1.37E-06
SC_3_23	1.39E-06	SC_7_23	1.39E-06	SC_11_23	1.39E-06	SC_15_23	1.39E-06
SC_3_24	1.41E-06	SC_7_24	1.41E-06	SC_11_24	1.41E-06	SC_15_24	1.41E-06
SC_3_25	1.47E-06	SC_7_25	1.47E-06	SC_11_25	1.47E-06	SC_15_25	1.47E-06
SC_3_26	1.49E-06	SC_7_26	1.49E-06	SC_11_26	1.49E-06	SC_15_26	1.49E-06
SC_3_27	1.50E-06	SC_7_27	1.50E-06	SC_11_27	1.50E-06	SC_15_27	1.50E-06
SC_4_1	1.00E-06	SC_8_1	1.00E-06	SC_12_1	1.00E-06	SC_16_1	1.00E-06
SC_4_2	1.02E-06	SC_8_2	1.02E-06	SC_12_2	1.02E-06	SC_16_2	1.02E-06
SC_4_3	1.04E-06	SC_8_3	1.04E-06	SC_12_3	1.04E-06	SC_16_3	1.04E-06
SC_4_4	1.06E-06	SC_8_4	1.06E-06	SC_12_4	1.06E-06	SC_16_4	1.06E-06
SC_4_5	1.07E-06	SC_8_5	1.07E-06	SC_12_5	1.07E-06	SC_16_5	1.07E-06
SC_4_6	1.09E-06	SC_8_6	1.09E-06	SC_12_6	1.09E-06	SC_16_6	1.09E-06
SC_4_7	1.11E-06	SC_8_7	1.11E-06	SC_12_7	1.11E-06	SC_16_7	1.11E-06
SC_4_8	1.13E-06	SC_8_8	1.13E-06	SC_12_8	1.13E-06	SC_16_8	1.13E-06
SC_4_9	1.14E-06	SC_8_9	1.14E-06	SC_12_9	1.14E-06	SC_16_9	1.14E-06
SC_4_10	1.16E-06	SC_8_10	1.16E-06	SC_12_10	1.16E-06	SC_16_10	1.16E-06
SC_4_11	1.18E-06	SC_8_11	1.18E-06	SC_12_11	1.18E-06	SC_16_11	1.18E-06
SC_4_12	1.20E-06	SC_8_12	1.20E-06	SC_12_12	1.20E-06	SC_16_12	1.20E-06
SC_4_13	1.21E-06	SC_8_13	1.21E-06	SC_12_13	1.21E-06	SC_16_13	1.21E-06
SC_4_14	1.23E-06	SC_8_14	1.23E-06	SC_12_14	1.23E-06	SC_16_14	1.23E-06
SC_4_15	1.25E-06	SC_8_15	1.25E-06	SC_12_15	1.25E-06	SC_16_15	1.25E-06
SC_4_16	1.27E-06	SC_8_16	1.27E-06	SC_12_16	1.27E-06	SC_16_16	1.27E-06
SC_4_17	1.28E-06	SC_8_17	1.28E-06	SC_12_17	1.28E-06	SC_16_17	1.28E-06
SC_4_18	1.30E-06	SC_8_18	1.30E-06	SC_12_18	1.30E-06	SC_16_18	1.30E-06
SC_4_19	1.32E-06	SC_8_19	1.32E-06	SC_12_19	1.32E-06	SC_16_19	1.32E-06
SC_4_20	1.34E-06	SC_8_20	1.34E-06	SC_12_20	1.34E-06	SC_16_20	1.34E-06
SC_4_21	1.35E-06	SC_8_21	1.35E-06	SC_12_21	1.35E-06	SC_16_21	1.35E-06
SC_4_22	1.37E-06	SC_8_22	1.37E-06	SC_12_22	1.37E-06	SC_16_22	1.37E-06
SC_4_23	1.39E-06	SC_8_23	1.39E-06	SC_12_23	1.39E-06	SC_16_23	1.39E-06
SC_4_24	1.41E-06	SC_8_24	1.41E-06	SC_12_24	1.41E-06	SC_16_24	1.41E-06
SC_4_25	1.47E-06	SC_8_25	1.47E-06	SC_12_25	1.47E-06	SC_16_25	1.47E-06
SC_4_26	1.49E-06	SC_8_26	1.49E-06	SC_12_26	1.49E-06	SC_16_26	1.49E-06
SC_4_27	1.50E-06	SC_8_27	1.50E-06	SC_12_27	1.50E-06	SC_16_27	1.50E-06

Tab. A.3-15 Cumulative inductances for each conductor of PF 6 coil at 200 kHz (H)

SC_1_1	9.88E-07	SC_5_1	9.88E-07	SC_9_1	9.88E-07	SC_13_1	9.88E-07
SC_1_2	1.01E-06	SC_5_2	1.01E-06	SC_9_2	1.01E-06	SC_13_2	1.01E-06
SC_1_3	1.02E-06	SC_5_3	1.02E-06	SC_9_3	1.02E-06	SC_13_3	1.02E-06
SC_1_4	1.04E-06	SC_5_4	1.04E-06	SC_9_4	1.04E-06	SC_13_4	1.04E-06
SC_1_5	1.06E-06	SC_5_5	1.06E-06	SC_9_5	1.06E-06	SC_13_5	1.06E-06
SC_1_6	1.07E-06	SC_5_6	1.07E-06	SC_9_6	1.07E-06	SC_13_6	1.07E-06
SC_1_7	1.09E-06	SC_5_7	1.09E-06	SC_9_7	1.09E-06	SC_13_7	1.09E-06
SC_1_8	1.11E-06	SC_5_8	1.11E-06	SC_9_8	1.11E-06	SC_13_8	1.11E-06
SC_1_9	1.13E-06	SC_5_9	1.13E-06	SC_9_9	1.13E-06	SC_13_9	1.13E-06
SC_1_10	1.14E-06	SC_5_10	1.14E-06	SC_9_10	1.14E-06	SC_13_10	1.14E-06
SC_1_11	1.16E-06	SC_5_11	1.16E-06	SC_9_11	1.16E-06	SC_13_11	1.16E-06
SC_1_12	1.18E-06	SC_5_12	1.18E-06	SC_9_12	1.18E-06	SC_13_12	1.18E-06
SC_1_13	1.19E-06	SC_5_13	1.19E-06	SC_9_13	1.19E-06	SC_13_13	1.19E-06
SC_1_14	1.21E-06	SC_5_14	1.21E-06	SC_9_14	1.21E-06	SC_13_14	1.21E-06
SC_1_15	1.23E-06	SC_5_15	1.23E-06	SC_9_15	1.23E-06	SC_13_15	1.23E-06
SC_1_16	1.25E-06	SC_5_16	1.25E-06	SC_9_16	1.25E-06	SC_13_16	1.25E-06
SC_1_17	1.26E-06	SC_5_17	1.26E-06	SC_9_17	1.26E-06	SC_13_17	1.26E-06
SC_1_18	1.28E-06	SC_5_18	1.28E-06	SC_9_18	1.28E-06	SC_13_18	1.28E-06
SC_1_19	1.30E-06	SC_5_19	1.30E-06	SC_9_19	1.30E-06	SC_13_19	1.30E-06
SC_1_20	1.31E-06	SC_5_20	1.31E-06	SC_9_20	1.31E-06	SC_13_20	1.31E-06
SC_1_21	1.33E-06	SC_5_21	1.33E-06	SC_9_21	1.33E-06	SC_13_21	1.33E-06
SC_1_22	1.35E-06	SC_5_22	1.35E-06	SC_9_22	1.35E-06	SC_13_22	1.35E-06
SC_1_23	1.37E-06	SC_5_23	1.37E-06	SC_9_23	1.37E-06	SC_13_23	1.37E-06
SC_1_24	1.38E-06	SC_5_24	1.38E-06	SC_9_24	1.38E-06	SC_13_24	1.38E-06
SC_1_25	1.44E-06	SC_5_25	1.44E-06	SC_9_25	1.44E-06	SC_13_25	1.44E-06
SC_1_26	1.45E-06	SC_5_26	1.45E-06	SC_9_26	1.45E-06	SC_13_26	1.45E-06
SC_1_27	1.47E-06	SC_5_27	1.47E-06	SC_9_27	1.47E-06	SC_13_27	1.47E-06
SC_2_1	9.88E-07	SC_6_1	9.88E-07	SC_10_1	9.88E-07	SC_14_1	9.88E-07
SC_2_2	1.01E-06	SC_6_2	1.01E-06	SC_10_2	1.01E-06	SC_14_2	1.01E-06
SC_2_3	1.02E-06	SC_6_3	1.02E-06	SC_10_3	1.02E-06	SC_14_3	1.02E-06
SC_2_4	1.04E-06	SC_6_4	1.04E-06	SC_10_4	1.04E-06	SC_14_4	1.04E-06
SC_2_5	1.06E-06	SC_6_5	1.06E-06	SC_10_5	1.06E-06	SC_14_5	1.06E-06
SC_2_6	1.07E-06	SC_6_6	1.07E-06	SC_10_6	1.07E-06	SC_14_6	1.07E-06
SC_2_7	1.09E-06	SC_6_7	1.09E-06	SC_10_7	1.09E-06	SC_14_7	1.09E-06
SC_2_8	1.11E-06	SC_6_8	1.11E-06	SC_10_8	1.11E-06	SC_14_8	1.11E-06
SC_2_9	1.13E-06	SC_6_9	1.13E-06	SC_10_9	1.13E-06	SC_14_9	1.13E-06
SC_2_10	1.14E-06	SC_6_10	1.14E-06	SC_10_10	1.14E-06	SC_14_10	1.14E-06
SC_2_11	1.16E-06	SC_6_11	1.16E-06	SC_10_11	1.16E-06	SC_14_11	1.16E-06
SC_2_12	1.18E-06	SC_6_12	1.18E-06	SC_10_12	1.18E-06	SC_14_12	1.18E-06
SC_2_13	1.19E-06	SC_6_13	1.19E-06	SC_10_13	1.19E-06	SC_14_13	1.19E-06
SC_2_14	1.21E-06	SC_6_14	1.21E-06	SC_10_14	1.21E-06	SC_14_14	1.21E-06
SC_2_15	1.23E-06	SC_6_15	1.23E-06	SC_10_15	1.23E-06	SC_14_15	1.23E-06
SC_2_16	1.25E-06	SC_6_16	1.25E-06	SC_10_16	1.25E-06	SC_14_16	1.25E-06
SC_2_17	1.26E-06	SC_6_17	1.26E-06	SC_10_17	1.26E-06	SC_14_17	1.26E-06
SC_2_18	1.28E-06	SC_6_18	1.28E-06	SC_10_18	1.28E-06	SC_14_18	1.28E-06
SC_2_19	1.30E-06	SC_6_19	1.30E-06	SC_10_19	1.30E-06	SC_14_19	1.30E-06
SC_2_20	1.31E-06	SC_6_20	1.31E-06	SC_10_20	1.31E-06	SC_14_20	1.31E-06
SC_2_21	1.33E-06	SC_6_21	1.33E-06	SC_10_21	1.33E-06	SC_14_21	1.33E-06
SC_2_22	1.35E-06	SC_6_22	1.35E-06	SC_10_22	1.35E-06	SC_14_22	1.35E-06
SC_2_23	1.37E-06	SC_6_23	1.37E-06	SC_10_23	1.37E-06	SC_14_23	1.37E-06
SC_2_24	1.38E-06	SC_6_24	1.38E-06	SC_10_24	1.38E-06	SC_14_24	1.38E-06
SC_2_25	1.44E-06	SC_6_25	1.44E-06	SC_10_25	1.44E-06	SC_14_25	1.44E-06
SC_2_26	1.45E-06	SC_6_26	1.45E-06	SC_10_26	1.45E-06	SC_14_26	1.45E-06
SC_2_27	1.47E-06	SC_6_27	1.47E-06	SC_10_27	1.47E-06	SC_14_27	1.47E-06
SC_3_1	9.88E-07	SC_7_1	9.88E-07	SC_11_1	9.88E-07	SC_15_1	9.88E-07

SC_3_2	1.01E-06	SC_7_2	1.01E-06	SC_11_2	1.01E-06	SC_15_2	1.01E-06
SC_3_3	1.02E-06	SC_7_3	1.02E-06	SC_11_3	1.02E-06	SC_15_3	1.02E-06
SC_3_4	1.04E-06	SC_7_4	1.04E-06	SC_11_4	1.04E-06	SC_15_4	1.04E-06
SC_3_5	1.06E-06	SC_7_5	1.06E-06	SC_11_5	1.06E-06	SC_15_5	1.06E-06
SC_3_6	1.07E-06	SC_7_6	1.07E-06	SC_11_6	1.07E-06	SC_15_6	1.07E-06
SC_3_7	1.09E-06	SC_7_7	1.09E-06	SC_11_7	1.09E-06	SC_15_7	1.09E-06
SC_3_8	1.11E-06	SC_7_8	1.11E-06	SC_11_8	1.11E-06	SC_15_8	1.11E-06
SC_3_9	1.13E-06	SC_7_9	1.13E-06	SC_11_9	1.13E-06	SC_15_9	1.13E-06
SC_3_10	1.14E-06	SC_7_10	1.14E-06	SC_11_10	1.14E-06	SC_15_10	1.14E-06
SC_3_11	1.16E-06	SC_7_11	1.16E-06	SC_11_11	1.16E-06	SC_15_11	1.16E-06
SC_3_12	1.18E-06	SC_7_12	1.18E-06	SC_11_12	1.18E-06	SC_15_12	1.18E-06
SC_3_13	1.19E-06	SC_7_13	1.19E-06	SC_11_13	1.19E-06	SC_15_13	1.19E-06
SC_3_14	1.21E-06	SC_7_14	1.21E-06	SC_11_14	1.21E-06	SC_15_14	1.21E-06
SC_3_15	1.23E-06	SC_7_15	1.23E-06	SC_11_15	1.23E-06	SC_15_15	1.23E-06
SC_3_16	1.25E-06	SC_7_16	1.25E-06	SC_11_16	1.25E-06	SC_15_16	1.25E-06
SC_3_17	1.26E-06	SC_7_17	1.26E-06	SC_11_17	1.26E-06	SC_15_17	1.26E-06
SC_3_18	1.28E-06	SC_7_18	1.28E-06	SC_11_18	1.28E-06	SC_15_18	1.28E-06
SC_3_19	1.30E-06	SC_7_19	1.30E-06	SC_11_19	1.30E-06	SC_15_19	1.30E-06
SC_3_20	1.31E-06	SC_7_20	1.31E-06	SC_11_20	1.31E-06	SC_15_20	1.31E-06
SC_3_21	1.33E-06	SC_7_21	1.33E-06	SC_11_21	1.33E-06	SC_15_21	1.33E-06
SC_3_22	1.35E-06	SC_7_22	1.35E-06	SC_11_22	1.35E-06	SC_15_22	1.35E-06
SC_3_23	1.37E-06	SC_7_23	1.37E-06	SC_11_23	1.37E-06	SC_15_23	1.37E-06
SC_3_24	1.38E-06	SC_7_24	1.38E-06	SC_11_24	1.38E-06	SC_15_24	1.38E-06
SC_3_25	1.44E-06	SC_7_25	1.44E-06	SC_11_25	1.44E-06	SC_15_25	1.44E-06
SC_3_26	1.45E-06	SC_7_26	1.45E-06	SC_11_26	1.45E-06	SC_15_26	1.45E-06
SC_3_27	1.47E-06	SC_7_27	1.47E-06	SC_11_27	1.47E-06	SC_15_27	1.47E-06
SC_4_1	9.88E-07	SC_8_1	9.88E-07	SC_12_1	9.88E-07	SC_16_1	9.88E-07
SC_4_2	1.01E-06	SC_8_2	1.01E-06	SC_12_2	1.01E-06	SC_16_2	1.01E-06
SC_4_3	1.02E-06	SC_8_3	1.02E-06	SC_12_3	1.02E-06	SC_16_3	1.02E-06
SC_4_4	1.04E-06	SC_8_4	1.04E-06	SC_12_4	1.04E-06	SC_16_4	1.04E-06
SC_4_5	1.06E-06	SC_8_5	1.06E-06	SC_12_5	1.06E-06	SC_16_5	1.06E-06
SC_4_6	1.07E-06	SC_8_6	1.07E-06	SC_12_6	1.07E-06	SC_16_6	1.07E-06
SC_4_7	1.09E-06	SC_8_7	1.09E-06	SC_12_7	1.09E-06	SC_16_7	1.09E-06
SC_4_8	1.11E-06	SC_8_8	1.11E-06	SC_12_8	1.11E-06	SC_16_8	1.11E-06
SC_4_9	1.13E-06	SC_8_9	1.13E-06	SC_12_9	1.13E-06	SC_16_9	1.13E-06
SC_4_10	1.14E-06	SC_8_10	1.14E-06	SC_12_10	1.14E-06	SC_16_10	1.14E-06
SC_4_11	1.16E-06	SC_8_11	1.16E-06	SC_12_11	1.16E-06	SC_16_11	1.16E-06
SC_4_12	1.18E-06	SC_8_12	1.18E-06	SC_12_12	1.18E-06	SC_16_12	1.18E-06
SC_4_13	1.19E-06	SC_8_13	1.19E-06	SC_12_13	1.19E-06	SC_16_13	1.19E-06
SC_4_14	1.21E-06	SC_8_14	1.21E-06	SC_12_14	1.21E-06	SC_16_14	1.21E-06
SC_4_15	1.23E-06	SC_8_15	1.23E-06	SC_12_15	1.23E-06	SC_16_15	1.23E-06
SC_4_16	1.25E-06	SC_8_16	1.25E-06	SC_12_16	1.25E-06	SC_16_16	1.25E-06
SC_4_17	1.26E-06	SC_8_17	1.26E-06	SC_12_17	1.26E-06	SC_16_17	1.26E-06
SC_4_18	1.28E-06	SC_8_18	1.28E-06	SC_12_18	1.28E-06	SC_16_18	1.28E-06
SC_4_19	1.30E-06	SC_8_19	1.30E-06	SC_12_19	1.30E-06	SC_16_19	1.30E-06
SC_4_20	1.31E-06	SC_8_20	1.31E-06	SC_12_20	1.31E-06	SC_16_20	1.31E-06
SC_4_21	1.33E-06	SC_8_21	1.33E-06	SC_12_21	1.33E-06	SC_16_21	1.33E-06
SC_4_22	1.35E-06	SC_8_22	1.35E-06	SC_12_22	1.35E-06	SC_16_22	1.35E-06
SC_4_23	1.37E-06	SC_8_23	1.37E-06	SC_12_23	1.37E-06	SC_16_23	1.37E-06
SC_4_24	1.38E-06	SC_8_24	1.38E-06	SC_12_24	1.38E-06	SC_16_24	1.38E-06
SC_4_25	1.44E-06	SC_8_25	1.44E-06	SC_12_25	1.44E-06	SC_16_25	1.44E-06
SC_4_26	1.45E-06	SC_8_26	1.45E-06	SC_12_26	1.45E-06	SC_16_26	1.45E-06
SC_4_27	1.47E-06	SC_8_27	1.47E-06	SC_12_27	1.47E-06	SC_16_27	1.47E-06

Tab. A.3-16 Cumulative inductances for each conductor of PF 6 coil at 295 kHz (H)

Annex A.4 FEM Models of the Bus Bars for Power Supply

(a) FEM Model of the Superconducting Bus Bars

Model Definition

Solver: Eddy Current Symmetry: XY-Plane Frequency 0 Hz

Drawing Size: X-direction: ±100 mm; Y-direction: ±100 mm

Materials

Cooling tube Vacuum, relative permittivity = 1, relative permeability = 1

Superconducting cable Copper at 4K, relative permittivity = 1, relative permeability = 1, conductivity = 6.4E9 S/m

Stainless steel jacket Stainless steel at 4K, relative permittivity = 1, relative permeability = 1, conductivity = 1.88e6 S/m

Insulation Epoxy resin, relative permittivity = 4, relative permeability = 1

Background: Vacuum, relative permittivity = 1, relative permeability = 1

Setup Boundaries and Sources

Current Source Superconducting bus bar with 45 kA

Boundary Balloon

Setup Executive Parameters

Only superconducting bus bar was chosen into the impedance matrix.

Return path of the current was set to default.

Setup Solution Options

Mesh: Manual mesh

Object	Insulation	Cooling Tube	Superconducting cable	Stainless steel jacket	Background
Number of triangles	182	34	1294	73	291

(b) FEM Model of the Water Cooled Bus Bars

Model Definition

Solver: Eddy Current Symmetry: XY-Plane Frequency 0 Hz

Drawing Size: X-direction: ±400 mm; Y-direction: ±400 mm

Materials

Water cooling tube Vacuum, relative permittivity = 1, relative permeability = 1

Aluminium bus bar Aluminium, relative permittivity = 1, relative permeability = 1, conductivity = 3.6e+7

Background: Vacuum, relative permittivity = 1, relative permeability = 1

Setup Boundaries and Sources

Current Source Water cooled bus bar with 45 kA

Boundary Balloon

Setup Executive Parameters

Water cooled bus bar was chosen into the impedance matrix.

Return path of the current was set to default.

Setup Solution Options

Mesh: Manual mesh

Object	Water Cooling Tube	Water Cooled Bus bar	Background
Number of triangles	34	1628	672

Annex B Detailed Data of the Network Models

Annex B.1 Network Model of CS PF Coil System

Name of the Element	Value of the Element	Name of the Element	Value of the Element
Cwcbb+CS1U	4.00E-10 F	Cwcbb-1CS1L	4.00E-10 F
Cwcbb+CS2L	4.00E-10 F	Cwcbb-1CS2L	4.00E-10 F
Cwcbb+CS2U	4.00E-10 F	Cwcbb-1CS2U	4.00E-10 F
Cwcbb+CS3L	4.00E-10 F	Cwcbb-1CS3L	4.00E-10 F
Cwcbb+CS3U	3.90E-10 F	Cwcbb-1CS3U	3.90E-10 F
Cwcbb+PF1	3.90E-10 F	Cwcbb-1PF1	3.90E-10 F
Cwcbb+PF2	4.00E-10 F	Cwcbb-1PF2	4.00E-10 F
C wcbb+PF3	4.00E-10 F	Cwcbb-1PF3	4.00E-10 F
Cwcbb+PF4	4.00E-10 F	Cwcbb-1PF4	4.00E-10 F
Cwcbb+PF5	4.00E-10 F	Cwcbb-1PF5	4.00E-10 F
Cwcbb+PF6	3.90E-10 F	Cwcbb-1PF6	3.90E-10 F
Cwcbb-2CS1L	5.90E-10 F	CwcbbCS1U	1.05E-09 F
Cwcbb-2CS2L	5.90E-10 F	CwcbbCS2L	1.05E-09 F
Cwcbb-2CS2U	4.00E-10 F	CwcbbCS2U	1.05E-09 F
Cwcbb-2CS3L	5.90E-10 F	CwcbbCS3L	1.05E-09 F
Cwcbb-2CS3U	4.00E-10 F	CwcbbCS3U	1.05E-09 F
Cwcbb-2PF1	4.00E-10 F	CwcbbPF1	1.05E-09 F
Cwcbb-2PF2	4.00E-10 F	CwcbbPF2	1.05E-09 F

Cwcbb-2PF3	4.00E-10 F	CwcbbPF3	1.05E-09 F
Cwcbb-2PF4	5.90E-10 F	CwcbbPF4	1.05E-09 F
Cwcbb-2PF5	5.90E-10 F	CwcbbPF5	1.05E-09 F
Cwcbb-2PF6	4.00E-10 F	CwcbbPF6	1.05E-09 F
Lwcbb+CS1U	4.20E-05 H	Lwcbb-1CS1L	4.20E-05 H
Lwcbb+CS2L	4.17E-05 H	Lwcbb-1CS2L	4.17E-05 H
Lwcbb+CS2U	4.17E-05 H	Lwcbb-1CS2U	4.17E-05 H
Lwcbb+CS3L	4.17E-05 H	Lwcbb-1CS3L	4.17E-05 H
Lwcbb+CS3U	4.17E-05 H	Lwcbb-1CS3U	4.17E-05 H
Lwcbb+PF1	4.17E-05 H	Lwcbb-1PF1	4.17E-05 H
Lwcbb+PF2	4.20E-05 H	Lwcbb-1PF2	4.20E-05 H
Lwcbb+PF3	4.20E-05 H	Lwcbb-1PF3	4.20E-05 H
Lwcbb+PF4	4.20E-05 H	Lwcbb-1PF4	4.20E-05 H
Lwcbb+PF5	4.20E-05 H	Lwcbb-1PF5	4.20E-05 H
Lwcbb+PF6	4.17E-05 H	Lwcbb-1PF6	4.17E-05 H
Lwcbb-2CS1L	6.30E-05 H	Rwcbb+CS1U	4.20E-05 Ω
Lwcbb-2CS2L	6.30E-05 H	Rwcbb+CS2L	4.17E-05 Ω
Lwcbb-2CS2U	4.33E-05 H	Rwcbb+CS2U	4.17E-05 Ω
Lwcbb-2CS3L	6.30E-05 H	Rwcbb+CS3L	4.17E-05 Ω
Lwcbb-2CS3U	4.33E-05 H	Rwcbb+CS3U	4.17E-05 Ω
Lwcbb-2PF1	4.33E-05 H	Rwcbb+PF1	4.17E-05 Ω

Lwcbb-2PF2	4.30E-05 H	Rwcbb+PF2	4.20E-05 Ω
Lwcbb-2PF3	4.30E-05 H	Rwcbb+PF3	4.20E-05 Ω
Lwcbb-2PF4	6.30E-05 H	Rwcbb+PF4	4.20E-05 Ω
Lwcbb-2PF5	6.30E-05 H	Rwcbb+PF5	4.20E-05 Ω
Lwcbb-2PF6	4.33E-05 H	Rwcbb+PF6	4.17E-05 Ω
Rwcbb-1CS1L	4.20E-05 Ω	Rwcbb-2CS1L	6.30E-05 Ω
Rwcbb-1CS2L	4.17E-05 Ω	Rwcbb-2CS2L	6.30E-05 Ω
Rwcbb-1CS2U	4.17E-05 Ω	Rwcbb-2CS2U	4.33E-05 Ω
Rwcbb-1CS3L	4.17E-05 Ω	Rwcbb-2CS3L	6.30E-05 Ω
Rwcbb-1CS3U	4.17E-05 Ω	Rwcbb-2CS3U	4.33E-05 Ω
Rwcbb-1PF1	4.17E-05 Ω	Rwcbb-2PF1	4.33E-05 Ω
Rwcbb-1PF2	4.20E-05 Ω	Rwcbb-2PF2	4.30E-05 Ω
Rwcbb-1PF3	4.20E-05 Ω	Rwcbb-2PF3	4.30E-05 Ω
Rwcbb-1PF4	4.20E-05 Ω	Rwcbb-2PF4	6.30E-05 Ω
Rwcbb-1PF5	4.20E-05 Ω	Rwcbb-2PF5	6.30E-05 Ω
Rwcbb-1PF6	4.17E-05 Ω	Rwcbb-2PF6	4.33E-05 Ω

Tab. B.1-1 Values for resistances, inductances and capacitances used in the network model of the CS PF coil system for the water cooled bus bars

Name of the Element	Value of the Element	Name of the Element	Value of the Element
Ck6+CS1L	1.98E-07 F	Lk6+CS1L	8.25E-07 H
Ck6+CS1U	2.09E-07 F	Lk6+CS1U	8.70E-07 H
Ck6+CS2L	1.01E-07 F	Lk6+CS2L	4.20E-07 H
Ck6+CS2U	1.58E-07 F	Lk6+CS2U	6.60E-07 H
Ck6+CS3L	7.20E-08 F	Lk6+CS3L	3.00E-07 H
Ck6+CS3U	1.30E-07 F	Lk6+CS3U	5.40E-07 H
Ck6+PF1	3.60E-08 F	Lk6+PF1	1.50E-07 H
Ck6+PF6	3.60E-08 F	Lk6+PF6	1.50E-07 H
Ck6-CS1L	1.80E-07 F	Lk6-CS1L	7.50E-07 H
Ck6-CS1U	2.09E-07 F	Lk6-CS1U	8.70E-07 H
Ck6-CS2L	1.01E-07 F	Lk6-CS2L	4.20E-07 H
Ck6-CS2U	1.58E-07 F	Lk6-CS2U	6.60E-07 H
Ck6-CS3L	7.20E-08 F	Lk6-CS3L	3.00E-07 H
Ck6-CS3U	1.30E-07 F	Lk6-CS3U	5.40E-07 H
Ck6-PF1	3.60E-08 F	Lk6-PF1	1.50E-07 H
Ck6-PF6	3.60E-08 F	Lk6-PF6	1.50E-07 H
Rk6+CS1L	4.57E-04 Ω	Rk6-CS1L	4.17E-04 Ω
Rk6+CS1U	4.83E-04 Ω	Rk6-CS1U	4.83E-04 Ω
Rk6+CS2L	2.33E-04 Ω	Rk6-CS2L	2.33E-04 Ω
Rk6+CS2U	3.66E-04 Ω	Rk6-CS2U	3.66E-04 Ω
Rk6+CS3L	1.67E-04 Ω	Rk6-CS3L	1.67E-04 Ω

Rk6+CS3U	3.00E-04 Ω	Rk6-CS3U	3.00E-04 Ω
Rk6+PF1	8.38E-05 Ω	Rk6-PF1	8.33E-05 Ω
Rk6+PF6	8.38E-05 Ω	Rk6-PF6	8.33E-05 Ω

Tab. B.1-2 Values for resistances, inductances and capacitances used in the network model of the CS PF coil system for the connection of the switching network units with switching network resistors

Name of the Element	Value of the Element	Name of the Element	Value of the Element
Ck2+CS1L	6.00E-08 F	Ck2-CS1L	9.60E-08 F
Ck2+CS1U	2.05E-07 F	Ck2-CS1U	2.12E-07 F
Ck2+CS2L	4.00E-08 F	Ck2-CS2L	4.00E-08 F
Ck2+CS2U	5.64E-08 F	Ck2-CS2U	5.64E-08 F
Ck2+CS3L	3.60E-08 F	Ck2-CS3L	3.80E-08 F
Ck2+CS3U	4.68E-08 F	Ck2-CS3U	4.68E-08 F
Ck2+PF1	2.40E-08 F	Ck2-PF1	2.40E-08 F
Ck2+PF2	3.60E-08 F	Ck2-PF2	3.60E-08 F
Ck2+PF3	1.05E-08 F	Ck2-PF3	1.05E-08 F
Ck2+PF4	6.00E-09 F	Ck2-PF4	1.26E-08 F
Ck2+PF5	6.00E-09 F	Ck2-PF5	1.30E-08 F
Ck2+PF6	6.00E-08 F	Ck2-CS1L	9.60E-08 F
Lk2+CS1L	2.25E-06 H	Lk2-CS1L	3.60E-06 H
Lk2+CS1U	8.50E-07 H	Lk2-CS1U	8.85E-07 H
Lk2+CS2L	1.48E-06 H	Lk2-CS2L	1.48E-06 H
Lk2+CS2U	2.11E-06 H	Lk2-CS2U	2.11E-06 H
Lk2+CS3L	1.35E-06 H	Lk2-CS3L	1.44E-06 H
Lk2+CS3U	1.75E-06 H	Lk2-CS3U	1.75E-06 H
Lk2+PF1	9.00E-07 H	Lk2-PF1	9.00E-07 H
Lk2+PF2	1.35E-06 H	Lk2-PF2	1.35E-06 H
Lk2+PF3	1.57E-06 H	Lk2-PF3	1.57E-06 H

Lk2+PF4	9.00E-07 H	Lk2-PF4	1.89E-06 H
Lk2+PF5	9.00E-07 H	Lk2-PF5	1.89E-06 H
Lk2+PF6	1.13E-06 H	Lk2-PF6	2.11E-06 H
Rk2+CS1L	1.25E-03 Ω	Rk2-CS1L	2.00E-03 Ω
Rk2+CS1U	4.75E-04 Ω	Rk2-CS1U	4.91E-04 Ω
Rk2+CS2L	8.25E-04 Ω	Rk2-CS2L	8.25E-04 Ω
Rk2+CS2U	1.18E-03 Ω	Rk2-CS2U	1.18E-03 Ω
Rk2+CS3L	7.50E-04 Ω	Rk2-CS3L	8.00E-04 Ω
Rk2+CS3U	9.75E-04 Ω	Rk2-CS3U	9.75E-04 Ω
Rk2+PF1	5.00E-04 Ω	Rk2-PF1	5.00E-04 Ω
Rk2+PF2	7.50E-04 Ω	Rk2-PF2	7.50E-04 Ω
Rk2+PF3	8.75E-04 Ω	Rk2-PF3	8.75E-04 Ω
Rk2+PF4	5.00E-04 Ω	Rk2-PF4	1.00E-03 Ω
Rk2+PF5	5.00E-04 Ω	Rk2-PF5	1.00E-06 Ω
Rk2+PF6	6.25E-04 Ω	Rk2-PF6	1.18E-03 Ω

Tab. B.1-3 Values for resistances, inductances and capacitances used in the network model of the CS PF coil system for the connection of the fast discharge units with fast discharge resistors

Name of the Element	Value of the Element	Name of the Element	Value of the Element
Cscbb+CS1L	7.20E-08 F	Cscbb-CS1L	7.20E-08 F
Cscbb+CS1U	7.20E-08 F	Cscbb-CS1U	7.20E-08 F
Cscbb+CS2L	6.98E-08 F	Cscbb-CS2L	6.98E-08 F
Cscbb+CS2U	6.40E-08 F	Cscbb-CS2U	6.40E-08 F
Cscbb+CS3L	6.60E-08 F	Cscbb-CS3L	6.60E-08 F
Cscbb+CS3U	6.10E-08 F	Cscbb-CS3U	6.10E-08 F
Cscbb+PF1	4.48E-08 F	Cscbb-PF1	4.48E-08 F
Cscbb+PF2	4.50E-08 F	Cscbb-PF2	4.50E-08 F
Cscbb+PF3	4.10E-08 F	Cscbb-PF3	4.10E-08 F
Cscbb+PF4	4.80E-08 F	Cscbb-PF4	4.80E-08 F
Cscbb+PF5	4.60E-08 F	Cscbb-PF5	4.60E-08 F
Cscbb+PF6	4.48E-08 F	Cscbb-PF6	4.48E-08 F
Lscbb+CS1L	5.60E-05 H	Lscbb-CS1L	5.60E-05 H
Lscbb+CS1U	5.60E-05 H	Lscbb-CS1U	5.60E-05 H
Lscbb+CS2L	5.46E-05 H	Lscbb-CS2L	5.46E-05 H
Lscbb+CS2U	5.04E-05 H	Lscbb-CS2U	5.04E-05 H
Lscbb+CS3L	5.18E-05 H	Lscbb-CS3L	5.18E-05 H
Lscbb+CS3U	4.76E-05 H	Lscbb-CS3U	4.76E-05 H
Lscbb+PF1	3.50E-05 H	Lscbb-PF1	3.50E-05 H
Lscbb+PF2	3.50E-05 H	Lscbb-PF2	3.50E-05 H
Lscbb+PF3	3.20E-05 H	Lscbb-PF3	3.20E-05 H

Lscbb+PF4	3.80E-05 H	Lscbb-PF4	3.80E-05 H
Lscbb+PF5	3.60E-05 H	Lscbb-PF5	3.00E-05 H
Lscbb+PF6	3.50E-05 H	Lscbb-PF6	3.50E-05 H
Rscbb+CS1L	4.00E-11 Ω	Rscbb-CS1L	4.00E-11 Ω
Rscbb+CS1U	4.00E-11 Ω	Rscbb-CS1U	4.00E-11 Ω
Rscbb+CS2L	3.90E-11 Ω	Rscbb-CS2L	3.90E-11 Ω
Rscbb+CS2U	3.60E-11 Ω	Rscbb-CS2U	3.60E-11 Ω
Rscbb+CS3L	3.70E-11 Ω	Rscbb-CS3L	3.70E-11 Ω
Rscbb+CS3U	3.40E-11 Ω	Rscbb-CS3U	3.40E-11 Ω
Rscbb+PF1	2.50E-11 Ω	Rscbb-PF1	2.50E-11 Ω
Rscbb+PF2	2.50E-11 Ω	Rscbb-PF2	2.50E-11 Ω
Rscbb+PF3	2.30E-11 Ω	Rscbb-PF3	2.30E-11 Ω
Rscbb+PF4	2.70E-11 Ω	Rscbb-PF4	2.70E-11 Ω
Rscbb+PF5	2.60E-11 Ω	Rscbb-PF5	2.60E-11 Ω
Rscbb+PF6	2.50E-11 Ω	Rscbb-PF6	2.50E-11 Ω

Tab. B.1-4 Values for resistances, inductances and capacitances used in the network model of the CS PF coil system for the connection of the coil terminal box with coil terminals with superconducting bus bars

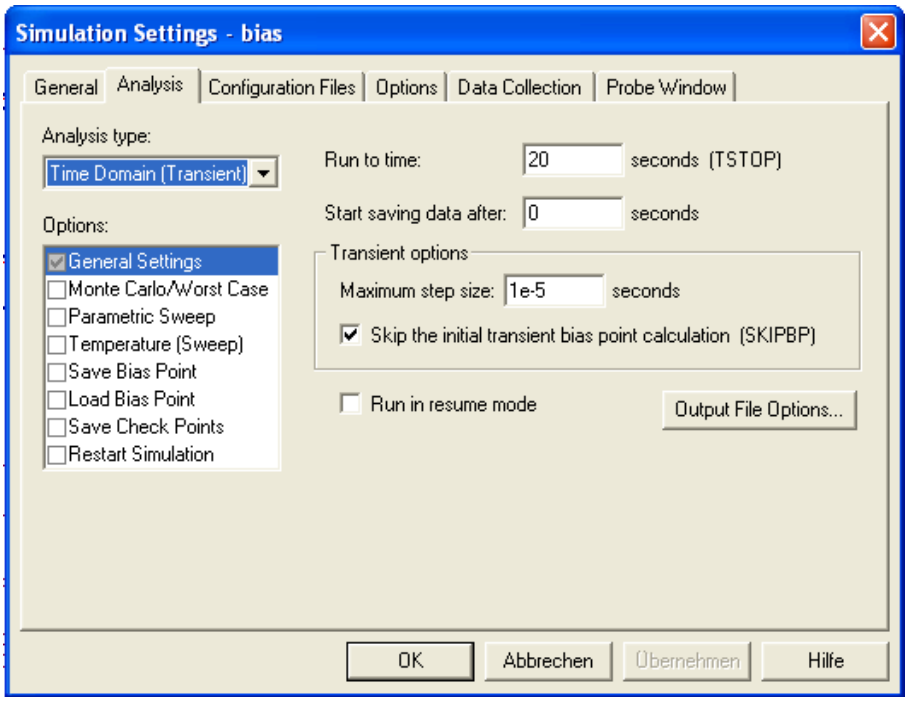

Fig. B.1-1 Simulation settings for analysis of the network model of the CS PF coil system

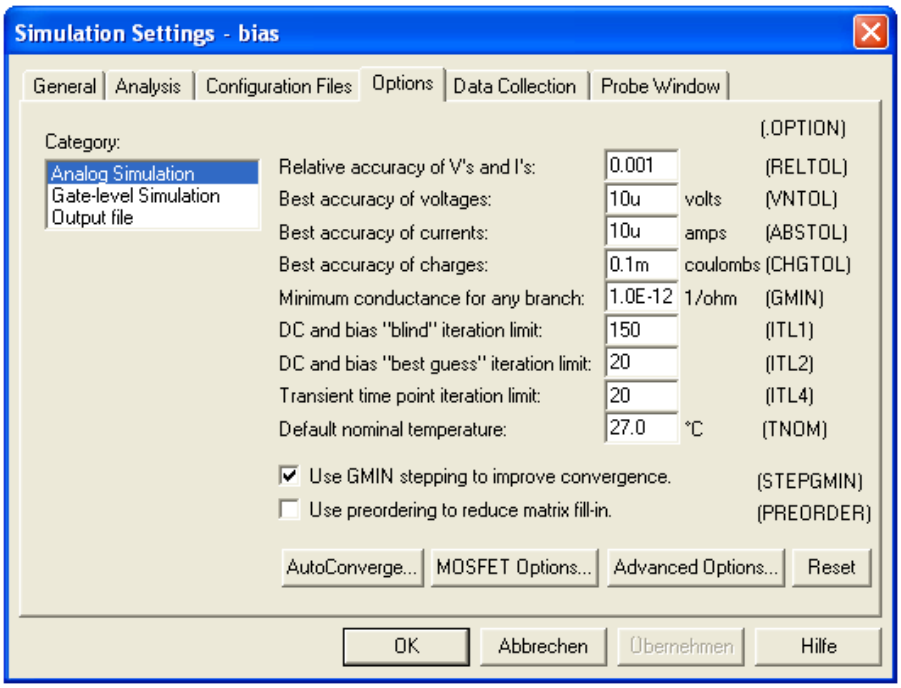

Fig. B.1-2 Simulation settings for options of the network model of the CS PF coil system

Annex B.2 Network Model of PF 3 Coil

(a) Calculations in Frequency Domain

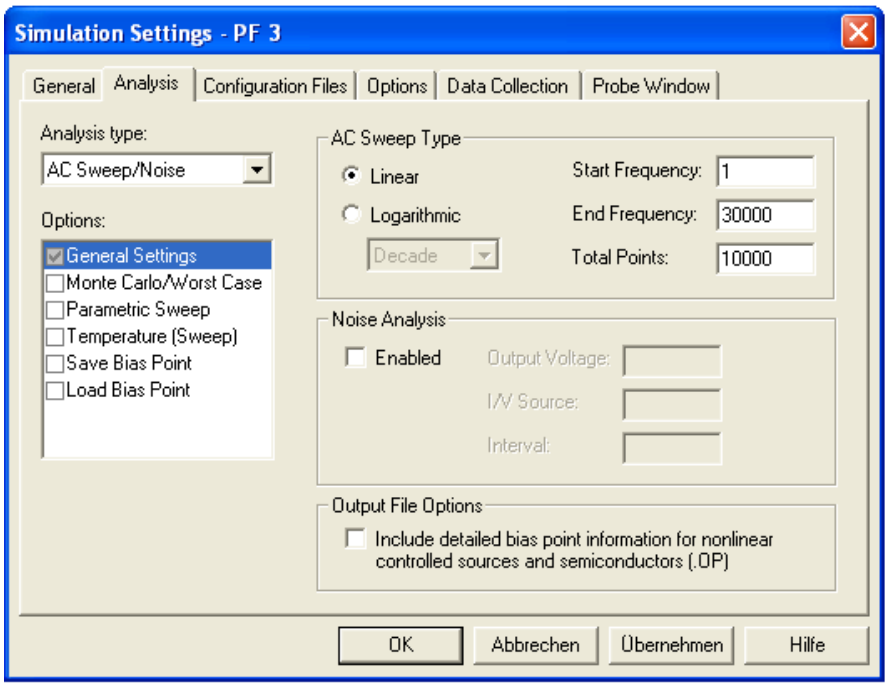

Fig. B.2-1 Simulation settings for analysis of the network model of the PF 3 coil in frequency domain

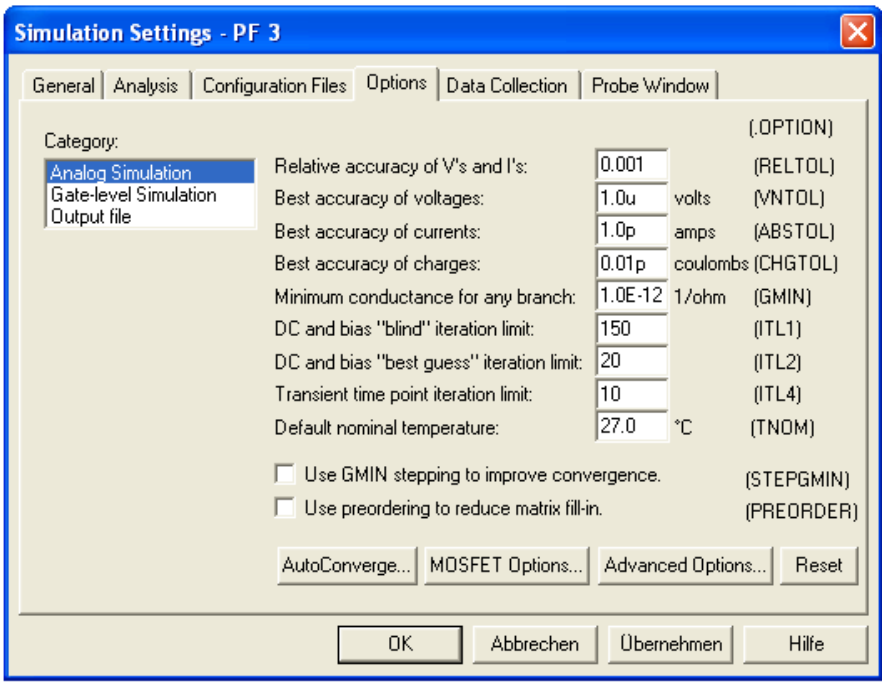

Fig. B.2-2 Simulation settings for options of the network model of the PF 3 coil in frequency domain

(b) Calculations in Time Domain

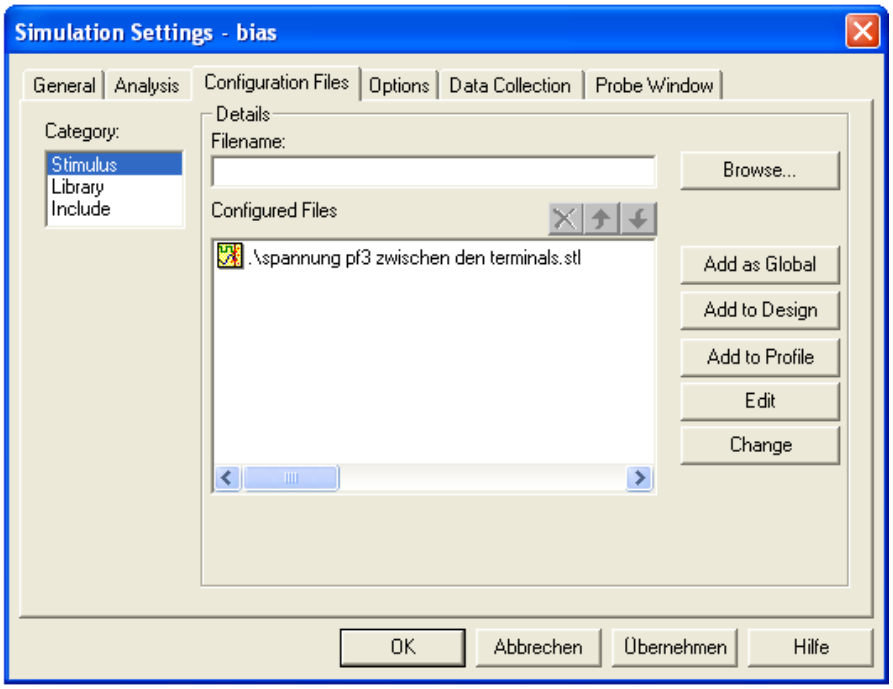

Fig. B.2-3 Simulation settings for configuration files of the network model of the PF 3 coil in time domain

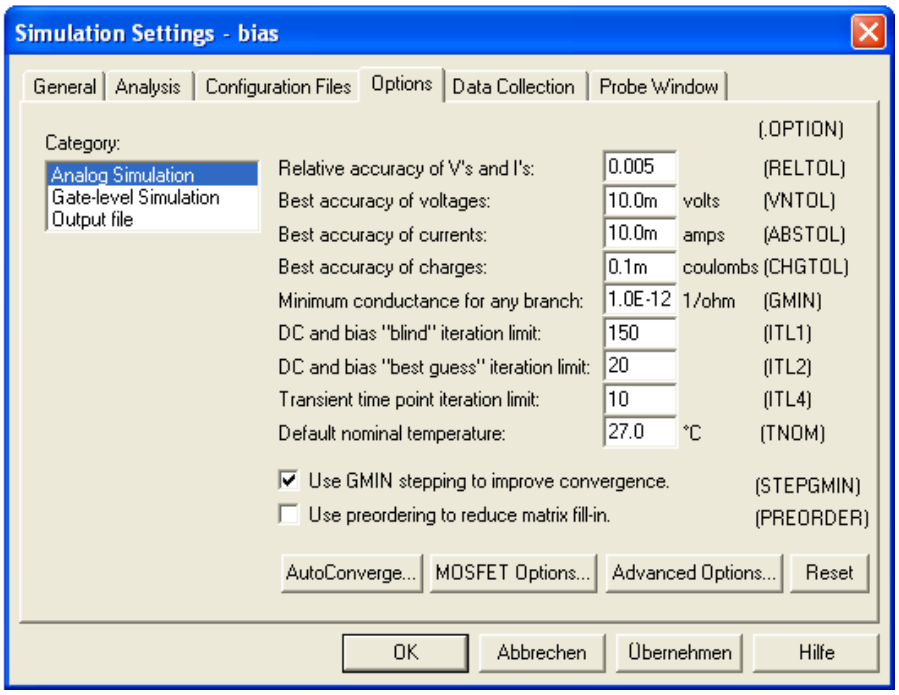

Fig. B.2-4 Simulation settings for options of the network model of the PF 3 coil in time domain

Annex B.3 Network Model of PF 6 Coil

(a) Calculations in Frequency Domain

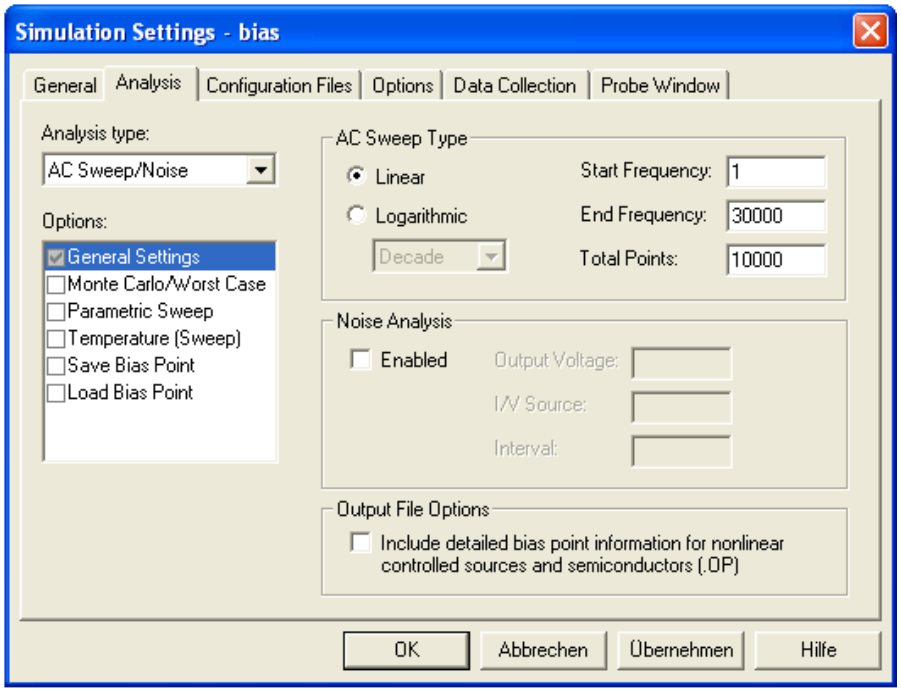

Fig. B.3-1 Simulation settings for analysis of the network model of the PF 6 coil in frequency domain

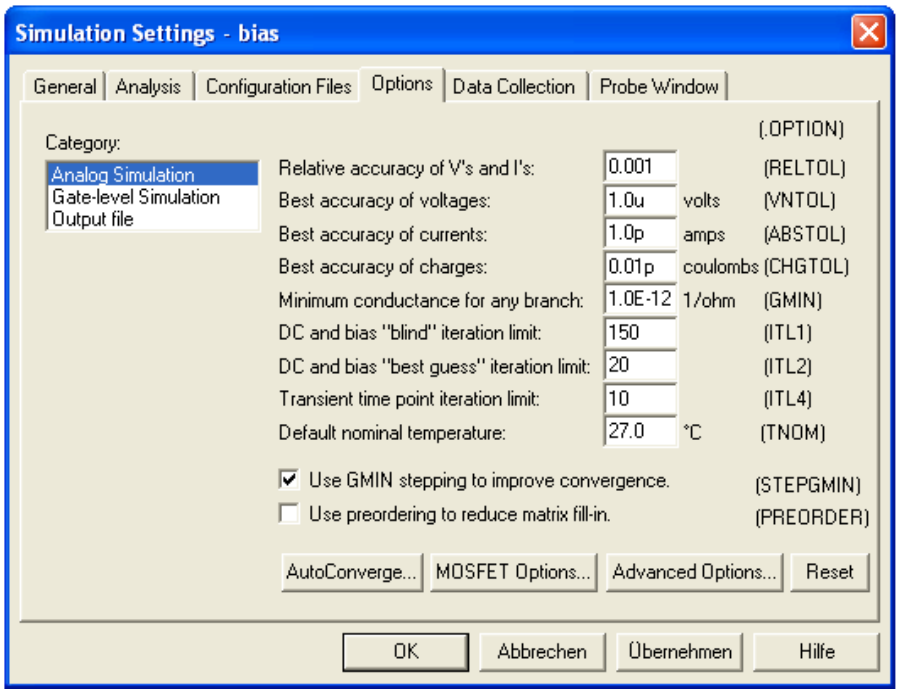

Fig. B.3-2 Simulation settings for options of the network model of the PF 6 coil in frequency domain

(b) Calculations in Time Domain

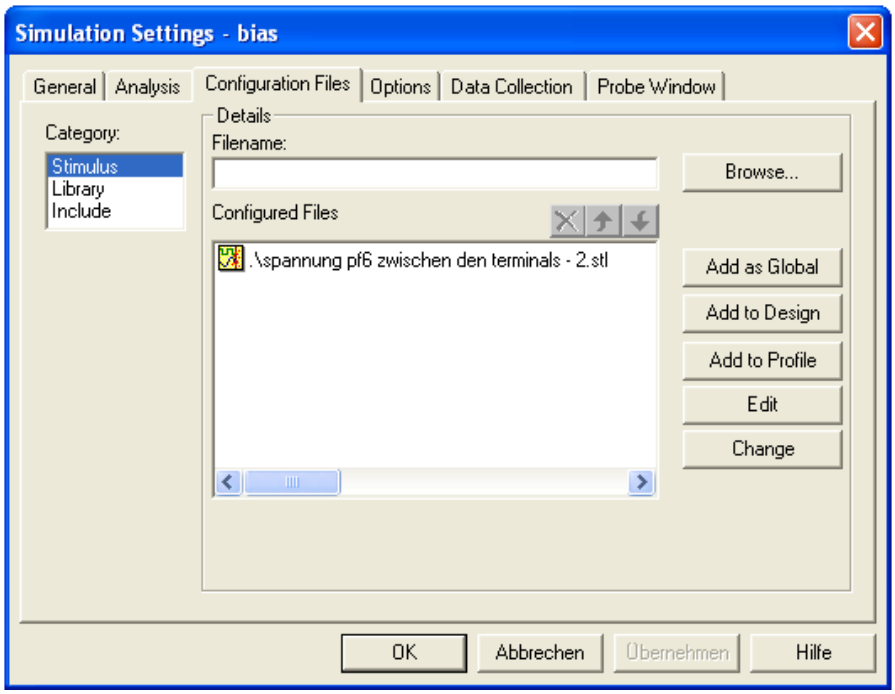

Fig. B.3-3 Simulation settings for configuration files of the network model of the PF 6 coil in time domain

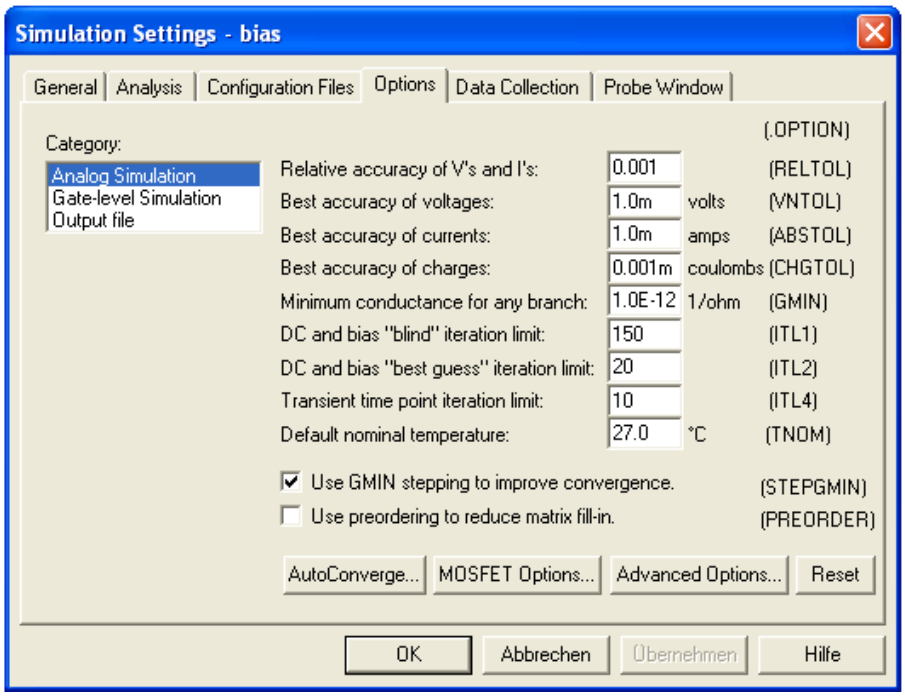

Fig. B.3-4 Simulation settings for options of the network model of the PF 6 coil in time domain